

# Learning Language Structures through Grounding

by

Haoyue Freda Shi

A thesis submitted  
in partial fulfillment of the requirements for  
the degree of

Doctor of Philosophy in Computer Science

at the  
TOYOTA TECHNOLOGICAL INSTITUTE AT CHICAGO  
Chicago, Illinois

June 2024

*Thesis Committee:*

Kevin Gimpel (Thesis Advisor)

Karen Livescu (Thesis Advisor)

Roger P. Levy

Luke Zettlemoyer

Copyright © 2024 by Haoyue Freda Shi.  
All rights reserved.

## Abstract

Language is highly structured, with syntactic and semantic structures, to some extent, agreed upon by speakers of the same language. With implicit or explicit awareness of such structures, humans can learn and use language efficiently and generalize to sentences that contain unseen words. Motivated by human language learning, in this dissertation, we consider a family of machine learning tasks that aim to learn language structures through *grounding*. We seek distant supervision from other data sources (i.e., grounds), including but not limited to other modalities (e.g., vision), execution results of programs, and other languages.

We demonstrate the potential of this task formulation and advocate for its adoption through three schemes, each shown in a separate part of this dissertation. In Part I, we consider learning syntactic parses through visual grounding. We propose the task of visually grounded grammar induction, which aims at learning to predict the constituency parse tree of a sentence by reading the sentence and looking at the corresponding image. We present the first models to induce syntactic structures from visually grounded text and speech, and find that the visual grounding signals can help improve the parsing quality over language-only models. As a side contribution, we propose a novel evaluation metric that enables the evaluation of speech parsing without text or automatic speech recognition systems involved. In Part II, we propose two execution-aware methods to map sentences into corresponding semantic structures (i.e., programs). One of them enables nearly perfect compositional generalization to unseen sentences with mild assumptions on domain knowledge, and the other significantly improves the performance of few-shot semantic parsing by leveraging the execution results of programs as a source of grounding signals. In Part III, we propose methods that learn language structures from annotations in other languages. Specifically, we propose a method that sets a new state-of-the-art performance on cross-lingual word alignment, without using any annotated parallel data. We then leverage the learned word alignments to improve the performance of zero-shot cross-lingual dependency parsing, by proposing a novel substructure-based projection method that preserves structural knowledge learned from the source language.

# Acknowledgements

I am incredibly fortunate to have Professors Kevin Gimpel and Karen Livescu as my Ph.D. advisors. Over the past years, Karen and Kevin have offered me the highest level of freedom (that I can imagine) on research topics while reminding me of my dissertation outline and have been incredibly supportive in everything. I usually filled our research meetings with scattered, vague, and probably crazy ideas, many of which did not make much sense, and many of them have not been realized yet. No matter how senseless the ideas were, my advisors always listened to me patiently and provided constructive feedback that helped make the ideas concrete and realistic. They answered all my beginner questions such as “*what is prosody*” and “*what is bitext*”, and responded with an absolute yes to almost all my unreasonable requests, from editing papers on holiday nights to having them as my secondary reviewer—as the advisor to my future students, I wish myself could be (even half) as kind and patient as them. I promise to keep the spirit of scientific rigor, curiosity, and kindness that they have shown to me, and I hope to be able to pass it on to my future students.

I have learned a lot from my mentors through internships and cross-institutional collaborations. I am grateful to Roger Levy and Luke Zettlemoyer for the training, guidance, and support they offered me, and for their feedback on this dissertation as committee members. I am fortunate to have been mentored twice by Sida Wang, the first author of my favorite ACL paper so far, and have learned a lot of concrete research skills from him. I am grateful to Denny Zhou for hosting me in the final internship and for his support on all my projects. I am also in debt to my academic mentors before coming to TTIC. Thanks to Lei Li and Hao Zhou for their guidance and continued support—I worked with them at the ByteDance AI lab, and now it is great to see they have both returned to academia and have started fostering the next generation of computer scientists. Thanks to Sam Bowman for the initial guidance when I entered the fantastic world of neural NLP and, perhaps

more importantly, for introducing TTIC to me.

Jiayuan Mao deserves special thanks for being my closest collaborator and friend over the past years, for brainstorming with me, for providing fruitful comments on almost all my papers, for sharing research or non-research stuff that amused me a lot, and for teaching me random knowledge in robotics, music, and photography.

I am grateful to Michael Bowling, Nidhi Hegde, and Dale Schuurmans—the extended definition of *grounding* in this dissertation has become much clearer and more articulable after the discussion with them at a wonderful dinner in Edmonton. Thanks to David McAllester for his insightful opinions on grounding—he is an anti-grounding person,<sup>1</sup> but his opinions have significantly helped me clarify my thoughts on grounding. Thanks to Yoav Artzi, Noriyuki Kojima, and Wentao Wang, as well as many anonymous conference reviewers, for their feedback on the work presented in this dissertation.

I am grateful to my coauthors, mentors and peers who have taught me a lot: thanks to Armen Aghajanyan, Xinyun Chen, Ed Chi, Dipanjan Das, David Dohan, Daniel Fried, Yoon Kim, Lingyu Gao, David Harwath, Jim Glass, Jessy Lin, Marjan Ghazvininejad, Vikram Gupta, Jeff Lai, Mike Lewis, Kanishka Misra, Puyuan Peng, Mrinmaya Sachan, Nathan Scales, Nathanael Schärli, Bowen Shi, Mirac Suzgun, Josh Tenenbaum, Shubham Toshniwal, Eric Wallace, Xuezhi Wang, Jason Wei, Jiajun Wu, Scott Yih, Ruiqi Zhong, and folks who organized and participated in the NL-Augmenter project for the wonderful collaboration; thanks to Allyson Ettinger, Sanghee Kim, Jiangtian Li, Jiaxuan Li, Zi Lin, Peng Qian, Weiwei Sun and Yuhan Zhang for inspiring conversations in linguistics and cognitive sciences; thanks to Hongyuan Mei and Lili Mou for discussions and encouragement around research ideas and career plans; thanks to the members of the TTIC speech and language reading group and the later TTIC-UChicago joint NLP reading group, especially Mingda Chen, Chung-Ming Chien, Ju-Chieh Chou, Kartik Goyal, Yushi Hu, Ruotian Luo, Richard Pang, Ankita Pasad, Shane Settle, Karl Stratos, Chenhao Tan, Qingming Tang, Chih-chan Tien, Lifu Tu, Haochen Wang, Sam Wiseman, Davis Yoshida, David Yunis, and Jiawei Zhou for all the delightful conversations.

TTIC is a fantastic place to do research, and I am grateful to the faculty and staff members for their efforts to make TTIC even better. I have benefitted a lot from the awesome courses and/or conversations with Avrim Blum, Julia Chuzhoy, Greg Shakhnarovich,

---

<sup>1</sup>Although I believe the definition of grounding (§2.2) in this dissertation is different from the one that David holds his opinion against.

Madhur Tulsiani, Matthew Turk, and Matthew Walter, as well as the (probably globally best) administrative support from Adam Bohlander, Rose Bradford, Erica Cocom, Chrissy Coleman, Jessica Jacobson, Deree Kobets, Mary Marre, Alicia McClarin, and Amy Minick.

I gratefully acknowledge that I have been supported by a Google Ph.D. fellowship since 2021. The fellowship is an honor, a financial endowment that provides me research freedom and, more importantly, great mental support during the darkest time caused by COVID-19 and the subsequent disasters on the faraway land I most care about.

I would like to express my gratitude to my friends and extended family for their support and encouragement. Thanks to Qian Li, Jingye Tian, and Yuemei Zhang for sharing news and thoughts with me and being super responsive whenever I pinged them for a random chat. Thanks to Xinyuan Zhang for all her cute arts. Thanks to Yvonne Han for always sharing her excellent cooking and brilliant tiny items, and for showing me that the world is much more fantastic than what I have already explored. Thanks to Xiao Han for being my amazing cousin and sharing his research, life stories, and thoughts with me. Thanks to Hexiang Hu and Tete Xiao for keeping me posted on all kinds of news and for discussing the industrial NLP breakthroughs with me. Thanks to Jiading Fang and Han Shao for their friendship and for keeping me more informed. Thanks to Hanqing Zhao, whom I consider the best poet I have ever had the pleasure to meet in person, for sharing her poems and thoughts with me, and for shaping me into (what I proudly call) a 0th-generation Hanqingist poetry critic. Thanks to friends in Canada for making my life there colorful (misspelled intentionally :)—we will have a longer journey together!

I never met the people listed below or was not even born when some of them passed away. However, I am grateful for their impact on my life: thanks to John Stith Pemberton for inventing Coca-Cola—I suspect that I would not have been able to complete this dissertation without Coke. Thanks to Adonis, Elizabeth Bishop, Luis Cernuda, and Wisława Szymborska for their great poetry that accompanied me during sleepless nights.

I have considered substituting the following paragraph with a banal one but eventually opted to retain it in its current form. I would indeed prefer not to be born if I had the option, but family is never a reason for my pessimism. I could not be more blessed to have my family—Mom, Dad, Yudong, and the furry family members Wisława, Ludwig, and Heinrich: thanks much to you all for always standing with me so that I gain enough courage to face the ridiculously meaningless life.

Fortunately, this dissertation is not solely about meaning, and we stand on the ground.

# DEDICATION

*To Mingxin Liu (1994–2019):  
Yet another piece of evidence that we miss you.*

# Contents

<b>1</b>	<b>Introduction</b>	<b>1</b>
1.1	Dissertation Structure and Contribution Summary . . . . .	3
1.2	A Quick Guide to Readers . . . . .	5
<b>2</b>	<b>Background</b>	<b>6</b>
2.1	Language Structures . . . . .	6
2.1.1	Phrase Structures and Phrase-Structure Grammars . . . . .	6
2.1.2	Dependency Syntax . . . . .	10
2.1.3	Executable Programs as Semantics . . . . .	11
2.1.4	Cross-Lingual Word Alignment . . . . .	13
2.2	Grounding . . . . .	15
<b>I</b>	<b>Learning to Parse through Cross-Modal Grounding</b>	<b>19</b>
<b>3</b>	<b>Syntax Acquisition from Visually Grounded Text</b>	<b>20</b>
3.1	Related Work . . . . .	22
3.2	The Visually Grounded Neural Syntax Learner . . . . .	23
3.2.1	Textual Representations and Structures . . . . .	24
3.2.2	Visual-Semantic Embeddings . . . . .	25
3.2.3	Training . . . . .	25
3.2.4	The Abstract-Initial Inductive Bias . . . . .	28
3.3	Experiments . . . . .	29



3.3.1	Datasets and Metrics . . . . .	29
3.3.2	Baselines . . . . .	29
3.3.3	Implementation Details . . . . .	31
3.3.4	Results: Unsupervised Constituency Parsing . . . . .	32
3.3.5	Results: Data Efficiency . . . . .	34
3.3.6	Analysis: Consistency with Linguistic Concreteness . . . . .	35
3.3.7	Analysis: Self Agreement as Model Selection Criterion . . . . .	35
3.3.8	Extension to Multiple Languages . . . . .	37
3.4	Conclusion and Discussion . . . . .	37
<b>4</b>	<b>Syntax Acquisition from Visually Grounded Speech</b>	<b>40</b>
4.1	Related Work . . . . .	41
4.2	Method . . . . .	43
4.2.1	Audio-Visual Word Segmentation and Representation . . . . .	44
4.2.2	Self-Training . . . . .	45
4.2.3	Unsupervised Decoding . . . . .	45
4.3	Experiments . . . . .	46
4.3.1	Setup . . . . .	46
4.3.2	Baselines and Toplines . . . . .	47
4.3.3	Evaluation Metrics . . . . .	47
4.3.4	Results: Unsupervised Word Segmentation . . . . .	48
4.3.5	Results: Unsupervised Phrase Structure Induction . . . . .	49
4.3.6	Analysis . . . . .	51
4.4	Conclusion and Discussion . . . . .	53
<b>5</b>	<b>STRUCT-IOU: A Structured Alignment-Based Evaluation Metric for Constituency Parsing</b>	<b>55</b>
5.1	Related Work . . . . .	57
5.2	Preliminaries . . . . .	58
5.2.1	Open Intereval Operations . . . . .	58

5.2.2	Relaxed Segment Trees . . . . .	58
5.3	The STRUCT-IOU Metric . . . . .	60
5.3.1	Problem Formulation . . . . .	60
5.3.2	Solution . . . . .	62
5.4	Experiments . . . . .	65
5.4.1	Speech Constituency Parsing Evaluation . . . . .	65
5.4.2	Text Constituency Parsing Evaluation: English . . . . .	69
5.4.3	Text Constituency Parsing Evaluation: Hebrew . . . . .	72
5.5	Conclusion and Discussion . . . . .	74
 <b>II Learning to Parse through Program Execution</b>		<b>75</b>
6	<b>Joint Syntax and Semantics Induction in Grounded Environments</b>	<b>76</b>
6.1	Related Work . . . . .	77
6.2	Grammar-Based Grounded Lexicon Learning . . . . .	79
6.2.1	Grounded Lexicon . . . . .	80
6.2.2	Program Execution . . . . .	83
6.2.3	Joint Chart Parsing and Expected Execution . . . . .	83
6.2.4	Learning . . . . .	87
6.3	Experiment . . . . .	87
6.3.1	Visual Reasoning . . . . .	87
6.3.2	Language-Driven Navigation . . . . .	96
6.4	Conclusion and Discussion . . . . .	102
7	<b>Learning Semantic Parses through Program Execution Consistency</b>	<b>104</b>
7.1	Related Work . . . . .	105
7.2	Proposed Approach: MBR-EXEC . . . . .	108
7.2.1	Sample Collection . . . . .	108
7.2.2	Execution-Based MBR Decoding . . . . .	109
7.3	Experiments . . . . .	109

7.3.1	Datasets and Evaluation Metrics . . . . .	110
7.3.2	Baselines . . . . .	113
7.3.3	Primary Results . . . . .	115
7.3.4	Analysis . . . . .	116
7.3.5	Oracle Performance . . . . .	121
7.4	Conclusion and Discussion . . . . .	122
<b>III Learning to Parse through Cross-Lingual Grounding</b>		<b>124</b>
<b>8</b>	<b>From Pre-Trained Contextualized Representations to Unsupervised Cross-Lingual Word Alignment</b>	<b>125</b>
8.1	Related Work . . . . .	126
8.2	Method . . . . .	127
8.2.1	Unsupervised Bitext Construction . . . . .	127
8.2.2	Feature-Based Word Aligner . . . . .	127
8.3	Experiments . . . . .	129
8.4	Conclusion and Discussion . . . . .	130
<b>9</b>	<b>Zero-Shot Cross-Lingual Dependency Parsing with Substructure Distribution Projection</b>	<b>132</b>
9.1	Related Work . . . . .	134
9.2	Method . . . . .	136
9.2.1	Background . . . . .	136
9.2.2	Preliminaries . . . . .	138
9.2.3	Dependency Distribution Projection . . . . .	139
9.2.4	Optimization . . . . .	142
9.3	Experiments . . . . .	142
9.3.1	Results: Fully Unsupervised Transfer . . . . .	144
9.3.2	Ablation Study . . . . .	144
9.3.3	Analysis: Effect of Alignment Methods . . . . .	146

9.3.4	Results: Multiple Source Languages . . . . .	147
9.3.5	Results: Transfer with Supervised Bitext . . . . .	148
9.4	Conclusion and Discussion . . . . .	150
<b>10</b>	<b>Conclusion and Discussion</b>	<b>152</b>

# List of Figures

2.1	The constituency parse tree of the sentence “ <i>The cat sat on the mat</i> ”.	7
2.2	Illustration of the bracket-based $F_1$ score.	9
2.3	The dependency parse tree of the sentence “ <i>The cat sat on the mat</i> ”, annotated following the Universal Dependencies (Nivre et al., 2020) scheme.	10
2.4	Illustration of how LAS and UAS work as dependency parsing metrics.	11
2.5	An example of a CCG derivation for the sentence “ <i>A cat drinks milk.</i> ”	13
2.6	Example of cross-lingual word alignment between English and German.	14
3.1	Illustration of visual correspondence of phrases.	21
3.2	Illustration of the VG-NSL model.	23
3.3	An illustration of how VG-NSL composes a constituency parse tree.	26
3.4	$F_1$ score and self $F_1$ score with respect to the amount of training data.	34
4.1	Illustration of the AV-NSL model.	41
4.2	An illustrative example of the evaluation metric used in Tseng et al. (2023).	43
4.3	Examples of VG-HuBERT word segmentation and segment insertion.	44
5.1	Illustration of STRUCT-IOU.	56
5.2	Examples of conflicted and non-conflicted node matchings.	61
5.3	STRUCT-IOU vs. PARSEVAL $F_1$ on NXT-SWBD.	66
5.4	Examples of perturbation.	67
5.5	STRUCT-IOU scores with respect to $\delta$ for different types of perturbations.	68
5.6	Corpus-level vs. sentence-level STRUCT-IOU scores.	69
5.7	STRUCT-IOU vs. PARSEVAL $F_1$ on PTB.	70

5.8	Example of syntactically ambiguous sentence (in English). . . . .	71
5.9	Example of syntactically ambiguous sentence (synthetic). . . . .	72
5.10	Parse trees of the Hebrew sentence ?פצועים פצויה with two possible morpho- logical analyses. . . . .	73
6.1	Illustration of idea of grounded lexicon learning. . . . .	77
6.2	Illustration of the G2L2 model. . . . .	80
6.3	Illustration of a lexicon entry in G2L2. . . . .	81
6.4	Illustration of two mergeable semantic programs. . . . .	84
7.1	Illustration of MBR-EXEC. . . . .	105
7.2	Primary evaluation results of MBR-EXEC. . . . .	115
7.3	Performance of the evaluated selection criteria across temperatures. . . . .	117
7.4	Performance with groups of 3-shot prompt vs. concatenation of 15 prompts. . . . .	118
7.5	Comparison between applying methods to all possible candidates vs. ap- plying methods to only executable candidates. . . . .	119
7.6	Comparison between soft and hard MBR-EXEC. . . . .	120
7.7	Sample size–oracle performance curves on the considered datasets. . . . .	121
8.1	Example of cross-lingual word alignment in English and German. . . . .	126
9.1	Illustration of SUBDP vs. Lacroix et al. (2016). . . . .	133
9.2	LAS on the Universal Dependencies v2.2 standard development set. . . . .	145
9.3	UAS on the Universal Dependencies v2.2 standard development set. . . . .	145
9.4	Data efficiency analysis for SUBDP. . . . .	149

# List of Tables

2.1	Language structures considered in this dissertation and the corresponding primary evaluation metrics. . . . .	14
2.2	The primary data source and ground in grounding settings in various scenarios. . . . .	18
3.1	Recall of specific typed phrases and overall $F_1$ score on MSCOCO. . . . .	33
3.2	Agreement between VG-NSL concreteness and existing concreteness estimation methods. . . . .	35
3.3	$F_1$ and self $F_1$ scores of VG-NSL and VG-NSL+AI with different model selection methods. . . . .	36
3.4	$F_1$ scores on the Multi30K. . . . .	37
4.1	English word segmentation results on the SpokenCOCO validation set. . . .	49
4.2	English phrase structure induction results on SpokenCOCO. . . . .	50
4.3	Results of self-training with s-Benepar. . . . .	50
4.4	PARSEVAL $F_1$ scores given oracle segmentation. . . . .	51
4.5	Phrase structure induction results on (spoken) German Multi30K. . . . .	51
4.6	Recall for specific typed phrases on SpokenCOCO. . . . .	52
4.7	PARSEVAL $F_1$ scores for ablations over word segmentation, visual representation, and speech representation. . . . .	53
5.1	Comparison of PARSEVAL $F_1$ and STRUCT-IOU scores on syntactically plausible trees. . . . .	72
6.1	The type system of the domain-specific language for visual reasoning. . . .	88

6.2	All operations in the domain-specific language for visual reasoning. . . . .	89
6.3	Execution trace of the program <code>count(filter(filter(scene(), CUBE), SHINY))</code> . . .	91
6.4	The learned lexicon entries associated with each word for a simple sentence: <i>are there any shiny cubes?</i> . . . . .	94
6.5	Accuracy on the CLEVR dataset. . . . .	95
6.6	All operations in the domain-specific language for language-driven navigation. . . . .	97
6.7	Sample semantic programs generated by the enumeration process based on our language-driven navigation DSL. . . . .	99
6.8	Accuracy on the SCAN dataset. . . . .	101
7.1	Prompt formatting for MBR-EXEC sample collection. . . . .	107
7.2	MBPP example prompt and response from Codex. . . . .	111
7.3	Spider example prompt and response from Codex. . . . .	112
7.4	NL2Bash example prompt and response from Codex. . . . .	113
7.5	Comparison between MBR-EXEC and baselines without selection process. . .	114
7.6	MBR-EXEC performance on greedily decoded and sampled programs. . . .	116
8.1	Average error rate (AER) for word alignment. . . . .	130
9.1	LAS and UAS on Universal Dependencies v2.2. . . . .	143
9.2	LAS and UAS on the Universal Dependencies v2.2 development set, using different alignment methods. . . . .	147
9.3	LAS on Universal Dependencies v2.0 with multiple source languages. . . .	148



# List of Algorithms

1	Constituency parsing based on given syntactic distances. . . . .	31
2	Constituency parsing based on concreteness estimation. . . . .	32
3	Polynomial time solution to Eq. (5.3) . . . . .	62
4	The CKY-E <sup>2</sup> algorithm. . . . .	85

# Chapter 1

## Introduction

Language is highly structured. Most natural languages naturally appear with sequential structures: sentences usually consist of a sequence of words; phrase structures are considered fundamental to natural languages for the ability of humans to handle nonadjacent and hierarchical dependencies between words (Chomsky, 1957, *inter alia*); over the past decades, multiple other syntactic and semantic structure formalisms have been proposed and studied (Tesnière, 1959; Joshi et al., 1975; Steedman, 2000, *inter alia*).

On the other hand, humans learn and use these language structures naturally and implicitly—through communication and interaction with others, humans develop the ability to understand and produce grammatical sentences to describe objects and scenarios in the world. Explicitly annotated structures, however, are almost never shown to humans during the learning process.

In this dissertation, we consider the following types of language structures as our representative targets of learning:

- **Phrase structures.** Phrase structures are fundamental to natural languages for the human ability to handle nonadjacent and hierarchical dependencies between words (Chomsky, 1957, *inter alia*). In this dissertation, we specifically consider the problem of learning phrase structures from parallel vision.
- **Dependency structures.** Dependency structures (Tesnière, 1959) are another syntactic structure widely used in NLP. Unlike phrase structures, dependency structures allow more flexibility by directly modeling word relationships. In this dissertation, we consider learning dependency structures through cross-lingual grounding signals,

where we start with a well-trained dependency parser in a high-resource language and use bitext to guide the learning process in low-resource languages.

- **Combinatory categorial grammar (CCG).** Beyond syntax, CCG provides a joint syntactic and semantic formalism for natural language. As a phrase-structure grammar,<sup>1</sup> CCG additionally provides a type-driven compositionality mechanism for semantic representation and composition. We consider the problem of learning CCG from parallel vision and execution results of the induced programs.
- **Executable programs.** We consider executable programs as semantic structures of corresponding natural language utterances, where executing them with optionally world knowledge as the input grounds the abstract sentences into the real world. To this end, we investigate the problem of execution-informed semantic parsing, which converts natural language to executable programs without explicit supervision.

Enabling machine learning of language structures resembling human-like learning holds both theoretical and practical potential. From a theoretical perspective, learning language structures without explicit supervision can benefit the study of syntax acquisition by providing evidence supporting or challenging the poverty of the stimulus hypothesis (Piattelli-Palmarini, 1980). From a practical perspective, language structures learned without explicit supervision can affordably enhance the compositional generalization ability of text processing systems to out-of-distribution data (Havrylov et al., 2019; Mao et al., 2021, *inter alia*), which provides an alternative to the traditional supervised learning paradigm that requires large-scale human annotations. Automatic learning and prediction of language structures can also benefit a wide range of natural language processing (NLP) applications, such as linguistics research, second language instruction, and program synthesis from natural language commands.

This dissertation addresses the challenges of learning language structures through grounding, from syntax to semantics. We are interested in exploring the potential of grounding signals that are naturally parallel to natural languages as a source of indirect supervision. We focus on using grounding signals in the real world, which typically require less human effort than those needed for supervised learning. In addition to providing

---

<sup>1</sup>We acknowledge that there are different conventions in defining phrase-structure grammar. For example, Jurafsky and Martin (2000) use the term *phrase-structure grammar* interchangeably with *context-free grammar*, which excludes CCG. Here, we use the term *phrase-structure grammar* to refer to a grammar that models the hierarchical phrase structures, in contrast to dependency grammar.

richer information about surrounding environments, these grounding signals enable more significant potential in real-world applications by offering a more comprehensive model of the environments where humans live. Specifically, we investigate several representative types of grounding signals, including:

- **Parallel vision.** Captions are often paired with images that share the same or similar meanings in a different modality. Thus, we can consider using visual information to supervise the learning of language structures.
- **Execution results of programs.** For natural language sentences with associated executable programs, we may execute the programs and use the execution results to guide the learning process of language structures. Given an optional input, a program can be executed with appropriate interpreters. The output, i.e., the execution results, can be considered a source of grounding signal.
- **Parallel sentences in other languages (bibtex).** There are around 7,000 languages all over the world. Sentences in different languages often have parallel ones with similar meanings in other languages. Once we have a reliable understanding of sentences in one language, we can use parallel sentences as grounding signals to improve or even enable understanding of other languages.

## 1.1 Dissertation Structure and Contribution Summary

This dissertation consists of three parts, exploring the potential of grounding in learning both syntactic and semantic structures of natural language. Before delving into the details of each part, we first provide a brief overview of the background by introducing the involved language structures and evaluation metrics for the learning systems and offering an extended definition of grounding (Chapter 2). Work in this dissertation can be formulated as learning language structures through grounding, where all work involved in this dissertation is based on the assumption that grounding signals provide indirect but useful supervision for learning language structures. We provide a different learning scheme to instantiate the general framework in each part.

In Part I, we discuss learning syntactic structures through visual grounding. We introduce the task of visually grounded grammar induction, which we use as a testbed to investigate the potential of grounding signals in learning syntactic structures. We present

VG-NSL (Chapter 3), a neural model that learns to parse sentences into its constituency parse structures by grounding them to corresponding visual scenes. Experiments show that VG-NSL can induce phrase structures from parallel vision, outperforming existing text-only grammar induction methods, and can be extended to multiple languages. We extend VG-NSL to induce syntactic structures from visually grounded speech (Chapter 4), and show that the model can induce meaningful phrase structures by breaking down an utterance into a few constituent-like segments. Along this line, we propose a new evaluation metric for speech constituency parsing (Chapter 5), to enable the evaluation of speech parsing models in the absence of ground-truth transcriptions or an automatic speech recognition system. This evaluation metric can be naturally extended to evaluate text constituency parsing, providing an additional perspective to the existing evaluation metrics, such as PARSEVAL (Black et al., 1991).

In Part II, we consider learning semantic structures through grounding with program execution. We first extend the task of syntax induction (Chapters 3 and 4) to joint syntax and semantics induction through joint visual grounding and program execution (Chapter 6). We show that the theoretically motivated model enables nearly perfect compositional generalization to unseen sentences and scenes, with mild assumptions on inductive biases and domain knowledge. Considering general-purpose semantic parsing that converts natural language utterances to executable programs, we ground the pre-trained language models to the real world by executing the induced programs and propose a new decoding method to improve the execution accuracy of output programs (i.e., semantic parses of sentences; Chapter 7). For the first time, we show that few-shot (e.g., fifteen examples) translation from natural language to executable programs can achieve the performance of supervised methods, which require thousands of annotated training examples.

In Part III, we investigate the potential of cross-lingual grounding signals in learning dependency parsing structures, another representative formalism of syntactic parsing. We first propose a lightweight method to extract cross-lingual word alignment, which may also be considered a type of language structure, from pre-trained contextualized language models (Chapter 8). Our system achieves state-of-the-art performance across languages without accessing parallel sentences usually used in previous work. We then propose a method to learn zero-shot cross-lingual dependency syntax by grounding it to a supervised parser trained on another language (Chapter 9). We demonstrate that our method efficiently preserves and transfers structural knowledge learned in the

source-language (i.e., ground) parsing system to the target language, achieving a new state-of-the-art performance in zero-shot cross-lingual dependency parsing.

Finally, we conclude the dissertation by discussing the contributions of each part and the potential future directions beyond learning language structures through grounding (Chapter 10).

## 1.2 A Quick Guide to Readers

This dissertation may be particularly interesting to readers interested in one or more of the following topics in natural language processing and computational linguistics: machine language acquisition and grounded language learning, syntactic and semantic parsing, program synthesis, lexical semantics, and cross-lingual NLP. Additionally, the evaluation metric proposed in Chapter 5 may be interesting to readers looking for a problem that can be solved in polynomial time with tree-based dynamic programming algorithms. We list the following topics and the relevant chapters in which they are discussed:

- Grounding: §2.2.
- Modeling language acquisition: Chapters 3, 4 and 6.
- Algorithms for structured prediction: Chapters 5, 6 and 9.
- Syntactic parsing: Chapters 3 to 6 and 9.
- Semantic parsing: Chapters 6 and 7.
- Cross-modal NLP: Chapters 3, 4 and 6.
- Cross-lingual NLP: Chapters 8 and 9.

We encourage readers familiar with each piece of work to read the corresponding discussions, i.e., the last section of each chapter. In these discussions, we provide a more comprehensive analysis, placing the work within the broader context of the field as of the year 2024 and suggesting potential directions for future research.

# Chapter 2

## Background

This chapter provides background information on the topics relevant to the work presented in this dissertation, including different types of language structures and grounding signals. In §2.1, we provide background knowledge on syntax (§§ 2.1.1 and 2.1.2), semantics (§2.1.3), and cross-lingual word alignment (§2.1.4) as language structures. For more details, we recommend readers refer to the textbooks on NLP, e.g., Jurafsky and Martin (2000). In §2.2, we discuss the concept of *grounding* in this dissertation. Our definition slightly extends the one given by Harnad (1990), and arguably covers the notion of *grounding* in natural language processing, (computational) linguistics, robotics, and cognitive sciences. In this dissertation, vision, program execution results, and cross-lingual supervision are considered representative types of grounding signals.

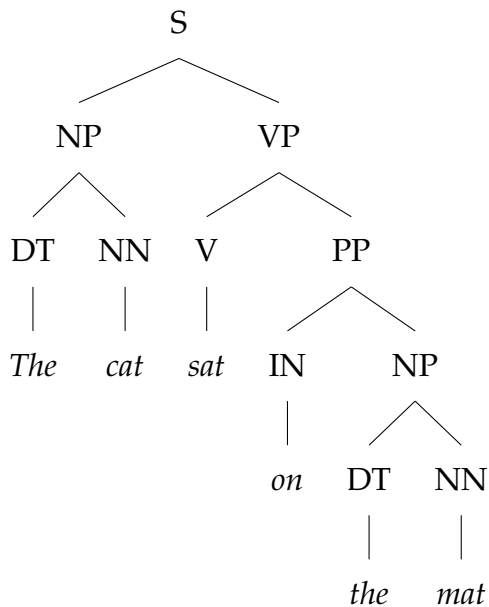
### 2.1 Language Structures

#### 2.1.1 Phrase Structures and Phrase-Structure Grammars

A group of words is considered as a *constituent*,<sup>1</sup> or a *phrase*, if it behaves as a single unit in a sentence. A *constituency parse tree* represents the hierarchical phrase structure of a sentence

---

<sup>1</sup>For simplicity in this dissertation, we only consider continuous constituents formed by consecutive words in a sentence—while this case covers most of the constituents in English declarative sentences, it is worth noting that there exist discontinuous constituents, which typically appear in English interrogative sentences, or even declarative sentences in other languages with more flexible word orders (e.g., German and Czech).



Symbol	Description
<i>Non-terminal symbols</i>	
S	Sentence
NP	Noun Phrase
VP	Verb Phrase
PP	Prepositional Phrase
<i>Pre-terminal symbols</i>	
DT	Determiner
NN	Noun
V	Verb
IN	Preposition

Figure 2.1: The constituency parse tree of the sentence “The cat sat on the mat”.

by recursively breaking down the sentence into constituents. For example, the sentence “The cat sat on the mat” can be parsed into a constituency parse tree in Figure 2.1. In this tree, the sentence (represented by the symbol S) is divided into a noun phrase (NP) and a verb phrase (VP), and the phrases are further divided into smaller constituents until the leaves are reached. The symbols in the tree can be classified into two categories: non-terminal symbols (e.g., S, NP, VP, and PP), which usually represent multi-word phrases in an NLP context, and pre-terminal symbols (e.g., DT, NN, V, and IN), which usually represents word categories (or more specifically, part-of-speech tags).

Constituency parse trees can be generated with *phrase-structure grammars*, which specifies a set of rules that describe how non-terminal symbols can be rewritten into sequences of terminal and non-terminal symbols. A representative formalism for phrase-structure grammar is *context-free grammar* (CFG), which consists of a set of production rules that



specify how non-terminal symbols can be rewritten into sequences of terminal and non-terminal symbols, and the rewriting process of one non-terminal symbol is independent of the context. For example, the CFG that generates the constituency parse tree in Figure 2.1 can be defined as follows:

$$\begin{aligned}S &\rightarrow \text{NP VP} \\ \text{NP} &\rightarrow \text{DT NN} \\ \text{VP} &\rightarrow \text{V PP} \\ \text{PP} &\rightarrow \text{IN NP}\end{aligned}$$

with additional lexical rules that rewrite the pre-terminal symbols into terminal symbols (i.e., words in this case).

In the past few decades, the task of supervised constituency parsing has been widely studied in NLP, and various methods have been proposed to predict constituency parse trees from sentences (Collins and Koo, 2005; Charniak and Johnson, 2005; McClosky et al., 2006, *inter alia*). At the training stage, the model is trained to predict the manually annotated constituency parse tree, e.g., the Penn Treebank (PTB; Marcus et al., 1993), given a sentence and optionally the ground-truth part-of-speech tags. For unsupervised constituency parsing or phrase-structure induction, the task is often formulated as predicting the constituency parse trees, given from a set of sentences without parse tree annotations (Klein and Manning, 2002, *inter alia*)—the model will induce the phrase structures from statistical patterns in the sentences and the inductive biases specified for the model.

Standard metrics exist for evaluating the quality of constituency parse trees by comparing the predicted parse tree with the gold parse tree. Among them, the most widely used metric is the  $F_1$  score over brackets (Black et al., 1991; Sekine and Collins, 1997), which is computed based on the precision and recall of constituents (represented by the brackets). Consider the trees presented in Figure 2.2 as an example. The predicted tree is compared with the gold tree to compute the precision, recall, and  $F_1$  score over brackets. In the evaluation process, the constituency parse trees are represented by brackets, where each bracket corresponds to the left and right boundaries (inclusive) of a constituent. In the example, there are five brackets in the gold tree and four brackets in the predicted tree. Among them, three brackets are in common, and the precision, recall, and  $F_1$  score, which

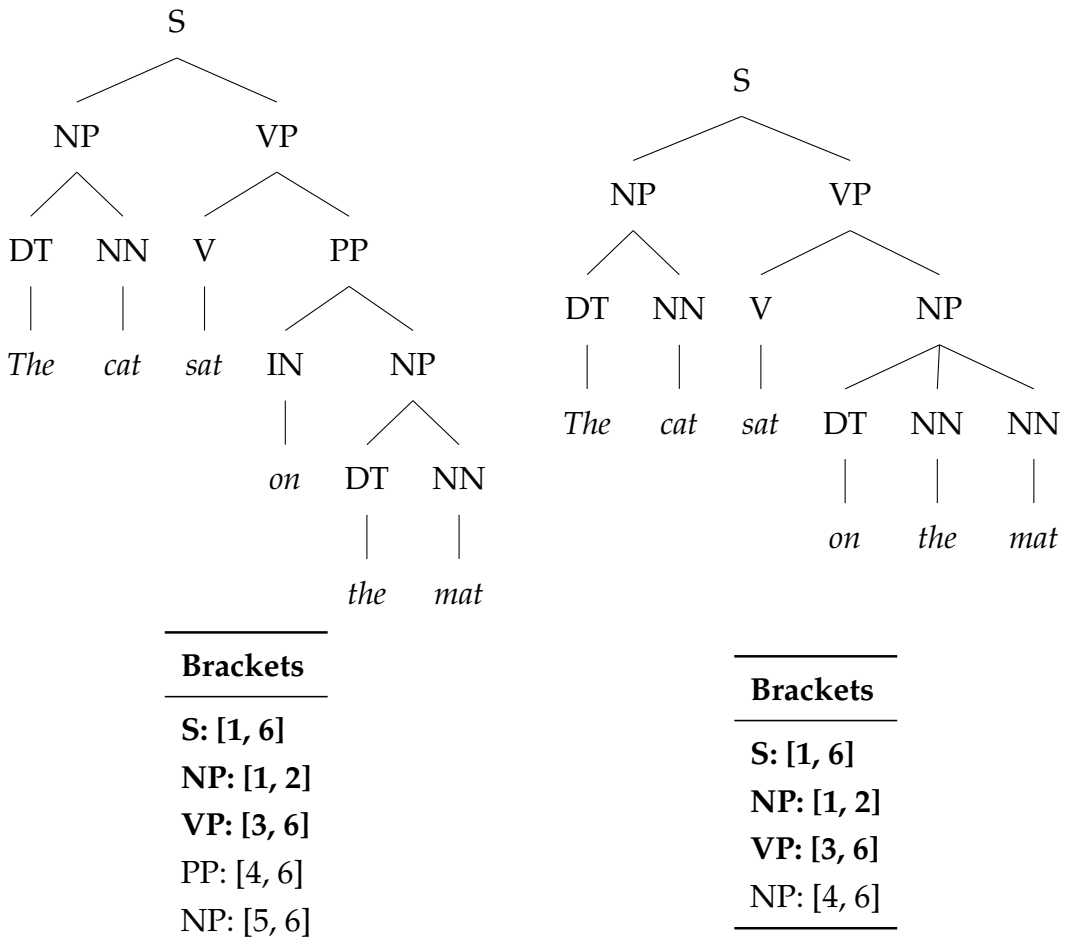
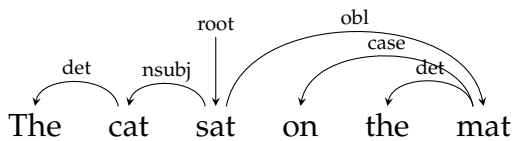


Figure 2.2: Illustration of the bracket-based  $F_1$  score. The predicted tree (right) is compared with the gold tree (left) to compute the precision, recall, and  $F_1$  score over brackets. The brackets that exist in both trees are in boldface.

is the harmonic mean between the precision and recall, are computed as follows:

$$\begin{aligned}
 \textit{Precision} &= \frac{3}{4}, \\
 \textit{Recall} &= \frac{3}{5}, \\
 F_1 &= \frac{2}{\frac{1}{\textit{Precision}} + \frac{1}{\textit{Recall}}} = \frac{2}{3}.
 \end{aligned}$$

The task of phrase-structure grammar induction (also known as unsupervised constituency parsing) aims to induce phrase-structure grammar from a set of sentences without



Relation	Description
nsubj	Nominal subject
det	Determiner
case	Case marker (e.g., preposition)
obl	Oblique nominal

Figure 2.3: The dependency parse tree of the sentence “*The cat sat on the mat*”, annotated following the Universal Dependencies (Nivre et al., 2020) scheme.

any explicit supervision. The task is often formulated as finding the best parse tree for each sentence in the training set and then inducing the grammar that generates the parse trees. Conventionally, the evaluation of phrase-structure grammar induction has been focused on comparing the unlabeled constituency parse trees, which ignore the specific labels of the non-terminal symbols; that is, all non-terminal symbols are treated as the same. Work on grammar induction presented in this dissertation (Chapters 3 and 4) also follows this convention, and the evaluation metrics are based on the unlabeled parse trees.

### 2.1.2 Dependency Syntax

In contrast to phrase-structure grammar, dependency grammar represents syntax by binary asymmetric relations between words in a sentence. A dependency parse tree represents the dependency relations between words in a sentence, where each word is a node in the tree, and the edges between the nodes represent the dependency relations (Tesnière, 1959). Each edge is directed from the *head* to the *dependent*, and the head of an entire sentence is denoted a special root node. According to the definition of a tree, each node has exactly one incoming edge (connecting itself as the dependent to its head) except for the root node, and there is a unique path from the root node to any other node in the tree. As an example, the dependency parse tree of the sentence “*The cat sat on the mat*” is shown in Figure 2.3.

In supervised dependency parsing (McDonald, 2006; Nivre, 2004, 2008, *inter alia*), the task is to predict the dependency parse tree of a sentence given the sentence and, optionally, the ground-truth part-of-speech tags. The predicted parse tree is evaluated by comparing it with the ground-truth parse tree, and the evaluation metrics include the labeled attachment score (LAS) and the unlabeled attachment score (UAS). The LAS is the percentage of words

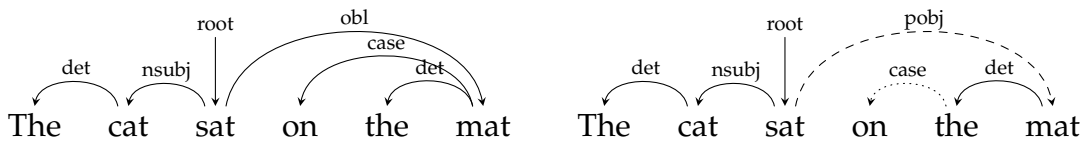


Figure 2.4: Illustration of how LAS and UAS work as dependency parsing metrics. The predicted tree (right) is compared with the gold tree (left) to compute the LAS and UAS. The edges in the predicted tree that LAS considers mismatched are dashed, whereas those by UAS (and, therefore, also LAS) are dotted.

in the sentence assigned with both the correct head and correct dependency relation, and the UAS is the percentage of words in the sentence assigned the correct head regardless of the dependency relation. Consider the trees presented in Figure 2.3 as an example. The predicted tree is compared with the gold tree to compute the LAS and UAS. There are six words (and, therefore, six edges). The predicted tree has four correct edges, one edge with the correct head and dependent but an incorrect label (*sat* to *mat*), and one edge with incorrect head (*the* to *on*), resulting in the LAS of  $\frac{4}{6}$  and the UAS of  $\frac{5}{6}$ .

### 2.1.3 Executable Programs as Semantics

#### Programs

In this dissertation, we follow existing work in NLP (Zelle and Mooney, 1996; Zettlemoyer and Collins, 2005; Liang et al., 2013, *inter alia*) to consider the task of semantic parsing as translating natural language utterances into logical forms. In addition, an executable program (e.g., a Python program) can be considered as a logical form in a relaxed sense, and we can therefore use the execution results to evaluate program semantics. For example, let  $u_i$  denote a natural-language utterance and  $p_i$  denote its paired ground-truth Python program. Suppose we have a test set of  $N$  pairs of utterances and ground-truth programs  $\{(u_1, p_1), \dots, (u_N, p_N)\}$ . The execution accuracy of predicted programs  $P' = \{p'_i\}$  is defined as the percentage of the programs that are executed correctly, i.e., the outputs of the program match the expected ones:

$$\text{Execution Accuracy}(P') = \frac{1}{N} \sum_{i=1}^N \mathbb{1} [\text{Execute}(p'_i) = \text{Execute}(p_i)],$$

where  $\mathbb{1}[\cdot]$  is the indicator function that returns 1 if the condition is true and 0 otherwise, and the function  $Execute(\cdot)$  maps a program to its execution results. For simplicity, we assume that the execution results are deterministic and can be represented as a string to support the comparison. Practically, some programs require input arguments to execute, and we synthesize a few input cases so that we can approximate the program semantics by comparing the execution results on specific input cases (see more discussions in Chapter 7). In addition, since some programs may not terminate, we empirically set a timeout threshold for the execution of each program and consider programs that exceed the threshold to have a different execution result from any other programs.

## Combinatory Categorical Grammars

Linguists have presented joint formalism of syntax and semantics. This dissertation considers the combinatory categorical grammars (CCGs; Steedman, 2000) as a representative formalism that combines syntax and semantics. Each word token in a sentence is associated with a syntactic category and a semantic program—the syntactic category here can be viewed as the function signature in a programming language, and the semantic program corresponds to the function implementation.<sup>2</sup>

For illustrative purposes, we provide the CCG derivation of the sentence “*A cat drinks milk*” in Figure 2.5. Each lexical entry is associated with a syntactic category (e.g.,  $NP$  and  $(S \setminus NP)/NP$ ) and a semantic program (represented by lambda calculus), and the derivation process combines the categories and programs of the words in the sentence to derive the final semantic program of the sentence. At each step, the derivation process applies a rule that combines the categories and programs of two adjacent words to derive a new category and program. The operators  $/$  and  $\setminus$  denote the forward and backward application, respectively—taking forward application as an example, the category  $X/Y$  expects an argument of category  $Y$  at the right side, and the category  $Y$  is combined with the category  $X/Y$  to derive a new category  $X$ . Note that the syntactic categories are not necessarily the same as the part-of-speech tags, and the semantic programs can be instantiated in executable programs. As a comprehensive example, we offer a detailed introduction of the instantiation of CCG we used in this dissertation in Chapter 6. In this work, we

---

<sup>2</sup>Generally, different word tokens with the same word type may be associated with different syntactic categories and semantic programs. A representative example is the word *word*, which can be a noun or a verb in different contexts.

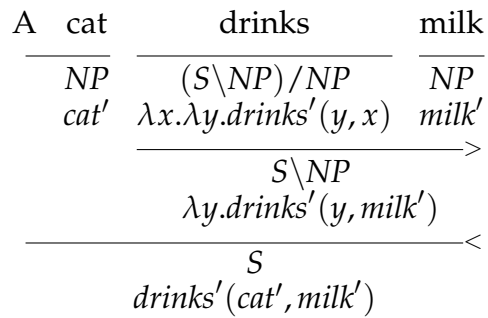


Figure 2.5: An example of a CCG derivation for the sentence “A cat drinks milk.” > and < denote forward and backward application, respectively.

consider the execution accuracy of the finally derived function (in the Figure 2.5 example,  $drinks'(cat', milk')$ ) as the primary evaluation metric.

### 2.1.4 Cross-Lingual Word Alignment

The final language structure considered in this dissertation is cross-lingual word alignment, which aims to align words in a sentence in one language to words in a sentence in another language. The alignment is typically represented as a set of word pairs, where each pair consists of a word in the source language and a word in the target language. Such word alignment is often used as a preprocessing step for various cross-lingual tasks, especially for statistical machine translation (Berger et al., 1994, *inter alia*). In addition to being a type of language structure, cross-lingual word alignment plays an important role in transferring knowledge from one language to another, and can therefore facilitate cross-lingual grounding (which we will discuss later in Chapter 9). As an example, Figure 2.6a shows the word alignment between the English sentence “Thank you” and German sentence “Danke.”

The annotations of word alignment pairs can be categorized into two types: required alignment and optional alignment. The required alignment is the word pairs that a word alignment model must align —the model will be penalized if it fails to align these pairs. In contrast, the optional alignment is the word pairs that the model may align, but the model is not penalized whether it aligns this pair or not. In addition, the model will also be penalized if it aligns the word pairs that are not in the ground-truth annotation as either a required or an optional alignment.

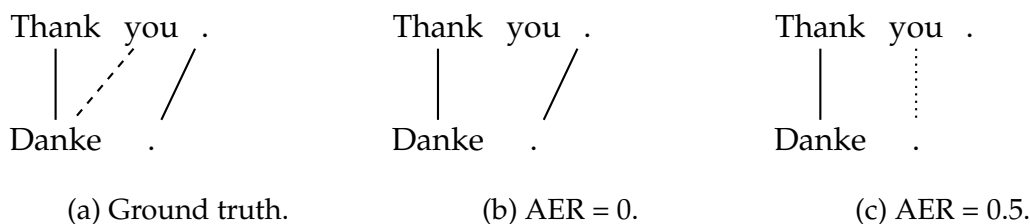


Figure 2.6: Example of cross-lingual word alignment between English and German. Solid line: required alignment; dashed line: optional alignment; dotted line: predicted alignment that does not exist in the ground truth.

	Language Structure	Evaluation Metric
(Chapter 3)	Constituency syntax	Bracket $F_1$
(Chapter 4)	Constituency syntax over spoken words	Bracket $F_1$ , Chapter 5
(Chapter 6)	Combinatory categorial grammars	Execution accuracy
(Chapter 7)	Python programs	Execution accuracy
(Chapter 8)	Word alignment	Alignment error rate
(Chapter 9)	Dependency syntax	LAS, UAS

Table 2.1: Language structures considered in this dissertation and the corresponding primary evaluation metrics.

The evaluation metric for cross-lingual word alignment is the alignment error rate, which is computed as follows. Let  $P = \{(s_i, t_i)\}$  denote the set of predicted alignment pairs,  $R$  denote the required alignment pairs (solid lines in Figure 2.6), and  $A$  denote the union of the required and optional alignments (both solid and dashed lines in Figure 2.6). The alignment error rate (AER) is defined by

$$AER = 1 - \frac{|P \cap A| + |P \cap R|}{|P| + |R|}.$$

Table 2.1 summarizes the language structures considered in this dissertation, along with the corresponding evaluation metrics.

## 2.2 Grounding

The symbol grounding problem (Harnad, 1990) presents a fundamental issue in the areas of artificial intelligence and cognitive sciences, which concerns how “*the semantic interpretation of a formal symbol system be made intrinsic to the system, rather than just parasitic on the meanings in our heads,*” and how “*the meanings of the meaningless symbol tokens, manipulated solely on the basis of their (arbitrary) shapes, be grounded in anything but other meaningless symbols.*” That is, the symbols in the system should be linked to meanings in the real world.<sup>3</sup> However, there are discrepancies in the definition of *grounding* under different contexts (Chai et al., 2018; Mollo and Millière, 2023). In addition to the high-level concept of interpreting symbols in the real world, grounding can be interpreted differently in various scenarios, including but not necessarily limited to the following NLP-centric ones,<sup>4</sup> where some of them are indeed instantiations of the high-level definition by Harnad (1990):

- **Scenario 1** (NLP and robotics): The process that links symbols (e.g., written words) and sequences of symbols (e.g., written sentences) to real-world entities and scenarios, represented by sensory signals, such as image (Plummer et al., 2015, *inter alia*) and audio (Settle et al., 2019, *inter alia*). While this definition follows the high-level concept of grounding, it is debatable whether all sensory signals represent meanings in an acceptable sense—for example, the spoken language is often considered a symbol system that lacks meanings; therefore, acoustically grounded word embeddings (Settle et al., 2019) do not ground the symbol system represented by words to their meanings. Similarly, it depends on the specific visual content to determine whether the visual signals represent meanings—for example, it is arguable that pictures of written text do not represent meanings in the same way as pictures of objects do.
- **Scenario 2** (NLP and computational linguistics): The process of linking entities in natural language to an existing knowledge base, which is also referred to as the entity linking task (Bunescu and Paşca, 2006, *inter alia*). This definition can be considered as an instantiation or extension of the symbol grounding problem in the context of

---

<sup>3</sup>We acknowledge that *meanings in the real world* is a vague description, and the definition of *meaning* can vary drastically depending on the context.

<sup>4</sup>Mollo and Millière (2023) have offered a comprehensive discussion from a more philosophical perspective. Roughly speaking, our Scenario 1 corresponds to their *referential grounding* and *sensorimotor grounding*, Scenario 2 corresponds to their *relational grounding* and *epistemic grounding*, and Scenario 3 corresponds to their *communicative grounding*.



NLP, with additional supervision (e.g., annotated links) being considered to train the machine processing systems.

- **Scenario 3** (NLP, pragmatics, and cognitive sciences): The common ground shared by the speaker and listener in a conversation in order to collaboratively communicate (Grice, 1975; Levinson, 1983; Clark and Brennan, 1991, *inter alia*). In NLP, this definition is often considered in the domain of dialogue systems (Zhou et al., 2018, *inter alia*)—the system should be able to share a common ground with the users to generate appropriate natural language utterances in contexts. This definition arguably contradicts the one offered by Harnad (1990) in a narrow and literal sense, as it does not necessarily require the symbols to be linked to meanings in the real world; instead, the interpretation of the utterances are left to the speaker and listener.

The discussion on the above scenarios is extended from the taxonomy offered by Chai et al. (2018), where they consider the term grounding in two senses: *semantic grounding* (Scenario 2, and part of Scenario 1) and *communicative grounding* (Scenario 3). For a detailed discussion covering more recent related work on language grounding, we recommend readers refer to the survey by Bisk et al. (2020). For a comprehensive discussion of recent work in NLP from a common-ground-centric view (i.e., Scenario 3 above), we recommend the survey by Chandu et al. (2021).

In this dissertation, we downplay the philosophical aspects of grounding and its connection with meanings, and give an extended definition of grounding from an arguably more natural perspective in machine learning. We consider grounding as a process that connects data from one source  $\mathcal{X}$  (analogous to language, as a symbol system in the definition by Harnad) to another source  $\mathcal{Y}$  (i.e., the ground, analogous to the real world), where we require:

1.  $\mathcal{X}$  is the primary source of data, and  $\mathcal{Y}$  provides information that can be helpful on the task associated with  $\mathcal{X}$ . At the inference phase,  $\mathcal{X}$  is the required input data to the trained model, and whether to involve  $\mathcal{Y}$  as an additional data source during inference can be optional.
2.  $\mathcal{X}$  and  $\mathcal{Y}$  have shared information (so that we can find meaningful correspondence between them).

In the following discussion, we will call  $\mathcal{X}$  the *primary data source* and  $\mathcal{Y}$  the *ground*. We will refer to the specific data used to represent  $\mathcal{Y}$  as the *grounding signals*.

We assume that the data from  $\mathcal{X}$  and  $\mathcal{Y}$  are sampled in a paired manner from the underlying joint distribution  $p(x, y)$ . In information theoretic terms, Condition 2 above can be expressed as

$$I(X; Y) = \mathbb{E}_{x, y \sim p(x, y)} \log \left( \frac{p(x, y)}{p(x)p(y)} \right) > 0,$$

where  $I(X; Y)$  denotes the mutual information between  $X$  and  $Y$ , which can be derived from the joint distribution  $p(x, y)$ .

In real-world applications, different data sources usually carry non-identical information and noise; therefore, the conditional entropy  $H(Y | X) = \mathbb{E}_{x, y \sim p(x, y)} \log p(x, y) - \log p(x)$  is almost always positive; that is, the ground  $\mathcal{Y}$  almost always contains additional information compared to what can be inferred from the primary data source  $\mathcal{X}$ . However, we do not require the conditional entropy  $H(Y | X)$  to be strictly positive in this dissertation. Consider the following synthetic data, where the primary data source gives written words *triangle* and *square*, and the ground gives only one corresponding shape of the same size for each word in visual signals. Such a setting arguably does not tell us much about the rules for recognizing triangles and squares—since there is only one visual shape presented for one word, there is no way to enable generalizability of the recognition without any built-in inductive bias—and the conditional entropy  $H(Y | X)$  is zero, but having  $\mathcal{Y}$  may still be better than nothing for recognizing the visual shape from the written words. In such cases, inductive biases associated with models, such as the localization bias introduced by the convolutional neural networks (LeCun et al., 1998), can be combined with the ground to help the specific task associated with the primary data source  $\mathcal{X}$ .

The core difference between the definition of grounding in this dissertation and most existing literature is whether to emphasize the roles of forms and meanings. In most existing literature, the term grounding is either explicitly or implicitly connected with linking *symbolic forms* to their *meanings*, where the symbolic forms considered are usually language. While our definition is compatible with this view, we do not require the ground to be meanings—in this dissertation, any additional data source that can be used for a specific task with primary data source  $\mathcal{X}$  can be considered as the ground, regardless of whether it is related to meanings or not. Similarly, the form of the source data  $\mathcal{X}$  may be extended beyond symbol systems—as an example, performing image segmentation with supervision solely from parallel text (Xu et al., 2022, *inter alia*) can be considered as a grounding process, where the primary data source is visual data and the textual data

	<b>Data Source <math>\mathcal{X}</math></b>	<b>Ground <math>\mathcal{Y}</math></b>
<i>Harnad</i>	Symbol system	Real-world meanings
<i>Scenario 1</i>	Natural language (text)	Sensory data
<i>Scenario 2</i>	Natural language (text)	Knowledge base
<i>Scenario 3</i>	Natural language	Shared common ground
<i>Chapter 3</i>	Natural language (text)	Vision
<i>Chapter 4</i>	Natural language (speech)	Vision
<i>Chapter 6</i>	Natural language (text)	Vision and/or program execution results
<i>Chapter 7</i>	Natural language (text)	Program execution results
<i>Chapter 8</i>	Natural language (text)	Natural language (text in another language)
<i>Chapter 9</i>	Natural language (text)	Natural language (text in another language)

Table 2.2: The primary data source and ground in various scenarios. The top section discusses the scenarios mentioned above in this section (§2.2), and the bottom section discusses the grounding settings considered in individual chapters of this dissertation.

serve as the ground.

The term grounding also differs from a few related machine learning terms. Compared to multi-view machine learning, such as canonical correlation analysis (CCA; Hotelling, 1936), the grounding process distinguishes the primary data source and the ground rather than treating them as two equally important views of the same data. The transfer learning (Bozinovski and Fulgosi, 1976) schema can also be considered as a special case of grounding, where the ground is the source domain and the primary data source is the target domain—work presented in Chapter 9 can also be considered as a transfer learning technique. However, transfer learning uses the same model architecture for the source and target domains, which is not required by grounding.

Table 2.2 analyzes the primary data source and the ground in the grounding settings considered in the above scenarios and individual chapters of this dissertation. Since this dissertation focuses on learning language structures, the primary data source is natural language in different forms, including text and speech. In contrast, we consider various data sources as the ground, including vision, program execution results, and other languages.

## **Part I**

# **Learning to Parse through Cross-Modal Grounding**

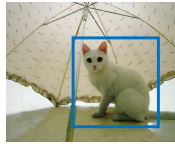
## Chapter 3

# Syntax Acquisition from Visually Grounded Text

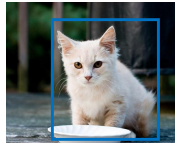
*Content in this chapter has been published as a conference paper at ACL 2019 (Shi et al., 2019). Jiayuan Mao has contributed significantly to this work.*

Consider images paired with descriptive texts (i.e., captions) in English (Figure 3.1). Given sufficiently many such pairs and no prior knowledge of English, one can infer the correspondence between certain words and visual attributes (e.g., recognizing that “a cat” refers to the objects in the blue boxes). Additionally, one can assume that visually concrete spans of words should be processed as a whole and thus form constituents in the sentence. Such a process can happen for noun phrases, verb phrases, and prepositional phrases. This intuition motivates using image-text pairs to facilitate automated language learning, including syntax and semantics. Specifically, in this chapter, we focus on learning syntactic structures, where we propose the Visually Grounded Neural Syntax Learner (VG-NSL; Figure 3.2).

VG-NSL acquires syntax in the form of phrase structures by looking at images and reading captions. The VG-NSL model consists of two modules: a textual module for inferring structures and representations for captions, and a visual-semantic module for matching constituents with images. At a high level, VG-NSL builds latent constituency trees of word sequences and recursively composes representations for constituents. Next, it matches the visual and textual representations. The training procedure is built on the hypothesis that a better syntactic structure contributes to a better representation of constituents, leading to better alignment between vision and language. We use no human-



A cat is sitting under an umbrella.  
There is an umbrella and a cat.  
A cat is standing under a white parasol.



A cat is standing by a bowl.  
A cat is sitting on the ground.  
There is a cat looking at you.

Figure 3.1: Illustration of visual correspondence of phrases. We propose to use image-caption pairs to extract constituents from text based on the assumption that similar textual spans (in blue) should be matched to similar visual objects (in blue boxes), and these concrete spans form constituents. Best viewed in color.

labeled constituency trees or other syntactic labeling (such as part-of-speech tags). Instead, we define a *concreteness* score of constituents based on their matching with images and use it to guide the parsing of sentences. At the test time, no images paired with the text are needed.

In our experiments, we compare VG-NSL with prior approaches to unsupervised constituency parsing, most of which do not use visual grounding. Our main findings are listed as follows:

1. VG-NSL improves over the best previous text-only approaches to unsupervised constituency parsing in terms of  $F_1$  scores with gold parse trees.
2. While many existing approaches are quite unstable to the choice of random initialization, VG-NSL exhibits consistent parsing results across multiple training runs.
3. Through analysis of the performance of different models on different types of constituents, we find that VG-NSL shows substantial improvement in noun phrases and prepositional phrases, which are common in image captions.
4. VG-NSL is more data-efficient than prior text-only grammar induction models and achieves comparable performance using only 20% of the training captions.
5. The *concreteness* score, which emerges during the matching between constituents and images, correlates well with a similar measure defined by linguists.

In addition, VG-NSL can be easily extended to multiple languages, which we evaluate on the Multi30K dataset (Elliott et al., 2016, 2017) consisting of German and French image

captions.

### 3.1 Related Work

**Phrase-structure grammar induction from text.** Recent work has proposed several approaches for inducing latent phrase structures (Choi et al., 2018; Yogatama et al., 2017; Maillard and Clark, 2018, *inter alia*) from the distant supervision of downstream tasks. However, many of the methods are not able to produce linguistically sound structures, or even consistent ones with fixed data and hyperparameters but different random initialization (Williams et al., 2018).

A related line of research is to induce latent syntactic structure via language modeling. This approach has achieved remarkable performance on unsupervised constituency parsing (Shen et al., 2018, 2019), especially in identifying the boundaries of higher-level (i.e., larger) constituents. To our knowledge, the Parsing-Reading-Predict Network (PRPN; Shen et al., 2018) and the Ordered Neuron LSTM (ON-LSTM; Shen et al., 2019) currently produce the best fully unsupervised constituency parsing results. One issue with PRPN, however, is that it tends to produce meaningless parses for lower-level (smaller) constituents (Htut et al., 2018).

Over the last two decades, there has been extensive study targeting unsupervised constituency parsing (Klein and Manning, 2002, 2004, 2005; Bod, 2006; Ponvert et al., 2011) and dependency parsing (Klein and Manning, 2004; Smith and Eisner, 2006; Spitkovsky et al., 2010; Han et al., 2017). However, all of these approaches are based on linguistic annotations. Specifically, they operate on the part-of-speech tags of words instead of word tokens. One exception is Spitkovsky et al. (2011), which produces dependency parse trees based on automatically induced pseudo tags.

**Grounded language acquisition.** Grounded language acquisition has been studied for image-caption data (Christie et al., 2016), video-caption data (Siddharth et al., 2014; Yu et al., 2015), and visual reasoning (Mao et al., 2019). However, existing approaches rely on human labels or rules for classifying visual attributes or actions. Instead, our model induces syntax structures with no human-defined labels or rules.

Meanwhile, encoding representations into a joint visual-semantic embedding space (Ngiam et al., 2011) is a widely studied approach, and has achieved remarkable results

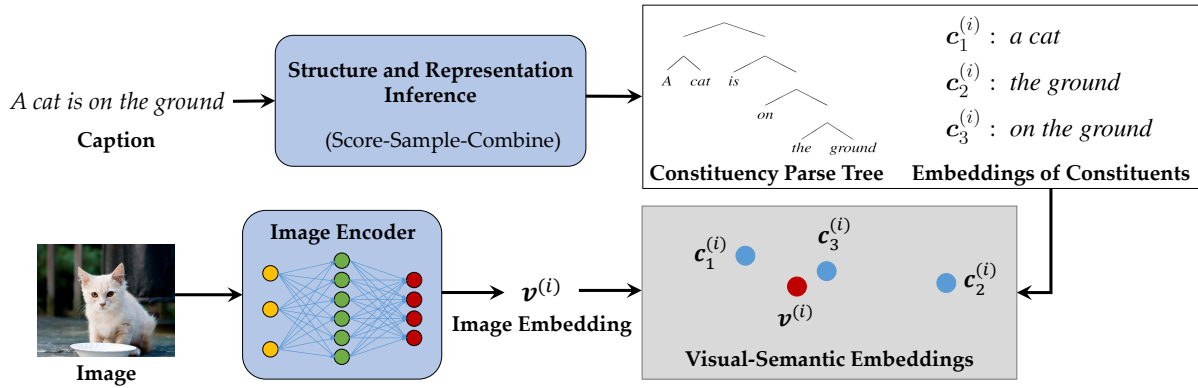


Figure 3.2: Illustration of the VG-NSL model. VG-NSL consists of two modules: a textual module for inferring structures and representations for captions, and a visual-semantic module for matching constituents with images. VG-NSL induces constituency parse trees of captions by looking at images and reading paired captions.

on image-caption retrieval (Kiros et al., 2014; Faghri et al., 2018; Shi et al., 2018), image caption generation (Kiros et al., 2014; Karpathy and Fei-Fei, 2015; Ma et al., 2015), and visual question answering (Malinowski et al., 2015). This work uses this idea to match visual and textual representations.

**Concreteness estimation.** Turney et al. (2011) define concrete words as those referring to things, events, and properties that we can perceive directly with our senses. Subsequent work has studied word-level concreteness estimation based on text (Turney et al., 2011; Hill et al., 2013), human judgments (Silberer and Lapata, 2012; Hill and Korhonen, 2014; Brysbaert et al., 2014), and multi-modal data (Hill and Korhonen, 2014; Hill et al., 2014; Kiela et al., 2014; Young et al., 2014; Hessel et al., 2018; Silberer et al., 2017). As with Hessel et al. (2018) and Kiela et al. (2014), our model uses multi-modal data to estimate concreteness. Compared with them, we define concreteness for spans instead of words and use it to induce linguistic structures.

### 3.2 The Visually Grounded Neural Syntax Learner

Given a set of paired images and captions, our goal is to learn representations and structures for words and constituents. Toward this goal, we propose the Visually Grounded Neural Syntax Learner (VG-NSL), an approach for the grounded acquisition of syntax of



natural language. VG-NSL is motivated by the idea of semantic bootstrapping (Pinker, 1984), which suggests that children acquire syntax by first understanding the meaning of words and phrases and linking them with the syntax of words.

At a high level (Figure 3.2), VG-NSL consists of two modules. First, given an input caption (i.e., a sentence or a phrase), as a sequence of tokens, VG-NSL builds a constituency parse tree, and recursively composes representations for every constituent. Next, it matches textual constituent representations with visual inputs. Both modules are jointly optimized with natural supervision: the model acquires constituency structures, composes textual representations, and links them with visual scenes, by looking at images and reading paired captions.

### 3.2.1 Textual Representations and Structures

VG-NSL starts by composing a binary constituency structure of the text, using an easy-first bottom-up parser. The composition of the tree from a caption of length  $n$  consists of  $n - 1$  steps. Let  $\mathbf{X}^{(t)} = (\mathbf{x}_1^{(t)}, \mathbf{x}_2^{(t)}, \dots, \mathbf{x}_k^{(t)})$  denote the textual representations of a sequence of constituents after step  $t$ , where  $k = n - t$ . For simplicity, we use  $\mathbf{X}^{(0)}$  to denote the *word embeddings* for all tokens (the initial representations).

At step  $t$ , a score function  $score(\cdot; \Theta)$ , parameterized by  $\Theta$ , is evaluated on all pairs of consecutive constituents, resulting in a vector  $score(\mathbf{X}^{(t-1)}; \Theta)$  of length  $n - t - 1$ :

$$score(\mathbf{X}^{(t-1)}; \Theta)_j \triangleq score([\mathbf{x}_j^{(t-1)}, \mathbf{x}_{j+1}^{(t-1)}]; \Theta).$$

We implement  $score(\cdot; \Theta)$  as a two-layer ReLU-activated feed-forward network.

A pair of constituents  $(\mathbf{x}_{j^*}^{(t-1)}, \mathbf{x}_{j^*+1}^{(t-1)})$  is sampled from all pairs of consecutive constituents, following the distribution produced by a softmax operator over the scores:<sup>1</sup>

$$p_{\Theta}(j^*) = \frac{\exp\left(score(\mathbf{X}^{(t-1)}; \Theta)_{j^*}\right)}{\sum_j \exp\left(score(\mathbf{X}^{(t-1)}; \Theta)_j\right)}.$$

The selected pair is combined to form a single new constituent, whereas the rest of the constituents are directly copied into the next step. Thus, after step  $t$ , the number of

---

<sup>1</sup> At test time, we take the argmax.

constituents is decreased by 1. The textual representation for the new constituent is defined as the L2-normalized sum of the component constituents:

$$\text{combine} \left( \mathbf{x}_{j^*}^{(t-1)}, \mathbf{x}_{j^*+1}^{(t-1)} \right) \triangleq \frac{\mathbf{x}_{j^*}^{(t-1)} + \mathbf{x}_{j^*+1}^{(t-1)}}{\left\| \mathbf{x}_{j^*}^{(t-1)} + \mathbf{x}_{j^*+1}^{(t-1)} \right\|_2}.$$

We find that using a more complex encoder for constituents, such as GRUs (Cho et al., 2014), will cause the representations to be highly biased towards a few salient words in the sentence (e.g., the encoder encodes only the word “cat” while ignoring the rest part of the caption; Shi et al., 2018; Wu et al., 2019). This significantly degrades the performance of linguistic structure induction.

We repeat the above score-sample-combine process for  $n - 1$  steps until all words in the input text have been combined into a single constituent (Figure 3.3), which denotes the ending of the inference process of the constituency parse tree. Since we combine two consecutive constituents at each time step, the derived tree  $\mathbf{t}$  contains  $2n - 1$  constituents (including  $n$  individual words as terminals and  $n - 1$  nonterminals).

### 3.2.2 Visual-Semantic Embeddings

We follow an approach similar to that of Kiros et al. (2014) to define the visual-semantic embedding (VSE) space for paired images and text constituents. Let  $\mathbf{v}^{(i)}$  denote the vector representation of an image  $i$ , and  $\mathbf{c}_j^{(i)}$  denote the vector representation of the  $j^{\text{th}}$  constituent of its corresponding text caption—during the matching with images, we ignore the tree structure and index the constituents as a list. A function  $m_\Phi(\cdot, \cdot)$  is defined as the matching score between images and texts:

$$m_\Phi(\mathbf{v}, \mathbf{c}) \triangleq \cos(\Phi \mathbf{v}, \mathbf{c}),$$

where the parameter vector  $\Phi$  aligns the visual and textual representations into a joint space.

### 3.2.3 Training

We optimize the visual-semantic representations (affected by parameters  $\Phi$  and the word embeddings) and constituency structures (affected by parameters  $\Theta$ ) iteratively. In each

**Step #6:** ((a cat) (is (sitting (on (the ground))))))

...

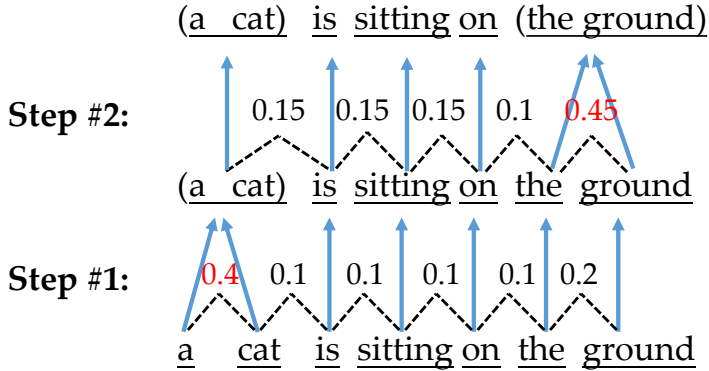


Figure 3.3: An illustration of how VG-NSL composes a constituency parse tree. At each step, the score function *score* is evaluated on all pairs of consecutive constituents (dashed lines). Next, a pair of constituents is sampled from all pairs, following a distribution computed by the softmax of all predicted scores. The selected two constituents are combined into a larger one, while the other constituents remain unchanged (solid lines). For the 7-word sentence shown in the figure, it requires 6 steps to compose the final parse tree.

iteration, given constituency parsing results of the caption,  $\Phi$  is optimized for matching the visual and the textual representations. Next, given the visual grounding of constituents,  $\Theta$  is optimized for producing constituents that can be better matched with images. Specifically, we optimize textual representations and the visual-semantic embedding space using a hinge-based triplet ranking loss:

$$\mathcal{L}(\mathcal{C}, \Phi; \mathcal{V}) = \sum_{i,k \neq i,j,\ell} \left[ m_{\Phi}(\mathbf{c}_{\ell}^{(k)}, \mathbf{v}^{(i)}) - m_{\Phi}(\mathbf{c}_j^{(i)}, \mathbf{v}^{(i)}) + \delta \right]_+ + \sum_{i,k \neq i,j} \left[ m_{\Phi}(\mathbf{c}_j^{(i)}, \mathbf{v}^{(k)}) - m_{\Phi}(\mathbf{c}_j^{(i)}, \mathbf{v}^{(i)}) + \delta \right]_+,$$

where  $i$  and  $k$  index over all image-caption pairs in the dataset, while  $j$  and  $\ell$  enumerate over all constituents of a specific caption ( $c^{(i)}$  and  $c^{(k)}$ , respectively),  $\mathcal{V} = \{\mathbf{v}^{(i)}\}$  is the set of corresponding image representations,  $\mathcal{C} = \{\mathbf{c}_j^{(i)}\}$  is the set of textual representations

of all constituents,  $\delta$  is a hyperparameter denoting a constant margin, and  $[\cdot]_+$  denotes  $\max(0, \cdot)$ . The loss  $\mathcal{L}$  extends the loss for image-caption retrieval of Kiros et al. (2014), by introducing the alignments between entire images and sub-sentence constituents. For simplicity, we use frozen image representation from a pre-trained image encoder and only optimize the textual representations  $\mathcal{C}$  and the linear transformation  $\Phi$  that projects the image representations into the joint space.

We also optimize textual structures for a better alignment between the derived constituents and the images. Intuitively, we would like adjectives to be associated (combined) with the corresponding nouns, and verbs and prepositions to be associated (combined) with the corresponding subjects and objects, respectively. Specifically, we use REINFORCE (Williams, 1992) as the gradient estimator for  $\Theta$ . Consider the parsing process of a specific caption  $c^{(i)}$ , and denote the corresponding image embedding  $\mathbf{v}^{(i)}$ . For a constituent  $\mathbf{c}_j^{(i)}$  of  $c^{(i)}$ , we define its (visual) concreteness  $concrete(\mathbf{c}_j^{(i)}; \mathcal{V}, \mathcal{C})$  as:

$$concrete(\mathbf{c}_j^{(i)}; \mathcal{V}, \mathcal{C}) = \sum_{k \neq i, p} \left[ m(\mathbf{c}_j^{(i)}, \mathbf{v}^{(i)}) - m(\mathbf{c}_p^{(k)}, \mathbf{v}^{(i)}) - \delta' \right]_+ + \sum_{k \neq i} \left[ m(\mathbf{c}_j^{(i)}, \mathbf{v}^{(i)}) - m(\mathbf{c}_j^{(i)}, \mathbf{v}^{(k)}) - \delta' \right]_+, \quad (3.1)$$

where  $\delta'$  is a fixed margin. At step  $t$ , we define the reward function for a combination of a pair of constituents  $(\mathbf{x}_q^{(t-1)}, \mathbf{x}_{q+1}^{(t-1)})$  as:

$$r(\mathbf{x}_q^{(t-1)}, \mathbf{x}_{q+1}^{(t-1)}) = concrete(\mathbf{z}, \mathbf{v}^{(i)}), \quad (3.2)$$

where  $\mathbf{z} \triangleq combine(\mathbf{x}_q^{(t-1)}, \mathbf{x}_{q+1}^{(t-1)})$ . In plain words, at each step, we encourage the model to compose a constituent that maximizes the alignment between the new constituent and the corresponding image. During training, we sample constituency parse trees of captions and reinforce each composition step using Eq. (3.2). Concretely, we update  $\Theta$  using the following gradient estimator:

$$\Theta \leftarrow \Theta + \eta \cdot \nabla_{\Theta} \sum_{i,j} p_{\Theta}(c_j^{(i)}) concrete(\mathbf{c}_j^{(i)}; \mathcal{V}, \mathcal{C}),$$

where  $\Theta$  denotes the parameters of the score function in the parser that account for the sampled constituency parse trees,  $\eta$  is the learning rate, and  $p_{\Theta}(c_j^{(i)})$  is the probability of selecting the constituent  $\mathbf{c}_j^{(i)}$  at the parsing step. At the inference stage, since we do not need to estimate the concreteness scores, no paired images of text are needed.

### 3.2.4 The Abstract-Initial Inductive Bias

English and many other Indo-European languages are usually head-initial (Baker, 2001). For example, in verb phrases or prepositional phrases, the verb (or the preposition) precedes the complements (e.g., the object of the verb). Consider the simple noun-phrase caption *a white cat on the lawn*. While the association of the adjective (*white*) can be induced from the visual grounding of phrases, whether the preposition (*on*) should be associated with *a white cat* or *the lawn* is more challenging to induce. Given an empirical observation that prepositions are less visually concrete than nouns, we impose the abstract-initial inductive bias to guide the learner to correctly associate prepositions with their complements, determiners with corresponding noun phrases, and complementizers with the corresponding relative clauses. Specifically, we discourage abstract constituents (i.e., constituents that cannot be grounded in the image) from being combined with a preceding constituent, by modifying the original reward definition (Eq. (3.2)) as:

$$r' \left( \mathbf{x}_j^{(t-1)}, \mathbf{x}_{j+1}^{(t-1)} \right) = \frac{r \left( \mathbf{x}_j^{(t-1)}, \mathbf{x}_{j+1}^{(t-1)} \right)}{\lambda \cdot \text{abstract} \left( \mathbf{x}_{j+1}^{(t-1)}; \mathcal{V}, \mathcal{C} \right) + 1}, \quad (3.3)$$

where  $\lambda$  is a scalar hyperparameter,  $\mathbf{v}^{(i)}$  is the image embedding corresponding to the caption being parsed, and *abstract* denotes the *abstractness* of the span, defined analogously to concreteness (Eq. (3.1)):

$$\begin{aligned} \text{abstract} \left( \mathbf{c}_j^{(i)}; \mathcal{V}, \mathcal{C} \right) &= \sum_{k \neq i, p} \left[ m(\mathbf{c}_p^{(k)}, \mathbf{v}^{(i)}) - m(\mathbf{c}_j^{(i)}, \mathbf{v}^{(i)}) + \delta' \right]_+ \\ &\quad + \sum_{k \neq i} \left[ m(\mathbf{c}_j^{(i)}, \mathbf{v}^{(k)}) - m(\mathbf{c}_j^{(i)}, \mathbf{v}^{(i)}) + \delta' \right]_+, \end{aligned}$$

The intuition here is that the initial heads for prepositional phrases (e.g., *on*) and relative clauses (e.g., *which*, *where*) are usually abstract words, especially in the domain of image captions. During training, we encourage the model to associate these abstract words with the succeeding constituents instead of the preceding ones. It is worth noting that such an inductive bias is language-specific, and cannot be applied to head-final languages such as Japanese (Baker, 2001). We leave the design of head-directionality inductive biases for other languages for future work.

## 3.3 Experiments

We evaluate VG-NSL for unsupervised parsing in a few ways:  $F_1$  score with gold trees, self-agreement across different choices of random initialization, performance on different types of constituents, and data efficiency. In addition, we find that the *concreteness* score acquired by VG-NSL is consistent with a similar measure defined by linguists. We focus on English for the main experiments but also extend to German and French.

### 3.3.1 Datasets and Metrics

We use the standard split of the MSCOCO dataset (Lin et al., 2014), following Karpathy and Fei-Fei (2015). It contains 82,783 images for training, 1,000 for development, and another 1,000 for testing. Each image is associated with five captions.

For the evaluation of constituency parsing, the Penn Treebank (PTB; Marcus et al., 1993) is a widely used, manually annotated dataset. However, PTB consists of sentences from abstract domains, e.g., the *Wall Street Journal* (WSJ), which are not visually grounded and whose linguistic structures can hardly be induced by VG-NSL. Here, we evaluate models on the MSCOCO test set, which is well-matched to the training domain; we leave the extension of our work to more abstract domains for future work. We apply Benepar (Kitaev and Klein, 2018),<sup>2</sup> an off-the-shelf constituency parser with state-of-the-art performance (95.52  $F_1$  score) on the WSJ test set,<sup>3</sup> to parse the captions in the MSCOCO test set as gold constituency parse trees. We evaluate all the investigated models using the  $F_1$  score compared to these gold parse trees.<sup>4</sup>

### 3.3.2 Baselines

We compare VG-NSL with various baselines for unsupervised tree structure modeling of texts, where we categorize the baselines by their training objective or supervision.

---

<sup>2</sup> <https://pypi.org/project/benepar>

<sup>3</sup> We also manually label the constituency parse trees for 50 captions randomly sampled from the MSCOCO test split, where Benepar has an  $F_1$  score of 95.65 with the manual labels. Details can be found at [https://home.ttic.edu/~freda/thesis\\_release/benepar\\_coco](https://home.ttic.edu/~freda/thesis_release/benepar_coco).

<sup>4</sup> Following convention (Black et al., 1991; Sekine and Collins, 1997), we report the  $F_1$  score across all constituents in the dataset, instead of the average of sentence-level  $F_1$  scores. Without further note, all parsing  $F_1$  scores reported in this dissertation are calculated in this way.

**Trivial tree structures.** Similarly to recent work on latent tree structures (Williams et al., 2018; Htut et al., 2018; Shi et al., 2018), we include three types of *trivial* baselines without linguistic information: random binary trees, left-branching binary trees, and right-branching binary trees.

**Syntax acquisition by language modeling and statistics.** Shen et al. (2018) propose the Parsing-Reading-Predict Network (PRPN), which predicts syntactic distances (Shen et al., 2018) between adjacent words, and composes a binary tree based on the syntactic distances to improve language modeling. The learned distances can be mapped into a binary constituency parse tree, by recursively splitting the sentence between the two consecutive words with the largest syntactic distance.

Ordered neurons (ON-LSTM; Shen et al., 2019) is a recurrent unit based on the LSTM cell (Hochreiter and Schmidhuber, 1997) that explicitly regularizes different neurons in a cell to represent short-term or long-term information. After being trained on the language modeling task, Shen et al. (2019) suggest that the gate values in ON-LSTM cells can be viewed as syntactic distances (Shen et al., 2018) between adjacent words to induce latent tree structures. We train both PRPN and ON-LSTM on all captions in the MSCOCO training set and use a fixed version of the syntactic distance method (Algorithm 1) to compose constituency parse trees.<sup>5</sup>

Motivated by the syntactic distance approaches (Shen et al., 2018, 2019), we also introduce another baseline, PMI, which uses negative pointwise mutual information between adjacent words as the syntactic distance. We compose constituency parse trees based on the distances in the same way as PRPN and ON-LSTM.

**Syntax acquisition from downstream tasks.** Choi et al. (2018) propose to compose binary constituency parse trees directly from downstream tasks using the Gumbel softmax trick Jang et al. (2017). We integrate a Gumbel tree-based caption encoder into the visual semantic embedding approach (Kiros et al., 2014), where the model is trained on the downstream task of image-caption retrieval with a hinge-based triplet ranking loss.

**Syntax acquisition from concreteness estimation.** Since we apply concreteness information to train VG-NSL, it is worth comparing against unsupervised constituency parsing

---

<sup>5</sup> As pointed out by Dyer et al. (2019), the original syntactic distance-based tree composition method (Shen et al., 2018) is biased towards right-branching trees. We fix this issue by treating the distances in all positions equally.

---

**Algorithm 1:** Constituency parsing based on given syntactic distances.

---

**Input:** text length  $m$ , list of syntactic distances  $\mathbf{d} = (d_1, d_2, \dots, d_{m-1})$ **Output:** Boundaries of constituents  $B = \{(L_i, R_i)\}_{i=1, \dots, m-1}$  $B = \text{parse}(\mathbf{d}, 1, m)$ **Function**  $\text{parse}(\mathbf{d}, \text{left}, \text{right})$ **if**  $\text{left} = \text{right}$  **then**| **return**  $\emptyset$ **end** $p = \arg \max_{j \in [\text{left}, \text{right}-1]} d_j$  $\text{boundaries} = \text{Union}(\{(\text{left}, \text{right})\}, \text{parse}(\mathbf{d}, \text{left}, p), \text{parse}(\mathbf{d}, p + 1, \text{right}))$ **return**  $\text{boundaries}$ 

---

based on previous approaches for predicting word concreteness. This set of baselines includes semi-supervised concreteness estimation (Turney et al., 2011), crowdsourced labeling (Brysbaert et al., 2014), and multimodal estimation (Hessel et al., 2018). Note that none of these approaches has been applied to unsupervised constituency parsing.

Based on the concreteness score of words, we introduce another baseline similar to VG-NSL (Algorithm 2). Specifically, at each step, we combine two consecutive constituents with the largest average concreteness and use the average concreteness as the score for the composed constituent. The algorithm generates binary constituency parse trees of captions. For a fair comparison, we implement a variant of this algorithm that also adopts the abstract-initial inductive bias (§3.2.4).

### 3.3.3 Implementation Details

Across all experiments and all models (including baselines such as PRPN, ON-LSTM, and Gumbel), the embedding dimension for words and constituents is 512. For VG-NSL, we use a pre-trained ResNet-152 (He et al., 2016), trained on ImageNet (Russakovsky et al., 2015), to extract vector embeddings for images. Thus,  $\Phi$  is a mapping from a 2048-D image embedding space to a 512-D visual-semantic embedding space. As for the *score* function in constituency parsing, we use a hidden dimension of 128 and ReLU activation. All VG-NSL models are trained for 30 epochs. We use an Adam optimizer (Kingma and Ba, 2015) with an initial learning rate  $5 \times 10^{-4}$  to train VG-NSL. The learning rate is re-initialized to



---

**Algorithm 2:** Constituency parsing based on concreteness estimation.

---

**Input:** list of normalized word concreteness scores  $\mathbf{a} = (a_1, a_2, \dots, a_m)$ ,  
hyperparameter  $\tau$  controlling the level of abstract-initiality

**Output:** Boundaries of constituents  $B = \{(L_i, R_i)\}_{i=1, \dots, m-1}$

**for**  $j = 1$  **to**  $m$  **do**  
     $left_j = j$   
     $right_j = j$   
**end**

**while**  $len(\mathbf{a}) > 1$  **do**  
     $p = \arg \max_j (a_j + \tau a_{j+1})$   
    add  $(left_p, right_{p+1})$  to  $B$   
     $\mathbf{a} = \mathbf{a}_{<p} + (\frac{a_p + a_{p+1}}{2}) + \mathbf{a}_{>p+1}$   
     $left = left_{<p} + (left_p) + left_{>p+1}$   
     $right = right_{<p} + (right_{p+1}) + right_{>p+1}$   
**end**

---

$5 \times 10^{-5}$  after 15 epochs. We tune other hyperparameters of VG-NSL on the development set using the self-agreement  $F_1$  score (Williams et al., 2018) over five runs with different choices of random initialization.

### 3.3.4 Results: Unsupervised Constituency Parsing

We evaluate the induced constituency parse trees via the overall  $F_1$  score, as well as the recall of four types of constituents: noun phrases (NP), verb phrases (VP), prepositional phrases (PP), and adjective phrases (ADJP) (Table 3.1). We also evaluate the robustness of models trained with fixed data and hyperparameters, but different random initialization, in two ways: via the standard deviation of performance across multiple runs, and via the self-agreement  $F_1$  score (Williams et al., 2018), which is the average  $F_1$  taken over pairs of different runs.

Among all of the models that do not require extra labels, VG-NSL with the abstract-initial inductive bias (VG-NSL+AI) achieves the best  $F_1$  score. PRPN (Shen et al., 2018) and a concreteness estimation-based baseline (Hessel et al., 2018) both produce competitive results. It is worth noting that the PRPN baseline reaches this performance without any

Model	NP	VP	PP	ADJP	Avg. F <sub>1</sub>	Self F <sub>1</sub>
Random	47.3 $\pm$ 0.3	10.5 $\pm$ 0.4	17.3 $\pm$ 0.7	33.5 $\pm$ 0.8	27.1 $\pm$ 0.2	32.4
Left	51.4	1.8	0.2	16.0	23.3	N/A
Right	32.2	23.4	18.7	14.4	22.9	N/A
PMI	54.2	16.0	14.3	39.2	30.5	N/A
PRPN (Shen et al., 2018)	72.8 $\pm$ 9.7	33.0 $\pm$ 9.1	61.6 $\pm$ 9.9	35.4 $\pm$ 4.3	52.5 $\pm$ 2.6	60.3
ON-LSTM (Shen et al., 2019)	74.4 $\pm$ 7.1	11.8 $\pm$ 5.6	41.3 $\pm$ 16.4	<b>44.0</b> $\pm$ 14.0	45.5 $\pm$ 3.3	69.3
Gumbel (Choi et al., 2018) <sup>†</sup>	50.4 $\pm$ 0.3	8.7 $\pm$ 0.3	15.5 $\pm$ 0.0	34.8 $\pm$ 1.6	27.9 $\pm$ 0.2	40.1
VG-NSL (ours) <sup>†</sup>	<b>79.6</b> $\pm$ 0.4	26.2 $\pm$ 0.4	42.0 $\pm$ 0.6	22.0 $\pm$ 0.4	50.4 $\pm$ 0.3	87.1
VG-NSL+AI (ours) <sup>†</sup>	74.6 $\pm$ 0.5	32.5 $\pm$ 1.5	<b>66.5</b> $\pm$ 1.2	21.7 $\pm$ 1.1	53.3 $\pm$ 0.2	<b>90.2</b>
VG-NSL+AI + FastText (ours) <sup>*†</sup>	78.8 $\pm$ 0.5	24.4 $\pm$ 0.9	65.6 $\pm$ 1.1	22.0 $\pm$ 0.7	<b>54.4</b> $\pm$ 0.4	89.8
<i>Concreteness estimation–based models</i>						
Turney et al. (2011)*	65.5	30.8	35.3	30.4	42.5	N/A
Turney et al. (2011)+HI*	74.5	26.2	47.6	25.6	48.9	N/A
Brysbaert et al. (2014)*	54.1	27.8	27.0	33.1	34.1	N/A
Brysbaert et al. (2014)+HI*	73.4	23.9	50.0	26.1	47.9	N/A
Hessel et al. (2018) <sup>†</sup>	50.9	21.7	32.8	27.5	33.2	N/A
Hessel et al. (2018)+HI <sup>†</sup>	72.5	<b>34.4</b>	65.8	26.2	52.9	N/A

Table 3.1: Recall of specific typed phrases and overall F<sub>1</sub> score, evaluated on the MSCOCO test set, averaged over 5 runs with different random initializations. We also include self-agreement F<sub>1</sub> score (Williams et al., 2018) across the 5 runs.  $\pm$  denotes standard deviation. \* denotes models requiring extra labels and/or corpus, and <sup>†</sup> denotes models requiring a pre-trained visual feature extractor. We highlight the best number in each column. The Left, Right, and PMI baselines, as well as concreteness estimation–based models have no standard deviation or self F<sub>1</sub> (shown as N/A) as they are deterministic given the training and/or testing data.

information from images. However, the performance of PRPN is less stable than that of VG-NSL across random initialization. In contrast to its state-of-the-art performance on the WSJ full set (Shen et al., 2019), we observe that ON-LSTM does not perform well on the MSCOCO caption dataset. However, it remains the best model for adjective phrases, which is consistent with the result reported by Shen et al. (2019).

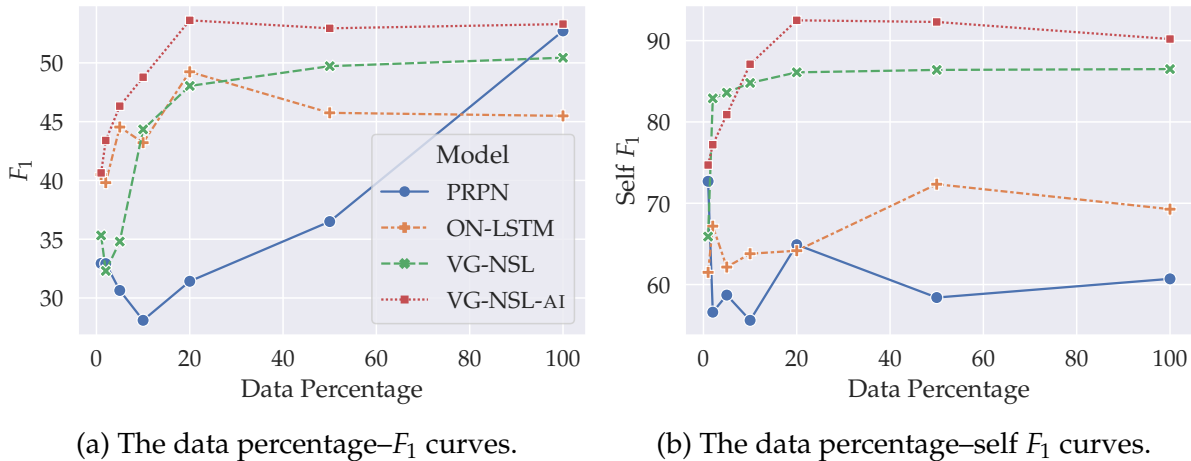


Figure 3.4:  $F_1$  score and self  $F_1$  score with respect to the amount of training data. All numbers are averaged over 5 runs with different random initialization.

In addition to the best overall  $F_1$  scores, VG-NSL+AI achieves competitive scores across most phrase types (NP, VP, and PP). Our models (VG-NSL and VG-NSL+AI) perform the best on NP and PP, which are the most common visually grounded phrases in the MSCOCO dataset. In addition, our models produce much higher self  $F_1$  than the baselines (Shen et al., 2018, 2019; Choi et al., 2018), showing that they reliably produce reasonable constituency parse trees with different initialization.

We also test the effectiveness of using pre-trained word embeddings. Specifically, for VG-NSL+AI + FastText, we use the pre-trained FastText embeddings (300-D; Joulin et al., 2016), concatenated with 212-D trainable embeddings, as the word embeddings. Using pre-trained word embeddings further improves performance to an average  $F_1$  of 54.4% while keeping a comparable self  $F_1$ .

### 3.3.5 Results: Data Efficiency

We compare the data efficiency for PRPN (the strongest baseline method), ON-LSTM, VG-NSL, and VG-NSL+AI. We train the models using 1%, 2%, 5%, 10%, 20%, 50% and 100% of the MSCOCO training set, and report the overall  $F_1$  and self  $F_1$  scores on the test set (Figure 3.4).

Compared to PRPN trained on the full training set, VG-NSL and VG-NSL+AI reach comparable performance using only 20% of the data (i.e., 8K images with 40K captions).

<b>Model/Method</b>	VG-NSL	(+AI)
Turney et al. (2011)	0.74	0.72
Brybaert et al. (2014)	0.71	0.71
Hessel et al. (2018)	0.84	0.85

Table 3.2: Agreement between our concreteness estimates and existing models or labels, evaluated via the Pearson correlation coefficient computed over the most frequent 100 words in the MSCOCO test set, averaged over 5 runs with different random initialization.

VG-NSL tends to quickly become more stable (in terms of the self  $F_1$  score) as the amount of data increases, while PRPN and ON-LSTM remain less stable.

### 3.3.6 Analysis: Consistency with Linguistic Concreteness

During training, VG-NSL acquires concreteness estimates for constituents via Eq. (3.1). Here, we evaluate the consistency between word-level concreteness estimates induced by VG-NSL and those produced by other methods (Turney et al., 2011; Brybaert et al., 2014; Hessel et al., 2018). Specifically, we measure the correlation between the concreteness estimated by VG-NSL on the MSCOCO test set and existing linguistic concreteness definitions (Table 3.2). For any word type  $z$ , we estimate its concreteness by taking the average of  $concrete(\mathbf{z}; \mathcal{V}, \mathcal{C})$ , across all word tokens of  $z$  in the dataset—the calculation of  $concrete(\mathbf{z}; \mathcal{V}, \mathcal{C})$  is based on the visual-semantic embeddings of constituents, and requires the corresponding image to the caption where the word token appears. The high correlation between VG-NSL and the concreteness scores produced by Turney et al. (2011) and Brybaert et al. (2014) supports the argument that the linguistic concept of concreteness can be acquired in an unsupervised way. Our model also achieves a high correlation with Hessel et al. (2018), which also estimates word concreteness based on visual information.

### 3.3.7 Analysis: Self Agreement as Model Selection Criterion

We introduce a novel hyperparameter tuning and model selection method based on the self-agreement  $F_1$  score.

Let  $\mathcal{M}_{\mathcal{H}}^{(i,j)}$  denote the  $j^{th}$  checkpoint of the  $i$ -th model trained with hyperparameters  $\mathcal{H}$ ,

Model	Criterion	Avg. $F_1$	Self $F_1$
VG-NSL	Self $F_1$	<b>50.4</b> $\pm 0.3$	<b>87.1</b>
VG-NSL	R@1	47.7 $\pm 0.6$	83.4
VG-NSL+AI	Self $F_1$	<b>53.3</b> $\pm 0.2$	<b>90.2</b>
VG-NSL+AI	R@1	53.1 $\pm 0.2$	88.7

Table 3.3: Average  $F_1$  scores and self  $F_1$  scores of VG-NSL and VG-NSL+AI with different model selection methods. R@1 denotes using recall at 1 (Kiros et al., 2014) as the model selection criterion. All hyperparameters are tuned with the self-agreement  $F_1$  score. The numbers are comparable to those in Table 3.1.

where  $\mathcal{M}_{\mathcal{H}}^{(i_1, \cdot)}$  and  $\mathcal{M}_{\mathcal{H}}^{(i_2, \cdot)}$  differ in their random initialization. The hyperparameters  $\mathcal{H}$  are tuned to maximize:

$$\sum_{1 \leq i < k \leq N} \max_{|j_i - j_k| < \delta} F_1 \left( \mathcal{M}_{\mathcal{H}}^{(i, j_i)}, \mathcal{M}_{\mathcal{H}}^{(k, j_k)} \right),$$

where  $F_1(\cdot, \cdot)$  denotes the  $F_1$  score between the trees generated by two models,  $N$  the number of different runs, and  $\delta$  the margin to ensure only nearby checkpoints are compared.<sup>6</sup>

After finding the best hyperparameters  $\mathcal{H}_0$ , we train the model for another  $N$  times with different random initialization, and select the best models by

$$\arg \max_{\{j_\ell\}_{\ell=1}^N} \sum_{1 \leq i < k \leq N} F_1 \left( \mathcal{M}_{\mathcal{H}_0}^{(i, j_i)}, \mathcal{M}_{\mathcal{H}_0}^{(k, j_k)} \right).$$

We compare the performance of VG-NSL selected by the self  $F_1$  score and that selected by recall at 1 in image-to-text retrieval (R@1 in Table 3.3; Kiros et al., 2014). As a model selection criterion, self  $F_1$  consistently outperforms R@1 (avg.  $F_1$ : 50.4 vs. 47.7 and 53.3 vs. 53.1 for VG-NSL and VG-NSL+AI, respectively). Meanwhile, it is worth noting that even if we select VG-NSL by R@1, it shows better stability compared with PRPN and ON-LSTM (Table 3.1), in terms of the score variance across different random initialization and self  $F_1$ . Specifically, the variance of avg.  $F_1$  is always less than 0.6 while the self  $F_1$  is greater than 80.

<sup>6</sup> In all of our experiments,  $N = 5, \delta = 2$ .

Model	EN	DE	FR
PRPN	30.8 $\pm$ 17.9	31.5 $\pm$ 8.9	27.5 $\pm$ 7.0
ON-LSTM	<b>38.7</b> $\pm$ 12.7	34.9 $\pm$ 12.3	27.7 $\pm$ 5.6
VG-NSL	33.5 $\pm$ 0.2	36.3 $\pm$ 0.2	34.3 $\pm$ 0.6
VG-NSL+AI	<b>38.7</b> $\pm$ 0.2	<b>38.3</b> $\pm$ 0.2	<b>38.1</b> $\pm$ 0.6

Table 3.4:  $F_1$  scores on the Multi30K test split (Young et al., 2014; Elliott et al., 2016, 2017), averaged over 5 runs with different random initialization.  $\pm$  denotes the standard deviation.

Note that the PRPN and ON-LSTM models are not tuned using self  $F_1$ , since these models are usually trained for hundreds or thousands of epochs and, thus, it is computationally expensive to evaluate self  $F_1$ . We leave the efficient tuning of these baselines by self  $F_1$  for future work.

### 3.3.8 Extension to Multiple Languages

We extend our experiments to the Multi30K dataset, which is built on the Flickr30K dataset (Young et al., 2014) and consists of English, German (Elliott et al., 2016), and French (Elliott et al., 2017) captions. For Multi30K, there are 29,000 images in the training set, 1,014 in the development set, and 1,000 in the test set. Each image is associated with one caption in each covered language.

We compare our models to PRPN and ON-LSTM in terms of overall  $F_1$  scores (Table 3.4). VG-NSL with the abstract-initial inductive bias consistently performs the best across the three languages, all of which are highly head-initial (Baker, 2001)—this set of results supports our intuition to implement the abstract-initial inductive bias. Note that the  $F_1$  scores here are not comparable to those in Table 3.1, since Multi30K (English) has 13 times fewer captions than MSCOCO.

## 3.4 Conclusion and Discussion

We have proposed a simple but effective model, the Visually Grounded Neural Syntax Learner, for visually grounded language structure acquisition. VG-NSL jointly learns

parse trees and visually grounded textual representations. In our experiments, we find that this approach to grounded language learning produces parsing models that are both accurate and stable. In addition, the learning process of VG-NSL is much more data-efficient than prior text-only approaches. Along the way, the model acquires estimates of word concreteness.

The results suggest multiple future research directions, which we discuss as follows:

1. VG-NSL matches text embeddings directly with embeddings of entire images. Its performance may be boosted by considering structured representations of both images (e.g., Lu et al., 2016; Wu et al., 2019) and texts. Evidence from recent work, such as Hong et al. (2021) and Wan et al. (2022), suggests that the awareness of image structures can improve the performance of text syntactic analysis. In a reversed direction, where vision is the primary modality to be processed, Xu et al. (2022) have also shown that text, as a secondary modality that provides distant supervision, can improve the performance of image segmentation, which is a crucial step towards a hierarchical understanding of images.

On the other hand, while different modalities—to some extent—share the structures, they also possess their unique features and information. We look forward to future work that integrates the structures of multiple modalities into a unified model while also considering the unique features of each modality.

2. Thus far, we have used a shared vector representation for both syntax and semantics, but it may be useful to disentangle their representations. In Chapter 6, we discuss the induction of combinatory categorial grammar (CCG; Steedman, 2000) from visually grounded text, which is a meaningful step towards this direction. In addition, the disentanglement of syntax and semantics may enable more interpretable and controllable study relevant to syntactic (Brown, 1957) and semantic (Pinker, 1984) bootstrapping.
3. Our best parsing model is based on the abstract-initial inductive bias, which is designed based on insights drawn from the structure of head-initial languages. However, automatically acquiring such effective inductive biases from data remains challenging (Kemp et al., 2006; Gauthier et al., 2018), and we suggest another future direction to learn inductive biases from data with plausibly minimal human intervention.

4. It may be possible to extend our approach to other linguistic tasks such as dependency parsing (Christie et al., 2016), coreference resolution (Kottur et al., 2018), and learning pragmatics beyond semantics (Andreas and Klein, 2016). Towards this line, we recommend readers to check out Su et al. (2021).

There are also limitations to the idea of grounded language acquisition. In particular, the current approach has thus far been applied to understanding grounded texts in a single domain (static visual scenes for VG-NSL), which fundamentally lacks the dynamics of real-world interactions. Its applicability may be extended by learning shared representations across multiple modalities (Castrejon et al., 2016) or integrating with pure text-domain models (e.g., integrating with probabilistic context-free grammars; Zhao and Titov, 2020).



## Chapter 4

# Syntax Acquisition from Visually Grounded Speech

*Content in this chapter has been published as a workshop paper at ASRU 2023 (Lai et al., 2023). Cheng-I Jeff Lai and Puyuan Peng have contributed significantly to this work.*

Given the results presented in Chapter 3 on parsing visually grounded text, we now focus on the problem of learning to parse visually grounded speech without explicit syntactic supervision.

In this chapter, we present a pipeline approach: the core idea is to first segment the speech waveform into sequences of word segments, and subsequently induce phrase structure using the inferred segment-level continuous representations. We introduce the Audio-Visual Neural Syntax Learner (AV-NSL; Figure 4.1) that learns phrase structures by listening to audio and looking at images, without ever being exposed to text. The speech utterances are represented by sequences of continuous speech segment representations derived from a pre-trained model that simultaneously discovers word-like units and learns segment representations (Peng and Harwath, 2022). Adapting the model structures of VG-NSL (Chapter 3), AV-NSL (1) learns to map the representations of speech segments and images into a shared embedding space, resulting in higher similarity scores for segments and images that convey similar meanings, (2) estimates the visual *concreteness* of speech segments using the learned embedding space, and (3) outputs speech segments with higher concreteness as the constituents. By training on paired images and spoken captions, AV-NSL can infer meaningful phrase structures comparable to those derived by naturally supervised text parsers, for both English and German. Our findings extend prior work in

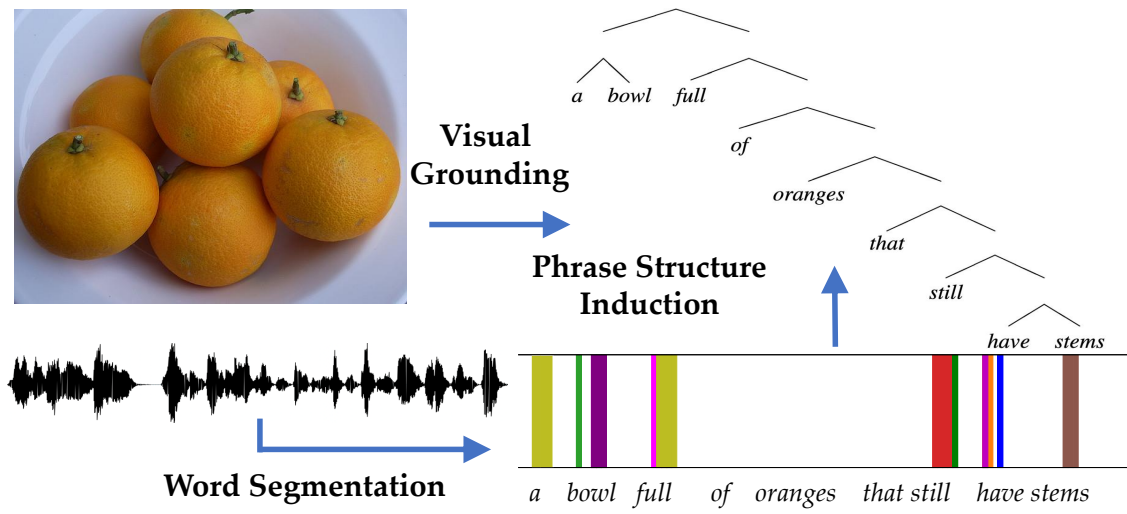


Figure 4.1: Illustration of the AV-NSL model. We adopt the VG-NSL model architecture to perform phrase structure induction from visually grounded speech.

unsupervised language acquisition from speech and grounded grammar induction and present one approach to bridge the gap between the two topics. As a by-product, we also improve over the previous state of the art in unsupervised word segmentation.

## 4.1 Related Work

**Grounded grammar induction.** Since the proposal of the visually grounded grammar induction task (Shi et al., 2019), there has been subsequent research on the topic (Zhao and Titov, 2020; Zhang et al., 2021; Wan et al., 2022, *inter alia*). To the best of our knowledge, existing work on grammar induction from distant supervision has been based almost exclusively on text input. The most relevant work to ours is Zhang et al. (2021), where speech features are treated as an auxiliary input for video-text grammar induction; that is, the model proposed by Zhang et al. (2021) still requires text data and an off-the-shelf automatic speech recognizer. In contrast to existing approaches, AV-NSL employs raw speech data and bypasses text to induce constituency parse trees, utilizing distant supervision from parallel audio-visual data.

**Spoken word discovery.** Following the pioneering work in spoken term discovery (Park and Glass, 2007), a line of work has been done to discover repetitive patterns or keywords from unannotated speech (Jansen and Van Durme, 2011; McInnes and Goldwater, 2011; Zhang, 2013, *inter alia*). Other related work has considered tasks such as unsupervised word segmentation and spoken term discovery (Lee et al., 2015; Kamper et al., 2017; Chorowski et al., 2021; Bhati et al., 2021, *inter alia*), and the ZeroSpeech challenges (Dunbar et al., 2022) have been a major driving force in the field. A recent line of work (Harwath and Glass, 2017; Harwath et al., 2018; Harwath and Glass, 2019; Harwath et al., 2020) has shown that word-like and phone-like units can be acquired from speech by analyzing audio-visual retrieval models. Peng and Harwath (2022) shows that word discovery naturally emerges from a visually grounded, self-supervised speech model, by analyzing the model’s self-attention heads. In contrast, AV-NSL attempts to induce phrase structure, in the form of constituency parsing on top of unsupervised word segments.

**Speech parsing and its applications.** Early work on speech parsing can be traced back to SParseval (Roark et al., 2006), a toolkit that evaluates text parsers given potentially errorful automatic speech recognition (ASR) results. In the past, syntax has also been studied in the context of speech prosody (Wagner and Watson, 2010; Köhn et al., 2018), and another line of work (Tran et al., 2018, 2019; Tran and Ostendorf, 2021) has incorporated acoustic-prosodic features for text parsing with auxiliary speech input. Lou et al. (2019) trains a text parser (Kitaev and Klein, 2018) to detect speech disfluencies, and Pupier et al. (2022) trains a text dependency parser from speech jointly with an ASR model. Concurrent work (Tseng et al., 2023) pipelines an unsupervised ASR system with DIORA (Drozdov et al., 2019) to perform unsupervised speech parsing. While the predicted parse trees are, in principle, comparable to the results in this work, the evaluation metric they adopted may introduce extra difficulty in interpreting the results—concretely, they use a bipartite matching algorithm to align the constituent spans in both trees by maximizing the sum of overlap time durations between aligned spans, treat the aligned spans as precise/recalled constituents, and report the  $F_1$  score as in PARSEVAL (Black et al., 1991). In an extreme case (Figure 4.2), such a metric assigns a perfect  $F_1$  score to two trees that are not similar in structural terms, which further motivates us to develop a new evaluation metric, STRUCT-IOU, in Chapter 5.

On the application side, syntactic parses of texts have been applied to prosody modeling in end-to-end text-to-speech (Guo et al., 2019; Tyagi et al., 2020; Kaiki et al., 2021). While

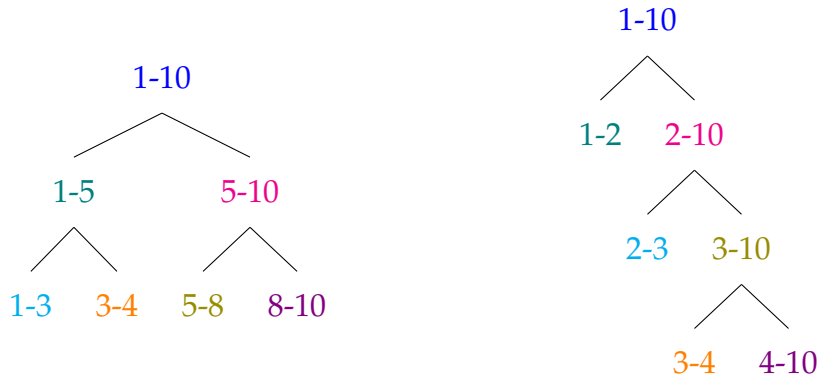
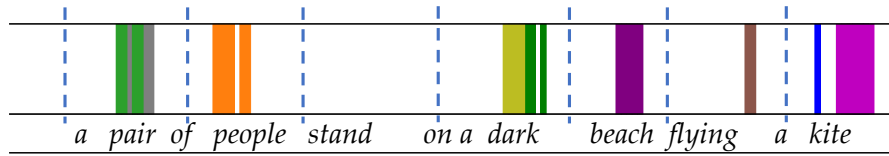


Figure 4.2: An illustrative example of the evaluation metric used in Tseng et al. (2023). Node labels represent the time spans of speech segments, measured in a specific unit (e.g., seconds). These two trees will receive a perfect  $F_1$  score under their metric. Best viewed in color: nodes in the same color are aligned by the max-sum-duration-based bipartite matching algorithm, and each pair of aligned nodes contributes 1 to the numerator of both precision and recall.

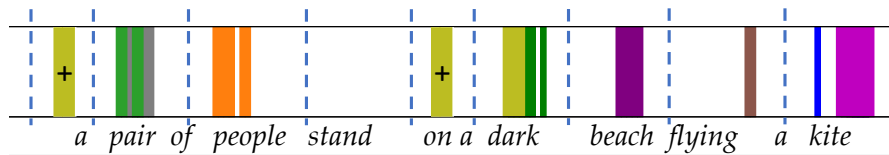
this work builds upon pre-existing text parsing algorithms, we focus on phrase structure induction in the absence of text.

## 4.2 Method

Given paired spoken captions and images, AV-NSL infers phrase structures from speech utterances without relying on text. The basis of AV-NSL is the Visually-Grounded Neural Syntax Learner (VG-NSL; Chapter 3), which learns to induce constituency parse trees by guiding a sequential sampling process with text-image matching. We refer the readers to Chapter 3 for a detailed description of VG-NSL, and here we focus on the modifications and extensions to VG-NSL that enable AV-NSL to parse speech. To implement AV-NSL, we obtain sequences of word segments and extract segment-level self-supervised representations. The extracted segment representations are then used to induce phrase structures, analogously to the randomly initialized word representations in VG-NSL. In this section, we describe in detail the unique components of AV-NSL.



(a) Example of VG-HuBERT word segmentation (top): different colors denote different attention heads, and color transparency represents the magnitude of the attention weights. Adjacent attention boundaries (vertical dashed lines) are used as the word boundaries.



(b) *Segment insertion* (bottom): short segments (marked with “+”) are placed in long enough gaps between existing segments to recover function words.

Figure 4.3: Examples of VG-HuBERT word segmentation and segment insertion (this work). Best viewed in color.

## 4.2.1 Audio-Visual Word Segmentation and Representation

We use VG-HuBERT (Peng and Harwath, 2022), a model trained to associate spoken captions with natural images via retrieval, for word segmentation. After training, spoken word segmentation emerges via magnitude thresholding of the self-attention heads of the audio encoder: at layer  $\ell$ , we (1) sort the attention weights from the [CLS] token to other tokens in descending order, and (2) apply a threshold  $p$  to retain the top  $p\%$  of the overall attention magnitude (Figure 4.3a).

Empirically, however, the VG-HuBERT word segmentation model tends to ignore function words such as *a* and *of*. This is natural because function words are often less visually grounded and may not be as salient in the attention maps. Therefore, we devise a simple heuristic to pick up function word segments by inserting a short word segment wherever there is a gap of more than  $s$  seconds that VG-HuBERT fails to place a segment (Figure 4.3b). We additionally apply unsupervised voice activity detection (Tan et al., 2020) to restrict segment insertion to only voiced regions. The length of the insertion gap  $s$ , the VG-HuBERT segmentation layer  $l$ , attention magnitude threshold  $p\%$ , and

model training snapshots across random seeds and training steps are all chosen in an unsupervised fashion using minimal Bayes risk decoding.

We use the word segments output by VG-HuBERT to calculate the representations. Let  $R = \{r_j\}_{j=1}^T$  denote the frame-level representation sequence, where  $T$  is the speech sequence length. Audio-visual word segmentation returns an alignment  $A(i) = r_{p:q}$  that maps the  $i^{\text{th}}$  word segment to the  $p^{\text{th}}$  to  $q^{\text{th}}$  acoustic frames. The segment-level continuous representation for the  $i^{\text{th}}$  word is  $w_i^0 = \sum_{t \in A(i)} a_{i,t} r_{i,t}$ , where  $a_{i,t}$  is the attention weights over the segments specified by  $A(i)$ . In AV-NSL,  $R$  is the layer representation from a pre-trained speech model (e.g., VG-HuBERT), and  $a_{i,t}$  is the [CLS] token attention weights over frames within each segment.

### 4.2.2 Self-Training

Shi et al. (2020) have shown that self-training can usually improve parsing performance: the approach involves training an additional parser to fit the output generated by a pre-existing learned parser. Concretely, they use Benepar Kitaev and Klein (2018), a supervised neural constituency parser, as the base model for self-training, where it (1) takes a sentence as the input, (2) maps it to word representations, and (3) predicts a score for all spans of being in the constituency parse tree. The model evaluates all possible tree structures for inference and outputs the highest-scoring one.

Following this idea, we apply self-training to improve AV-NSL. We extend Benepar to the speech domain and introduce s-Benepar, which takes segment-level continuous mean-pooling HuBERT representations instead of discrete words as the input and outputs the constituency parse trees.

### 4.2.3 Unsupervised Decoding

Following the decoding design of VG-NSL, we extend consistency-based decoding to AV-NSL, which is also similar in spirit to minimum Bayes risk (MBR) decoding (Chapter 7), for both spoken word segmentation and phrase-structure induction. Given a loss function  $\ell_{MBR}(O_1, O_2)$  between two outputs  $O_1$  and  $O_2$ , and a set of  $k$  outputs  $\mathcal{O} = \{O_1, \dots, O_k\}$ , we select the optimal output

$$\hat{O} = \arg \min_{O' \in \mathcal{O}} \sum_{O'' \in \mathcal{O}} \ell_{MBR}(O', O'').$$

The output candidate set  $\mathcal{O}$  is obtained by sampling from the output distribution. We defer more detailed discussions regarding MBR decoding to Chapter 7.

For word segmentation, we define the loss between two segmentation proposals  $\mathcal{S}_1$  and  $\mathcal{S}_2$  as  $\ell_{MBR}(\mathcal{S}_1, \mathcal{S}_2) = -\text{MIOU}(\mathcal{S}_1, \mathcal{S}_2)$ , where  $\text{MIOU}(\cdot, \cdot)$  denotes the mean intersection over union ratio across all matched pairs of predicted word spans. We match the predicted word spans using the maximum weight-matching algorithm (Galil, 1986), where word spans correspond to vertices, and we define edge weights by the temporal overlap between the corresponding spans.

For phrase structure induction, the loss function between two parse trees  $\mathcal{T}_1$  and  $\mathcal{T}_2$  is  $\ell_{MBR}(\mathcal{T}_1, \mathcal{T}_2) = 1 - F_1(\mathcal{T}_1, \mathcal{T}_2)$ , where  $F_1(\cdot, \cdot)$  denotes the  $F_1$  score between the two trees.

## 4.3 Experiments

### 4.3.1 Setup

**Datasets.** We first evaluate models on SpokenCOCO (Hsu et al., 2021), the spoken version of MSCOCO (Lin et al., 2014), where humans verbally read the text captions in English. It contains 83k/5k/5k images for training, validation, and testing. Each image has five corresponding captions.

We also extend our experiments to German, where we synthesize German speech from the Multi30K captions (Elliott et al., 2016).<sup>1</sup> It contains 29k/1k/1k images for training, validation, and testing. Each image has one corresponding caption. Following VG-NSL (Chapter 3), we use pre-trained English Benepar (Kitaev and Klein, 2018) to generate the oracle parse trees for captions.

**Preprocessing.** We use the Montreal Forced Aligner (McAuliffe et al., 2017) trained on the specific language (i.e., English or German) to obtain the oracle word segmentation. We remove utterances that have mismatches between ASR transcripts and text captions.

---

<sup>1</sup> Synthesized with the pre-trained German Tacotron2 model (<https://github.com/thorstenMueller/Thorsten-Voice>).

### 4.3.2 Baselines and Toplines

We consider the following baselines and modeling alternatives to examine each component of AV-NSL:

1. **Trivial tree structures.** Following VG-NSL (Chapter 3), we include baselines without linguistic information: random binary trees, left-branching binary trees, and right-branching binary trees.
2. **AV-cPCFG.** We train compound probabilistic context-free grammars (cPCFG; Kim et al., 2019) on word-level discrete speech tokens given by VG-HuBERT. Unlike in AV-NSL, the segment representations are discretized via k-means to obtain word-level indices. AV-cPCFG uses visual cues only for segmentation and segment representations, not for phrase structure induction.
3. **DPDP-cPCFG.** In contrast to AV-cPCFG, DPDP-cPCFG does not rely on any visual grounding throughout. We use DPDP (Kamper, 2022) and pre-trained HuBERT (Hsu et al., 2021) followed by k-means to obtain discrete word indices.<sup>2</sup>
4. **Oracle AV-NSL (topline).** To remove the uncertainty of unsupervised word segmentation, we directly train AV-NSL on top of the oracle word segmentation via forced alignment. Due to the absence of VG-HuBERT, the frame-level representations  $R$  are obtained from pre-trained HuBERT while the attention weights  $a_{i,t}$  are parameterized by a 1-layer MLP, jointly trained with the tree sampling module instead.

### 4.3.3 Evaluation Metrics

**Word segmentation.** We use the standard word boundary prediction metrics (precision, recall, and the  $F_1$  score), calculated by comparing the temporal position between inferred and forced-aligned word boundaries. An inferred boundary located within  $\pm 20ms$  of a forced aligned boundary is considered a successful prediction.

**Parsing.** For parsing with the oracle word segmentations, we use PARSEVAL (Black et al., 1991) to calculate the  $F_1$  score between the predicted and reference parse trees. For parsing with inferred word segmentation, due to the mismatch in the number of nodes between

---

<sup>2</sup> We sweep the number of word clusters over  $\{1k, 2k, 4k, 8k, 12k, 16k\}$ .



the predicted and reference parse trees, we use the structured average intersection-over-union ratio (STRUCT-IOU) as an additional metric—this is a new metric developed in this dissertation, which will be presented in details in Chapter 5.

STRUCT-IOU considers both word segmentation quality and temporal overlap between induced constituents. Concretely, the input is two constituency parse trees over the same speech utterance,  $\mathcal{T}_1 = \{a_i\}_{i=1}^n$  and  $\mathcal{T}_2 = \{b_j\}_{j=1}^m$ , where  $a_i$  and  $b_j$  are time spans. Suppose  $a_i$  from  $\mathcal{T}_1$  is aligned to  $b_j$  from  $\mathcal{T}_2$ . In a valid alignment, the following conditions must be satisfied:

1. Any descendant of  $a_i$  may either align to a descendant of  $b_j$  or be left unaligned;
2. Any ancestor of  $a_i$  may either align to an ancestor of  $b_j$  or be left unaligned;
3. Any descendant of  $b_j$ , may either align to a descendant of  $a_i$  or be left unaligned;
4. Any ancestor of  $b_j$ , may either align to an ancestor of  $a_i$  or be left unaligned.

Given a Boolean matrix  $\mathbf{A}$ , where  $A_{i,j} = 1$  denotes that  $a_i$  aligns to  $b_j$ , we compute the structured average IOU between  $\mathcal{T}_1$  and  $\mathcal{T}_2$  over  $\mathbf{A}$  by

$$\text{STRUCT-IOU}(\mathcal{T}_1, \mathcal{T}_2; \mathbf{A}) = \frac{2}{n + m} \left( \sum_{i=1}^{n_1} \sum_{j=1}^{n_2} A_{i,j} \text{IOU}(a_i, b_j) \right),$$

and the final evaluation result is obtained by maximizing the STRUCT-IOU score across all valid alignments. Dynamic programming allows us to calculate the optimal STRUCT-IOU score within  $\mathcal{O}(n^2m^2)$  time. We will describe the detailed problem formulation and algorithm of STRUCT-IOU in Chapter 5.

### 4.3.4 Results: Unsupervised Word Segmentation

We validate the effectiveness of our unsupervised word segmentation approach. We first compare our improved VG-HuBERT with segment insertion to the original VG-HuBERT (Peng and Harwath, 2022) and DPDP (Kamper, 2022), a speech-only word segmentation method (Table 4.1). We find that segment insertion improves the recall and hurts the precision while achieving the highest  $F_1$  score.

Next, we compare MBR-based and supervised decoding. For practice efficiency, we implement MBR-based decoding as follows: we first run a pilot hyperparameter selection, performing word segmentation on all candidates in the SpokenCOCO validation set, and

Method	Decoding	Precision	Recall	$F_1$
DPDP (Kamper, 2022)	supervised	17.37	9.00	11.85
VG-HuBERT (Peng and Harwath, 2022)	supervised	<b>36.19</b>	27.22	31.07
VG-HuBERT	supervised	34.34	29.85	31.94
w/ seg. ins. (ours)	MBR	33.31	<b>34.90</b>	<b>34.09</b>

Table 4.1: English word segmentation results on the SpokenCOCO validation set. Supervised decoding methods require an annotated development set to choose the best hyperparameters. The best number in each column is in boldface. VG-HuBERT with segment insertion and MBR decoding achieves the best boundary  $F_1$ .

subsequently choose the 10 most selected sets of hyperparameters to perform another round of MBR selection on the training set.

For German word segmentation, we employ identical models and settings as those used for English, as Peng et al. (2023) have shown that the word segmentation capability of English VG-HuBERT demonstrates cross-lingual generalization without any adaptation. On German Multi30K, our method achieves an  $F_1$  score of 37.46 with MBR, which outperforms supervised hyperparameter tuning (36.45).

### 4.3.5 Results: Unsupervised Phrase Structure Induction

We quantitatively show that AV-NSL learns meaningful phrase structure given word segments (Table 4.2). The best performing AV-NSL is based on our improved VG-HuBERT with MBR top 10 selection for word segmentation, VG-HuBERT layers as the segment representations, and another MBR decoding over phrase structure induction hyperparameters, including training checkpoints and segment representation layers. Comparing AV-NSL against AV-cPCFG and AV-cPCFG against DPDP-cPCFG, we empirically show the necessity of training AV-NSL on *continuous* segment representation instead of discretized speech tokens, and the effectiveness of visual grounding in our overall model design.

Next, we compare the performance of AV-NSL with and without self-training (Table 4.3) and find that self-training with an s-Benepar backbone improves the best AV-NSL performance from 0.521 (Table 4.2) to 0.538.

Syntax Induction	Model		Output	STRUCT-IOU
	Segmentation	Seg. Repr.	Selection	
Right-Branching	VG-HuBERT			<b>0.546</b>
Right-Branching	DPDP			0.478
AV-cPCFG	VG-HuBERT	discrete	supervised	0.499
AV-cPCFG	VG-HuBERT	discrete	supervised	0.481
DPDP-cPCFG	DPDP	discrete	supervised	0.465
AV-NSL	VG-HuBERT	continuous	MBR	0.516
AV-NSL	VG-HuBERT	continuous	MBR	0.521

Table 4.2: English phrase structure induction results on SpokenCOCO. Subscripts denote layer number, e.g., HuBERT<sub>10</sub> denotes the 10<sup>th</sup> layer representation from HuBERT. We list the best-performing hyperparameters for each modeling choice.

Segment Representation	Output Selection	STRUCT-IOU
HuBERT	last ckpt.	<b>0.538</b>
HuBERT <sub>2,4,6,8,10,12</sub>	MBR	0.536

Table 4.3: Results of self-training with s-Benepar, trained on outputs from the best AV-NSL model (STRUCT-IOU = 0.521) from Table 4.2. Inputs to s-Benepar are segment-level HuBERT representations instead of VG-HuBERT representations.

Thirdly, Table 4.4 isolates phrase structure induction from word segmentation quality with oracle AV-NSL. Unlike in Table 4.2, we can adopt the PARSEVAL  $F_1$  score (Black et al., 1991) for evaluation since there is no mismatch in the number of tree nodes. Unsupervised oracle AV-NSL matches or outperforms text-based VG-NSL with proper segment-level representations. Similarly to Table 4.3, self-training with s-Benepar on oracle AV-NSL trees further improves the syntax induction results, almost matching that of right-branching trees.

Perhaps surprisingly, right-branching trees (RBT) with oracle and VG-HuBERT word segmentation reach the best English STRUCT-IOU and  $F_1$  scores on SpokenCOCO, respectively. We note that the RBTs highly align with the head initiality of English (Baker, 2001),

Model		Output	$F_1$
Syntax Induction	Seg. Representation	Selection	
Right-Branching	N/A	N/A	<b>57.39</b>
VG-NSL	word embeddings	Supervised	53.11
oracle AV-NSL	HuBERT <sub>2</sub>	Supervised	55.51
oracle AV-NSL $\rightarrow$ s-Benepar	HuBERT <sub>2</sub>	MBR	57.24

Table 4.4: PARSEVAL  $F_1$  scores given oracle segmentation. The best number is in boldface.

Model		Output	SAIoU
Induction	Segmentation	Selection	
Right-Branching	VG-HuBERT+MBR <sub>10</sub>	N/A	0.456
Left-Branching	VG-HuBERT+MBR <sub>10</sub>	N/A	0.461
AV-NSL	VG-HuBERT+MBR <sub>10</sub>	MBR	<b>0.487</b>

Table 4.5: Phrase structure induction results on the (spoken) German Multi30K test set. The best number is in boldface.

especially in our setting where all punctuation marks were removed. In contrast, our experiments on German show that AV-NSL outperforms both RBTs and left-branching trees in terms of STRUCT-IOU (Table 4.5).<sup>3</sup>

### 4.3.6 Analysis

**Recall of each type of constituent.** Similarly to Chapter 3, we present the recall of specific types of constituents (Table 4.6). While VG-NSL benefits from the abstract-initial bias, where abstract words are encouraged to appear at the beginning of a constituent, AV-NSL outperforms all variations of VG-NSL on all constituent categories except NP. We hypothesize that the spoken utterances are noisier than the written text, and it is, therefore, more challenging for AV-NSL to capture the noun phrases; however, the spoken utterances

<sup>3</sup>For German grammar induction with oracle segmentation, oracle AV-NSL attains 33.94  $F_1$  while LBT/RBT attain 26.70/25.30  $F_1$  respectively.

Model	$F_1$	Constituent Recall			
		NP	VP	PP	ADJP
VG-NSL (Shi et al., 2019)	50.4	<b>79.6</b>	26.2	42.0	22.0
VG-NSL+AI	53.3	74.6	32.5	66.5	21.7
VG-NSL+AI + FastText	54.4	78.8	24.4	65.6	22.0
oracle AV-NSL	<b>55.5</b>	55.5	<b>68.1</b>	<b>66.6</b>	<b>22.1</b>

Table 4.6: Recall of specific typed phrases, including noun phrases (NP), verb phrases (VP), prepositional phrases (PP), and adjective phrases (ADJP), as well as the overall  $F_1$  score, evaluated on SpokenCOCO test set. VG-NSL numbers are the same as those in Chapter 3.

contain arguably more information, such as prosody, that can be used to infer other types of constituents. We leave the investigation of these hypotheses to future work.

**Ablation study.** We introduce three ablations to evaluate the efficacy of high-quality word segmentation, visual representation, and speech representation (Table 4.7). Concretely, we train AV-NSL with the following modifications:

1. Given the number of words  $n$ , we divide the speech utterances uniformly into  $n$  chunks to get the word segmentation and use the same visual representations as AV-NSL.
2. We replace visual representations with random vectors, where each pixel is independently sampled from a uniform distribution, and use the oracle word segmentation.
3. We replace the self-supervised speech representations (i.e., HuBERT) with log-Mel spectrograms.

We observe significant performance drops in all settings, compared to AV-NSL with oracle word segmentations. This set of results complements Table 4.2, stressing that precise word segmentation and both high-quality visual and speech representations are all necessary for phrase structure induction from speech.

Model		Visual	$F_1$
Word Segmentation	Seg. Repr.		
MFA	HuBERT <sub>2</sub>	ResNet 101	55.51
Uniform	HuBERT <sub>2</sub>	ResNet 101	48.97
MFA	HuBERT <sub>2</sub>	random	31.23
MFA	logMel spec	ResNet 101	42.01

Table 4.7: PARSEVAL  $F_1$  scores for ablations over word segmentation, visual representation, and speech representation.

## 4.4 Conclusion and Discussion

Previous research has achieved notable progress in zero-resource speech processing and grammar induction by employing multi-modal techniques. In our study, we propose an approach to model human language acquisition that leverages the visual modality as the source of grounding signals. Our approach, AV-NSL, encompasses extracting word-level representations from speech and deriving syntactic structures from those representations, thereby eliminating the reliance on text. Through quantitative and qualitative analyses, we demonstrate in both English and German experiments that our proposed model infers meaningful constituency parse trees based on continuous word segment representations. Our work represents the initial step in grammar induction within textless settings, paving the way for future research endeavors, which include but are not limited to (1) building end-to-end models that take spoken utterances and produce their syntactic analysis, (2) understanding the contribution of various grounding signals to grammar induction, and (3) modeling human language acquisition in grounded environments.

As a side contribution, we find that an unsupervised word segmentation model, VG-HuBERT, and heuristics-based segment insertion outperform the previous state-of-the-art method in unsupervised word segmentation. This result suggests that we may combine the advantages of audio-visual (Peng and Harwath, 2022, *inter alia*) and speech-only (Kamper, 2022, *inter alia*) word segmentation models to improve the quality of word segmentation further: intuitively, the former better extracts word boundaries of more visually concrete words (see more discussions in Chapter 3), whereas the latter provides a general option

for a broader range of words.

Lastly, we note that the work presented in this chapter should be considered a preliminary exploration of unsupervised speech parsing, together with Tseng et al. (2023). While it is clear that visually grounded text parsing models can significantly outperform right-branching baselines (Chapter 3), our best-performing visually grounded speech parsing model still lags behind the simple right-branching trees in English. As discussed in the prior content, we note that the right-branching trees highly align with the head initiality of English, and the results presented in this chapter are nontrivial as we do not incorporate any linguistic priors. On the other hand, this set of results also implies significant room for improvement in the quality of visually grounded speech parsing. In particular, an end-to-end approach that jointly learns word segmentation and phrase structure induction may be a promising direction for future research.

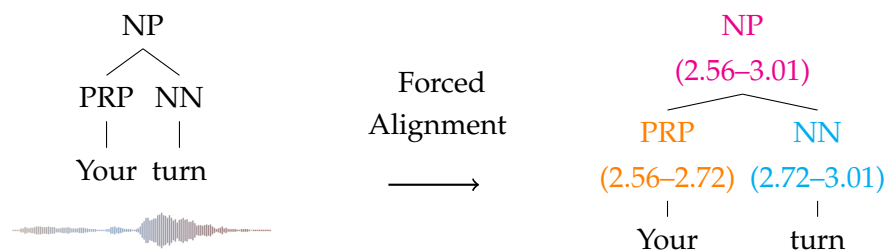
## Chapter 5

# STRUCT-IOU: A Structured Alignment-Based Evaluation Metric for Constituency Parsing

Models for *textless* constituency parsing have been proposed in Chapter 4 (Lai et al., 2023) and other concurrent work (Tseng et al., 2023). In contrast to earlier work that parses manually labeled (Charniak and Johnson, 2001, *inter alia*) or automatic (Kahn and Ostendorf, 2012, *inter alia*) speech transcriptions, these models construct constituency parse trees over automatically recognized spoken word boundaries, where each word is represented with a time range of the spoken utterance, without using any form of text. To evaluate these textless models, we need a metric that compares the predicted tree (over spoken word boundaries) with the manually labeled ground-truth tree (over written words) and faithfully reflects the parsing quality. Since the automatically recognized word boundaries may be imperfect, the metric should also reflect the changes in parsing quality due to word boundary errors. To the best of our knowledge, none of the existing metrics meets these requirements, as they are all designed to compare parse trees over discrete word sequences instead of continuous time ranges.

Motivated by the need for textless speech parsing evaluation (Lai et al., 2023; Tseng et al., 2023), in this work, we introduce the structured average intersection-over-union ratio (STRUCT-IOU; Figure 5.1), a metric that compares two parse trees over time ranges. We relax the definition of segment trees (Bentley, 1977) to represent speech constituency parse trees, where each node is associated with an interval that represents the time range





(a) Ground-truth speech parse tree (right), obtained by forced alignment between the ground-truth text parse tree (left, top) and the spoken utterance (left, bottom).



(b) Predicted tree with good word boundaries and an errorful tree structure (left), or that with errorful word boundaries and a perfect tree structure (right).

Figure 5.1: Illustration of how STRUCT-IOU evaluates textless speech constituency parsing. Best viewed in color, where nodes with the same color are aligned. Numbers in parentheses are the starting and ending times of the corresponding spans (in seconds).

of the corresponding spoken word or constituent. To obtain the “ground-truth” speech parse trees, we use the forced alignment algorithm (McAuliffe et al., 2017), a supervised and highly accurate method that aligns written words to time ranges of the corresponding spoken utterance, to project the ground-truth text parses onto the time domain. STRUCT-IOU is calculated by aligning the same-label nodes in the predicted and ground-truth parse trees, following structured constraints that preserve parent-child relations. The calculation of STRUCT-IOU can be formulated as an optimization problem (§5.3.1) with a polynomial-time solution (§5.3.2) in terms of the number of tree nodes.

Although STRUCT-IOU is designed to evaluate speech parsing, it is also applicable to text parsing evaluation. We analyze STRUCT-IOU for both purposes: in speech parsing evaluation, STRUCT-IOU robustly takes into account both the structure information and

word boundaries; in text parsing evaluation, while maintaining a high correlation with the PARSEVAL  $F_1$  score, STRUCT-IOU shows a higher tolerance to potential syntactic ambiguity.

## 5.1 Related Work

**Text constituency parsing and evaluation.** In the past decades, there has been much effort in building and improving constituency parsing models (Collins and Koo, 2005; Charniak and Johnson, 2005; McClosky et al., 2006; Durrett and Klein, 2015; Cross and Huang, 2016; Dyer et al., 2016; Choe and Charniak, 2016; Stern et al., 2017; Kitaev and Klein, 2018, *inter alia*). PARSEVAL (Black et al., 1991) has been the standard evaluation metric for constituency parsing in most scenarios, which takes the ground truth and predicted trees and calculates the harmonic mean of precision and recall of labeled spans. For morphologically rich languages, TEDEVAl (Tsarfaty et al., 2012) extends PARSEVAL to accept multiple morphological analyses over sequences of words. All of these metrics are designed to evaluate parses over discrete word sequences and cannot be easily extended to evaluate speech parses over continuous time ranges. Although our metric, STRUCT-IOU, is designed to evaluate speech constituency parsing, it can be easily extended for text parsing evaluation, reflecting a different aspect from existing metrics (§5.4.2).

**Speech constituency parsing and its evaluation.** Work on conversational speech parsing has focused on addressing the unique challenges posed by speech, including speech recognition errors (Kahn and Ostendorf, 2012; Marin and Ostendorf, 2014), unclear sentence boundaries (Kahn et al., 2004), disfluencies (Jamshid Lou and Johnson, 2020; Kahn et al., 2005; Lease and Johnson, 2006), as well as integrating prosodic features into the parsing systems (Tran et al., 2018; Tran and Ostendorf, 2021). On the evaluation side, the closest work to ours is SPARSEVAL (Roark et al., 2006), which extends PARSEVAL to account for speech recognition errors by allowing for word-level insertion, deletion, and substitution. In contrast, our metric STRUCT-IOU applies to the cases where no speech recognizer is applied or available.

**Other structured evaluation metrics for parsing.** There have been evaluation metrics of abstract meaning representations (AMRs; Cai and Knight, 2013), where two AMR graphs are matched by solving an NP-complete integer linear programming problem. While our work shares the spirit with theirs, we focus on the evaluation of speech constituency

parsing over continuous word boundaries. A polynomial-time exact solution exists for our optimization problem.

## 5.2 Preliminaries

For simplicity, we use real-valued open intervals to represent speech spans, although most of the following definitions and conclusions can be easily extended to closed and half-open intervals. We start with basic operations over open intervals (§5.2.1) and then introduce relaxed segment trees (§5.2.2), which are used to represent parse trees.

### 5.2.1 Open Interval Operations

**Definition 5.1.** The **length** of a real-valued open interval  $I = (a, b)$ , where  $a < b$ , is  $|I| = b - a$ .

**Definition 5.2.** The **intersection size** of open intervals  $I_1$  and  $I_2$  is

$$\mathcal{I}(I_1, I_2) = \begin{cases} 0 & \text{if } I_1 \cap I_2 = \emptyset \\ |I_1 \cap I_2| & \text{otherwise.} \end{cases}$$

**Definition 5.3.** The **union size** of open intervals  $I_1$  and  $I_2$  is  $\mathcal{U}(I_1, I_2) = |I_1| + |I_2| - \mathcal{I}(I_1, I_2)$ .

**Definition 5.4.** The **intersection over union (IOU)** ratio between open intervals  $I_1$  and  $I_2$  is

$$\text{IOU}(I_1, I_2) = \frac{\mathcal{I}(I_1, I_2)}{\mathcal{U}(I_1, I_2)}.$$

We will use IOU as the similarity metric between two intervals.

### 5.2.2 Relaxed Segment Trees

To represent parse trees, we relax the definition of a segment tree (Bentley, 1977) as follows.

**Definition 5.5.** A **node**  $n$  of a relaxed segment tree is a triple  $n = \langle I_n, C_n, \ell_n \rangle$ , where

1.  $I_n = (s_n, e_n)$  is an open interval (i.e., segment) associated with the node  $n$ , where  $s_n < e_n$ ;

2.  $C_n$  is a finite set of disjoint children nodes of  $n$ : for any  $p, q \in C_n (p \neq q)$ ,  $I_p \cap I_q = \emptyset$ .  
 $C_n = \emptyset$  if and only if  $n$  is a terminal node;
3. For a nonterminal node  $n$ ,  $s_n = \min_{p \in C_n} s_p$ , and  $e_n = \max_{p \in C_n} e_p$ .

**Corollary 5.6.** For nodes  $p, n$ , if  $p \in C_n$ , then  $I_p \subseteq I_n$ .

*Proof.* According to the definition of open intervals and Definition 5.5 (3),

$$\begin{aligned} a_n &\leq a_p < b_p \leq b_n \\ \Rightarrow I_p = (a_p, b_p) &\subseteq (a_n, b_n) = I_n. \end{aligned}$$

□

**Definition 5.7.** Node  $p$  is an **ancestor** of node  $q$  if there exists a sequence of nodes  $n_0, n_1, \dots, n_k (k \geq 1)$  such that (i.)  $n_0 = p$ , (ii.)  $n_k = q$ , and (iii.) for any  $i \in [k]$ ,<sup>1</sup>  $n_i \in C_{n_{i-1}}$ .

**Corollary 5.8.** If node  $p$  is an ancestor of node  $q$ , then  $I_p \supseteq I_q$ .

*Proof.* According to Definition 5.7, there exists a sequence of nodes  $n_0, n_1, \dots, n_k (k \geq 1)$  such that (1)  $n_0 = p$ , (2)  $n_k = q$  and (3) for any  $i \in [k]$ ,  $n_i \in C_{n_{i-1}}$ .

Corollary 5.6 implies that for any  $i \in [k]$ ,  $I_{n_{i-1}} \supseteq I_{n_i} \Rightarrow I_{n_0} \supseteq I_{n_k} \Rightarrow I_p \supseteq I_q$ . □

**Definition 5.9.** Node  $p$  is a **descendant** of node  $q$  if  $q$  is an ancestor of  $p$ .

**Definition 5.10.** A **relaxed segment tree**  $\mathcal{T} = \langle r_{\mathcal{T}}, N_{\mathcal{T}} \rangle$  is a tuple, where

1.  $r_{\mathcal{T}}$  is the root node of  $\mathcal{T}$ ;
2.  $N_{\mathcal{T}} = \{r_{\mathcal{T}}\} \cup \{n : n \text{ is a descendant of } r_{\mathcal{T}}\}$  is a finite set of all nodes in  $\mathcal{T}$ .

**Example 5.11.** A relaxed segment tree can represent a constituency parse tree over spoken word time ranges (Figure 5.1a).

**Corollary 5.12.** A relaxed segment tree can be uniquely characterized by its root node.

*Proof.* ( $\Rightarrow$ ) Definition 5.10 implies that each relaxed segment tree has one root node.

( $\Leftarrow$ ) Given a specific node  $n$ , we have the unique set  $\mathcal{N} = \{n\} \cup \{n' : n' \text{ is a descendant of } n\}$ , and therefore extract the set of all nodes in the relaxed segment tree rooted at  $n$ . □

---

<sup>1</sup> $[k] = \{1, 2, \dots, k\}$ , where  $k \in \mathbb{N}$ .

In the following content, we use  $\mathcal{T}(\mathbf{n})$  to denote the relaxed segment tree rooted at  $\mathbf{n}$ .

**Proposition 5.13.** For a relaxed segment tree  $\mathcal{T}$  and  $\mathbf{p}, \mathbf{q} \in N_{\mathcal{T}}$ ,  $\mathbf{p}$  is neither an ancestor nor a descendant of  $\mathbf{q} \Leftrightarrow I_{\mathbf{p}} \cap I_{\mathbf{q}} = \emptyset$ .

*Proof.* ( $\Rightarrow$ ) Let  $z$  denote the least common ancestor of  $\mathbf{p}$  and  $\mathbf{q}$ . There exists  $\mathbf{p}', \mathbf{q}' \in C_z(\mathbf{p}' \neq \mathbf{q}')$  such that  $I_{\mathbf{p}'} \supseteq I_{\mathbf{p}}$  and  $I_{\mathbf{q}'} \supseteq I_{\mathbf{q}}$ ; therefore

$$I_{\mathbf{p}} \cap I_{\mathbf{q}} \subseteq I_{\mathbf{p}'} \cap I_{\mathbf{q}'} \stackrel{\text{Definition 5.5 (2)}}{=} \emptyset \Rightarrow I_{\mathbf{p}} \cap I_{\mathbf{q}} = \emptyset.$$

( $\Leftarrow$ ) If  $I_{\mathbf{p}} \cap I_{\mathbf{q}} = \emptyset$ , according to Definition 5.5 (3) and Definition 5.7,  $\mathbf{p}$  is not an ancestor of  $\mathbf{q}$  and vice versa.  $\square$

## 5.3 The STRUCT-IOU Metric

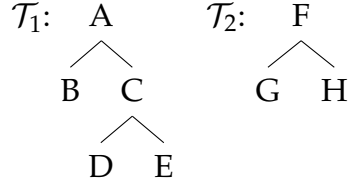
We present the definition of the structured average IOU (STRUCT-IOU) metric in §5.3.1, which measures the similarity between two relaxed segment trees. We also introduce a polynomial-time algorithm to compute the STRUCT-IOU metric in §5.3.2.

### 5.3.1 Problem Formulation

Given relaxed segment trees  $\mathcal{T}_1$  and  $\mathcal{T}_2$  with node sets  $N_{\mathcal{T}_1} = \{\mathbf{n}_{1,i}\}_{i=1}^{|N_{\mathcal{T}_1}|}$  and  $N_{\mathcal{T}_2} = \{\mathbf{n}_{2,j}\}_{j=1}^{|N_{\mathcal{T}_2}|}$ , we can align the trees by matching their same-label nodes. Let  $\mathbf{n}_{1,i} \leftrightarrow \mathbf{n}_{2,j}$  denote the matching between the nodes  $\mathbf{n}_{1,i}$  and  $\mathbf{n}_{2,j}$ .

**Definition 5.14** (conflicted node matchings; Figure 5.2). The matchings  $\mathbf{n}_{1,i} \leftrightarrow \mathbf{n}_{2,j}$  and  $\mathbf{n}_{1,k} \leftrightarrow \mathbf{n}_{2,\ell}$  are *conflicted* if any of the following conditions holds:

1.  $\mathbf{n}_{1,i}$  is an ancestor of  $\mathbf{n}_{1,k}$ , and  $\mathbf{n}_{2,j}$  is not an ancestor of  $\mathbf{n}_{2,\ell}$ ;
2.  $\mathbf{n}_{1,i}$  is not an ancestor of  $\mathbf{n}_{1,k}$ , and  $\mathbf{n}_{2,j}$  is an ancestor of  $\mathbf{n}_{2,\ell}$ ;
3.  $\mathbf{n}_{1,i}$  is a descendant of  $\mathbf{n}_{1,k}$ , and  $\mathbf{n}_{2,j}$  is not a descendant of  $\mathbf{n}_{2,\ell}$ ;
4.  $\mathbf{n}_{1,i}$  is not a descendant of  $\mathbf{n}_{1,k}$ , and  $\mathbf{n}_{2,j}$  is a descendant of  $\mathbf{n}_{2,\ell}$ .



- A  $\leftrightarrow$  G and E  $\leftrightarrow$  H: conflicted (violating rule 1)
- C  $\leftrightarrow$  F and A  $\leftrightarrow$  H: conflicted (violating rules 2 and 3)
- B  $\leftrightarrow$  H and C  $\leftrightarrow$  F: conflicted (violating rule 4)
- A  $\leftrightarrow$  F and C  $\leftrightarrow$  H: not conflicted

Figure 5.2: Examples of conflicted and non-conflicted node matchings (Definition 5.14).

Intuitively, we would like the alignment to be consistent with the ancestor-descendant relationship between nodes.

The optimal (i.e., maximally IOU-weighted) structured alignment between  $\mathcal{T}_1$  and  $\mathcal{T}_2$  is given by the solution to the following problem:

**Problem 5.15** (maximally IOU-weighted alignment).

$$\mathbf{A}^* = \arg \max_{\mathbf{A}} \sum_{i=1}^{|\mathcal{N}_{\mathcal{T}_1}|} \sum_{j=1}^{|\mathcal{N}_{\mathcal{T}_2}|} a_{i,j} \text{IOU} \left( I_{n_{1,i}}, I_{n_{2,j}} \right)$$

$$s.t. \sum_j a_{i,j} \leq 1 (\forall i \in [|\mathcal{N}_{\mathcal{T}_1}|]), \tag{5.1}$$

$$\sum_i a_{i,j} \leq 1 (\forall j \in [|\mathcal{N}_{\mathcal{T}_2}|]), \tag{5.2}$$

$$a_{i,j} + a_{k,\ell} \leq 1 \quad \text{if } n_{1,i} \leftrightarrow n_{2,j} \text{ and } n_{1,k} \leftrightarrow n_{2,\ell} \text{ are conflicted.}$$

$\mathbf{A} \in \{0, 1\}^{|\mathcal{N}_{\mathcal{T}_1}| \times |\mathcal{N}_{\mathcal{T}_2}|}$  denotes an alignment matrix:  $a_{i,j} = 1$  indicates that the matching  $n_{1,i} \leftrightarrow n_{2,j}$  is selected, otherwise  $a_{i,j} = 0$ . The last constraint of Problem 5.15 ensures that no conflicted matchings are selected. (5.1) and (5.2) imply one-to-one matching between nodes; that is, in a valid tree alignment, each node in  $\mathcal{T}_1$  can be matched with at most one node in  $\mathcal{T}_2$ , and vice versa. The solution to Problem 5.15 gives the maximal possible sum of IOU over aligned node pairs.

---

**Algorithm 3:** Polynomial time solution to Eq. (5.3)

---

**Input:**  $\mathcal{T}_1, \mathcal{T}_2$

**Output:** Eq. (5.3) =  $g[\mathcal{T}_1, \mathcal{T}_2, e_{r_{\mathcal{T}_1}}, e_{r_{\mathcal{T}_2}}]$

$g[\mathcal{T}_1, \mathcal{T}_2, x, y] \leftarrow 0, \forall x, y$

$g'[\mathcal{T}_1, \mathcal{T}_2, x, y] := \max_{x' < x, y' < y} g[\mathcal{T}_1, \mathcal{T}_2, x', y']$

$d_1 \leftarrow$  sequence of descendants of  $r_{\mathcal{T}_1}$ , sorted in increasing order of right endpoint

$d_2 \leftarrow$  sequence of descendants of  $r_{\mathcal{T}_2}$ , sorted in increasing order of right endpoint

**for**  $i \leftarrow 1 \dots, |d_1|$  **do**

**for**  $j \leftarrow 1 \dots, |d_2|$  **do**

$g[\mathcal{T}_1, \mathcal{T}_2, e_{d_{1,i}}, e_{d_{2,j}}] \leftarrow$

$\max \left( g[\mathcal{T}_1, \mathcal{T}_2, e_{d_{1,i}}, e_{d_{2,j}}], f_{\mathcal{T}(d_{1,i}), \mathcal{T}(d_{2,j})} + g'[\mathcal{T}_1, \mathcal{T}_2, s_{d_{1,i}}, s_{d_{2,j}}] \right)$

        update  $g'$  accordingly within  $\mathcal{O}(1)$  time

**end**

**end**

**return**  $g[\mathcal{T}_1, \mathcal{T}_2, e_{r_{\mathcal{T}_1}}, e_{r_{\mathcal{T}_2}}]$

---

**Definition 5.16.** The **structured average IOU** (STRUCT-IOU) between  $\mathcal{T}_1$  and  $\mathcal{T}_2$  is given by

$$\overline{\text{IOU}}(\mathcal{T}_1, \mathcal{T}_2) = \frac{1}{|N_{\mathcal{T}_1}| + |N_{\mathcal{T}_2}|} \sum_{i=1}^{|N_{\mathcal{T}_1}|} \sum_{j=1}^{|N_{\mathcal{T}_2}|} a_{i,j}^* \text{IOU}(I_{n_{1,i}}, I_{n_{2,j}}),$$

where  $A^* = \{a_{i,j}^*\}$  is the solution to Problem 5.15.

### 5.3.2 Solution

We present a polynomial-time algorithm for the exact solution to Problem 5.15 by breaking it down into structured subproblems and solving them recursively with dynamic programming.

We define the subproblem as follows: given relaxed segment trees  $\mathcal{T}_1$  and  $\mathcal{T}_2$ , we would like to find the maximum IOU weighted alignment of  $\mathcal{T}_1$  and  $\mathcal{T}_2$ , where the roots of  $\mathcal{T}_1$  and  $\mathcal{T}_2$  are aligned. Without loss of generality, we assume that the root nodes of  $\mathcal{T}_1$  and  $\mathcal{T}_2$  are both indexed by 1. Formally,

**Problem 5.17** (maximum IOU weighted alignment, with root nodes aligned).

$$f_{\mathcal{T}_1, \mathcal{T}_2} = \max_{\mathbf{A}} \sum_{i=1}^{|\mathcal{T}_1|} \sum_{j=1}^{|\mathcal{T}_2|} a_{i,j} \text{IOU} \left( I_{n_{1,i}}, I_{n_{2,j}} \right)$$

$$\text{s.t. } a_{1,1} = 1;$$

$$\sum_j a_{i,j} \leq 1 (\forall i \in [|\mathcal{T}_1|]),$$

$$\sum_i a_{i,j} \leq 1 (\forall j \in [|\mathcal{T}_2|]),$$

$$a_{i,j} + a_{k,\ell} \leq 1 \quad \text{if } n_{1,i} \leftrightarrow n_{2,j} \text{ and } n_{1,k} \leftrightarrow n_{2,\ell} \text{ are conflicted,}$$

where  $\mathbf{A} \in \{0,1\}^{|\mathcal{T}_1| \times |\mathcal{T}_2|}$  is the alignment matrix.

While Problems 5.15 and 5.17 are not equivalent in principle, Problem 5.15 can be reduced to Problem 5.17 within  $\mathcal{O}(1)$  time, by adding a dummy root node to each tree that associates with segments covering all the segments in both trees. We now present a polynomial-time solution to Problem 5.17.

**Definition 5.18.** Given a node  $n$  of a relaxed segment tree,  $\mathbf{D} = (n_1, n_2, \dots, n_k)$  is an **ordered disjoint descendant sequence** of  $n$  if

1. (ordered) for any  $i, j \in [k]$  and  $i < j$ ,  $s_{n_i} < s_{n_j}$ , where  $s_{n_i}$  and  $s_{n_j}$  are left endpoint of the associated intervals;
2. (disjoint) for any  $i, j \in [k]$  and  $i \neq j$ ,  $I_{n_i} \cap I_{n_j} = \emptyset$ ;
3. (descendant) for any  $i \in [k]$ ,  $n_i$  is a descendant of  $n$ .

**Corollary 5.19.** In an ordered disjoint descendant sequence  $\mathbf{D} = (n_1, n_2, \dots, n_k)$  of  $n$ ,  $e_{n_i} \leq s_{n_{i+1}}$  for any  $i \in [k-1]$ .

*Proof.* If there exists  $i \in [k-1]$  such that  $b_{n_i} > a_{n_{i+1}}$ , then

$$\begin{aligned} & I_{n_i} \cap I_{n_{i+1}} \\ &= (a_{n_i}, b_{n_i}) \cap (a_{n_{i+1}}, b_{n_{i+1}}) \\ &= \{x : \max(a_{n_i}, a_{n_{i+1}}) < x < \min(b_{n_i}, b_{n_{i+1}})\} \\ &= \{x : a_{n_{i+1}} < x < \min(b_{n_i}, b_{n_{i+1}})\} \quad (\text{Definition 5.18 (1)}). \end{aligned}$$



Since  $b_{n_{i+1}} > a_{n_{i+1}}$  (definition of open intervals),

$$a_{n_{i+1}} < \min(b_{n_i}, b_{n_{i+1}}) \Rightarrow I_{n_i} \cap I_{n_{i+1}} \neq \emptyset.$$

This conflicts with Definition 5.18 (2). □

The solution to Problem 5.17 is given by the following recursion:

$$f_{\mathcal{T}_1, \mathcal{T}_2} = \text{IOU} \left( I_{r_{\mathcal{T}_1}}, I_{r_{\mathcal{T}_2}} \right) + \max_{|\mathbf{D}_1|=|\mathbf{D}_2|} \sum_{i=1}^{|\mathbf{D}_1|} f_{\mathcal{T}(d_{1,i}), \mathcal{T}(d_{2,i})}, \quad (5.3)$$

where  $r_{\mathcal{T}_1}$  and  $r_{\mathcal{T}_2}$  denote the root nodes of  $\mathcal{T}_1$  and  $\mathcal{T}_2$  respectively;  $|\cdot|$  denotes the length of a sequence;  $\mathbf{D}_1 = (d_{1,1}, d_{1,2}, \dots, d_{1,|\mathbf{D}_1|})$  and  $\mathbf{D}_2 = (d_{2,1}, d_{2,2}, \dots, d_{2,|\mathbf{D}_2|})$  are same-length ordered disjoint descendant sequences of  $r_{\mathcal{T}_1}$  and  $r_{\mathcal{T}_2}$  respectively. Eq. (5.3) can be computed within polynomial time by solving a knapsack-style problem with dynamic programming. Specifically, let

$$g[\mathcal{T}_1, \mathcal{T}_2, e_1, e_2] = \max_{|\mathbf{D}_1^{e_1}|=|\mathbf{D}_2^{e_2}|} \sum_{j=1}^{|\mathbf{D}_1^{e_1}|} f_{\mathcal{T}(d_{1,j}^{e_1}), \mathcal{T}(d_{2,j}^{e_2})},$$

where  $e_1$  and  $e_2$  are arbitrary scalars denoting the constraints of endpoints;

$\mathbf{D}_1^{e_1} = (d_{1,1}^{e_1}, \dots, d_{1,|\mathbf{D}_1^{e_1}|}^{e_1})$  is an ordered disjoint descendant sequence of  $r_{\mathcal{T}_1}$ , where for any  $j \in [|\mathbf{D}_1^{e_1}|]$ , the right endpoint of the corresponding node  $e_{d_{1,j}^{e_1}} \leq e_1$ ; similarly,  $\mathbf{D}_2^{e_2} = (d_{2,1}^{e_2}, d_{2,2}^{e_2}, \dots, d_{2,|\mathbf{D}_2^{e_2}|}^{e_2})$  is a disjoint descendant sequence of  $r_{\mathcal{T}_2}$  of which the right endpoint of each node does not exceed  $e_2$ . Algorithm 3 computes  $g$  and Eq. (5.3) within polynomial time, and therefore leads to a polynomial-time solution to Problem 5.17.

**Complexity analysis.** Suppose  $|\mathcal{T}_1| = n$  and  $|\mathcal{T}_2| = m$ . To compute  $f_{\mathcal{T}_1, \mathcal{T}_2}$ , all we need to compute is  $g[\mathcal{T}'_1, \mathcal{T}'_2, e'_1, e'_2]$  for all  $\mathcal{T}'_1, \mathcal{T}'_2, e'_1$  and  $e'_2$ . Here,  $\mathcal{T}'_1$  and  $\mathcal{T}'_2$  enumerate over all subtrees of  $\mathcal{T}_1$  and  $\mathcal{T}_2$ , respectively, and  $e'_1$  and  $e'_2$  enumerate over the endpoints of all nodes in both trees, respectively. The update process requires  $\mathcal{O}(1)$  time for each  $\mathcal{T}_1, \mathcal{T}_2, e_1, e_2$ . The edge cases, i.e.,  $g$  values of terminal nodes, can be directly computed in  $\mathcal{O}(1)$  time, and therefore, the overall time complexity to solve Problem 5.17 is  $\mathcal{O}(n^2m^2)$ .

## 5.4 Experiments

We present two example applications of STRUCT-IOU: speech constituency parsing evaluation (§5.4.1) and text constituency parsing evaluation (§5.4.2), where the former is our main focus. In each part, we show the connection between STRUCT-IOU and existing metrics in appropriate settings and present the unique features of STRUCT-IOU.

### 5.4.1 Speech Constituency Parsing Evaluation

#### Datasets and Setups

We use the NXT-Switchboard (NXT-SWBD; Calhoun et al., 2010) dataset to train and evaluate models, where the parser can access the forced alignment word boundaries in both training and testing stages. We train an off-the-shelf supervised constituency parsing model for speech transcriptions (Jamshid Lou and Johnson, 2020) on the training set of NXT-SWBD, do early-stopping using PARSEVAL  $F_1$  on the development set, and perform all the analysis below on the development set. The model achieves  $F_1 = 85.4$  and STRUCT-IOU (averaged across sentences)<sup>2</sup> = 0.954 on the standard development set.

#### Comparison to the PARSEVAL $F_1$ score

Since the forced alignment word boundaries are accessible by the models, the PARSEVAL  $F_1$  metric can be directly calculated between the predicted speech constituency parse tree and the ground truth. We compare the values of STRUCT-IOU and PARSEVAL (Sekine and Collins (1997) implementation with default parameters) in the settings with forced-alignment word segmentation (Figure 5.3), and find a strong correlation between the two metrics.

#### Analysis: STRUCT-IOU with Perturbed Word Boundaries

In textless speech parsing (Lai et al., 2023; Tseng et al., 2023), the word boundaries are unknown, and the parser-predicted word boundaries are usually imperfect. As a con-

---

<sup>2</sup>Unless otherwise specified, all STRUCT-IOU scores reported in this dissertation are computed by averaging across STRUCT-IOU scores of individual sentences. We compare and discuss sentence-level and corpus-level STRUCT-IOU in §5.4.1

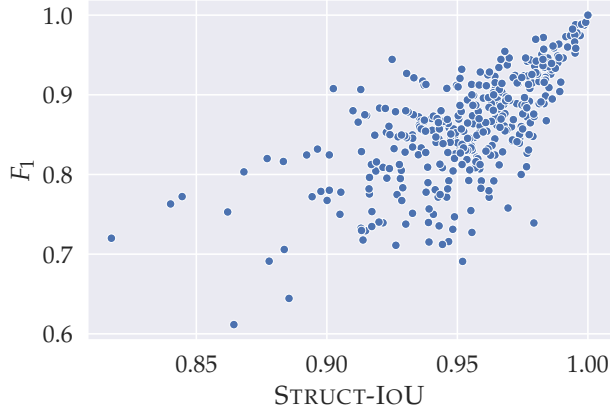


Figure 5.3: STRUCT-IOU vs. PARSEVAL  $F_1$  on NXT-SWBD (Spearman’s correlation  $\rho = 0.689$ , p-value= $1.79 \times 10^{-54}$ ). Each dot represents the results of the base model ( $F_1=85.4$  on the full development set) on ten random examples from the development set.

trolled simulation to such settings, we perturb the forced alignment word boundaries of the predicted parse tree (Figure 5.4), and calculate the STRUCT-IOU score between the perturbed parse tree and the ground truth over the original forced alignment word boundaries. Specifically, we suppose the word boundaries of a sentence with  $n$  words are  $\mathcal{B} = b_0, b_1, \dots, b_n$ ,<sup>3</sup> and consider the following types of perturbation with a hyperparameter  $\delta \in [0, 1]$  controlling the perturbation level:

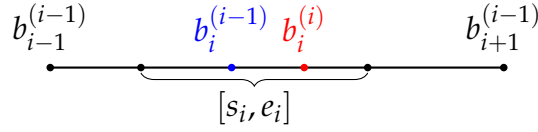
- **Noise- $\delta$ .** We start with  $\mathcal{B}^{(0)} = \mathcal{B}$ , and update the boundaries iteratively as follows. For each  $i \in [n - 1]$ , we randomly draw a number  $r_i$  from the uniform distribution  $U(-\delta, \delta)$ , and let  $b_i^{(i)} = b_i^{(i-1)} + |r_i| * \left( b_{i+\text{sgn}(r_i)}^{(i-1)} - b_i^{(i-1)} \right)$ , where  $\text{sgn}(\cdot) : \mathbb{R} \rightarrow \{1, -1\}$  denotes the sign function

$$\text{sgn}(x) = \begin{cases} 1 & \text{if } x \geq 0; \\ -1 & \text{if } x < 0. \end{cases}$$

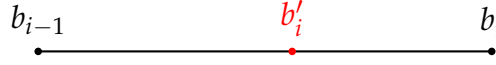
For all  $j \neq i$  and  $j \in [n]$ , we let  $b_j^{(i)}$  remain the same as  $b_j^{(i-1)}$ . Finally, we take  $\mathcal{B}^{(n-1)}$  as the perturbed word boundaries for the predicted tree.

- **Insert- $\delta$ .** We randomly draw a number  $r_i$  from the uniform distribution for each boundary index  $i \in [n]$ . If  $r_i < \delta$ , we insert a word boundary at the position  $b'_i$ ,

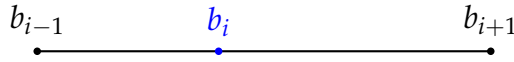
<sup>3</sup>We assume no silence between spoken words; if any inter-word silence exists, we remove it.



(a) Noise- $\delta$ , where  $s_i = b_i^{(i-1)} - \delta \cdot (b_i^{(i-1)} - b_{i-1}^{(i-1)})$  and  $e_i = b_i^{(i-1)} + \delta \cdot (b_{i+1}^{(i-1)} - b_i^{(i-1)})$  denote the most left and right possible position of  $b_i^{(i)}$ .



(b) Insert- $\delta$ , with  $r_i < \delta$ ; otherwise  $b'_i$  will not be inserted.



(c) Delete- $\delta$ , with  $r_i < \delta$ ; otherwise  $b_i$  will not be deleted.

Figure 5.4: Examples of three types of perturbation: when applicable, the added boundaries are shown in red, and the deleted boundaries are shown in blue. Best viewed in color.

randomly drawn from the uniform distribution  $U(b_{i-1}, b_i)$ , breaking the  $i^{\text{th}}$  spoken word into two (i.e.,  $[b_{i-1}, b'_i]$  and  $[b'_i, b_i]$ ).

- **Delete- $\delta$ .** Similarly to the insertion-based perturbation, we randomly draw a number  $r_i$  from the uniform distribution  $U(0, 1)$  for each boundary index  $i \in [n - 1]$ , and delete the boundary  $b_i$  if  $r_i < \delta$ . Since such boundary deletion may break the predicted tree structure, we use the base model (§5.4.1) to re-predict the parse tree with the new word boundaries, where words concatenated by space are taken as the textual input (Jamshid Lou and Johnson, 2020).

A larger  $\delta$  means a higher level of perturbation is applied, and we, therefore, expect a lower STRUCT-IOU score;  $\delta = 0$  means no perturbation is applied, and the STRUCT-IOU score is the same as that for the predicted parse trees with forced alignment word boundaries.

For each  $\delta \in \{0.1, 0.2, \dots, 1.0\}$ , starting from the base model (for deletion-based perturbation) or its predicted parse trees (for noise and insertion-based perturbation), we run the perturbation five times and report both the mean and the standard deviation of the STRUCT-IOU result after perturbation.

**Results and discussion.** We present how the STRUCT-IOU value changes with respect to  $\delta$  for different types of perturbation (Figure 5.5). The figure’s standard deviation is nearly invisible, showing that our metric is stable under a specific setting. As desired, a

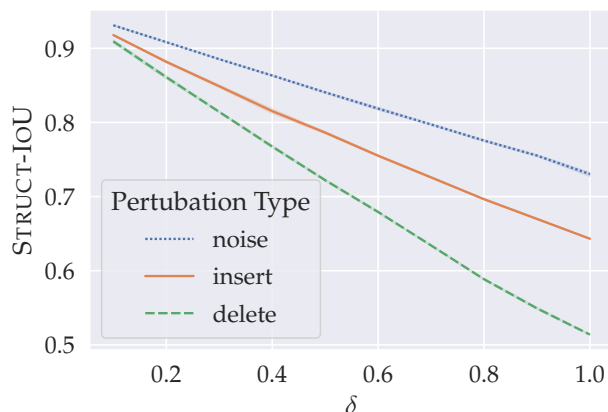


Figure 5.5: STRUCT-IoU scores with respect to  $\delta$  for different types of perturbations.

larger  $\delta$  leads to a lower STRUCT-IoU score for all three types of perturbation. Among the perturbation types, STRUCT-IoU is the most sensitive to deletion and the least sensitive to noise-based perturbation. Although the results are not comparable across perturbation types in the most rigorous sense, this reflects that STRUCT-IoU, to some extent, is more sensitive to structural change of the trees than simple word boundary changes.

Although both word boundary insertion and deletion change the predicted tree structures, the former has less impact on the STRUCT-IoU scores. This also aligns with our expectation: boundary insertion only splits some of the spoken words into two and keeps the longer constituents; however, deletion may significantly change the tree structure, especially when it happens at the boundary of two long constituents.

### Corpus-Level vs. Sentence-Level Metric

Note that 39.7% utterances in the NXT-SWBD development set contain only one spoken word, and the STRUCT-IoU score of such sentences is always high—the metric degenerates to the IoU score between two intervals. Averaging the STRUCT-IoU scores across all sentence pairs in the dataset may therefore overly emphasize these short utterances. To address this, we introduce the corpus-level STRUCT-IoU score as an alternative, where Definition 5.16 is modified as follows:

**Definition 5.20.** The corpus-level STRUCT-IoU between two sets of parsed trees  $\mathcal{D}_1 =$

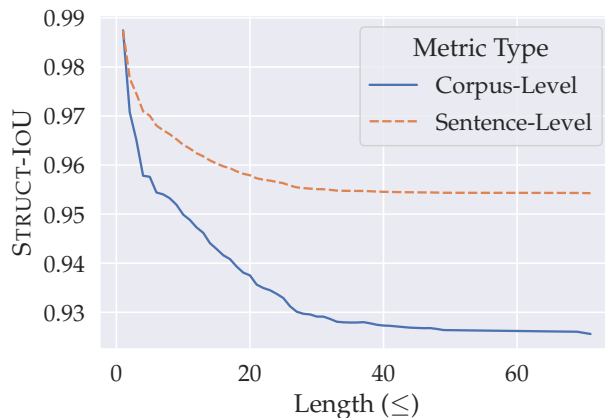


Figure 5.6: Corpus-level and sentence-level STRUCT-IOU scores of the predicted parse trees of the base model ( $F_1 = 85.4$  on the development set), evaluated on development examples with less than or equal to a certain number of spoken words.

$\{\mathcal{T}_{1,k}\}$  and  $\mathcal{D}_2 = \{\mathcal{T}_{2,k}\}$  is given by

$$\overline{\text{IOU}}(\mathcal{D}_1, \mathcal{D}_2) = \frac{\sum_{k=1}^{|\mathcal{D}_1|} (|\mathcal{T}_{1,k}| + |\mathcal{T}_{2,k}|) \overline{\text{IOU}}(\mathcal{T}_{1,k}, \mathcal{T}_{2,k})}{\sum_{k'=1}^{|\mathcal{D}_1|} |\mathcal{T}_{1,k'}| + |\mathcal{T}_{2,k'}|},$$

where  $|\mathcal{D}_1| = |\mathcal{D}_2|$ , and a pair of  $\mathcal{T}_{1,k}$  and  $\mathcal{T}_{2,k}$  denotes the parse trees of the  $k^{\text{th}}$  sentence in the corpus respectively.

We compare the corpus-level and sentence-level STRUCT-IOU scores (Figure 5.6). As desired, the corpus-level STRUCT-IOU score has lower absolute values than the sentence-level one, and the difference is more significant when longer sentences are considered. A similar phenomenon has also been found in text constituency parsing (Kim et al., 2019) where corpus-level PARSEVAL  $F_1$  scores are lower than sentence-level ones.

#### 5.4.2 Text Constituency Parsing Evaluation: English

We extend our experiment to the evaluation of text constituency parsing. In this subsection, we suppose every written word corresponds to a segment of the same unit length—analogously, this can be considered speech parsing with evenly distributed word boundaries for both predicted and ground-truth trees.

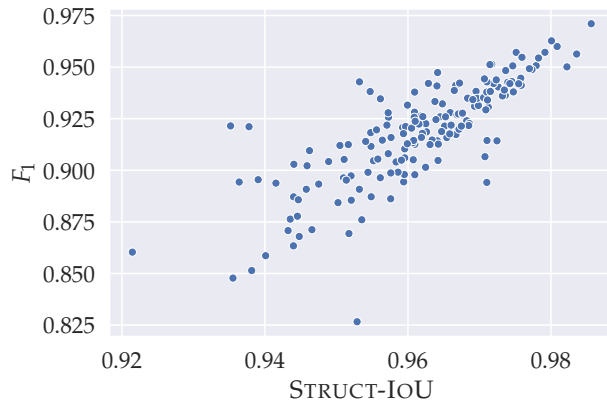


Figure 5.7: Comparison of STRUCT-IOU and PARSEVAL  $F_1$  (Spearman’s rank correlation  $\rho = 0.821$ ,  $p\text{-value} = 8.16 \times 10^{-43}$ ). Each dot represents the results of the base model on 10 random examples from the PTB development set.

### Correlation with PARSEVAL $F_1$ Scores on the Penn Treebank

We use the Penn Treebank (PTB; Marcus et al., 1993) dataset to train and evaluate Benepar (Kitaev and Klein, 2018), a state-of-the-art text constituency parsing model, doing early-stopping using labeled PARSEVAL  $F_1$  on the development set. The base model achieves PARSEVAL  $F_1 = 94.4$  and STRUCT-IOU (averaged across sentences) = 0.962 on the standard development set.

We compare the STRUCT-IOU scores with the PARSEVAL  $F_1$  scores on the development set (Figure 5.7). As in the speech parsing experiment, we find a strong correlation between the two metrics, showing that STRUCT-IOU is consistent with the existing metric in the text parsing domain.

### STRUCT-IOU vs. PARSEVAL $F_1$ on Syntactically Ambiguous Sentences

We consider a particular setting of parsing syntactically ambiguous sentences, where the syntactically plausible parse tree of a sentence may not be unique (see examples in Figure 5.8). We simplify the case shown in Figure 5.8 and generate synthetic sentences with syntactic ambiguity with the template  $N (P N)\{n\}$ , where  $P$  denotes a preposition and  $N$  denotes a noun, and  $n$  determines how many times the  $P N$  pattern is repeated. For  $N (P N)\{2\}$ , the two potential parse trees are shown in Figure 5.9.

We compare the PARSEVAL and STRUCT-IOU in the following scenarios, choosing a

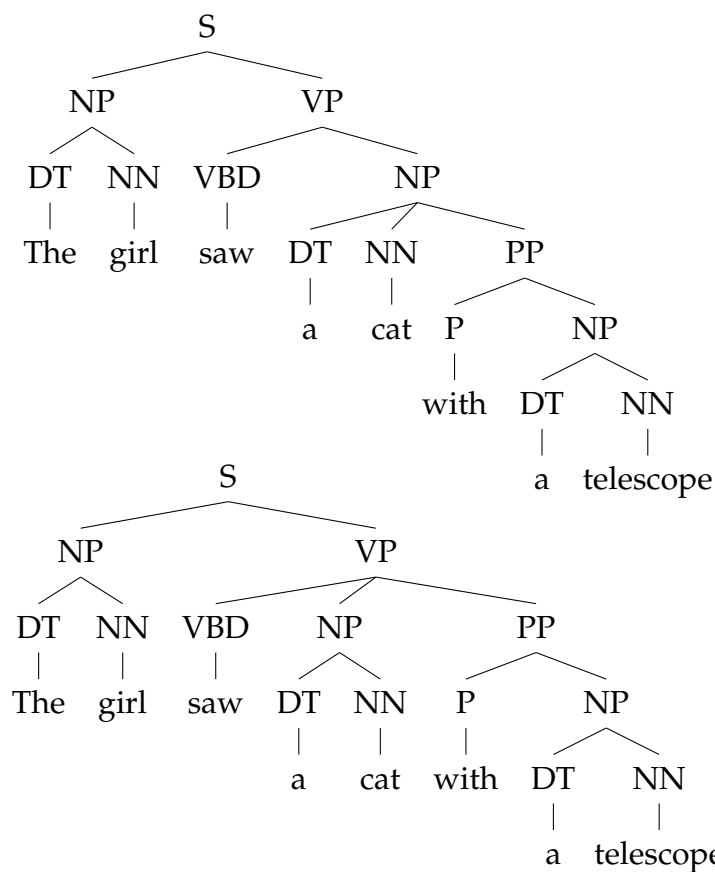


Figure 5.8: An example syntactically ambiguous sentence: *The girl saw a cat with a telescope*. Both parses are syntactically valid, but the first one implies that *a cat* was holding the telescope, whereas the second implies *the girl* was using the telescope.

random syntactically plausible parse tree as the ground truth:

- **Ground truth vs. random parse trees**, where the random parse trees are constructed by recursively combining random consecutive words (or word groups) into a binary tree. We construct 100 random parse trees and report the average.
- **Ground truth vs. syntactically plausible parse trees**, where we report the lowest possible score between the ground truth and other syntactically plausible trees.

As shown in Table 5.1, the lowest possible PARSEVAL  $F_1$  score between the ground truth and another syntactically plausible tree is significantly lower than the score achieved by meaningless random trees; however, STRUCT-IOU consistently assigns higher scores to the syntactically plausible parses, showing more tolerance to syntactic ambiguity.



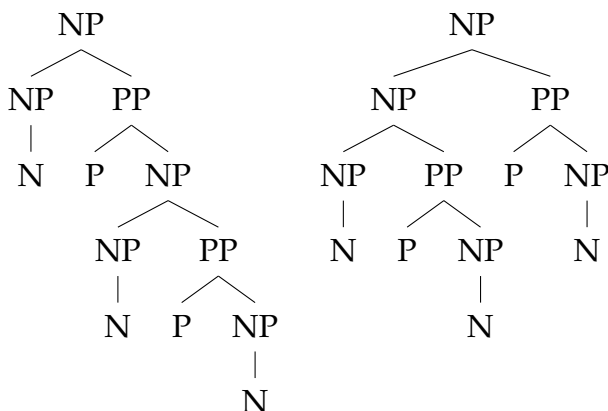


Figure 5.9: Two syntactically plausible parses of the  $N (P N)^2$ , where NP denotes a noun phrase, and PP denotes a prepositional phrase.

Metric	Ground-Truth vs. Random, Average
PARSEVAL $F_1$	27.3
STRUCT-IOU	61.9
Ground-Truth vs. Plausible, Lowest	
PARSEVAL $F_1$	12.5
STRUCT-IOU	63.6

Table 5.1: Average PARSEVAL  $F_1$  and STRUCT-IOU scores between the ground truth and a random binary tree, and the lowest possible scores between the ground truth and another syntactically plausible tree. Experiments are done on the string “ $N (P N)^8$ ”. For simplicity, we report the unlabeled scores, where all nonterminals are treated as having the same label.

### 5.4.3 Text Constituency Parsing Evaluation: Hebrew

We extend our experiment to the evaluation of text constituency parsing on Hebrew, a morphologically rich language that allows different tokenizations of the same sentence. In this subsection, we suppose every written character (instead of a word for English; §5.4.2) corresponds to a segment of the same unit length. We evaluate STRUCT-IOU by running a pre-trained Hebrew constituency parsing model (benepar\_he2; Kitaev et al., 2019) on the SPMRL 2013 Hebrew development set (Seddah et al., 2013). Similarly to the English text

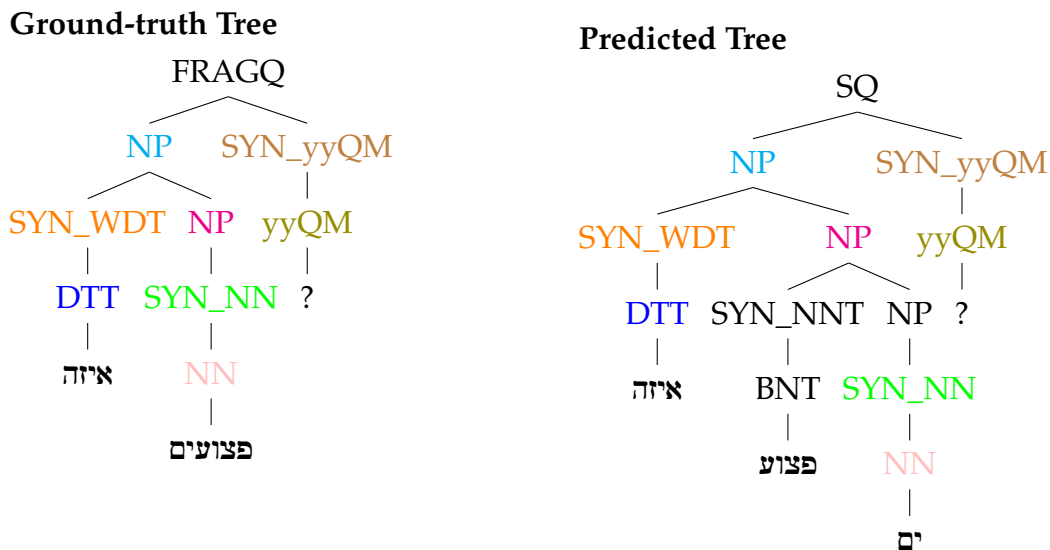


Figure 5.10: Parse trees of the Hebrew sentence `איזה פצעים?` with two possible morphological analyses (STRUCT-IOU = 0.635). The plural morpheme `ים` appears as a separate token in the right-hand side tree. Best viewed in color: the aligned nodes on both sides are shown in the same color.

parsing evaluation result (§5.4.2), we obtain a high Spearman rank correlation coefficient of 0.823 (over 10-sentence buckets) between STRUCT-IOU (0.959 averaged across sentences) and PARSEVAL F1 scores measured by EVALB-SPMRL (93.3).

In addition, we demonstrate that STRUCT-IOU naturally provides a metric that supports misaligned morphological analysis. The default tokenization in the SPMRL dataset does not extract the plural morphemes `ות` and `ים`; therefore, simply extracting the plural morphemes forms another acceptable tokenization strategy (see Figure 5.10 for an example). We break the nouns ending with these two morphemes and feed the new tokenization to the `benepar_he2` model.<sup>4</sup> The prediction with our new tokenization receives a STRUCT-IOU of 0.907 against the ground-truth—as desired, it is lower than 0.959 with the ground-truth tokenization. However, the STRUCT-IOU score remains high, reflecting the facts that (1) the manipulation introduces misalignment between parses, and (2) the Benepar model is fairly robust to such mismatch on tokenization (see Footnote 4). In contrast to TEDEVAL (Tsarfaty et al., 2012), which aligns the tree structures by deleting

<sup>4</sup>The `benepar_he2` model is not trained on this tokenization; however, we expect the model still works well, since it uses XLM-R (Conneau et al., 2020) as the word embeddings, which provides syntactic information of the new tokenization.

and adding nodes (Bille, 2005) and takes into account these edits in the PARSEVAL-based evaluation, STRUCT-IOU provides an alternative way to evaluate the parsing quality under misaligned morphological analyses: instead of treating all the misaligned nodes as errors that result in the same penalization in the final metric, STRUCT-IOU assigns partial credit to the aligned same-label nodes with  $\text{IOU} > 0$ .

## 5.5 Conclusion and Discussion

In this chapter, we present STRUCT-IOU, the first metric that computes the similarity between two parse trees over continuous spoken word boundaries. STRUCT-IOU enables the evaluation of textless speech parsing (Lai et al., 2023; Tseng et al., 2023), where no text or speech recognizer is used or available to parse spoken utterances.

In the canonical text and speech parsing settings, STRUCT-IOU complements the existing evaluation metrics (Black et al., 1991; Roark et al., 2006; Tsarfaty et al., 2012). Even for the evaluation of English constituency parsing, STRUCT-IOU shows a higher tolerance to potential syntactic ambiguity under certain scenarios, providing an alternative interpretation of the parsing quality.

Faithful evaluation of parsing quality is crucial for developing both speech and text parsing models. In supervised parsing, it has been common sense that higher evaluation metric scores (i.e., PARSEVAL  $F_1$ ) imply better models. However, as we discussed in Shi et al. (2020), the misalignment between linguistically annotated ground truths and model predictions, especially unsupervised parsing model predictions, does not necessarily indicate poor parsing quality of the models—instead, the models may have learned different but equally valid structures. Conversely, annotations made by linguistic experts (such as the Penn Treebank) may exhibit discrepancies when compared to the responses of native speakers who lack formal linguistic training. We suggest that future work investigate what properties of the parses are emphasized by each evaluation metric, and consider multi-dimensional evaluation metrics (Kasai et al., 2022, *inter alia*).

## **Part II**

# **Learning to Parse through Program Execution**

## Chapter 6

# Joint Syntax and Semantics Induction in Grounded Environments

*Content in this chapter has been published as a conference paper at NeurIPS 2021 (Mao et al., 2021). Jiayuan Mao is the lead author of this work.*

We now start to consider program execution results as another source of grounding signals and consider using distant supervisions from both vision and program execution for grammar induction. In this chapter, we present Grammar-Based Grounded Lexicon Learning (G2L2), a lexicalist approach toward learning a compositional and grounded meaning representation of language from grounded data, such as paired images and texts. At the core of G2L2 is a collection of lexicon entries, which map each word to a tuple of a syntactic type and a neuro-symbolic semantic program. In Figure 6.1, for example, the word *shiny* has a syntactic type of *adjective*; its neuro-symbolic semantic program has the *symbolic* form  $\lambda x.filter(x, \mathbf{SHINY})$ , where the concept **SHINY** is associated with a *neural network* embedding, which will be used to classify shiny objects. Given an input sentence, G2L2 first looks up the lexicon entries associated with each token. It then derives the meaning of the sentence as an executable neuro-symbolic program by composing lexical meanings based on syntax. These programs can be executed on grounded inputs. To facilitate learning in an exponentially growing compositional space, we introduce a joint parsing and expected execution algorithm (CKY-E<sup>2</sup>), which does local marginalization over derivations to reduce the training time. We evaluate G2L2 on two domains: visual reasoning and language-driven navigation. Results show that G2L2 can generalize from small amounts of data to novel compositions of words.

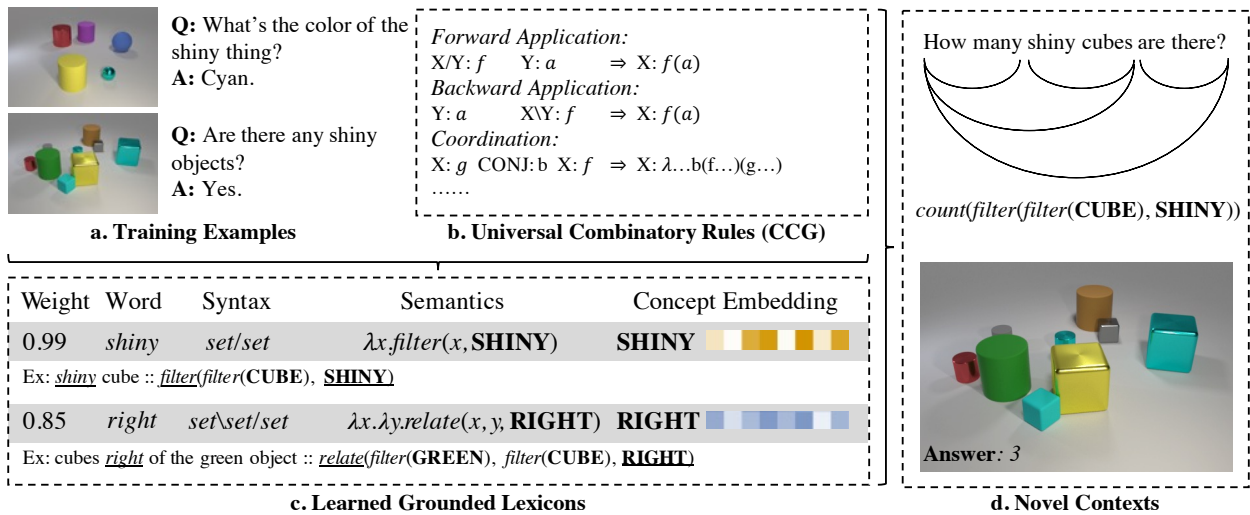


Figure 6.1: Illustration of idea of grounded lexicon learning. The model learns from grounded language data, for example, by looking at images and reading parallel question-answer pairs. It learns a collection of grounded lexicon entries comprised of weights, syntax types, semantics forms, and, optionally, grounded embeddings associated with semantic concepts. These lexicon entries can be used to parse questions into programs.

## 6.1 Related Work

**Lexicalist theories.** The lexicalist theories of syntax (Pollard and Sag, 1994; Steedman, 2000; Bresnan et al., 2016) argue that (1) the key syntactic principles by which words and phrases combine are extremely simple and general, and (2) nearly all of the complexity in syntax can be attributed to rich and detailed lexical entries for the words in the language. For example, whereas the relationship between the active and passive voice, e.g., “Kim saw a balloon” versus “A balloon was seen by Kim”, was treated in pre-lexicalist theories as a special syntactic rule converting between the sentences, in lexicalist theories, this relationship derives simply from the knowledge that the passive participle for the verb “see” is “seen,” which interacts with knowledge of other words to make both the active and passive forms of the sentence possible. In lexicalist theories, the problem for the language learner thus becomes a problem of learning the words in the language, not a problem of learning numerous abstract rule schemas. The combinatory categorial grammar (CCG; Steedman, 2000) framework we use is a well-established example of a lexicalist theory: there is a universal inventory of just three combinatory rules (Figure 6.1a), but those rules

can only be applied once richly specified lexical entries are learned for the words in a sentence. We believe that this lexicalist-theory approach is a particularly good fit for the problem of grounded language learning: the visual context provides clues to the meaning of a word, and the grammatical behavior of the word is tied closely to this meaning. This linking makes learning efficient.

**Compositional generalization in NLP.** Improving the compositional generalization of NLP systems has drawn great attention in recent years (Baroni, 2020). Most recent approaches towards this goal are built on deep learning-based models. There are two representative approaches: building structured neural networks with explicit phrase-based structures or segments (Socher et al., 2013; Zhu et al., 2015; Tai et al., 2015; Shi et al., 2018; Saqur and Narasimhan, 2020); and using data augmentation techniques (Andreas, 2020; Guo et al., 2020; Akyürek et al., 2021). However, these approaches either rely on additional annotation or pre-trained models for phrase structure inference or require domain-specific heuristics in data augmentation. In contrast to both approaches, we propose to use combinatory grammar rules to constrain the learning of word meanings and how they are composed.

**Neural latent trees.** CKY-E<sup>2</sup> is related to recent work using CKY-style modules for inducing latent trees. However, our model is fundamentally different from work on unsupervised constituency parsing (Kim et al., 2019; Shi et al., 2021, *inter alia*), which use the CKY algorithm for inference over scalar span scores and those compute span representation vectors with CKY-style algorithms (Maillard and Clark, 2018; Drozdov et al., 2019, *inter alia*). Our key contribution is introducing the expected execution mechanism, where each span is associated with weighted, compressed programs. Beyond enumerating all possible parsing trees as in (Maillard and Clark, 2018), G2L2 considers all possible programs associated with each span. Our expected execution procedure works for different types (object set, integer, etc.) and even functor types, which makes our approximation exact for linear cases with polynomial complexity.

**Grammar-based grounded language learning.** There have also been work that learns grammatical structures from grounded texts (Artzi and Zettlemoyer, 2013; Shi et al., 2019; Zhao and Titov, 2020; Jin and Schuler, 2020). However, these approaches either rely on pre-defined lexicon entries (Artzi and Zettlemoyer, 2013) or only focus on inducing syntactic structures such as phrase-structure grammar (Shi et al., 2019, *inter alia*). Different from them, G2L2 jointly learns the syntactic types, semantic programs, and concept grounding,

only based on a small set of combinatory grammar rules.

Grammar-based and grounded language learning has also been studied in linguistics, with related work to ours studying how humans use grammar as constraints in learning meaning (Steedman, 2000) and how learning syntactic rules and semantic meanings in language bootstrap each other (Abend et al., 2017; Taylor and Gelman, 1988). However, most previous computational models have focused only on explaining small-scale lab experiments and do not address grounding in visual perception (Fazly et al., 2010; Gauthier et al., 2018). In contrast, G2L2 is a neuro-symbolic model that integrates the combinatory categorial grammar formalism (Steedman, 2000) with joint perceptual learning and concept learning to learn meanings from images and texts directly.

**Neuro-symbolic models for language grounding.** Integrating symbolic structures such as programs and neural networks has shown success in modeling compositional queries in various domains, including image and video reasoning (Hu et al., 2017; Mascharka et al., 2018), knowledge base query (Andreas et al., 2016), and robotic planning (Andreas et al., 2017). This work uses symbolic domain-specific languages with neural network embeddings for visual reasoning in images and navigation sequence generation, following NS-CL (Mao et al., 2019). However, in contrast to using a neural network-based semantic parser as in the aforementioned work, our model G2L2 focuses on learning grammar-based lexicon for compositional generalization in linguistic structures, such as novel word composition.

## 6.2 Grammar-Based Grounded Lexicon Learning

Our framework, G2L2, learns grounded lexicons from cross-modal data, such as paired images and texts. This section will use the visual reasoning task, specifically visual question answering (VQA), as the example. However, the idea itself can be applied to other tasks and domains, such as image captioning and language-driven navigation.

G2L2 learns from a collection of VQA data tuples containing an image, a question, and an answer to the question. In G2L2, each word type  $w$  is associated with one or multiple lexical entries comprising their syntactic types and semantic programs. Given the input question, G2L2 first looks up the lexicon entries associated with each token in the sentence (Figure 6.2I). G2L2 then uses a chart parsing algorithm to derive the



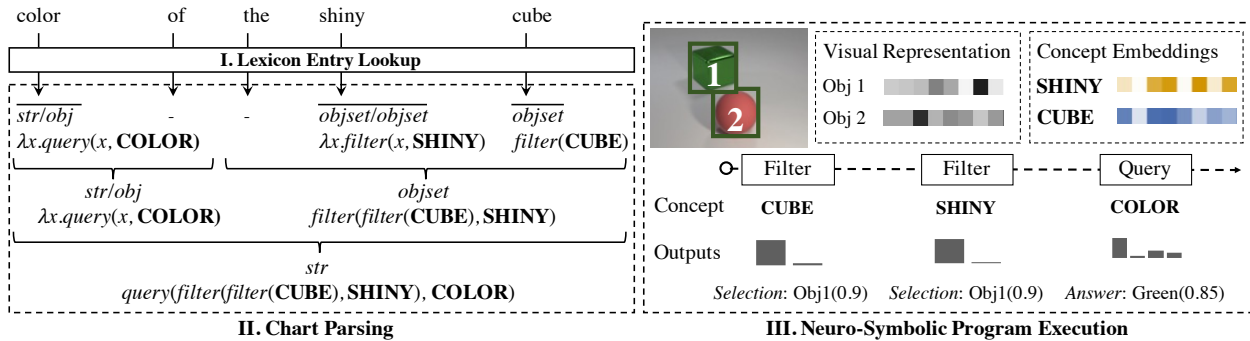


Figure 6.2: G2L2 parses the input sentence into an executable neuro-symbolic program by first (I) lookup the lexicon entry associated with each word, followed by (II) computes the most probable parsing tree and the corresponding tree with a chart parsing algorithm. The derived program can be grounded and executed on an image with a neuro-symbolic reasoning process (Mao et al., 2019) (III).

programmatically meaning representation of the entire sentence by recursively composing meanings based on syntax (Figure 6.2II). To answer the question, we execute the program on the image representation (Figure 6.2III). During training, we compare the answer derived from the model with the groundtruth answer to form the supervision for the entire system. No additional supervision is needed, such as lexicon entries for certain words or concept labels.

### 6.2.1 Grounded Lexicon

At a high level, G2L2 follows the combinatory categorical grammar (CCG; Steedman, 2000) formalism to maintain lexicon entries and parse sentences. Illustrated in Figure 6.3, each word  $w$  (e.g., *shiny*) is associated with one or multiple entries. Each entry  $e_w^{(i)}$  is a tuple comprised of a syntax type  $syn_w^{(i)}$  (e.g., *objset/objset*), and a semantic meaning form  $sem_w^{(i)}$  (e.g.,  $\lambda x.filter(x, \mathbf{SHINY})$ ).  $sem_w^{(i)}$  is a symbolic program represented in a typed domain-specific language (DSL) and can be executed on the input image. Some programs contain concepts (in this case, **SHINY**) that can be visually grounded.

**Typed domain-specific language.** G2L2 uses a DSL to represent word meanings. For the visual reasoning domain, we use the CLEVR DSL (Johnson et al., 2017). It contains object-level operations such as selecting all objects with a particular attribute (e.g., the

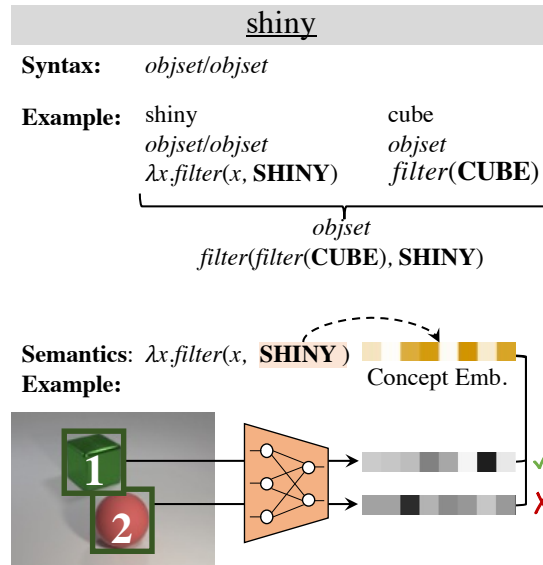


Figure 6.3: Illustration of a lexicon entry in G2L2. Each word is associated with a grounded lexicon, comprised of its syntactic type and a neuro-symbolic semantic program.

shiny objects) or selecting all objects with a specific relationship with a certain object (e.g., the objects left of the cube). It also supports functions that respond to user queries, such as counting the number of objects or querying a specific attribute (e.g., shape) of an object. The language is typed: most functions take a set of objects or a single object as their inputs and produce another set of objects. For example, the operation *filter* has the signature  $filter(objset, concept) \rightarrow objset$  and returns all objects that have *concept* (e.g., all *shiny* objects) in the input set.

**Syntactic types.** There are two types of syntactic types in G2L2: primitive and complex.<sup>1</sup> The primitive types are defined in the typed domain-specific language (e.g.,  $objset, int$ ). A complex type, denoted as  $X/Y$  or  $X \setminus Y$ , is a functor type that takes an argument of type  $Y$  and returns an object of type  $X$ . The direction of the slash indicates word order: for  $X/Y$ , the argument  $Y$  must appear on the right, whereas in  $X \setminus Y$ , it must appear on the left. Note that  $X$  and  $Y$  can themselves be complex types, which allows us to define functor types with multiple arguments, such as  $(X \setminus Y)/Z$ , or even functors with functor arguments (e.g.,  $(X \setminus Y)/(Z/Z)$ ).

In G2L2, the semantic type of a word (in the DSL), together with a set of directional and

<sup>1</sup>In some domains we also use conjunctions (*CONJ*) in the coordination rule.

ordering settings for its arguments (that reflects how the word and its arguments should be linearized in text), uniquely determines the syntactic type of a word. For example, the syntactic type for word *shiny* is *objset/objset*. It first states that *shiny* acts as a function in meaning composition, which takes a subprogram that outputs a set of objects (e.g.,  $filter(\mathbf{CUBE})$ ) as its argument, and produces a new program whose output is also a set of objects, in this case,  $filter(filter(\mathbf{CUBE}), \mathbf{SHINY})$ . Second, it states the direction of the argument, which should come from its right.

**Neuro-symbolic programs.** Some DSL functions involve concepts that are grounded in other modalities, such as the visual appearance and spatial relationships of objects. Taking the function *filter* as an example: its secondary argument *concept* should be associated with the visual representation of objects. In G2L2, the meaning of each lexicon entry may involve one more constants (called “concepts”) that are grounded on other modalities, possibly via deep neural embeddings. In the case of *shiny*:  $\lambda x.filter(x, \mathbf{SHINY})$ . The concept **SHINY** is associated with a vector embedding in a joint visual-semantic embedding space, following Kiros et al. (2014). During program execution, we will be comparing the embedding of concept **SHINY** with object embeddings extracted from the input image to filter out all *shiny* objects.

**Lexicon learning.** G2L2 learns lexicon entries in the following three steps. (i) First, we enumerate all possible semantic meaning programs derived from the DSL. For example, in the visual reasoning domain, a candidate program is  $\lambda x.filter(x, ?)$ , where  $?$  denotes a concept argument. When we try to associate this lexicon entry to the word *shiny*, the program is instantiated as  $\lambda x.filter(x, \mathbf{SHINY})$ , where **SHINY** is a new concept associated with a vector embedding. Typically, we set a maximum number of arguments for each program and constrain its depth. (ii) Next, for programs that have a primitive type, we use its semantic type as the syntactic type (e.g., *objset*). For programs that function with arguments, we enumerate possible arguments in the ordering of the arguments. For example, the program  $\lambda x.filter(x, \mathbf{SHINY})$  has two candidate syntactic types: *objset/objset* (the argument is on its right in language) and *objset\objset* (the argument is on its left). (iii) Finally, we associate each candidate lexicon entry with a learnable scalar weight  $\tau(\cdot)$ . It is typical for a single word to have tens or hundreds of candidate entries, and we optimize these lexicon entry weights in the training process. In practice, we assume no lexical ambiguity, i.e., *each word type has only one lexical entry*. Thus, the ambiguity of parsing only comes from different syntactic derivation orders for the same lexical entries. This

also allows us to prune lexicon entries that do not lead to successful derivations during training.

### 6.2.2 Program Execution

Any fully grounded programs (i.e., programs without unbound arguments) can be executed based on the image representation. We implement the Neuro-Symbolic Concept Learner (NS-CL; Mao et al., 2019) as our differentiable program executor, which consists of a collection of deterministic functional modules to realize the operations in the DSL. NS-CL represents execution results in a “soft” manner: in the visual reasoning domain, a set of objects is represented as a vector mask  $m$  of length  $N$ , where  $N$  is the number of objects in the scene. Each element,  $m_i$  can be interpreted as the probability that object  $i$  is in the set. For example, the operation  $\lambda x.filter(x, \mathbf{SHINY})$  receives an input mask  $m$  and produces a mask  $m'$  that selects all shiny objects in the input set. The computation has two steps: (i) compare the vector embedding of concept **SHINY** with all objects in the scene to obtain a mask  $m^{(\mathbf{SHINY})}$ , denoting the probability of each object being *shiny*; (ii) compute the element-wise multiplication  $m' = m \odot m^{\mathbf{SHINY}}$ , which can be further used as the input to other functions. In NS-CL, the execution result of any program is fully differentiable with respect to the input image representation and concept embeddings (e.g., **SHINY**).

### 6.2.3 Joint Chart Parsing and Expected Execution

G2L2 extends a standard dynamic programming algorithm for chart parsing (i.e., the CKY algorithm (Kasami, 1966; Younger, 1967; Cocke, 1969)) to compose sentence meaning from lexical meaning forms, based on syntax. Denote  $w_i$  as the input word sequence.  $e_i^j$  the  $j$ -th lexicon entry associated with word  $w_i$ , and  $\tau(e_i^j)$  the corresponding weight. Consider all possible derivation of the question  $\{derivation_k\}, k = 1, 2, \dots$ . We define the following context-free probability distribution of derivations as:

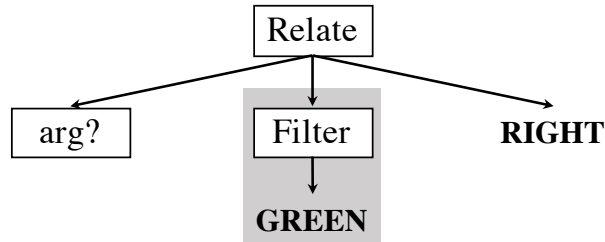
$$p(derivation_k) \propto \exp \left( \sum_{e \in derivation_k} \tau(e) \right).$$

The probability is exponentially proportional to the total weights  $\tau(e)$  of all lexicon entries  $e \in derivation_k$  used by the specific derivation.

**Span: right of the green object**

**Candidate 1:**

$\lambda x. \text{relate}(x, \text{filter}(\text{GREEN}), \text{RIGHT})$



**Candidate 2:**

$\lambda x. \text{relate}(x, \text{relate}(\text{filter}(\text{THE}), \text{filter}(\text{OBJECT}), \text{GREEN}), \text{RIGHT})$

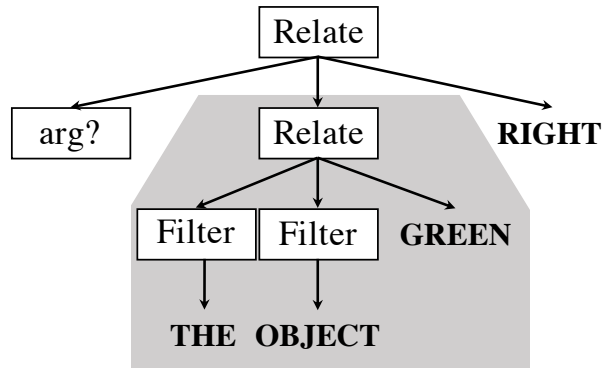


Figure 6.4: An illustrative example of two semantic programs that can be merged by computing the expected execution results of two subtrees (highlighted in gray). Both subtrees output a vector of scores that indicates the selected objects.

A straightforward implementation to support joint learning of lexicon weights  $\tau$  and neural modules (e.g.,  $\text{filter}(x, \text{SHINY})$ ), is to simply execute all possible derivations on the input image, and compare the answer with the groundtruth. However, the number of possible derivations grows exponentially as the question length, making such computation intractable. For example, in SCAN (Lake and Baroni, 2018), each word has 178 candidate lexicons, and the number of lexicon combinations of a sentence with five words will be  $178^5 \approx 10^{11}$ . To address this issue, we introduce the idea of expected execution, which essentially computes the “expected” execution result of all possible derivations. We further accelerate this process by taking local marginalization.

---

**Algorithm 4:** The CKY-E<sup>2</sup> algorithm.

---

**Input:** $w_i$ : the input sentence; $L$ : sentence length; $e_i^j$ : the  $j$ -th lexicon entry associated with word  $w_i$ ; $\tau(e_i^j)$ : lexicon weights.**Output:**  $exe_k$  the execution result of the all possible derivations and their weights $\tau(exe_k)$ .**for**  $i \leftarrow 0$  to  $L - 1$  **do**| Initialize  $dp[i, i + 1]$  with lexicon entries  $e_i^*$  and weights  $\tau(e_i^*)$ **end****for**  $length \leftarrow 1$  to  $L$  **do**| **for**  $left \leftarrow 0$  to  $L - length$  **do**| |  $right \leftarrow left + length$ | |  $dp[left, right] \leftarrow$  empty list| | **for**  $k \leftarrow left + 1$  to  $right - 1$  **do**| | | Try to combine nodes in  $dp[left, k]$  and  $dp[k, right]$ | | | Append successful combination to  $dp[left, right]$ | | **end**| | EXPECTEDEXECUTION( $dp[left, right]$ )| **end****end****Function** EXPECTEDEXECUTION( $a$ : a list of derivations)**while**  $\exists x, y \in a$  are identical except for subtrees of the same type **do**| Create  $z$  from  $x$  and  $y$  by computing the expected execution results for  
| non-identical subtrees|  $\tau(z) \leftarrow \tau(x) + \tau(y)$ | Replace  $x$  and  $y$  in  $a$  with  $z$ **end**

---

Our CKY-E<sup>2</sup> algorithm is illustrated in Algorithm 4. It processes all spans  $[left, right)$  sequentially ordered by their length. The composition for derivations of  $[left, right)$  has two stages. First, it enumerates possible split point  $k$  and tries to combine the derivation of  $[left, k)$  and  $[k, right)$ . This step is identical to the standard CKY parsing algorithm.

Next, suppose there are two derivations  $x$  and  $y$  of span  $[i, j)$ , whose program structures are identical except for subtrees that can be partially evaluated (i.e., do not contain any unbounded arguments). In that case, we will compress these two derivations into one, by marginalizing the execution result for that subtree.

See the example from Figure 6.4. Two programs have an identical structure, except for the second argument to the outer-most *relate* operation. However, these sub-trees, highlighted in gray, can be partially evaluated on the input image, and both of them output a vector of scores indicating the objects being selected. Denote  $\tau_1$  and  $\tau_2$  as the weight associated with two derivations, and  $v_1$  and  $v_2$  the partial evaluation results (vectors) for two subtrees. We will replace these two candidate meaning forms with  $z$ :

$$z := \lambda x. \text{relate}(x, v', \mathbf{RIGHT}), \quad \text{where } v' := \frac{\exp(\tau_1)v_1 + \exp(\tau_2)v_2}{\exp(\tau_1) + \exp(\tau_2)}, \quad \tau(z) := \tau_1 + \tau_2.$$

**Complexity.** Intuitively, once we have determined the semantics of a constituent in the question, the actual concrete meaning form of the derivation does not matter for future program execution, if the meaning form can already be partially evaluated on the input image. This joint parsing and expected execution procedure significantly reduces the exponential space of possible parsing to a polynomial space with respect to the number of possible program layouts that can not be partially evaluated, which, in practice, is small. The complexity of CKY-E2 is polynomial with respect to the length  $L$  of the sentence, and  $M$  is the number of candidate lexicon entries. More specifically,  $O(L^3M)$ , where  $O(L^3)$  comes from the chart parsing algorithm, and the number of derivations after the expected execution procedure is  $O(M)$ . This result is obtained by viewing the maximum arity for functor types as a constant (e.g., 2). Intuitively, for each span, all possible derivations associated with this span can be grouped into four categories: derivations of a primitive type, derivations of a 1-ary functor type, derivations of a 2-ary functor type, and derivations of a 2-ary functor type, with one argument binded. All these numbers grow linearly with respect to  $M$ .

**Correctness.** One can theoretically prove that if all operations in the program layout are commutative with the expectation operator, i.e., if  $\mathbb{E}([f(x)] = f(\mathbb{E}[x]))$ , our CKY-E<sup>2</sup> produces exact computation of the expected execution result. These operations include tensor addition, multiplication (if tensors are independent), and concatenation, which cover most of the computation we will do in neuro-symbolic program execution. For example, for *filter*, taking the expectation over different inputs before doing the filtering is the same

as taking the expectation over the filter results of different inputs. However, there are operations such as quantifiers whose semantics are not commutative with the expectation operator. In practice, it is possible to still use the expected expectation framework to approximate. We leave the application of other approximated inference techniques as future work.

## 6.2.4 Learning

Our model, G2L2, can be trained end-to-end by looking at images and reading paired questions and answers. We denote  $\ell$  as a loss function that compares the output of a program execution (e.g., a probability distribution over possible answers) and the groundtruth. More precisely, given all possible derivations  $derivation_k$ , the image representation  $I$ , the answer  $A$ , and the executor  $\mathcal{E}(\cdot, I)$ , we optimize all parameters by minimizing the loss  $\mathcal{L}$ :

$$\mathcal{L} = \sum_k (p(derivation_k) \cdot \ell(\mathcal{E}(derivation_k, I), A)).$$

In practice, we use gradient-based optimization for both the neural network weights in concept grounding modules and the lexicon weights  $\tau$ .

## 6.3 Experiment

We evaluate G2L2 on two domains: visual reasoning in CLEVR (Johnson et al., 2017) and language-driven navigation in SCAN (Lake and Baroni, 2018). Beyond the grounding accuracy, we also evaluate the compositional generalizability and data efficiency, comparing G2L2 with end-to-end neural models and modular neural networks.

### 6.3.1 Visual Reasoning

We first evaluate G2L2 on the visual reasoning tasks in the CLEVR domain (Johnson et al., 2017), where the task is to reason and answer questions about images. Our study uses a subset of the CLEVR dataset, which does not include sentences that involve coreference resolution and words with multiple meanings in different contexts.



Type	Note	Representation
ObjConcept	Object-level concepts	An embedding vector.
Attribute	Object-level attributes	A vector of length $K_{obj}$ , where $K_{obj}$ is the number of
RelConcept	Relational concepts	An embedding vector.
ObjectSet	A set of objects in the scene	A vector $\mathbf{m}$ of length $N$ , where $N$ is the number of objects in the scene. Each entry $\mathbf{m}_i$ is a real value in $[0, 1]$ , can be interpreted as the probability that object $i$ is in this set.
Integer	An integer	A single non-negative real value, can be interpreted as the “expected” value of this integer.
Bool	A Boolean value	A single real value in $[0, 1]$ , can be interpreted as the probability that this Boolean value is true.

Table 6.1: The type system of the domain-specific language for visual reasoning.

## Domain-Specific Language

Our DSL is based on the CLEVR DSL introduced in Johnson et al. (2017), and the neuro-symbolic realization of each functional module is extended from the Neuro-Symbolic Concept Learner (NS-CL; Mao et al., 2019). We refer readers to the original papers for a detailed introduction to the DSL and neuro-symbolic program execution. Here, we only highlight the key aspects of our language and its neuro-symbolic realization, and discuss the difference between our implementation and the ones in the original papers.

Our visual reasoning DSL is a subset of CLEVR, containing six types and eight primitive operations. Table 6.1 illustrates all six types and how they are internally represented in neuro-symbolic execution.

Table 6.2 further shows all operations in the DSL. There are two main differences between the DSL used by G2L2 and the original CLEVR DSL. First, we have removed the *unique* operation, whose semantic meaning was to return the single object in a set of

Signature	Note
$scene() \rightarrow \text{ObjectSet}$	Return all objects in the scene.
$filter(\mathbf{a}: \text{ObjectSet}, c: \text{ObjConcept}) \rightarrow \text{ObjectSet}$	Filter out a set of objects having the object-level concept (e.g., red) from the input object set.
$relate(\mathbf{a}: \text{ObjectSet}, \mathbf{b}: \text{ObjectSet}, c: \text{RelConcept}) \rightarrow \text{ObjectSet}$	Filter out a set of objects in set $\mathbf{a}$ that have the relational concept (e.g., left) with the input object $\mathbf{b}$ .
$intersection(\mathbf{a}: \text{ObjectSet}, \mathbf{b}: \text{ObjectSet}) \rightarrow \text{ObjectSet}$	Return the intersection of set $\mathbf{a}$ and set $\mathbf{b}$ .
$union(\mathbf{a}: \text{ObjectSet}, \mathbf{b}: \text{ObjectSet}) \rightarrow \text{ObjectSet}$	Return the union of set $\mathbf{a}$ and set $\mathbf{b}$ .
$query(\mathbf{a}: \text{ObjectSet}, c: \text{Attribute}) \rightarrow \text{ObjConcept}$	Query the attribute (e.g., color) of the input object $\mathbf{a}$ .
$exist(\mathbf{a}: \text{ObjectSet}) \rightarrow \text{Bool}$	Check if the set is empty.
$count(\mathbf{a}: \text{ObjectSet}) \rightarrow \text{Integer}$	Count the number of objects in the input set.

Table 6.2: All operations in the domain-specific language for visual reasoning.

objects. For example, it can be used to represent the meaning of the word “*the*” in “*the red object*”, in which the semantic program of “*red object*” yields a set of red objects and the semantic program of “*the*” selects the unique object in that set. However, the meaning of “*the*” may have a slightly different semantic type in different contexts, for example, “*what is the color of ...*”. Since this has violated our assumption about each word having only one lexicon entry, we choose to remove this operation to simplify the learning problem. Meanwhile, to handle the “uniqueness” of the object being referred to, in our realization of related operations, such as *relate* and *query*, we will implicitly choose the unique object being referred to, which we will detail in the following paragraphs.

**Object-centric scene representation.** In our visual reasoning domain, we have assumed access to a pre-trained object-detector that generates a list of bounding boxes of objects in

the scene. In our implementation, following Mao et al. (2019), we use a pre-trained Mask R-CNN He et al. (2017) to generate bounding boxes for each object proposal. These bounding boxes, paired with the original image, are then sent to a ResNet-34 (He et al., 2016) to extract a region-based representation (by RoI Align) and image-based representation, respectively. We concatenate them to form a vector embedding for each object in the image.

**Neuro-symbolic realization.** The high-level idea for the program execution is to build a collection of functions that realize the semantics of each operation based on the vector embeddings of objects and concepts. Taking the *filter* operation as an example, denote  $\mathbf{a}$  as a vector representation of the input set,  $o_i$  the object embeddings, and  $e_c$  the concept embedding. We compute the vector representation  $\mathbf{b}$  of the output set as:

$$\mathbf{b}_i = \mathbf{a}_i \cdot \sigma(\langle o_i, e_c \rangle),$$

where  $\sigma$  is the sigmoid function, and  $\langle \cdot, \cdot \rangle$  is the inner product of two vectors. Intuitively, we first compute the inner product between the concept embedding  $e_c$  and each object embedding, which gives us a vector of scores of whether object  $i$  has concept  $c$ . Next, we compute the element-wise multiplication between two vectors.

A key difference between our realization of these operations and the one in Mao et al. (2019) is that we use element-wise multiplication to simulate the intersection between two sets, and  $1 - (1 - \mathbf{a})(1 - \mathbf{b})$  for union. In contrast, Mao et al. (2019) use element-wise min operation for intersection and max for union. Both realizations can be motivated by real-valued logic: product logic vs. Gödel logic.

**Example.** Here, we run a concrete example to illustrate the execution process of a program in the visual reasoning domain. Suppose we have an image containing three objects  $o_1$ ,  $o_2$  and  $o_3$ . We have two additional vector embeddings for concepts **SHINY** and **CUBE**. Furthermore,  $\sigma(\langle o_i, e_{\text{SHINY}} \rangle) = [0.1, 0.8, 0.9]$ , and  $\sigma(\langle o_i, e_{\text{CUBE}} \rangle) = [0.8, 0.1, 0.9]$ .

Consider the input sentence “How many shiny cubes are there”. Table 6.3 illustrates a step-by-step execution of the underlying program:

$$\text{count}(\text{filter}(\text{filter}(\text{scene}(), \text{CUBE}), \text{SHINY})).$$

**Expected execution.** In the visual reasoning domain, we have only implemented the expected execution mechanism for subordinate program trees whose type is *objset*, although

Program	Type	Value
$scene()$	ObjectSet	$[1, 1, 1]$
$filter(scene(), \mathbf{CUBE})$	ObjectSet	$[0.8, 0.1, 0.9]$
$filter(filter(scene(), \mathbf{CUBE}), \mathbf{SHINY})$	ObjectSet	$[0.08, 0.08, 0.81]$ $= [0.8, 0.1, 0.9] \odot [0.1, 0.8, 0.9]$
$count(filter(filter(scene(), \mathbf{CUBE}), \mathbf{SHINY}))$	Integer	$0.97 = sum([0.08, 0.08, 0.81])$

Table 6.3: Execution trace of the program  $count(filter(filter(scene(), \mathbf{CUBE}), \mathbf{SHINY}))$ .  $sum$  denotes the “reduced sum” operation of a vector, which returns the summation of all entries in that vector.  $\odot$  denotes element-wise multiplication for two vectors.

many other types such as *integer* and *bool* also naturally support expected execution. This is because types such as *integer* and *bool* only appear at the sentence level, and thus, computing the “expectation” of such programs does not reduce the overall complexity.

Formally, the expected execution process compresses a list of semantic programs, denoted by  $v_1, v_2, \dots, v_K$ , and their corresponding weights  $\tau(v_i)$  into a single semantic program  $v^*$  with weight  $\tau(v^*)$ . Suppose all  $v_i$ ’s have type *objset*. We use  $\bar{v}_i$  to denote the execution result of these programs. Each of them is a vector of length  $N$ , where  $N$  is the number of objects in the scene. We compute  $\bar{v}^*$  and  $\tau(v^*)$  as the following:

$$\bar{v}^* = \frac{1}{\sum_i \exp(\tau(v_i))} \sum_i (\exp(\tau(v_i)) \cdot \bar{v}_i),$$

$$\tau(v^*) = \log \sum_i \exp(\tau(v_i)).$$

Intuitively, we normalize the weights using a softmax function to translate them into a distribution, and then compute the expectation of the vectors.

**Candidate lexicons.** Recall that the process of lexicon learning has three stages. First, we generate an extensive collection of candidate semantic programs. Second, we generate candidate lexicon entries for each word by enumerating all possible candidate semantic programs generated in the first step and all possible ordering (linearization in a sentence) of its arguments. Third, we apply our CKY-E<sup>2</sup> and gradient-based optimization to update the weights associated with each lexicon entry.

In our visual reasoning domain, we only consider the following candidate semantic programs and linearizations:

1. Syntactic type: *objset*, semantic program: *scene()* (English noun).
2. Syntactic type: *objset*, semantic program: *filter(scene(), ?)* (English noun).
3. Syntactic type: *objset/objset*, semantic program:  $\lambda x. filter(x, ?)$  (English adjective).
4. Syntactic type: *objset \setminus objset / objset*, semantic program:  $\lambda x. \lambda y. relate(x, y, ?)$  (English preposition I).
5. Syntactic type: *objset \setminus objset / objset*, semantic program:  $\lambda x. \lambda y. relate(y, x, ?)$  (English preposition II)
6. Syntactic type: *bool / objset*, semantic program:  $\lambda x. exist(x)$ .
7. Syntactic type: *integer / objset*,  $\lambda x. count(x)$ .
8. Syntactic type: *word / objset*,  $\lambda x. query(x, ?)$ .
9. Syntactic type:  $CONJ_{AND}$ ,  $\lambda f. \lambda g. (\lambda x. intersect(f(x), g(x)))$  (generalized conjunction).
10. Syntactic type:  $CONJ_{OR}$ ,  $\lambda x. \lambda y. (\lambda z. intersect(z, union(x, y)))$  (generalized disjunction).

As we will see later, when we compare the candidate lexicon entries for the visual reasoning domain and the language-driven navigation domain, the visual reasoning domain contains significantly fewer entries than the navigation domain. This is because much of the learning process in this domain is associated with learning the concept embeddings. In the following few paragraphs, we will explain how we instantiate concepts based on these lexicon entry templates and implement generalized conjunction and disjunction in our domain.

First, for each word (more precisely, word type), e.g., *shiny*, we will instantiate ten lexicon entries. For semantic programs that contain unbounded concept arguments (? marks), we will introduce a series word-type-specific concepts. Specifically in this domain, each word type will be associated with 3 concept representations:  $\mathbf{SHINY}_{ObjConcept}$ ,  $\mathbf{SHINY}_{RelConcept}$ , and  $\mathbf{SHINY}_{Attribute}$ . Based on Table 6.2, the first two concepts will be represented as two embedding vectors, and the third concept will be represented as a vector, indicating which concepts belong to this attribute category. Next, we will instantiate these lexicon entries by filling in these concept representations. For example,

one of the candidate lexicon entry for *shiny* is syntactic type: *objset*, semantic program:  $filter(scene(), \mathbf{SHINY}_{ObjConcept})$ . During training, all these vector embeddings and the weights associated with each lexicon entry, will be optimized jointly.

Next, we discuss the implementation for two conjunctive lexicon entries. The grammar rule for  $CONJ_{AND}$  is:

$$T \text{ CONJ}_{AND} T \rightarrow T,$$

where  $T$  is an arbitrary syntactic type (thus called generalized conjunction). There are two typical use cases: what is the shape of the red and shiny object, and what is the shape of the object that is left of the cube and right of the sphere. In the first case, both arguments have syntactic type *objset / objset*. In the second case, both arguments have syntactic type *objset \ objset*. Note that CLEVR contains only the second case.

The grammar rule for  $CONJ_{OR}$  is:

$$objset \text{ CONJ}_{OR} objset \rightarrow objset \setminus objset.$$

It covers the case: *how many objects are blue cubes or red spheres*. Our implementation is slightly different with human-defined lexicon entries for the word *or*, in particular, because the DSL we use is a small set of set-theoretic operations, which does not fully match the expressiveness of truth-conditional semantics. Thus, the current DSL does not support the representation of all words in the dataset (in particular, *or* and *are*). Thus, we have implemented this ad-hoc fix to handle disjunction.

Finally, we would like to emphasize again that since our DSL does not support representing all semantic programs of words, we allow certain words to be associated with an “empty” lexicon entry. This entry can be combined with any words or constituents next to it and does not participate in the composition of syntactic types and semantic programs. In Table 6.4, we show the lexicon entry associated with each word in the sentence “*are there any shiny cubes?*”, learned by our model, G2L2.

**Setup.** Instead of using manually defined heuristics for curriculum learning or self-paced learning as in previous work (Mao et al., 2019; Li et al., 2020), we employ a curriculum learning setup that is simply based on sentence length: we gradually add longer sentences into the training set. This helps the model to learn basic words from very short sentences (6 words), and use the acquired lexicon to facilitate learning longer sentences (20 words). Since CLEVR does not provide test set annotations, for all models, we hold out 10% of the training data for model development and test them on the CLEVR validation split.

Word Type	Syntactic Type	Semantic Program
are	<EMPTY>	<EMPTY>
there	<EMPTY>	<EMPTY>
any	<i>bool / objset</i>	$\lambda x. exist(x)$
shiny	<i>objset / objset</i>	$\lambda x. filter(x, \mathbf{SHINY}_{ObjConcept})$
cubes	<i>objset</i>	$filter(scene(), \mathbf{CUBE}_{ObjConcept})$

Table 6.4: The learned lexicon entries associated with each word for a simple sentence: *are there any shiny cubes?* The derived semantic program for the full sentence is  $exist(filter(filter(scene(), \mathbf{CUBE}_{ObjConcept}), \mathbf{SHINY}_{ObjConcept}))$

## Baselines

We compare G2L2 with 4 baselines. (1) MAC (Hudson and Manning, 2018) is an end-to-end approach based on attention. (2) TbD-Net (Mascharka et al., 2018) uses a pre-trained semantic parser to parse the question into a symbolic program and executes the program with a neural module network (Andreas et al., 2016). (3) Similarly, NS-VQA (Yi et al., 2018) also parses the question into a symbolic program. It also extracts an abstract scene representation with pre-trained neural recognition models (He et al., 2017). It executes the program based on the abstract scene representation. Both approaches require additional supervision for training the semantic parser, and NS-VQA requires additional annotation for training the visual recognition model. (4) NS-CL (Mao et al., 2019) jointly learns a neural semantic parser and concept embeddings by looking at images and reading paired questions and answers. It requires the annotation for all concepts in the domain (e.g., colors and shapes). In contrast, G2L2 can *automatically* discover visual concepts from texts.

## Results

Table 6.5 summarizes the results. We consider any model that performs in the 95–100 range to have more or less solved the task. Small differences in numeric scores in this range, such as the fact that NS-CL outperforms our model on the “purple” generalization task by 0.2%, are less important than the fact that our model far outperforms all competitors on “count” compositional generalization and the “depth” generalization task, both of which all competitor models are far from solving.

Model	Prog?	Concept?	Standard		Compositional Generalization			Depth
			10%	100%	<i>purple</i>	<i>right of</i>	<i>count</i>	
MAC	N/N	N/N	85.39	98.61	97.14	90.85	54.87	77.40
TbD-Net	Y/Y	N/N	44.52	98.04	89.57	49.92	63.37	53.13
NS-VQA	Y/Y	Y/Y	<b>98.57</b>	98.57	95.52	<b>99.80</b>	81.81	50.45
NS-CL	Y/N	Y/N	98.51	<b>98.91</b>	<b>98.02</b>	99.01	18.88	81.60
G2L2 (ours)	Y/N	Y/N	98.11	98.25	97.82	98.59	<b>96.76</b>	<b>98.49</b>

Table 6.5: Accuracy on the CLEVR dataset. Our model achieves a comparable results with state-of-the-art approaches on the standard training-testing split. It significantly outperforms all baselines on generalization to novel word compositions and to sentences with deeper structures. The best number in each column is bolded. The second column indicates whether the model uses program-based representation of question meaning and whether it needs program annotation for training questions. The third column indicates whether the model explicitly models individual concepts and whether it needs concept annotation for objects during training.

We first compare different models on the **standard** training-testing split. We train different models with either 10% or 100% of the training data and evaluate them on the validation set. Our model achieves a comparable performance in terms of its accuracy and data efficiency.

Next, we systematically build three **compositional generalization** test splits: *purple*, *right of*, and *count*. Essentially, we remove about 90% of the sentences containing the word *purple*, the phrase *right*, and *counting operations*, such as *how many ...?* and *what number of ...?*. We only keep sentences up to a certain length (6 for *purple*, 11 for *right*, and 8 for *count*). We ensure that each use case of these words appears in training questions. After training, we test these models on the validation set with questions containing these words. Overall, our model G2L2 outperforms all baselines on all three generalization splits. In particular, it significantly outperforms other methods on the *count* split. The *count* split is hard for the baseline methods because this split requires models to generalize to sentences with deeper structures, for example, from “*how many red objects are there?*” to “*how many red objects are right of the cube?*” Note that, during training, all models have seen example



uses of similar structures such as *“what’s the shape of the red object”* and *“what’s the shape of the red object right of the cube?”*

Finally, we test generalization to sentences with deeper structures (**depth**). Specifically, we define the “hop number” of a question as the number of intermediate objects being referred to, in order to locate the target object. For example, the “hop number” of the question *“how many red objects are right of the cube?”* is 1. We train different models on 0-hop and 1-hop questions and test them on 2-hop questions. Our model strongly outperforms all baselines.

The results on the **compositional generalization** and **depth** splits yield two conclusions. First, disentangling grounded concept learning (associating words with visual appearances) and reasoning (e.g., filtering or counting subsets of objects in a given scene) improves data efficiency and generalization. On CLEVR, neuro-symbolic approaches that separately identify concepts and perform explicit reasoning (NS-VQA, NS-CL, and G2L2) consistently generalize better than approaches that do not (MAC, TbD). The comparison between TbD and NS-VQA is informative: TbD fails on the “right of” task even in the case where the semantic parser is providing correct programs, while NS-VQA, which uses the same parser but explicitly represents compositional symbolic concepts for reasoning, succeeds in this task. Crucially, of the three neuro-symbolic methods, G2L2 achieves strong performance with less domain-specific knowledge than other methods: NS-VQA needs groundtruth programs; NS-CL needs the concept vocabulary; G2L2 requires neither. Second, our model is the only one to perform well on the hardest “out-of-sample” generalization tests: holding out “count” and generalizing to deeper embeddings. The other, easier generalization tests all have close neighbors in the training set, differing by just one word. In contrast, the length, depth, and “count” tests require generalizing to sentences that differ in multiple words from any training example. They appear to require—or at least benefit especially well from—G2L2 lexical-grammatical approach to capturing the meaning of complex utterances with explicit constituent-level (as opposed to simply word-level) composition.

### 6.3.2 Language-Driven Navigation

The second domain we consider is language-driven navigation. We evaluate models on the SCAN dataset (Lake and Baroni, 2018): a collection of sentence and navigational action

Signature	Note
$empty() \rightarrow \text{ActSeq}$	Create an empty string (of length 0).
$newprim() \rightarrow \text{ActSeq}$	Create a string containing only one primitive action. In SCAN, there are in total 6 primitives.
$newint() \rightarrow \text{Integer}$	Create a single integer. In SCAN, we only support integers {2, 3, 4}.
$concat(\mathbf{a}: \text{ActSeq}, \mathbf{c}: \text{ActSeq}) \rightarrow \text{ActSeq}$	Concatenate two input strings.
$repeat(\mathbf{a}: \text{ActSeq}, \mathbf{b}: \text{Integer}) \rightarrow \text{ActSeq}$	Repeat the input string for multiple times.

Table 6.6: All operations in the domain-specific language for language-driven navigation.

sequence pairs. There are six primitive actions: *jump*, *look*, *walk*, *run*, *lturn*, and *rturn*, where an instruction *turn left twice and run* will be translated to *lturn lturn run*. All instructions are generated from a finite context-free grammar, so that we can systematically construct train-test splits for different types of compositional generalizations.

### Domain-Specific Language

Our DSL for the language-driven navigation domain is a simple string manipulation language that supports creating new strings, concatenating two strings, and repeating a string multiple times. Our DSL contains only two primitive types: action sequence, abbreviated as `ActSeq`, and integer. Formally, we summarize the list of operations in our language-driven navigation domain in Table 6.6.

**Probabilistic string representation.** We represent each string in a “probabilistic” manner. In particular, each string  $s$  is represented as a tuple  $\langle L^s, C^s \rangle$ .  $L^s$  is a categorical distribution of the length.  $C^s$  is a three-dimensional tensor, indexed by  $\ell, k, c$ , where  $C_{\ell, k, c}^s = p(s[k] = c | \text{length}(s) = \ell)$ . Thus,  $C$  has the shape  $[L + 1, L, |V|]$ , where  $L$  is the max length of a string and  $V$  is the action vocabulary. For simplicity, we constrain that  $C_{\ell, k, c}^s \equiv 0$  for all  $k > \ell$ .

It is straightforward to represent empty strings:  $L_0 = 1$ , or strings with a single action primitive  $a$ :  $L_1 = 1$  and  $C_{1, 0, a} = 1$ . Now we explain our implementation of the *concat* and the *repeat* operation.

For  $z = \text{concat}(x, y)$ :

$$L_\ell^z = \sum_{0 \leq i \leq \ell} \left( L_i^x \cdot L_{(\ell-i)}^y \right);$$

$$C_{\ell,k,c}^z = \frac{1}{L_\ell^z} \sum_{0 \leq i \leq \ell} \left( L_i^x \cdot L_{(\ell-i)}^y \cdot (C_{i,k,c}^x + C_{\ell-i,k-i,c}^y) \right).$$

The high-level idea is to enumerate the possible length of both strings.

Similarly, for  $z = \text{repeat}(x, m)$ ,

$$L_\ell^z = \begin{cases} L_{\ell/m}^x & \text{if } \ell \bmod m = 0 \\ 0 & \text{otherwise} \end{cases}$$

$$C_{\ell,k,c}^z = \begin{cases} L_{\ell/m, k \bmod (\ell/m), c}^x & \text{if } \ell \bmod m = 0 \text{ and } k < \ell \\ 0 & \text{otherwise} \end{cases}.$$

**Expected execution.** In this domain, we only perform expected execution for semantic programs of type `ActSeq`, whose execution results can be represented using the probabilistic string representation. Denote  $\bar{s}_i$  as the execution results for  $K$  programs, and  $\tau(s_i)$  the corresponding weights. We define  $p(s_i) = \text{softmax}(\{\tau(s_i)\})_i = \frac{\exp \tau(s_i)}{\sum_j \exp \tau(s_j)}$ . We compute the expected string  $\bar{s}$  and its weight  $\tau(s)$  as:

$$L_\ell^s = \sum_i p(s_i) L_\ell^{s_i}; \quad C_{\ell,k,c}^s = \frac{\sum_i \left( p(s_i) L_\ell^{s_i} \cdot C_{\ell,k,c}^{s_i} \right)}{L_\ell^s}.$$

**Candidate lexicons.** We use a simple enumerate algorithm to generate candidate lexicon entries for our language-driven navigation DSL. Specifically, we first enumerate candidate semantic programs for each lexicon entry that satisfy the following constraints:

1. There are at most three operations.
2. There are at most two arguments.
3. There is at most one argument whose type is a functor.
4. There is no argument of type *Integer*.

Table 6.7 lists a couple of programs generated by the algorithm and their corresponding types.

Based on the candidate semantic types, we first instantiate candidate lexicon entries by enumerating possible ordering (linearization) of the arguments. For example, the

Type	Program (Note)
ActSeq	$walk()$ The simplest program that constructs a string with a single action primitive: <b>WALK</b> .
$(\text{ActSeq}) \rightarrow \text{ActSeq}$	$\lambda x.concat(look(), x)$ Prepend a <b>LOOK</b> action to an input string.
$(\text{ActSeq}, \text{ActSeq}) \rightarrow \text{ActSeq}$	$\lambda x.\lambda y.concat(x, y)$ Concatenate two strings.
$(\text{ActSeq}, \text{ActSeq}) \rightarrow \text{ActSeq}$	$\lambda x.\lambda y.concat(repeat(x, 2), y)$ Repeat the first string twice and concatenate with the second string.
$((\text{ActSeq} \rightarrow \text{ActSeq}, \text{ActSeq}) \rightarrow \text{ActSeq})$	$\lambda x.\lambda y.concat(y, x(walk()))$ The first argument ( $x$ ) is a function which maps a ActSeq to another ActSeq. The second argument $y$ is an ActSeq. The function invokes $x$ with a simple string <b>WALK</b> , and concatenate the result with $y$ .

Table 6.7: Sample semantic programs generated by the enumeration process based on our language-driven navigation DSL.

simple program  $\lambda x.concat(look(), x)$  has two possible linearizations:  $ActSeq/ActSeq$  and  $ActSeq \setminus ActSeq$ . As discussed in the main paper, in order to handle parsing ambiguities, we further introduce two finer-grained syntactic types for the  $ActSeq$  type:  $S$  and  $V$ . In practice, we only allow the following set of syntactic types:  $V, V/V, V \setminus V, V \setminus V/V, V \setminus V/(V \setminus V)$ , and  $S \setminus V/V$ . In total, we have 178 candidate lexicon entries for each word.

**Setup.** We use a string-editing domain-specific language (DSL) for modeling the meaning of words in the SCAN dataset. At a high level, the model supports three primitive operations: constructing a new constant string (consisting of primitive operations), concatenating two strings, and repeating the input string a number of times.

For G2L2, we generate candidate lexicons by enumerating functions in the string-editing DSL with up to 2 arguments, and the function body has a maximum depth of 3.

We also allow at most one of the arguments to be functor-typed, for example,  $V \setminus V / (V \setminus V)$ . To handle parsing ambiguities, we use two primitive syntax types  $S$  and  $V$ , while both of them are associated with the semantic type of *string*. In total, we have 178 candidate lexicon entries for each word.

## Baselines

We compare G2L2 to seven baselines. (1) Seq2seq (Sutskever et al., 2014) trains an LSTM-based encoder-decoder model. We follow the hyperparameter setups of (Lake and Baroni, 2018). (2) Transformer (Vaswani et al., 2017) is a 4-head Transformer-based autoregressive seq2seq model. We tuned the hidden size (i.e., the dimension of intermediate token representations) within  $\{100, 200, 400\}$ , as well as the number of layers (for both the encoder and the decoder) from  $\{2, 4, 8\}$ . Other methods are based on different data augmentation schemes for training an LSTM seq2seq model. Specifically, (3) GECA augments the original training splits using heuristic span recombination rules; (4) WordDrop (Guo et al., 2020) performs random dropout for input sequence (while keeping the same label); (5) similarly, SwitchOut (Wang et al., 2018) randomly replaces an input token with a random token from the vocabulary; (6) SeqMix (Guo et al., 2020) uses soft augmentation techniques following (Zhang et al., 2017), which composes an “weighted average” of different input sequences; (7) recomb-2 (Akyürek et al., 2021) learns recombination and resampling rules for augmentation.

## Results

We compare models on three train-test splits (Table 6.8). In **Simple**, the training and test instructions are drawn from the same distribution. We compare the data efficiency of various models by using either 10% or 100% of the training data and test them on the same test split. While all models can achieve a nearly-perfect accuracy with 100% training data, our model G2L2 shows an advantage with only a small amount of data. Next, in **Compositional**, we have held out the sentences containing certain phrases, such as *jump* and *around right*. For these held-out phrases, only valid non-contextual examples containing them (i.e., *jump* in isolation and no example for *around right*) are available during training. During the test, algorithms need to make systematical generalizations of these phrases in novel contexts. Finally, in **Length**, all training examples have an

Model	Simple		Compositional Generalization		Length
	10%	100%	<i>jump</i>	<i>around right</i>	
seq2seq	0.93±0.05	0.99±0.01	0.00±0.00 <sup>†</sup>	0.00±0.00 <sup>†</sup>	0.15±0.02
Transformer	0.71±0.24	0.78±0.11	0.00±0.00	0.10±0.08	0.02±0.01
GECA	0.99±0.00	0.98±0.01	0.87±0.05 <sup>†</sup>	0.82±0.11 <sup>†</sup>	0.15±0.02
WordDrop *	0.56±0.02	0.62±0.02	0.52±0.02	0.70±0.06	0.18±0.01
SwitchOut *	0.99±0.01	0.99±0.01	0.98±0.02	0.97±0.02	0.17±0.02
SeqMix *	–	–	0.98 <sup>‡</sup>	0.89 <sup>‡</sup>	–
recomb-2	–	–	0.88±0.07 <sup>†</sup>	0.82±0.08 <sup>†</sup>	–
G2L2 (ours)	<b>1.00±0.00</b>	<b>1.00±0.00</b>	<b>1.00±0.00</b>	<b>1.00±0.00</b>	<b>1.00±0.00</b>

Table 6.8: Accuracy on the SCAN dataset, averaged across 10 valid runs when applicable,  $\pm$  denotes standard deviation. The best number in each column is bolded. <sup>†</sup>: results taken from Akyürek et al. (2021); <sup>‡</sup>: results taken from Guo et al. (2020). Both papers have only presented results on the compositional generalization split. \*: applied after GECA. The results for GECA are based on the released implementation by the authors. All the models are selected with respect to the accuracy on the training set.

action length less than or equal to 22, while that of a test example is up to 48. Our model consistently reaches perfect performance in all considered settings, even on the cross-length generalization task where GECA does not help improve performance. These results are consistent with the conclusions we derived from the CLEVR dataset. Specifically, data-augmentation techniques for SCAN can solve simple generalization tests (e.g., *jump*, where tests all have close neighbors in the training set, differing by just one word) but not the hard ones (e.g., *length*, where test sentences can differ in multiple words from any training examples).

## Case Study

G2L2 is expressive enough to achieve perfect accuracy on the SCAN dataset: a set of lexicon entries matches the groundtruth in SCAN. However, our learning algorithm does not always converge on the correct lexicon, but when it fails, the failure can be identified based on training-set accuracy. So, we perform model selection based on the training

accuracy for G2L2: after a sufficient number of epochs, if the model has not reached perfect accuracy (100%), we re-initialize the weights and train the model again. Our results show that, among 100 times of training, the model reaches 100% accuracy 74% of the time. For runs that do not achieve 100% accuracy, the average performance is 0.94.

Since G2L2 directly learns human-interpretable lexicon entries associated with each individual word, we can further inspect the failure cases made by it when the training accuracy does not converge to 0. We find that the most significant failure mode is the word *and* (e.g., *jump and run*) and *after* (e.g., *jump after run*). Both of them are treated as connectives in SCAN. Sometimes G2L2 fails to pick the syntax type  $S \setminus V/V$  over the type  $V \setminus V/V$ . The entry  $V \setminus V/V$  will succeed in parsing most cases (e.g., *jump and run*), except that it will introduce ambiguous parsing for sentences such as “*jump and run twice*”: *jump and run twice* vs. *jump and run twice*. Based on the definition of the SCAN, only the first derivation is valid. In contrast, using  $S \setminus V/V$  resolves this ambiguity. Depending on the weight initialization and the example presentation order, G2L2 sometimes gets stuck at the local optima of  $V \setminus V/V$ . However, we can quickly identify this by the training accuracies—G2L2 can reach perfect performance on all considered splits by simply retraining with another random seed; therefore, we only select those with 100% training accuracy as valid models.

## 6.4 Conclusion and Discussion

In this chapter, we have presented G2L2, a lexicalist approach towards learning the compositional and grounded meaning of words. G2L2 builds in a compact but potentially universal set of combinatory grammar rules and learns grounded lexicon entries from a collection of sentences and their grounded meaning without human annotated lexicon entries. The lexicon entries represent the semantic type of the word, the ordering settings for its arguments, and the grounding of concepts in its semantic program. To facilitate lexicon entry induction in an exponentially growing space, we introduced CKY-E<sup>2</sup> for joint chart parsing and *expected execution*.

Through systematical evaluation on both visual reasoning and language-driven navigation domains, we demonstrate the data efficiency and compositional generalization capability G2L2, and its general applicability in different domains. The design of G2L2 suggests several research directions. First, in G2L2, we have made strong assumptions

on the context-independence of the lexicon entry and the application of grammar rules; handling linguistic ambiguities and pragmatics needs further exploration (Frank and Goodman, 2012). Second, meta-learning models that can leverage learned words to bootstrap the learning of novel words, such as syntactic bootstrapping (Gauthier et al., 2018), is a meaningful direction. Finally, future work may consider integrating G2L2 with program-synthesis algorithms (Ellis et al., 2023) for learning more generic and complex semantic programs.



# Chapter 7

## Learning Semantic Parses through Program Execution Consistency

*Content in this chapter has been published as a conference paper at EMNLP 2022 (Shi et al., 2022).*

We now focus on learning semantic parses in realistic settings, such as translating natural language into executable code using generative models (Chen et al., 2021; Austin et al., 2021; Li et al., 2022, *inter alia*). While these models do not explicitly incorporate program semantics (i.e., execution results) during training, they can generate correct solutions for many problems. However, choosing a *single* correct program from a generated set for each problem remains challenging.

In this work, we introduce execution result-based minimum Bayes risk decoding (MBR-EXEC; Figure 7.1) for program selection and show that it improves the few-shot performance of pre-trained code models on natural-language-to-code tasks. We select output programs from a generated candidate set by marginalizing over program implementations that share the same semantics. Because exact equivalence is intractable, we execute each program on a small number of test inputs to approximate semantic equivalence. Across datasets, execution or simulated execution significantly outperforms the methods that do not involve program semantics. We find that MBR-EXEC consistently improves over all investigated execution-unaware selection methods, suggesting it is an effective approach for natural language-to-code translation.

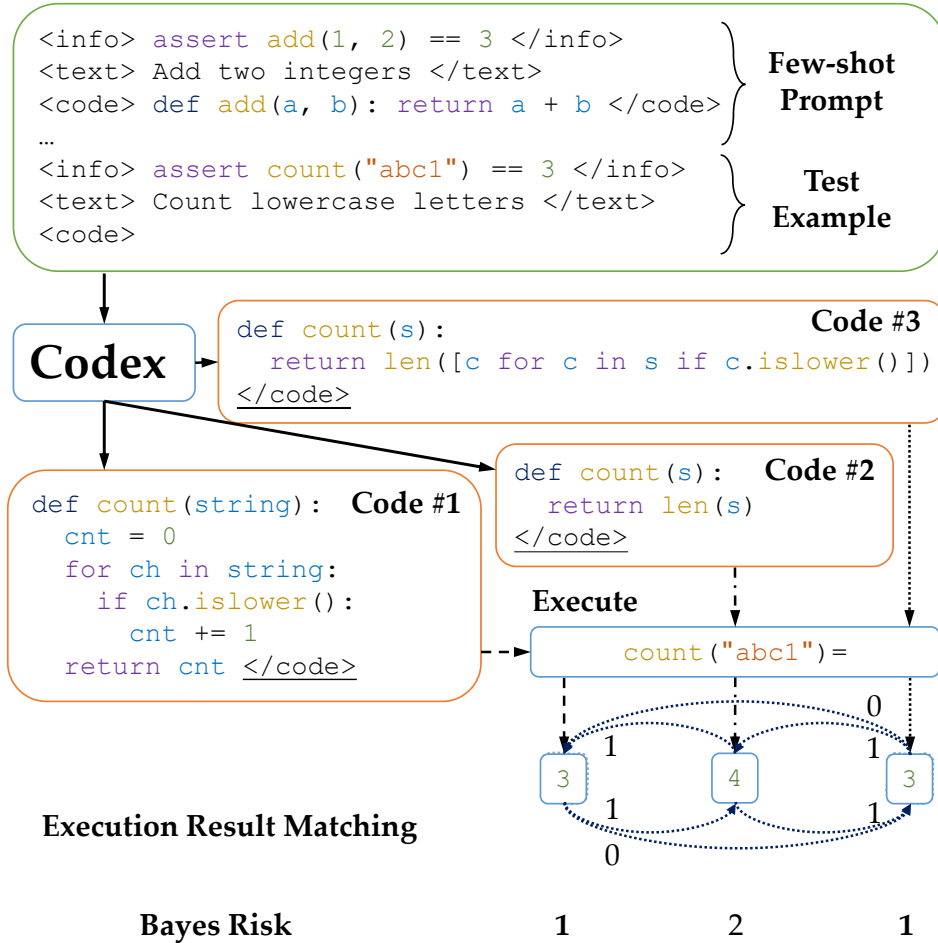


Figure 7.1: Illustration of MBR-EXEC on translating natural language to Python code: we (1) sample programs from a pre-trained language-to-code model such as Codex (Chen et al., 2021), (2) execute each program on one test case, and (3) select the example with the minimal execution result-based Bayes risk. Numbers around dotted lines denote the 0/1 matching loss between execution results, while the Bayes risk of a program is defined by the sum of the loss between itself and other examples. In the figure, either Code #1 or Code #3 can be selected. Ground-truth program output is not needed for selection.

## 7.1 Related Work

**Language to code translation with neural networks.** With the progress of neural network-based language modeling and conditioned text generation, there has been much work

exploring natural language to code generation with end-to-end neural model architectures (Xiao et al., 2016; Ling et al., 2016; Rabinovich et al., 2017; Dong and Lapata, 2018; Suhr et al., 2018; Xu et al., 2020; Lachaux et al., 2021, *inter alia*). Recently, large Transformer-based (Vaswani et al., 2017) pre-trained code models have shown surprisingly strong generation performance across programming languages (Chen et al., 2021; Austin et al., 2021; Li et al., 2022, *inter alia*). In this work, we explore selection (i.e., inference) methods to apply to these pre-trained models, showing that selecting programs using their execution results can greatly improve program generation.

Multiple benchmarks have been proposed to evaluate code model performance (Yin et al., 2018; Miceli Barone and Sennrich, 2017; Lu et al., 2021, *inter alia*). In this work, we evaluate on three text-to-code datasets: MBPP (Python; Austin et al., 2021), Spider (SQL; Yu et al., 2018) and NL2Bash (Bash; Lin et al., 2018), covering a range of programming languages.

**Prompting pre-trained language models.** The GPT-2 (Radford et al., 2019) and GPT-3 (Brown et al., 2020) models have shown strong prompting performance: after conditioning on a task-related prompt, the language models are often able to make accurate output predictions for unseen inputs. These results lead to prompt-based approaches for few-shot or zero-shot text classification (Shin et al., 2020; Gao et al., 2021; Min et al., 2022, *inter alia*), question answering (Khashabi et al., 2020), machine translation (Radford et al., 2019), and evaluation of generated text (Yuan et al., 2021), where no more than a few examples are used to construct the prompts. Few-shot examples are usually formatted into natural language prompts, and continuations generated by the models for these prompts are then converted to task-specific predictions. The prompt formatting can be either manually designed (Jiang et al., 2020) or automatically learned (Li and Liang, 2021; Lester et al., 2021). We refer the readers to Liu et al. (2023) for a more comprehensive survey.

In this work, we prompt a pre-trained code model (Codex; Chen et al., 2021) in a few-shot setting (§7.2.1) and perform execution-based selection over the samples. We also find that the Codex model performs well with fairly programming-language-agnostic prompt formatting (Table 7.1).

**Minimum Bayes risk decoding.** In structured prediction, minimum Bayes risk (MBR) decoding (Bickel and Doksum, 1977) selects a structured output that minimizes the expected errors in the structure by introducing an explicit loss function to the decision criterion.

<b>General Template</b>	
<code>&lt;info&gt;[INFO]&lt;/info&gt;</code>	<i>(optional)</i>
<code>&lt;text&gt;[TEXT]&lt;/text&gt;</code>	
<code>&lt;code&gt;[CODE]&lt;/code&gt;</code>	
<b>Instantiation 1: Python, One-Shot Example</b>	
<b>Exemplar</b>	
<code>&lt;info&gt;assert add(1, 2) == 3&lt;/info&gt;</code>	
<code>&lt;text&gt;Write a function that adds 2 integers&lt;/text&gt;</code>	
<code>&lt;code&gt;def add(a, b): return a + b&lt;/code&gt;</code>	
<b>Query</b>	
<code>&lt;info&gt;assert cat() == "cat"&lt;/info&gt;</code>	
<code>&lt;text&gt;Write a function that outputs the string "cat"&lt;/text&gt;</code>	
<code>&lt;code&gt;</code>	
<b>Instantiation 2: Bash, One-Shot Example</b>	
<b>Exemplar</b>	
<code>&lt;text&gt;show the files in the current directory&lt;/text&gt;</code>	
<code>&lt;code&gt;ls&lt;/code&gt;</code>	
<b>Query</b>	
<code>&lt;text&gt;show the first 5 lines of a.txt&lt;/text&gt;</code>	
<code>&lt;code&gt;</code>	

Table 7.1: Prompt formatting template for queries to pre-trained code models. For instantiation, we substitute [TEXT] and [CODE] with natural language descriptions and corresponding code snippets, respectively. We also provide compatibility for an optional [INFO] section to provide the model extra information (e.g., the desired function identifier and example function calls) that helps code generation. In general, we expect the pre-trained code models to generate a `</code>` token at the end of each code snippet given its pattern following ability (Brown et al., 2020; Chen et al., 2021). Otherwise, we will truncate the generated code to 1024 tokens.

This method has outperformed the maximum a posteriori (MAP) method on many tasks, including syntactic parsing (Titov and Henderson, 2006; Shi et al., 2019; Zhang et al., 2020),

statistical machine translation (Kumar and Byrne, 2004; Zhang and Gildea, 2008), and neural machine translation (Eikema and Aziz, 2020, 2022).

In machine translation, MBR decoding is usually implemented by reranking candidates (Goel and Byrne, 2000; Kumar and Byrne, 2004; Tromble et al., 2008, *inter alia*). Let  $F$  denote the input and  $E$  denote the corresponding ground-truth translation. Given a loss function  $\ell(\cdot, \cdot)$  between translations and a probability model  $P(E | F)$ , MBR decoding can be formulated as

$$\hat{E} = \arg \min_{E' \in \mathcal{E}_h} \sum_{E \in \mathcal{E}_e} \ell(E, E') P(E | F), \quad (7.1)$$

where  $\mathcal{E}_h$  is the *hypothesis space*, and  $\mathcal{E}_e$  is the *evidence space*: both are sets of possible translations.

We define execution-based MBR loss functions and show they are crucial in the selection processes for natural language to code with a pre-trained large language model.

## 7.2 Proposed Approach: MBR-EXEC

Our execution-based framework consists of two parts: (1) collecting samples from a pre-trained code model (§7.2.1) and (2) selecting the best candidate using minimum Bayes risk decoding (§7.2.2).

### 7.2.1 Sample Collection

To obtain the corresponding code, we query the pre-trained code model with few-shot prompts followed by the text description, using a unified mark-up style few-shot prompting template (Table 7.1).<sup>1</sup> In addition to the generated programs themselves, most existing models also allow us to have the associated probability of generating each generated token  $w_i$  conditioned on the prompt tokens  $C = \langle c_1, \dots, c_n \rangle$  and all the previously generated tokens  $w_1, \dots, w_{i-1}$ , denoted by  $P(w_i | C, w_1, \dots, w_{i-1})$ .

---

<sup>1</sup>While existing work on prompting language models usually requires a task-specific design of prompts (Shin et al., 2020; Zhong et al., 2021; Gao et al., 2021, *inter alia*), we find that a fairly general pattern (Table 7.1), which does not involve any programming language-specific information, works well across programming languages on Codex.

## 7.2.2 Execution-Based MBR Decoding

Given a problem in its natural language description  $C$ , we sample a set of programs  $\mathcal{P} = \{p_i\}_{i=1}^N$  using the method in §7.2.1. We formulate the execution-based MBR (MBR-EXEC) decoding by selecting

$$\begin{aligned}\hat{p} &= \arg \min_{p \in \mathcal{P}} \mathcal{L}_{MBR}(p; \mathcal{P}) \\ &= \arg \min_{p \in \mathcal{P}} \sum_{p_{ref} \in \mathcal{P}} \ell(p, p_{ref})\end{aligned}\tag{7.2}$$

as the best candidate, where  $\mathcal{L}_{MBR}(\cdot; \cdot)$  denotes the MBR loss of a program conditioned on a set of references, and  $\ell$  is a predefined, execution-based loss function that examines the discrepancy between two programs. Intuitively, this finds a consensus candidate which has a low loss relative to all other candidates. The above implementation is an unbiased estimation of Eq (7.1).

We introduce the following execution result-based loss function:

$$\ell(p_i, p_j) = \max_{t \in \mathcal{T}} \mathbb{1} [p_i(t) \neq p_j(t)],$$

where  $\mathcal{T}$  is the set of available test inputs,<sup>2</sup> and  $p_i(t)$  denotes the execution result of program  $p_i$  when having  $t$  as the input. When a program fails to execute on a test case, it is considered not equivalent to any other programs, even if they fail to execute as well. Intuitively,  $\ell$  assigns equivalence (0 loss) if and only if two programs have the same output on all considered test cases.

There may be multiple programs receiving the same MBR loss  $\mathcal{L}_{MBR}(\cdot; \mathcal{P})$ , which are all minima. We break any ties by selecting the program with the largest likelihood among them.

## 7.3 Experiments

We evaluate (§7.3.3) and analyze (§7.3.4) the performance of MBR-EXEC, starting with introducing the datasets and evaluation metrics (§7.3.1), as well as non-execution-based

---

<sup>2</sup>Our MBR-EXEC decoding process does not involve any ground-truth test case output, nor the ground-truth programs. This is compatible with many real scenarios, e.g., in a programming competition, where valid test inputs are easier to access than ground-truth output.

baselines (§7.3.2) for MBR-EXEC. Finally, we show and discuss oracle performances on the considered tasks (§7.3.5).

### 7.3.1 Datasets and Evaluation Metrics

We consider three datasets that cover a range of programming languages: MBPP (Python; Austin et al., 2021), Spider (SQL; Yu et al., 2018), and NL2Bash (Bash; Lin et al., 2018).

**MBPP.** The MBPP dataset (Austin et al., 2021)<sup>3</sup> consists of 974 basic Python programming problems, with 500 used for testing and the rest for training or few-shot prompting. There are ground-truth programs and three assertions (i.e., test cases with input and ground-truth output) associated with the description of each problem. When collecting the samples, we use one assertion as the extra information ([INFO]; Table 7.1).<sup>4</sup> Programs are evaluated with execution accuracy, where a program is considered as passing if all three test cases are correct.

**Spider.** The Spider dataset (Yu et al., 2018)<sup>5</sup> is a text-to-SQL dataset, which requires a model to translate text descriptions into SQL commands. There are 7,000 examples for training and 1,034 for development. When prompting models to produce candidate commands, we concatenate the corresponding SQL table and column names as the [INFO]. Commands are evaluated with execution accuracy, where a command is considered as passing if it returns the same result as the ground-truth command when executed on the same database.

**NL2Bash.** The NL2Bash dataset (Lin et al., 2018) aims to translate natural language to bash commands. We omit [INFO] in the sample collection process. Because it is challenging to execute bash commands in a sandbox, we split a bash command with `bashlex`,<sup>6</sup> a rule-based bash parser, and use the token-level BLEU-4 score between commands as the estimation of execution result similarity. We consider a command not executable when `bashlex` fails to parse it. Following Lin et al. (2018), commands are evaluated with character-level BLEU-4 score.

---

<sup>3</sup><https://github.com/google-research/google-research/tree/master/mbpp>

<sup>4</sup>The main goal of [INFO] in MBPP is to inform Codex about the desired function name for more straightforward evaluation – while the assertions are not a necessary part of the prompt, we use them as [INFO] for simplicity and compatibility with past work (Austin et al., 2021).

<sup>5</sup><https://yale-lily.github.io/spider>

<sup>6</sup><https://pypi.org/project/bashlex/>

---

**MBPP: Prompt**

---

```
<info>assert camel_to_snake('GoogleAssistant') == 'google_assistant'</info>
<text>Write a function to convert camel case string to snake case string by using regex.</
text>
<code>import re
def camel_to_snake(text):
    str1 = re.sub('(.[A-Z][a-z]+)', r'\1_\2', text)
    return re.sub('[a-z0-9]([A-Z])', r'\1_\2', str1).lower()</code>
<info>assert sort_dict_item({(5, 6) : 3, (2, 3) : 9, (8, 4): 10, (6, 4): 12} ) == {(2, 3): 9,
(6, 4): 12, (5, 6): 3, (8, 4): 10}</info>
<text>Write a function to sort dictionary items by tuple product of keys for the given
dictionary with tuple keys.</text>
<code>def sort_dict_item(test_dict):
    res = {key: test_dict[key] for key in sorted(test_dict.keys(), key = lambda ele: ele[1] *
ele[0])}
    return (res)
</code>
<info>assert reverse_list_lists([[1, 2, 3, 4], [5, 6, 7, 8], [9, 10, 11, 12], [13, 14, 15,
16]])==[[4, 3, 2, 1], [8, 7, 6, 5], [12, 11, 10, 9], [16, 15, 14, 13]]</info>
<text>Write a function to reverse each list in a given list of lists.</text>
<code>def reverse_list_lists(lists):
    for l in lists:
        l.sort(reverse = True)
    return lists </code>
<info>assert remove_Occ("hello", "l") == "heo"</info>
<text>Write a python function to remove first and last occurrence of a given character from
the string.</text>
<code>
```

---

**MBPP: Response**

---

```
def remove_Occ(str1 ,ch):
    return str1[:str1.index(ch)] + str1[str1.rindex(ch)+1:]</code>
```

---

Table 7.2: MBPP example prompt and response from Codex: we use the first assertion in the dataset as the extra information (i.e., [INFO] in Table 7.1). The content in the last `<info>...</info>` and `<text>...</text>` marks in the prompt corresponds to the test problem.

Across datasets, we use 15 examples from the training set for few-shot prompting. Detailed examples showing prompt formatting can be found in Tables 7.2 to 7.4. Unless otherwise specified, we collect samples by querying Codex with five different prompts, each containing three examples, using temperature 0.3. We combine the candidates sampled across the five prompts to get a set of candidate samples to use in our selection methods. For execution on MBPP and Spider, we apply a memory limit of 128GB and a



---

**Spider: Prompt**

---

<info>e\_learning | \* | Course\_Authors\_and\_Tutors : author\_id , author\_tutor\_ATB , login\_name , password , personal\_name , middle\_name , family\_name , gender\_mf , address\_line\_1 | Students : student\_id , date\_of\_registration , date\_of\_latest\_logon , login\_name , password , personal\_name , middle\_name , family\_name | Subjects : subject\_id , subject\_name | Courses : course\_id , author\_id , subject\_id , course\_name , course\_description | Student\_Course\_Enrolment : registration\_id , student\_id , course\_id , date\_of\_enrolment , date\_of\_completion | Student\_Tests\_Taken : registration\_id , date\_test\_taken , test\_result</info>

<text>Which course authors teach two or more courses? Give me their addresses and author IDs .</text>

```
<code>SELECT T1.address_line_1 , T2.author_id FROM Course_Authors_and_Tutors AS T1 JOIN Courses AS T2 ON T1.author_id = T2.author_id GROUP BY T2.author_id HAVING Count(*) >= 2</code>
```

<info>flight\_1 | \* | flight : flno , origin , destination , distance , departure\_date , arrival\_date , price , aid | aircraft : aid , name , distance | employee : eid , name , salary | certificate : eid , aid</info>

<text>Show origin and destination for flights with price higher than 300.</text>

```
<code>SELECT origin , destination FROM Flight WHERE price > 300</code>
```

<info>driving\_school | \* | Addresses : address\_id , line\_1\_number\_building , city , zip\_postcode , state\_province\_county , country | Staff : staff\_id , staff\_address\_id , nickname , first\_name , middle\_name , last\_name , date\_of\_birth , date\_joined\_staff , date\_left\_staff | Vehicles : vehicle\_id , vehicle\_details | Customers : customer\_id , customer\_address\_id , customer\_status\_code , date\_became\_customer , date\_of\_birth , first\_name , last\_name , amount\_outstanding , email\_address , phone\_number , cell\_mobile\_phone\_number | Customer\_Payments : customer\_id , datetime\_payment , payment\_method\_code , amount\_payment | Lessons : lesson\_id , customer\_id , lesson\_status\_code , staff\_id , vehicle\_id , lesson\_date , lesson\_time , price</info>

<text>When did the staff member with first name as Janessa and last name as Sawayn leave the company?</text>

```
<code>SELECT date_left_staff FROM Staff WHERE first_name = \"Janessa\" AND last_name = \"Sawayn\";</code>
```

<info>concert\_singer | \* | stadium : Stadium\_ID , Location , Name , Capacity , Highest , Lowest , Average | singer : Singer\_ID , Name , Country , Song\_Name , Song\_release\_year , Age , Is\_male | concert : concert\_ID , concert\_Name , Theme , Stadium\_ID , Year | singer\_in\_concert : concert\_ID , Singer\_ID</info>

<text>How many singers do we have?</text>

```
<code>
```

---

**Spider: Response**

---

```
SELECT COUNT(*) FROM singer;</code>
```

---

Table 7.3: Spider example prompt and response from Codex: following Xie et al. (2022), we use the concatenation of corresponding table and column names in the dataset as the extra information (i.e., [INFO] in Table 7.1). The content in the last <info>...</info> and <text>...</text> marks in the prompt corresponds to the test problem.

---

**NL2Bash: Prompt**

---

```
<text>Print file information of command \"bash\"</text>
<code>echo $(ls -l $(which bash))</code>
<text>Recursively change the owner and group of all files in \"/your/directory/to/fuel/" to
  \"nginx\"</text>
<code>chown nginx:nginx /your/directory/to/fuel/ -R</code>
<text>Copy \"src/prog.js\" and \"images/icon.jpg\" to \"/tmp/package\" keeping relative path
  names</text>
<code>rsync -R src/prog.js images/icon.jpg /tmp/package</code>
<text>Adds execution permissions on a script ./etc/bash_completion within Homebrew home
  folder path.</text>
<code>
```

---

---

**NL2Bash: Response**

---

```
chmod +x /usr/local/etc/bash_completion</code>

[breaklines=true]
```

---

Table 7.4: NL2Bash example prompt and response from Codex: we did not use any extra information. The content in the last `<text>...</text>` marks in the prompt corresponds to the test problem.

time limit of 10 seconds on a single Intel(R) Xeon(R) CPU E5-2698 v4 @ 2.20GHz CPU, and consider the programs that exceed these limits as inexecutable; unless otherwise specified, we only execute each program on the first test input provided for the example and use the output for calculating the Bayes risk in the inference process.

### 7.3.2 Baselines

We compare the most basic baselines with no selection, prompting Codex with three examples in Table 7.1 format:<sup>7</sup>

- **Greedy decoding.** We perform token-by-token greedy decoding to generate the output.
- **Sampling.** We sample the output token by token with a fixed temperature, where we set the temperature as 0.3 in all of our experiments.

In addition, we consider the following baseline sample selection methods:

- **Maximizing likelihood (ML).** Given a set of sampled candidate programs, we select

---

<sup>7</sup>We use the code-davinci-001 engine throughout this work.

Method	MBPP	Spider	NL2Bash
Greedy (3-shot)	47.3 ± 2.5	50.8 ± 2.6	52.8 ± 2.9
Sample (3-shot)	47.7 ± 1.5	48.5 ± 2.6	53.0 ± 2.9
MBR-EXEC	<b>58.2 ± 0.3</b>	<b>63.6 ± 0.8</b>	<b>58.5 ± 0.3</b>

Table 7.5: Comparison between MBR-EXEC and baselines without a selection process. For both MBR-EXEC and Sample (3-shot), we collected samples with a temperature of 0.3. All numbers involve the same set of 125 samples for each case: for greedy and sample baselines, we report the average performance of them all; for MBR-EXEC, we report the result with 25 examples, averaged across five experiments.

the one with the largest log-likelihood. Formally, we select

$$\hat{p} = \arg \max_{p \in \mathcal{P}} \prod_{i=1}^{n_p} P(w_{p,i} \mid C, w_{p,1}, \dots, w_{p,i-1}),$$

where  $n_p$  denotes the number of tokens in a generated program  $p$ , and  $w_{p,i}$  denotes its  $i$ -th token.

- **Maximizing average log likelihood** (MALL) across tokens. In order to address the practical issue that ML typically favors shorter sequences, we follow Chen et al. (2021) and propose another baseline that uses the average log-likelihood across tokens as the selection criterion, where we select

$$\hat{p} = \arg \max_{p \in \mathcal{P}} \frac{1}{n_p} \sum_{i=1}^{n_p} \log P(w_{p,i} \mid C, w_{p,1}, \dots, w_{p,i-1}).$$

- **BLEU score based MBR** (MBR-BLEU). To study the effect of execution-based MBR in sample selection, we consider BLEU-based MBR, where the Bayes risk is calculated using the following risk function:

$$\ell_{BLEU}(p_i, p_j) = -BLEU(p_i, p_j),$$

where  $BLEU(p_i, p_j)$  is the BLEU score of the two programs. We use character-level (MBR-charBLEU) or token-level (MBR-tokenBLEU) BLEU-4 in all of our experiments.

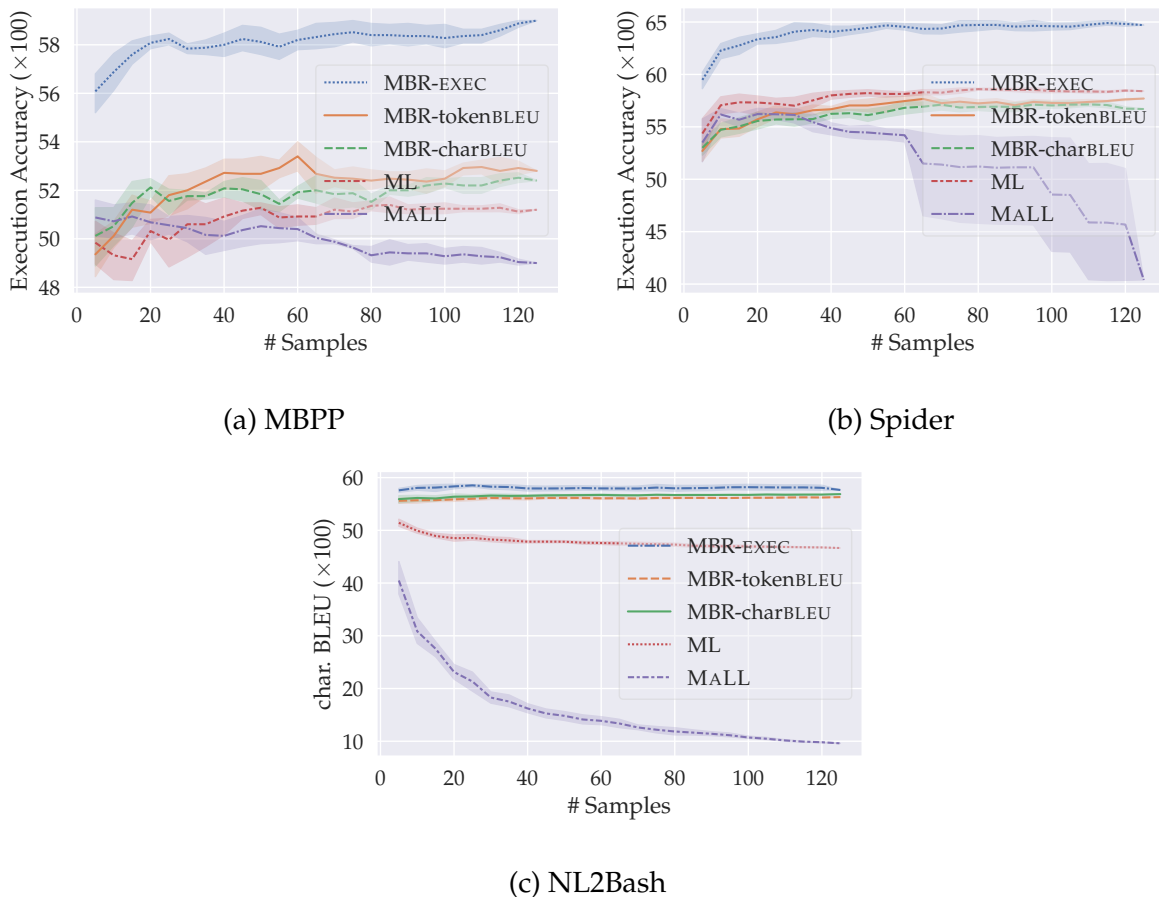


Figure 7.2: Primary evaluation results of MBR-EXEC: performance of the evaluated selection criteria (best viewed in color). For each sample size, we evaluate the methods on five different groups of samples and report the average performance (lines) and the standard deviations (shaded regions). All samples are collected from Codex with a temperature of 0.3.

### 7.3.3 Primary Results

We evaluate MBR-EXEC on the three datasets (§7.3.1) with dataset-specific metrics, using one test case for each problem. MBR-EXEC outperforms all baselines without a selection process by a significant margin (Table 7.5). In addition, we find that MBR-EXEC outperforms all baseline selection methods (Figure 7.2) and is especially effective on the two datasets (MBPP and Spider) that use execution-based evaluation. In addition, the MBR-BLEU metrics are also solid and robust across datasets, suggesting the effectiveness

Dataset	Greedy ( $\tau = 0$ )	Sample ( $\tau = 0.3$ )
MBPP	56.0	<b>58.2</b> $\pm$ 0.3
Spider	62.1	<b>63.6</b> $\pm$ 0.8
NL2Bash	58.4	<b>58.5</b> $\pm$ 0.3

Table 7.6: MBR-EXEC performance on greedily decoded and sampled programs: for each problem, we use 25 groups of 3-shot prompts, decode or sample one program with each prompt, and use MBR-EXEC to select the best program. For sampling with temperature 0.3, we repeat the process five times and report the average performance and standard deviations. The dataset-specific metric can be found at §7.3.1. The best number in each row is in boldface. Note that the greedy performances are different from those reported in Table 7.5, as we perform MBR-EXEC here over greedy decoding outputs while reporting the average performance in Table 7.5.

of finding a consensus candidate with generally low discrepancy with other samples.

While more samples lead to better performance for most methods, MALL consistently performs worse with larger sample size, as we find that MALL generally favors programs with unnecessary repetitions,<sup>8</sup> and a larger sample size generally leads to a more significant chance to have such a sample.

### 7.3.4 Analysis

We analyze the performance of MBR-EXEC from the following perspectives: the effectiveness across different sample collection temperatures (§7.3.4), the effectiveness of using groups of 3-shot prompts (§7.3.4), and the contribution of using execution results instead of simply checking the executability of programs (§7.3.4).

#### Effect of Sample Temperature

We first compare sampling with temperature 0.3 to greedy decoding (i.e., temperature  $\tau = 0$ ) from the Codex model (Table 7.6). When having the same number of examples,

<sup>8</sup>This issue has been found in existing open-ended text generation models, while methods such as unlikelihood training (Welleck et al., 2020) may help reduce degeneration (i.e., the generation of unnecessarily repetitive output).

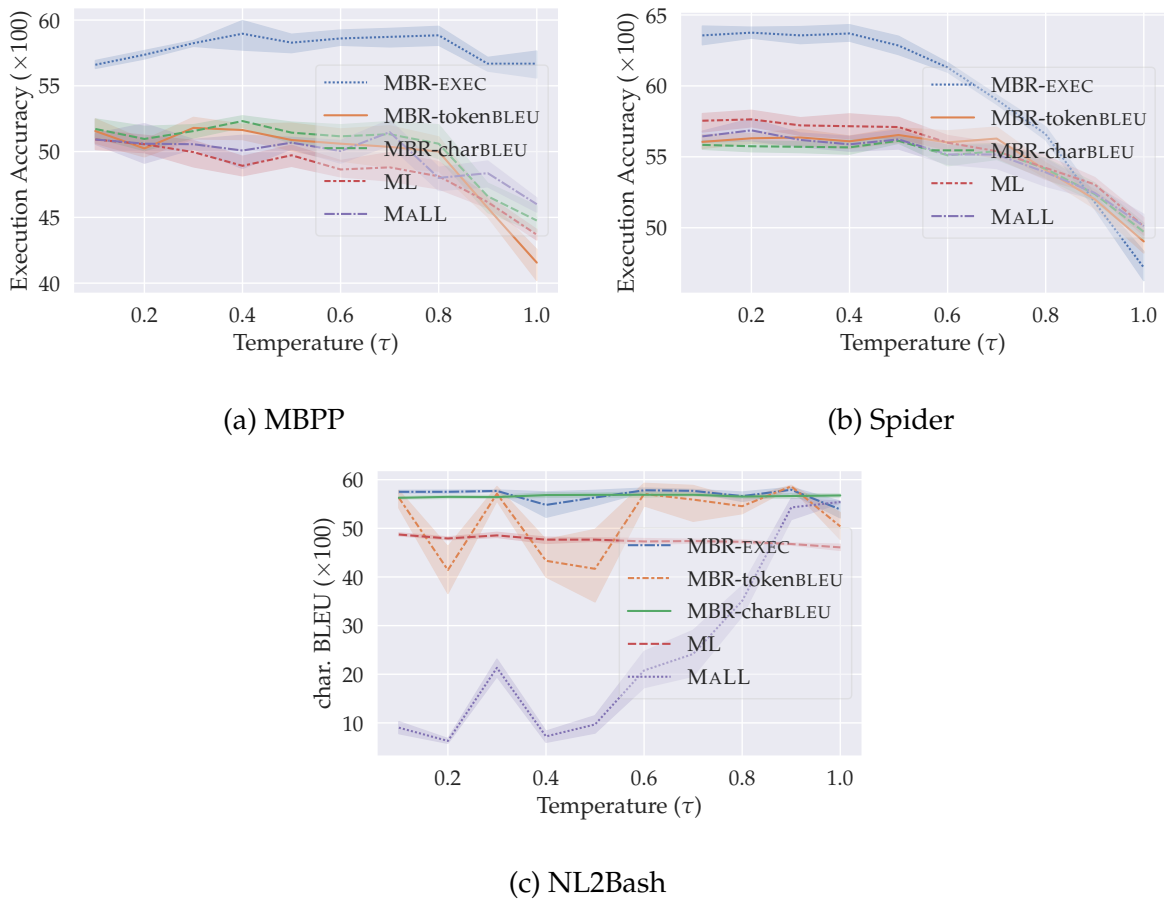


Figure 7.3: Performance of the evaluated selection criteria across temperatures (best viewed in color). We perform the methods for each temperature on five groups of 25 examples and report the average performance (lines) and the standard deviations (shaded regions).

MBR-EXEC on sampled candidates with temperature 0.3 consistently reaches competitive or better performance than that on greedy decoded candidates.

We plot the performance of MBR-EXEC for various sampling temperatures (Figure 7.3). Across datasets, we find that MBR-EXEC with a decoding temperature lower than 0.5 usually leads to reasonably good performance. When the temperature approaches 1.0, the results rapidly drop for all considered selection methods on MBPP and Spider; however, MALL generally achieves higher performance on NL2bash with a higher temperature.

According to the evidence discussed above, we recommend sampling with a low temperature (specifically, lower than 0.5) for candidate sample collection and performing



Figure 7.4: Performance with different types of prompts, where *groups of 3-shot* denotes the prompt formatting in Table 7.1, while *concatenation of 15* denotes concatenating all available 15 examples as prompts for data collection.

MBR-EXEC for final program selection for better results.

### Effect of Different 3-shot Prompts

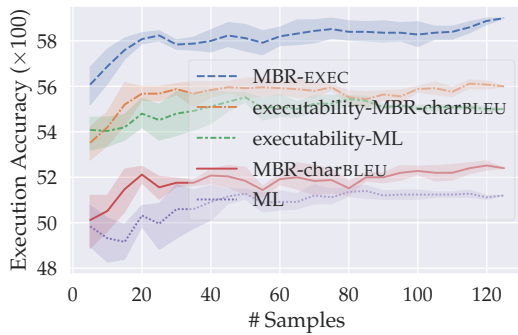
We analyze the necessity of choosing multiple groups of 3-shot instead of simply concatenating the available 15 examples as the prompt (Figure 7.4).<sup>9</sup> We allow different orders of the 15 examples when collecting samples. On both MBPP and NL2Bash datasets, we find that using different groups of 3-shot prompts outperforms concatenating all 15 examples, suggesting that different groups of fewer-shot prompts followed by post-hoc decoding may be more effective than using all available examples for all time.

### Executability vs. Execution Results

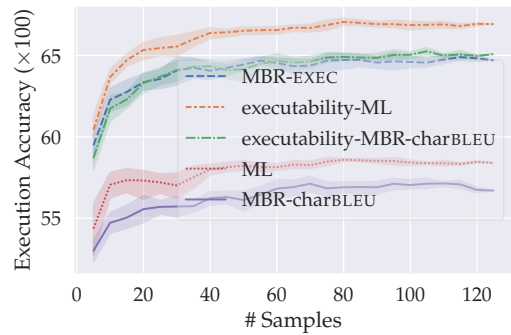
We perform an ablation study to identify the contribution of execution results vs. program executability (Figure 7.5) on the MBPP and Spider datasets.<sup>10</sup> We try to execute all candidates on the test cases and perform baseline candidate methods only on the candidates that

<sup>9</sup>We only include MBPP and NL2Bash results here as concatenating 15 Spider examples usually results in exceeding the token number limit of the pre-trained models.

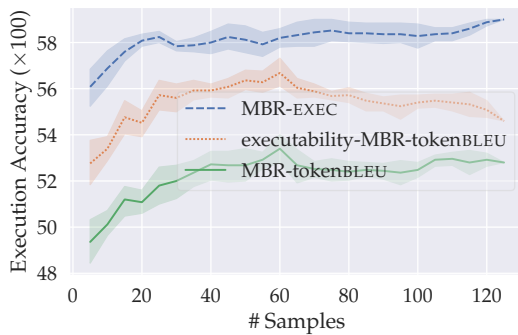
<sup>10</sup>We did not include NL2bash since MBR-EXEC does not execute the commands. However, the comparison between MBR-EXEC and MBR-tokenBLEU in Figure 7.3(c) shows that using an external bash parser as an executability estimator leads to more consistent and generally better performance.



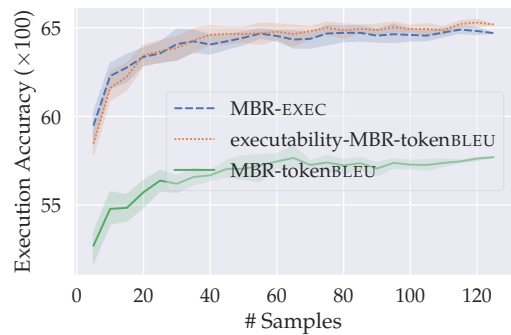
(a) MBPP



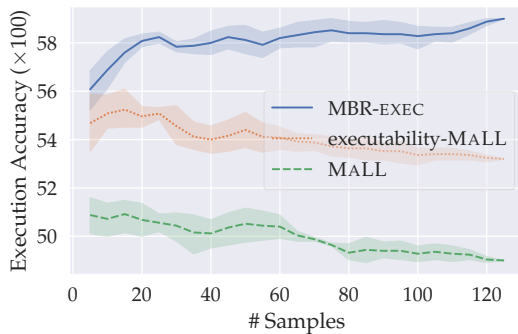
(b) Spider



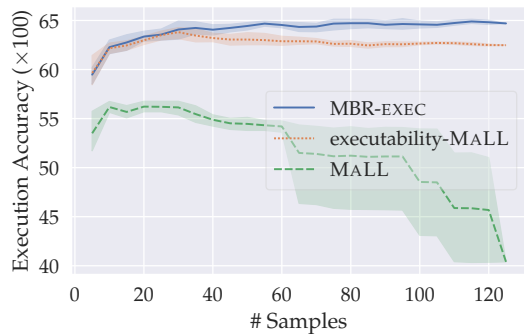
(c) MBPP (MBR-tokenBLEU)



(d) Spider (MBR-tokenBLEU)



(e) MBPP (MALL)



(f) Spider (MALL)

Figure 7.5: Comparison between applying methods to all possible candidates vs. applying methods to only executable candidates (best viewed in color), where executability- $X$  denotes applying selection criteria  $X$  on executable candidates only. We present MBR-tokenBLEU and MALL and their combination with executability check separately for clarity.



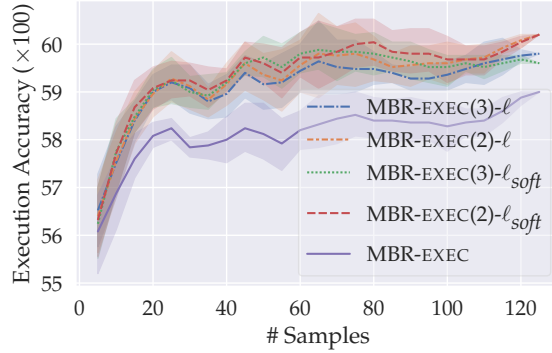


Figure 7.6: Execution accuracies with respect to sample size on the MBPP dataset, where the number in the parentheses denotes the number of test cases per problem used for MBR-EXEC. Best viewed in color.

successfully execute within the time limit. On both datasets, we find that simply involving executability checking significantly helps improve the performance of all non-semantic feature-based selection methods; on Spider, applying ML over executable commands even outperforms MBR-EXEC across sample sizes.

### Soft Loss as the Bayes Risk Function

While all the above evaluations are based on executing one test case per problem, more test cases can lead to more accurate judgments of semantic equivalence between programs (Zhong et al., 2020). Therefore, we introduce more test cases and compare  $\ell$  (§7.2.2) with  $\ell_{soft}$ , a soft version of the loss function, as the Bayes risk function in MBR-EXEC. We define  $\ell_{soft}$  as follows:

$$\ell_{soft}(p_i, p_j) = \frac{1}{|\mathcal{T}|} \sum_{t \in \mathcal{T}} \mathbb{1}[p_i(t) \neq p_j(t)],$$

which assesses equivalence based on the number of test cases that receive the same output. If only one test case is available,  $\ell$  and  $\ell_{soft}$  are equivalent.

We experiment with the MBPP dataset (Figure 7.6) as it provides three test cases per problem. While multiple test cases clearly outperform MBR-EXEC with one test case across sample sizes, we did not find a significant difference between  $\ell_{hard}$  and  $\ell_{soft}$ , nor between using two or three test cases.

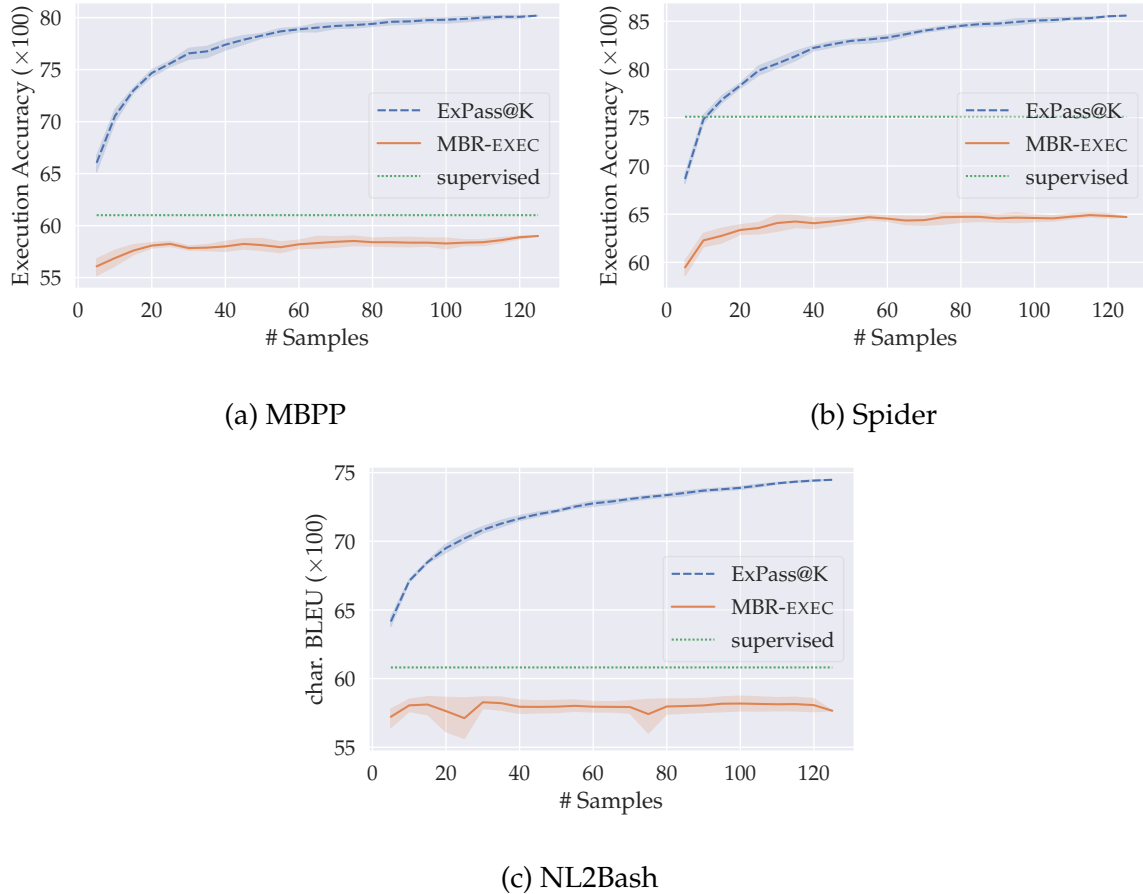


Figure 7.7: Sample size–oracle performance curves on the considered datasets. We calculate each expected Pass@K with five different sets of candidates for each sample size while using the same sets to perform MBR-EXEC for fair comparison.

### 7.3.5 Oracle Performance

We report the upper bound performance of all inference methods (Figure 7.7). Here, we define the expected Pass@K on one problem  $q$  by

$$ExPass@K(q) = \mathbb{E}_{|\mathcal{P}|=K} \left[ \max_{p \in \mathcal{P}} \min_{t \in \mathcal{T}_q} \mathbb{1}[p(t) = G(t)] \right],$$

where  $G(t)$  denotes the ground-truth output for test case input  $t$ . Intuitively, to calculate the performance upper bound, a problem  $q$  is considered to be solved if one program in the candidate sample set  $P$  passes all associated test cases  $\mathcal{T}_q$ . The dataset-level expected Pass@K is defined as the average expected Pass@K across all problems.

In addition, we report the supervised performance on these datasets, where all available training data are used for model training or finetuning: for MBPP, the results are from Austin et al. (2021), where they use all 374 training examples to finetune their pre-trained code model; for Spider, we compare to the current state-of-the-art result (Scholak et al., 2021); for NL2Bash, we finetune GPT-2 (Radford et al., 2019) with all training examples with the same prompting set up as Table 7.1.

However, it is worth noting that the upper bounds outperform the state-of-the-art supervised performances on all datasets by a significant margin when a reasonable sample is given. This further demonstrates the effectiveness of the pre-trained code models and points out a potential next step in the direction: while such models can generate correct programs, designing an effective inference algorithm may be a promising way to translate natural language commands to code in real-world applications.

## 7.4 Conclusion and Discussion

In this chapter, we present and systematically analyze MBR-EXEC, an execution-based inference algorithm for pre-trained language to code models, on datasets that cover three representative programming languages. Our results showed that doing execution, even with access only to inputs (not outputs) for test cases, or with only access to an executability checker, substantially helps improve the quality of generated programs, especially in the settings that use execution accuracy as the evaluation metric (MBPP and Spider). Given the consistently strong performance, we suggest future work on program synthesis with large pre-trained models consider MBR-EXEC as an effective selection algorithm. When we are not able to execute programs, or there are no test inputs available, our results suggest considering an alternative MBR metric (e.g., MBR-BLEU) as the selection algorithm.

The method proposed in this chapter connects deeply with Holtzman et al. (2021). In addition to the potentially insufficient training of models, Holtzman et al. (2021) offers a potential interpretation of why the maximum-probability program does not always give the correct execution results—they may compete with each other in terms of the surface form probability. In contrast to the domain-specific pointwise mutual information solution for question answering proposed by Holtzman et al. (2021), we directly consider the external execution results, which are arguably more interpretable and reliable in noisy real-world settings.

Our results also align with the concurrent work by Wang et al. (2023), where they propose using consistency-based selection for mathematical reasoning. More concretely, they sample multiple intermediate reasoning paths from the pre-trained large language models, and have them perform majority voting to select the final answer. Indeed, there are three potential views of both work presented in this chapter and Wang et al. (2023):

- **Majority voting.** Each of the sampled programs (this work) or reasoning paths (Wang et al., 2023) is considered as a vote, and the final answer is selected by majority voting.
- **Minimum Bayes risk decoding.** Unifying in the theoretical framework proposed in this work, it can be viewed that Wang et al. (2023) (1) define a Bayes risk function that considers the discrepancy between reasoning paths by  $\mathbb{1}[x \neq y]$ , where  $x$  and  $y$  are two reasoning paths of the same problem, and (2) select the final answer by minimizing the expected discrepancy.
- **Sample-based marginal distribution estimation.** Arguably more naturally, both methods can be viewed as estimating the marginal probability of execution results (this work) or final answers to a math problem (Wang et al., 2023) by sampling. Here, the models sample multiple examples and marginalize over all possible program forms (this work) or reasoning paths (Wang et al., 2023) that share the same execution results (this work) or final answers (Wang et al., 2023) to select the final program or answer.

The Bayes risk minimization framework provides a more flexible way to design new variants of the underlying probability distribution, compared to the other two views, through flexible modification of the Bayes risk function. While this work estimates the semantics of programs in an arguably more reliable way, we also acknowledge that Wang et al. (2023) have offered a more general approach that can only rely on pre-trained models without any external sources.

This work and Wang et al. (2023) also share a common limitation: both methods are computationally expensive due to the need for multiple examples from the pre-trained models. We suggest that future work explore more efficient ways to estimate the marginal distribution of programs or reasoning paths, which may lead to more practical applications of these methods in real-world scenarios.

## **Part III**

# **Learning to Parse through Cross-Lingual Grounding**

## Chapter 8

# From Pre-Trained Contextualized Representations to Unsupervised Cross-Lingual Word Alignment

*Content in this has been published as part of a conference paper at ACL 2021 (Shi et al., 2021), of which the main research question is on bilingual lexicon induction.*

This chapter presents a method for learning cross-lingual word alignment from contextualized representations. The task of cross-lingual word alignment aims to find the word correspondences between two mutually translatable sentences in different languages (Figure 8.1). Prior work, SimAlign (Jalili Sabet et al., 2020), has proposed to directly adapt pre-trained contextualized multilingual language models, calculate the similarity between the representations of words in different languages, and then use different inference strategies to obtain the final alignment. Following SimAlign, our method, which is initially designed for bilingual lexicon induction (Shi et al., 2021), fuses multiple inference strategies to improve the alignment quality by learning a multi-layer perceptron (MLP) that takes statistical features, such as word frequency, cooccurring word pairs, and the similarity between the representations of words in different languages, as the input, and predicts the alignment probability. Results on cross-lingual word alignment benchmarks show that our method outperforms SimAlign and builds a new state of the art for the task.

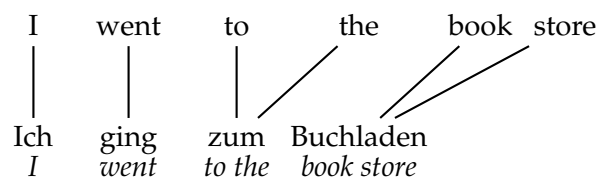


Figure 8.1: Example of cross-lingual word alignment in English and German. The lines indicate the word correspondences between the two sentences. The word alignment relations include both one-to-one (e.g., I and Ich) and many-to-one (e.g., book store and Buchladen) correspondences.

## 8.1 Related Work

**Word alignment.** Word alignment is a fundamental problem in statistical machine translation, of which the goal is to align words that are translations of each within parallel sentences (Brown et al., 1993). Most methods assume parallel sentences for training data (Och and Ney, 2003; Dyer et al., 2013; Peter et al., 2017, *inter alia*). Following the approach of IBM models (Brown et al., 1993), existing work has achieved decent performance with statistical methods (Och and Ney, 2003; Dyer et al., 2013). Recent work has demonstrated the potential of neural networks on the task (Peter et al., 2017; Garg et al., 2019; Zenkel et al., 2019, *inter alia*). In contrast, Jalili Sabet et al. (2020) propose SimAlign, which does not train on parallel sentences but instead aligns words that have the most similar pre-trained multilingual representations (Devlin et al., 2019; Conneau et al., 2020). SimAlign achieves competitive or superior performance compared to conventional alignment methods despite not using parallel sentences, and it provides one of the baseline components for our work. This work presents a simple yet effective method to improve performance over SimAlign (§8.2).

**Bitext mining/parallel corpus mining.** Bitext mining has been a long studied task (Resnik, 1999; Shi et al., 2006; Abdul-Rauf and Schwenk, 2009, *inter alia*). Most methods train neural multilingual encoders on bitext, which are then used with efficient nearest neighbor search to expand the training set (España-Bonet et al., 2017; Schwenk, 2018; Guo et al., 2018; Artetxe and Schwenk, 2019, *inter alia*). Recent work has also shown that unsupervised mining is possible (Tran et al., 2020; Keung et al., 2020). We use CRISS (Tran et al., 2020)<sup>1</sup>

<sup>1</sup><https://github.com/pytorch/fairseq/tree/master/examples/criss>

as one of our component models.

## 8.2 Method

### 8.2.1 Unsupervised Bitext Construction

We follow Tran et al. (2020) to perform bitext construction through encoding-based retrieval: taking the average across the contextualized embeddings of tokens as sentence representation, we perform nearest neighbor search, and mine bitext using the margin-based max-score method (Artetxe and Schwenk, 2019). We use CRISS (Tran et al., 2020) as the base model in this work.

The margin score between sentence representations  $\mathbf{s}$  and  $\mathbf{t}$  is defined by

$$score(\mathbf{s}, \mathbf{t}) = \frac{\cos(\mathbf{s}, \mathbf{t})}{\sum_{\mathbf{t}' \in NN_k(\mathbf{t})} \frac{\cos(\mathbf{s}, \mathbf{t}')}{2k} + \sum_{\mathbf{s}' \in NN_k(\mathbf{s})} \frac{\cos(\mathbf{s}', \mathbf{t})}{2k}}, \quad (8.1)$$

where  $NN_k(\cdot)$  denotes the set of  $k$  nearest neighbors of a vector in the corresponding space. In this work, we keep the top 20% of the sentence pairs with scores larger than one as the constructed bitext.

### 8.2.2 Feature-Based Word Aligner

Let  $\mathcal{B} = \{\langle \mathbf{s}_i, \mathbf{t}_i \rangle\}_{i=1}^N$  denote the constructed bitext, where  $N$  denotes the number of sentence pairs, and  $\mathbf{s}_i$  and  $\mathbf{t}_i$  denote a pair of sentences in the source and target language respectively. In a pair of bitext  $\langle \mathbf{s}, \mathbf{t} \rangle$ ,  $\mathbf{s} = \langle s_1, \dots, s_{\ell_s} \rangle$  and  $\mathbf{t} = \langle t_1, \dots, t_{\ell_t} \rangle$  denote sentences consisting of  $\ell_s$  and  $\ell_t$  word tokens respectively.

For a pair of bitext, SimAlign with a specified inference algorithm produces word alignment  $\mathcal{A} = \{\langle a_i, b_i \rangle\}_i$ , denoting that the word tokens  $s_{a_i}$  and  $t_{b_i}$  are aligned. Jalili Sabet et al. (2020) has proposed different algorithms to induce alignment from the same similarity matrix, and the best method varies across language pairs. In this work, we consider the relatively conservative (i.e., having higher precision) *argmax* and the higher recall *itermax* algorithm, and denote the alignments by  $\mathcal{A}_{argmax}$  and  $\mathcal{A}_{itermax}$  respectively. Concretely, let  $\mathcal{S} \in \mathbb{R}^{\ell_s \times \ell_t}$  denote the similarity matrix between two sentences, the *argmax* algorithm



aligns any word pair  $\langle s_i, t_j \rangle$  that satisfies

$$i = \arg \max_{i'} S_{i',j},$$

$$j = \arg \max_{j'} S_{i,j'}.$$

A word pair  $\langle s_i, t_j \rangle$  will be aligned by the *itermax* algorithm if their similarity is both row-wise and column-wise maximum in the similarity matrix. The *itermax* algorithm applies *argmax* iteratively—at each step, it appends all word pairs selected by *argmax* to the alignment set and mask-out those selected positions,<sup>2</sup> and repeats the process until no word pair can be selected. It is obvious that  $\mathcal{A}_{argmax} \subseteq \mathcal{A}_{itermax}$ , since the first step of the latter produces the same result as the former.

We consider the following features for each word token pair  $\langle s_i, t_j \rangle$ :

- Count of alignment: we consider both one-to-one alignment and many-to-one alignment of  $s$  and  $t$  separately as two features since the task of lexicon induction is arguably biased toward one-to-one alignment.
- Count of co-occurrence in the mined bitext.
- The count of  $s$  in the source language and  $t$  in the target language.
- Contextualized word similarity: we feed the words in contexts into CRISS, use the average pooling of the output subword embeddings, and consider both cosine similarity and dot-product similarity as features.

We formulate word alignment as the task of ternary classification. For a pair of word tokens  $\langle s_i, t_j \rangle$ , the gold label  $y_{\langle s_i, t_j \rangle}$  is defined as

$$\mathbb{1}[\langle i, j \rangle \in \mathcal{A}_{argmax}] + \mathbb{1}[\langle i, j \rangle \in \mathcal{A}_{itermax}].$$

Intuitively, the labels 0 and 2 represent confident alignment or non-alignment by both methods, while the label 1 models the potential alignment.

The MLP takes the features  $\mathbf{x}_{\langle s_i, t_j \rangle} \in \mathbb{R}^7$  of the word token pair and computes the

---

<sup>2</sup>Empirically, this can be done by setting the corresponding row and column of the similarity matrix to a sufficiently small value.

probability of each label  $y$  by

$$\begin{aligned}\hat{\mathbf{h}} &= \text{ReLU}(\mathbf{W}_1 \mathbf{x}_{\langle s_i, t_j \rangle} + \mathbf{b}_1) \\ \mathbf{g} &= \mathbf{W}_2 \cdot \hat{\mathbf{h}} + \mathbf{b}_2 \\ P_{\Phi}(y \mid s_i, t_j, \mathcal{S}, \mathcal{T}) &= \frac{\exp(g_y)}{\sum_{y'} \exp(g_{y'})}\end{aligned}$$

where  $\Phi = \{\mathbf{W}_1 \mathbf{W}_2, \mathbf{b}_1, \mathbf{b}_2\}$ . On the training stage, we maximize the log-likelihood of ground-truth labels:

$$\Phi^* = \arg \max_{\Phi} \sum_{\langle \mathcal{S}, \mathcal{T} \rangle \in \mathcal{B}} \sum_{s_i \in \mathcal{S}} \sum_{t_j \in \mathcal{T}} \log P_{\Phi}(y_{\langle s_i, t_j \rangle} \mid s_i, t_j, \mathcal{S}, \mathcal{T}).$$

On the inference stage, we keep all word token pairs  $\langle s_i, t_j \rangle$  that have

$$\mathbb{E}_P[y] := \sum_y y \cdot P(y \mid s_i, t_j, \mathcal{S}, \mathcal{T}) > 1$$

as the prediction.

### 8.3 Experiments

We evaluate different word alignment methods (Table 8.1) on existing word alignment datasets,<sup>3</sup> following Jalili Sabet et al. (2020). We investigate four language pairs: German–English (de-en), English–French (en-fr), English–Hindi (en-hi), and Romanian–English (ro-en). While Jalili Sabet et al. (2020) initially implement SimAlign with an XLM-R backbone, we also consider mBART (Liu et al., 2020) and CRISS (Tran et al., 2020) as the backbone model. Indeed, we find that, in general, backbone models that achieve better performance on general-purpose multilingual benchmarks also perform better on word alignment. The CRISS-based SimAlign already achieves competitive performance with the state-of-the-art method (Garg et al., 2019), which requires supervised bitext for training. By ensembling the *argmax* and *itermax* CRISS-based SimAlign results, we set the new state of the art of word alignment without using any bitext supervision.

<sup>3</sup><http://www-i6.informatik.rwth-aachen.de/goldAlignment> (de-en);  
<https://web.eecs.umich.edu/~mihalcea/wpt> (en-fr and ro-en);  
<https://web.eecs.umich.edu/~mihalcea/wpt05> (en-hi)

Model	de-en	en-fr	en-hi	ro-en
GIZA++ (Och and Ney, 2003) <sup>†</sup>	0.22	0.09	0.52	0.32
Fast Align (Dyer et al., 2013) <sup>†</sup>	0.30	0.16	0.62	0.32
Garg et al. (2019)	0.16	0.05	N/A	0.23
Zenkel et al. (2019)	0.21	0.10	N/A	0.28
SimAlign (Jalili Sabet et al., 2020)				
XLM-R (Conneau et al., 2020)- <i>argmax</i> <sup>†</sup>	0.19	0.07	0.39	0.29
mBART (Liu et al., 2020)- <i>argmax</i>	0.20	0.09	0.45	0.29
CRISS (Tran et al., 2020)- <i>argmax</i> *	0.17	0.05	0.32	0.25
CRISS (Tran et al., 2020)- <i>itermax</i> *	0.18	0.08	0.30	0.23
MLP (ours)*	<b>0.15</b>	<b>0.04</b>	<b>0.28</b>	<b>0.22</b>

Table 8.1: Average error rate (AER) for word alignment (lower is better). The best numbers in each column are bolded. Models in the top section require ground-truth bitext, while those in the bottom section do not. \*: models that involve unsupervised bitext construction. †: results copied from Jalili Sabet et al. (2020).

## 8.4 Conclusion and Discussion

This chapter discusses a lightweight and effective method to extract word alignment relations from pre-trained contextualized multilingual language models. In the next chapter, we will discuss how such cross-lingual word alignment can bridge languages and enable grounding the syntax of one language to another.

Since SimAlign was proposed, it has become common wisdom that the cross-lingual word alignment information is encoded in the representations of pre-trained multilingual language models. By calculating the similarity between the representations of words in different languages, SimAlign has achieved competitive performance without using parallel sentences, significantly saving the cost of obtaining bitext. Following this line, our work demonstrates that fully unsupervised word alignment can even outperform methods requiring supervised bitexts. While the feature-based MLP method is one of many possible ways to improve the alignment quality, it takes advantage of simplicity and interpretability.

While the method was initially designed for bilingual lexicon induction (Shi et al., 2021),

where we used statistical features from pre-trained contextualized multilingual models to induce mutually translatable word pairs, it is easily adapted to the word alignment task. The improvement over single-model SimAlign suggests that pre-trained language models may be generally more potent than directly using their representations. The method can be further improved by incorporating more sophisticated features and models.

## Chapter 9

# Zero-Shot Cross-Lingual Dependency Parsing with Substructure Distribution Projection

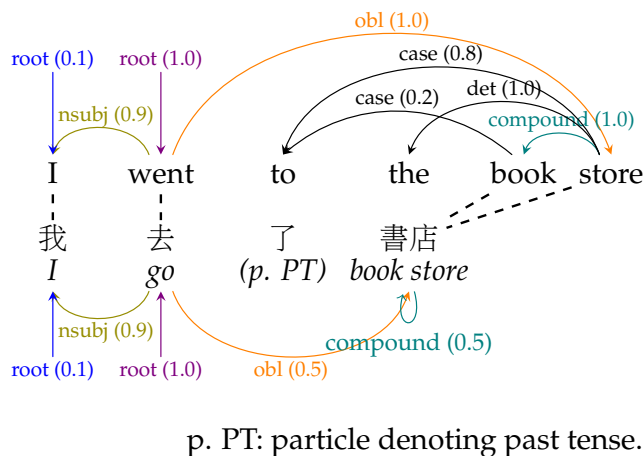
*Content in Chapter 9 has been published as a conference paper at ACL 2022 (Shi et al., 2022).*

Zero-shot cross-lingual dependency parsing requires the prediction of dependency parses without seeing any parsing example in the target language; instead, the model may use annotated parses in other languages. This chapter discusses how high-quality zero-shot cross-lingual dependency parsing can be achieved with unsupervised word alignment (Jalili Sabet et al., 2020; Shi et al., 2021, *inter alia*) as the bridge between languages.

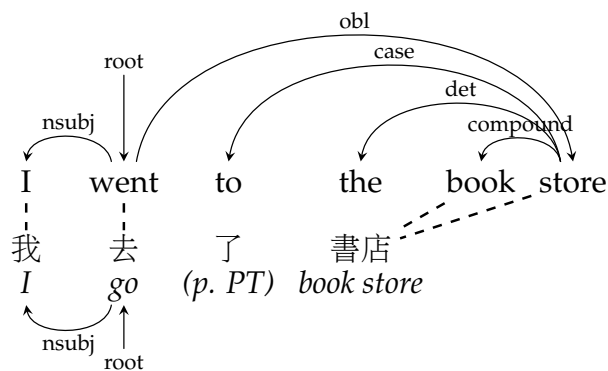
We present substructure distribution projection (SUBDP), a technique that projects a distribution over structures in one domain to another by projecting substructure distributions separately. Models for the target domain can then be trained using the projected distributions as soft silver labels. Our motivation is to address the limitations of existing annotation projection methods, which typically project “hard” structures and usually have a low recall for the target structures.<sup>1</sup> As illustrated in Figure 9.1b, most annotation projection methods typically output partial hard dependency trees, where there either is or is not an arc between any pair of words. In addition, most bitext-based work has relied on one-to-one word alignment between bitext pairs (Ma and Xia, 2014; Lacroix et al.,

---

<sup>1</sup>Throughout this chapter, we refer to dependency parse trees with 0/1 arc and label probabilities, i.e., conventional dependency trees, as *hard trees*; in contrast, we refer to collections of per-word head distributions and per-arc label distributions with continuous probabilities as *soft trees*.



(a) Soft trees projected by SUBDP. The self-loops are discarded when training models.



(b) Hard trees projected with only one-to-one alignments (Lacroix et al., 2016).

Figure 9.1: Illustration of SUBDP vs. Lacroix et al. (2016). The English sentence (up) is projected to German (bottom) using the dependency arcs as substructures. Same-colored solid arcs denote corresponding arcs in the source and target trees, while dashed arcs exist in the ground truth but are not projected. The arcs are projected separately, and the target parser is trained on the projected distributions. Best viewed in color.

2016; Rasooli et al., 2021, *inter alia*), discarding information in many-to-one alignments. In contrast, SUBDP (Figure 9.1a) projects substructure distributions, i.e., the conditional probability distribution of the corresponding head given a word.<sup>2</sup> When the source parse

<sup>2</sup>Projection of the distribution over whole parse trees has been considered by Ma and Xia (2014), while

is a hard tree, SUBDP has the same behavior as prior work (e.g., Lacroix et al., 2016) for arcs that are only involved in one-to-one alignments; for many-to-one alignments, SUBDP projects the corresponding arcs into *soft* arc distributions in the target language. Therefore, in SUBDP, a target language word may have multiple heads in the projected trees, where their probabilities sum to one. More generally, SUBDP may take dependency arc or label distributions (i.e., soft trees) in the source language(s) instead of hard trees as the input. As in annotation projection approaches, the projected soft trees are then used to train a target language parser.

We evaluate SUBDP on zero-shot cross-lingual dependency parsing, taking dependency arcs as substructures: we project the predicted dependency arc distributions in the source language(s) to target language(s) and train a target language parser on the resulting distributions. Given an English treebank as the only source of human supervision, SUBDP achieves higher unlabeled attachment scores than all prior work on the Universal Dependencies v2.2 (Nivre et al., 2020) test set across eight diverse target languages, as well as the best-labeled attachment score on six languages. In addition, SUBDP improves zero-shot cross-lingual dependency parsing with very few (e.g., 50) supervised bitext pairs across a broader range of target languages.

## 9.1 Related Work

**Zero-shot cross-lingual dependency parsing.**<sup>3</sup> Existing approaches can be classified into the following categories:

1. **Delexicalized training** (Zeman and Resnik, 2008; McDonald et al., 2011; Cohen et al., 2011; Durrett et al., 2012; Rosa and Žabokrtský, 2015, *inter alia*), which only considers delexicalized features (e.g., part-of-speech tags) in training. However, in most recent work, the availability of pre-defined delexicalized features is not assumed.
2. **Transfer with cross-lingual embeddings** (Täckström et al., 2012; Guo et al., 2015; Schuster et al., 2019, *inter alia*), which assumes that cross-lingual word representations, including word clusters (Täckström et al., 2012; Ammar et al., 2016), word type embeddings (Guo et al., 2015, 2016; Duong et al., 2015; Ammar et al., 2016; Wick et al.,

---

SUBDP has a much lower time complexity—see §9.1 for more discussion.

<sup>3</sup>Also referred to as zero-shot dependency parsing in recent literature (Schuster et al., 2019; Wang et al., 2019).

2016), or contextualized cross-lingual word embeddings (Schuster et al., 2019; Wang et al., 2019; He et al., 2019; Ahmad et al., 2019,)), provide shared features for words with similar syntactic roles.

3. **Trebank translation**, which translates treebanks in the source language(s) into the target language(s) (Tiedemann et al., 2014; Tiedemann, 2015; Tiedemann and Agić, 2016) or a code-switching mode (Zhang et al., 2019), and uses them to train target language parsers.
4. **Annotation projection**,<sup>4</sup> which trains a parser in the source language(s) and projects the predicted source language parse trees to the target language(s) using bitext (Hwa et al., 2005; Ma and Xia, 2014; Agić et al., 2016). Additional strategies are usually used to improve the projection quality, such as keeping confident edges only (Li et al., 2014; Lacroix et al., 2016), projection from multiple source languages (Täckström et al., 2013; Agić et al., 2016; Rasooli and Collins, 2017), density based iterative filtering (Rasooli and Collins, 2015, 2017, 2019), and noisy self-training (Kurniawan et al., 2021).

These approaches make different assumptions on annotation availability, such as gold part-of-speech tags (Zeman and Resnik, 2008; Cohen et al., 2011; Durrett et al., 2012, *inter alia*), a reasonably good translator, which uses extra annotated data in the training process (Tiedemann et al., 2014; Tiedemann, 2015; Zhang et al., 2019), high-quality bilingual lexicons (Durrett et al., 2012; Guo et al., 2015, 2016, *inter alia*), or language-specific constraints (Meng et al., 2019). Most bitext-based work assumes annotated bitext (Ma and Xia, 2014; Li et al., 2014; Lacroix et al., 2016, *inter alia*) or bitext constructed from extra signals (e.g., Wikipedia; Rasooli et al., 2021). However, He et al. (2019), Schuster et al. (2019), Ahmad et al. (2019,)), and Kurniawan et al. (2021) only require minimal annotations (i.e., source language treebanks and unlimited raw text in relevant languages). We are mainly interested in the minimal annotation setting and will compare it to this line of work.

Our proposed method, SUBDP, falls into the category of annotation projection. Some of the benefits of SUBDP relative to prior work are that it works well with minimal annotations, allows soft word alignment (§9.2.2), supports both labeled and unlabeled parsing,

---

<sup>4</sup>We use *annotation projection* to denote the projection of predicted parses following Rasooli and Collins (2019) and Zhang et al. (2019), and *trebank translation* for the projection of human-annotated trees following Tiedemann et al. (2014).



and has a low time complexity  $\mathcal{O}(n^2)$  for non-projective parsing.<sup>5</sup> SUBDP can be easily extended to other tasks, such as sequence labeling, where we can define substructures (Shi et al., 2021) and substructure distributions.

**Multilingual contextualized representations.** Recent contextualized models pre-trained on multilingual text (Devlin et al., 2019; Conneau et al., 2020; Tran et al., 2020, *inter alia*) are effective across a wide range of cross-lingual NLP tasks, including bitext retrieval (Tran et al., 2020), bilingual lexicon induction (Shi et al., 2021), cross-lingual named entity recognition (Pires et al., 2019; Mulcaire et al., 2019), and cross-lingual dependency parsing (Schuster et al., 2019; Wang et al., 2019). In this work, we apply two of the contextualized pre-trained models, XLM-R (Conneau et al., 2020) and CRISS (Tran et al., 2020), to generate unsupervised bitext.

**Soft-label methods.** Calculating the cross entropy loss between model output and a soft distribution (instead of one-hot labels) has been applied to knowledge distillation (Hinton et al., 2015; You et al., 2017; Sanh et al., 2019, *inter alia*), cross-lingual named entity recognition (Wu et al., 2020), and for handling annotation discrepancy (Fornaciari et al., 2021). Our approach is a soft-label method with additional post-processing to the output of the original models.

## 9.2 Method

Our pipeline for zero-shot cross-lingual dependency parsing consists of three steps: (1) train a bi-affine dependency parser  $\mathcal{P}_1$  in the source language  $L_1$ , (2) project annotations on  $L_1$  sentences to their parallel sentences in the target language  $L_2$  (§9.2.3), and (3) train another bi-affine dependency parser  $\mathcal{P}_2$  for  $L_2$  (§9.2.4). We first present some background (§9.2.1) and preliminaries (§9.2.2).

### 9.2.1 Background

**Bi-affine dependency parser.** For a sentence with  $n$  words  $\langle w_1, \dots, w_n \rangle$ ,<sup>6</sup> we denote the word features when acting as heads and dependents by  $\mathbf{H} \in \mathbb{R}^{n \times d_h}$  and  $\mathbf{D} \in \mathbb{R}^{n \times d_d}$

---

<sup>5</sup>In contrast, Ma and Xia (2014) require  $\mathcal{O}(n^4)$  time for non-projective unlabeled dependency parsing.

<sup>6</sup>For convenience, we assume that  $w_1$  is an added dummy word that has one dependent – the root word of the sentence.

respectively, where  $d_h$  and  $d_d$  denote the dimensionality of the corresponding features. The probability of word  $w_i$  having head  $w_j$  can be formulated as an  $n$ -way classification problem:

$$\mathbf{S}^{(arc)} = \mathbf{D}\mathbf{W}^{(arc)}\mathbf{H}^\top \quad (9.1)$$

$$P(w_j | w_i) = \frac{\exp(\mathbf{S}_{i,j}^{(arc)})}{\sum_{k=1}^n \exp(\mathbf{S}_{i,k}^{(arc)})}, \quad (9.2)$$

where  $\mathbf{W}^{(arc)} \in \mathbb{R}^{d_d \times d_h}$  is the parameters of the bi-affine module.<sup>7</sup> Given  $\log P(w_j | w_i)$  for every pair of  $i$  and  $j$ , the dependency trees can be inferred by finding the spanning arborescence of maximum weight using the Chu–Liu–Edmonds algorithm (Chu and Liu, 1965; Edmonds, 1968). We use the algorithm proposed by Tarjan (1977), which has an  $\mathcal{O}(n^2)$  time complexity for each sentence.

We denote the candidate dependency label set by  $L$ . Parameterized by  $\mathbf{W}^{(label)} \in \mathbb{R}^{d_d \times d_h \times |L|}$ , we define the probability that the arc from head  $w_j$  to dependent  $w_i$  has the label  $\ell$  by

$$\mathbf{S}_{i,j,\ell}^{(label)} = \sum_p \sum_q \mathbf{D}_{i,p} \mathbf{W}_{p,q,\ell}^{(label)} \mathbf{H}_{j,q}$$

$$P(\ell | w_j \rightarrow w_i) = \frac{\exp(\mathbf{S}_{i,j,\ell}^{(label)})}{\sum_{k=1}^{|L|} \exp(\mathbf{S}_{i,j,k}^{(label)})}, \quad (9.3)$$

Given the probability definitions above, we train the model to maximize the log-likelihood of the training data. More details can be found in Dozat and Manning (2017).

We use bi-affine dependency parsers as the backbone for all parsers in this work, though it is worth noting that SUBDP works for any parser that produces a set of arc and label distributions.

**CRISS.** CRISS (Tran et al., 2020) is an unsupervised machine translation model trained with monolingual corpora, starting from mBART (Liu et al., 2020), a multilingual pre-trained sequence-to-sequence model with a mask-filling denoising objective. During the training process, CRISS iteratively (1) encodes sentences in the monolingual corpora with

---

<sup>7</sup>While Eq. (9.1) is in a bi-linear form, in practice, we can always append a constant feature column to both  $\mathbf{H}$  and  $\mathbf{D}$ , resulting in a bi-affine model.

its encoder, (2) mines bitext based on encoding similarity, and (3) uses the mined bitext to fine-tune the model with a machine translation objective. In this work, we use CRISS to generate an unsupervised translation of English sentences to construct bitext and apply its encoder to extract word features for an ablation study.

**SimAlign.** SimAlign (Jalili Sabet et al., 2020) is a similarity-based word aligner: given a pair of source and target sentence  $\langle s, t \rangle$ , SimAlign computes a contextualized representation for each token in both  $s$  and  $t$  using multilingual pre-trained models (Devlin et al., 2019; Conneau et al., 2020), and calculates the similarity matrix  $S$ , where  $S_{i,j}$  represents the cosine similarity between tokens  $s_i$  and  $t_j$ . The argmax inference algorithm selects position pairs  $\langle i, j \rangle$ , where  $S_{i,j}$  is both horizontal and vertical maximum and outputs the word pairs corresponding to such position pairs as the word alignment. This work uses XLM-R (Conneau et al., 2020) based SimAlign with the argmax algorithm to extract word alignment for SUBDP. Notably, pre-trained multilingual models usually use subwords, a more fine-grained level than words, for tokenization. The argmax algorithm may therefore generate many-to-one alignments. More details can be found in Jalili Sabet et al. (2020).

Unlike bitext-based word alignment (Och and Ney, 2003; Dyer et al., 2013), such as GIZA++ (Och and Ney, 2003) and `fast_align` (Dyer et al., 2013), SimAlign does not require any bitext to produce high-quality alignments, and therefore better fits the low-resource scenario with very few bitext pairs available.

## 9.2.2 Preliminaries

**Dependency annotations in  $L_1$ .** As in the most common data settings for supervised dependency parsing, we assume access to sentences with dependency annotations: for a sentence  $\langle w_1, \dots, w_n \rangle$ , there is a dummy word  $w_1$ , whose unique dependent is the root word; every other word  $w_i$  is labeled with  $h_i$  and  $r_i$ , denoting that the head of  $w_i$  is  $w_{h_i}$ , with the dependency relation  $r_i$ . We use these annotations to train an  $L_1$  bi-affine dependency parser  $\mathcal{P}_1$ , following the procedure described in §9.2.1.

**Bitext.** We denote the available  $m$  pairs of bitext by  $\mathcal{B} = \{\langle s^{(k)}, t^{(k)} \rangle\}_{k=1}^m$ , where  $\{s^{(k)}\}$  and  $\{t^{(k)}\}$  are sentences in  $L_1$  and  $L_2$  respectively.

**Word alignment.** For a bitext pair  $\langle s, t \rangle$ , we generate the word alignment matrix  $\tilde{A} \in \{0, 1\}^{|s| \times |t|}$  with SimAlign, where  $\tilde{A}_{i,j} = 1$  denotes that there exists an alignment between

$s_i$  and  $t_j$ .

We would like the word alignment matrices to be right stochastic, i.e., (1) each element is non-negative and (2) each row sums to one, to ensure that the results after projection remain distributions. To handle words that have zero or more than one aligned words in the other language, we introduce the following two matrix operators.

**The *add-dummy-position* operator  $\Delta(\cdot)$ :**

$$\begin{aligned}\Delta &: \mathbb{R}^{r \times c} \rightarrow \mathbb{R}^{(r+1) \times (c+1)} (\forall r, c \in \mathbb{N}_+) \\ \Delta(\mathbf{M})_{i,j} &= \mathbf{M}_{i,j} (1 \leq i \leq r, 1 \leq j \leq c); \\ \Delta(\mathbf{M})_{i,c+1} &= \mathbf{0}[\mathbf{M}_{i,1}, \dots, \mathbf{M}_{i,c}] (1 \leq i \leq r); \\ \Delta(\mathbf{M})_{r+1,j} &= \mathbf{0} (1 \leq j \leq c); \\ \Delta(\mathbf{M})_{r+1,c+1} &= 1,\end{aligned}$$

where  $\mathbf{0}[\cdot] = 1$  when all input values are zero and otherwise 0.

**The *row normalization* operator  $\mathcal{N}^{\mathcal{R}}(\cdot)$ :**

$$\begin{aligned}\mathcal{N}^{\mathcal{R}} &: \mathbb{R}^{r \times c} \rightarrow \mathbb{R}^{r \times c} (\forall r, c \in \mathbb{N}_+) \\ \mathcal{N}^{\mathcal{R}}(\mathbf{M})_{i,j} &= \frac{\mathbf{M}_{i,j}}{\sum_{\ell} \mathbf{M}_{i,\ell}}.\end{aligned}$$

Intuitively, the added dummy positions correspond to *null* words in the word alignment literature (Dyer et al., 2013; Schulz et al., 2016; Jalili Sabet et al., 2020, *inter alia*). We denote the source-to-target alignment matrix by  $\mathbf{A}^{s \rightarrow t} = \mathcal{N}^{\mathcal{R}}(\Delta(\tilde{\mathbf{A}}))$ , and the target-to-source alignment matrix by  $\mathbf{A}^{t \rightarrow s} = \mathcal{N}^{\mathcal{R}}(\Delta(\tilde{\mathbf{A}}^\top))$ . Both are right stochastic matrices by definition.

### 9.2.3 Dependency Distribution Projection

**Arc distribution projection.** We consider a pair of bitext  $\langle s, t \rangle$ . Let  $P_1(s_j | s_i)$  denote the arc probability produced by the parser  $\mathcal{P}_1$ . Like the dummy position notation, we specify a dummy  $(|s| + 1)^{th}$  word whose head is itself, that is,

$$P_1(s_i | s_{|s|+1}) = 0, P_1(s_{|s|+1} | s_{|s|+1}) = 1.$$

We project  $P_1(\cdot | \cdot)$  to  $\hat{P}_2(t_q | t_p)$ , the arc probability distributions in the parallel  $L_2$  example  $t$ ,

$$\hat{P}_2(t_q | t_p) = \sum_{i=1}^{|s|+1} \sum_{j=1}^{|s|+1} \mathbf{A}_{p,i}^{t \rightarrow s} P_1(s_j | s_i) \mathbf{A}_{j,q}^{s \rightarrow t}. \quad (9.4)$$

It is guaranteed that  $\hat{P}_2(\cdot | t_p)$  is a distribution for any  $t_p$ .

**Proposition 9.1.** Suppose that  $P_1(\cdot | s_i)$  is a probability distribution for any  $s_i$ , and that  $\mathbf{A}^{t \rightarrow s}$  and  $\mathbf{A}^{s \rightarrow t}$  are right-stochastic matrices (i.e., each row of the matrices defines a probability distribution). Let  $P_2(t_p | t_q) = \sum_{i=1}^{|s|+1} \sum_{j=1}^{|s|+1} \mathbf{A}_{p,i}^{t \rightarrow s} P_1(s_j | s_i) \mathbf{A}_{j,q}^{s \rightarrow t}$ . We have that  $P_2(\cdot | t_p)$  is a distribution for any  $t_p$ .

*Proof.* First, for any combination of  $i, j, p, q$ , we have that  $\mathbf{A}_{p,i}^{t \rightarrow s} \geq 0$ ,  $P_1(s_j | s_i) \geq 0$ ,  $\mathbf{A}_{j,q}^{s \rightarrow t} \geq 0$ , therefore,

$$P_2(t_q | t_p) = \sum_{i=1}^{|s|+1} \sum_{j=1}^{|s|+1} \mathbf{A}_{p,i}^{t \rightarrow s} P_1(s_j | s_i) \mathbf{A}_{j,q}^{s \rightarrow t} \geq 0$$

On the other hand,

$$\begin{aligned} & \sum_{q=1}^{|t|+1} P_2(t_q | t_p) \\ &= \sum_{q=1}^{|t|+1} \sum_{i=1}^{|s|+1} \sum_{j=1}^{|s|+1} \mathbf{A}_{p,i}^{t \rightarrow s} P_1(s_j | s_i) \mathbf{A}_{j,q}^{s \rightarrow t} \\ &= \sum_{i=1}^{|s|+1} \sum_{j=1}^{|s|+1} \mathbf{A}_{p,i}^{t \rightarrow s} P_1(s_j | s_i) \left( \sum_{q=1}^{|t|+1} \mathbf{A}_{j,q}^{s \rightarrow t} \right) \\ &= \sum_{i=1}^{|s|+1} \sum_{j=1}^{|s|+1} \mathbf{A}_{p,i}^{t \rightarrow s} P_1(s_j | s_i) \\ &= \sum_{i=1}^{|s|+1} \mathbf{A}_{p,i}^{t \rightarrow s} \left( \sum_{j=1}^{|s|+1} P_1(s_j | s_i) \right) \\ &= \sum_{i=1}^{|s|+1} \mathbf{A}_{p,i}^{t \rightarrow s} \\ &= 1. \end{aligned}$$

□

Note that if we adopt matrix notations, where we denote  $\hat{P}_2(t_q | t_p)$  by  $\hat{\mathbf{P}}_{p,q}^{(2)}$  and denote  $P_1(s_j | s_i)$  by  $\mathbf{P}_{i,j}^{(1)}$ , Eq. (9.4) is equivalent to

$$\hat{\mathbf{P}}^{(2)} = \mathbf{A}^{t \rightarrow s} \mathbf{P}^{(1)} \mathbf{A}^{s \rightarrow t}.$$

**Label distribution projection.** Let  $P_1(\ell | s_j \rightarrow s_i)$  denote the label probability produced by  $\mathcal{P}_1$ . For dummy positions, we simply add a uniform distribution, that is,

$$P_1(\ell | s_j \rightarrow s_i) = \frac{1}{L} \quad \text{if } i \text{ or } j = |s| + 1.$$

We project  $P_1(\cdot | \cdot \rightarrow \cdot)$  to  $\hat{P}_2(\ell | t_q \rightarrow t_p)$ , the label distributions in the parallel  $L_2$  example  $t$ , by

$$\hat{P}_2(\ell | t_q \rightarrow t_p) = \sum_{i=1}^{|s|+1} \sum_{j=1}^{|s|+1} \mathbf{A}_{p,i}^{t \rightarrow s} P_1(\ell | s_j \rightarrow s_i) \mathbf{A}_{q,j}^{t \rightarrow s}$$

$\hat{P}_2(\cdot | t_q \rightarrow t_p)$  is provably a distribution for any pair of  $t_p$  and  $t_q$ .

**Proposition 9.2.** Suppose that  $P_1(\cdot | s_j \rightarrow s_i)$  is a probability distribution for any combination of  $s_i$  and  $s_j$ , and that  $\mathbf{A}^{t \rightarrow s}$  is a right-stochastic matrix. Let  $P_2(\ell | t_q \rightarrow t_p) = \sum_{i=1}^{|s|+1} \sum_{j=1}^{|s|+1} \mathbf{A}_{p,i}^{t \rightarrow s} P_1(\ell | s_j \rightarrow s_i) \mathbf{A}_{q,j}^{t \rightarrow s}$ . We have that  $P_2(\cdot | t_q | t_p)$  is a probability distribution for any  $t_p$  and  $t_q$ .

*Proof.* Similarly to the proof of Proposition 9.1, it is easy to show that for any  $\ell, t_p, t_q$ ,

$$P_2(\ell | t_q \rightarrow t_p) \geq 0.$$

We next consider the sum over  $\ell$  for a specific pair of  $t_p$  and  $t_q$ , where we have

$$\begin{aligned} & \sum_{\ell=1}^{|L|} P_2(\ell | t_q \rightarrow t_p) \\ &= \sum_{\ell=1}^{|L|} \sum_{i=1}^{|s|+1} \sum_{j=1}^{|s|+1} \mathbf{A}_{p,i}^{t \rightarrow s} P_1(\ell | s_j \rightarrow s_i) \mathbf{A}_{q,j}^{t \rightarrow s} \\ &= \sum_{i=1}^{|s|+1} \sum_{j=1}^{|s|+1} \mathbf{A}_{p,i}^{t \rightarrow s} \mathbf{A}_{q,j}^{t \rightarrow s} \left( \sum_{\ell=1}^{|L|} P_1(\ell | s_j \rightarrow s_i) \right) \\ &= \sum_{i=1}^{|s|+1} \sum_{j=1}^{|s|+1} \mathbf{A}_{p,i}^{t \rightarrow s} \mathbf{A}_{q,j}^{t \rightarrow s} \\ &= \sum_{i=1}^{|s|+1} \mathbf{A}_{p,i}^{t \rightarrow s} \left( \sum_{j=1}^{|s|+1} \mathbf{A}_{q,j}^{t \rightarrow s} \right) \\ &= \sum_{i=1}^{|s|+1} \mathbf{A}_{p,i}^{t \rightarrow s} \\ &= 1. \end{aligned}$$

□

### 9.2.4 Optimization

We train another bi-affine dependency parser  $\mathcal{P}_2$  on language  $L_2$ , by minimizing the cross entropy between its produced probability  $P_2$  and the soft silver labels  $\hat{P}_2$ . Note that the added dummy word denoting the null alignment is not eventually used in the final dependency inference process and may introduce extra noise to the model, so we instead calculate the *partial* cross-entropy loss, which does not consider elements involving dummy words. Concretely, we compute the partial arc cross-entropy loss for one example  $t$  as follows:

$$\mathcal{L}_{arc}^{(t)}(P_2, \hat{P}_2) = - \sum_{p=1}^{|t|} \sum_{q=1}^{|t|} \hat{P}_2(t_q | t_p) \log P_2(t_q | t_p)$$

Similarly, the partial label cross-entropy loss can be computed as follows:

$$\mathcal{L}_{label}^{(t)}(P_2, \hat{P}_2) = - \sum_{\ell=1}^{|L|} \sum_{p=1}^{|t|} \sum_{q=1}^{|t|} \hat{P}_2(\ell | t_q \rightarrow t_p) \log P_2(\ell | t_q \rightarrow t_p)$$

Finally, we train the parameters of  $\mathcal{P}_2$  to minimize

$$\sum_{\langle s, t \rangle \in \mathcal{B}} \mathcal{L}_{arc}^{(t)}(P_2, \hat{P}_2) + \mathcal{L}_{label}^{(t)}(P_2, \hat{P}_2). \quad (9.5)$$

## 9.3 Experiments

Throughout all experiments, the subword representation is a weighted sum of layer-wise representation from a frozen pre-trained model, where each layer has a scalar weight optimized together with other network parameters to minimize Eq. (9.5). We convert subword features to word features by endpoint concatenation, following Toshniwal et al. (2020). We use the Adam optimizer (Kingma and Ba, 2015) to train all models, where the source language parser is trained for 100 epochs with initial learning rate  $2 \times 10^{-3}$  following the baseline implementation by Zhang et al. (2020), and the target language

Method	<i>distant languages</i>				<i>nearby languages</i>			
	ar	hi	ko	tr	de	es	fr	it
<b>LAS</b>								
Meng et al.	—	—	—	—	—	—	—	—
He et al.	—	—	—	—	—	—	—	—
Ahmad et al.	27.9	28.0	16.1	—	61.8	65.8	73.3	75.6
Kurniawan et al.	38.5	28.3	16.1	20.6	63.5	69.2	<b>74.5</b>	<b>77.7</b>
SUBDP (ours)	<b>41.3</b>	<b>38.9</b>	<b>31.2</b>	<b>33.5</b>	<b>71.7</b>	<b>70.4</b>	71.0	75.0
<b>UAS</b>								
Meng et al.	47.3	52.4	37.1	35.2	70.8	75.8	79.1	82.0
He et al.	55.4	33.2	37.0	36.1	69.5	64.3	67.7	70.7
Ahmad et al.	27.9	28.0	16.1	—	61.8	65.8	73.3	75.6
Kurniawan et al.	48.3	36.4	34.6	38.4	74.1	78.3	80.6	83.7
SUBDP (ours)	<b>63.8</b>	<b>58.3</b>	<b>54.3</b>	<b>56.9</b>	<b>82.8</b>	<b>83.9</b>	<b>84.8</b>	<b>88.2</b>

Table 9.1: Labeled attachment scores (LAS) and unlabeled attachment scores (UAS) on the Universal Dependencies v2.2 (Nivre et al., 2020) standard test set, transferring from English. Following Kurniawan et al. (2021), our results are averaged across five runs with different random seeds; the best number in each column is in boldface.

parser is trained for 30 epochs with initial learning rate  $5 \times 10^{-4}$ .<sup>8</sup> We use the loss against silver projected distributions on the development set for SUBDP and the development LAS against projected trees for baselines for early stopping.<sup>9</sup> For evaluation, we ignore all punctuation following the most common convention (Ma and Xia, 2014; Rasooli and Collins, 2015; Kurniawan et al., 2021, *inter alia*). If not specified,

- All models in target languages are initialized with the trained source language parser.
- All word alignments are obtained by XLM-R based SimAlign (Jalili Sabet et al., 2020), using BPE tokenization and the argmax algorithm.
- XLM-R is used as the feature extractor.

We report results on the standard development sets to avoid tuning on the test sets for analysis purposes.

<sup>8</sup>We do not observe further training loss decrease when training for more epochs. The learning rate for SUBDP is tuned to optimize the development loss for German, where the German gold trees remain unused.

<sup>9</sup>SUBDP does not provide a set of hard silver trees for LAS and UAS calculation.



### 9.3.1 Results: Fully Unsupervised Transfer

We compare SUBDP to prior work in the minimal annotation setting (Table 9.1), where an English dependency treebank is the only annotation that involves human effort. We select target languages from the overlap between those considered by Kurniawan et al. (2021), those covered by XLM-R (Conneau et al., 2020) training corpora, and those supported by CRISS (Tran et al., 2020), resulting in eight languages: Arabic (ar), Hindi (hi), Korean (ko), Turkish (tr), German (de), Spanish (es), French (fr), and Italian (it).

We translate English sentences using the unsupervised model CRISS to construct the required bitext.<sup>10</sup> To ensure the quality of the unsupervised bitext, we discard (1) translations where at least 80% of words appear in the corresponding source sentences, which are likely to be copied, (2) those containing a CRISS language token other than the target language, which are likely to be false translation into another language, and (3) those with 80% or more words appearing in the translated sentence more than once, which are likely to be repetitions.

Transferring from an English parser, SUBDP achieves the best UAS across all eight target languages and the best LAS on six languages out of eight. In addition, we find that SUBDP is consistent across random seeds, with a standard deviation less than 0.8 for every number in Table 9.1.

### 9.3.2 Ablation Study

We introduce the following baselines with the same annotated data availability for an ablation study:

1. **Direct transfer of English models (DT).** We train a bi-affine dependency parser on English treebanks and test the model on other languages. This approach is expected to outperform a random baseline as it has a pre-trained cross-lingual language model-based feature extractor, which may implicitly enable cross-lingual transfer. For this baseline, we test both XLM-R and CRISS encoders, as SUBDP benefits from both models.
2. **Self-training (ST).** Following Kurniawan et al. (2021), we apply an XLM-R DT parser

---

<sup>10</sup>In experiments, we translate English treebank sentences; in more general cases, any source language sentence can be taken for bitext construction.

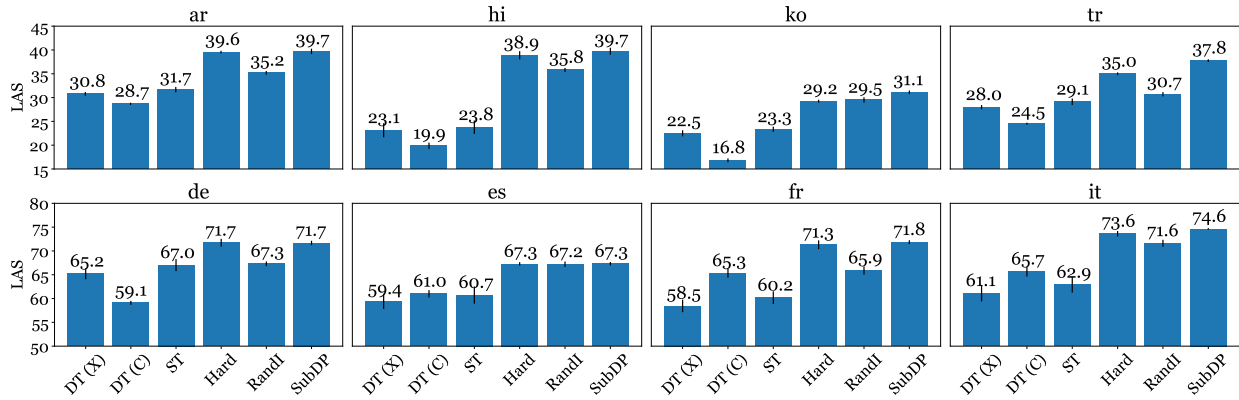


Figure 9.2: LAS on the Universal Dependencies v2.2 standard development set. The standard deviations are denoted by black lines at the top of the bars. All numbers are averaged across five runs. DT(X): direct transfer by XLM-R representations; DT (C): direct transfer by CRISS representations.

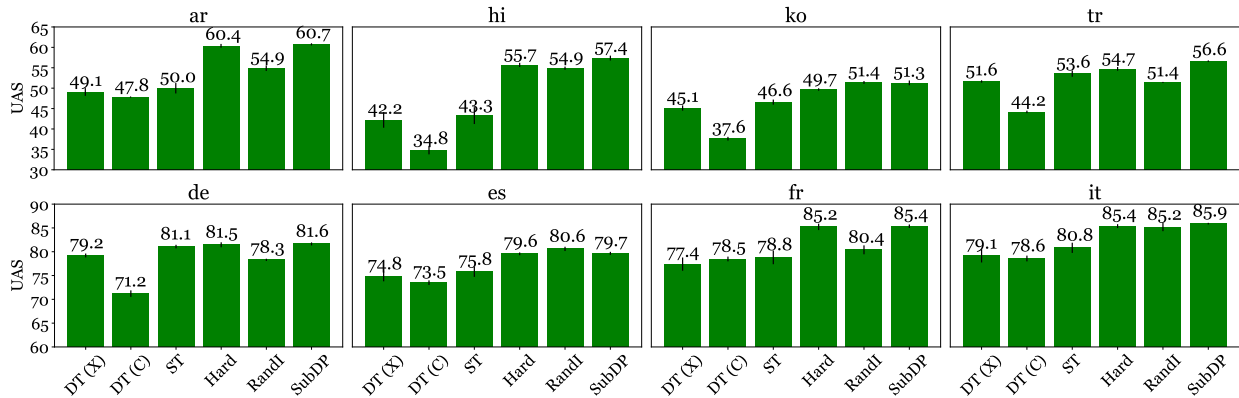


Figure 9.3: UAS on the Universal Dependencies v2.2 standard development set. The standard deviations are denoted by black lines at the top of the bars. All numbers are averaged across five runs. DT(X): direct transfer by XLM-R representations; DT (C): direct transfer by CRISS representations.

to the target language,<sup>11</sup> and train another parser on the predicted hard trees.

3. **Hard projection (Hard).** It is intuitive to compare SUBDP against the hard tree projection baseline (Lacroix et al., 2016), where we use the same set of bitext and alignments to project trees to the target languages, keeping only the edges with both

<sup>11</sup>We only consider XLM-R as the feature extractor for ST as it achieves better average DT results.

sides aligned in a one-to-one alignment. We use the projected trees to train a parser in the target language.

4. **Random target parser initialization (RandI).** Instead of using the trained English model as the initialization of target parsers, we randomly initialize the weights in this baseline. This approach matches with SUBDP in every component except the target parser initialization.

All baselines use bi-affine dependency parsers, with pre-trained cross-lingual language models (XLM-R or CRISS) as feature extractors.

We compare the LAS and UAS between SUBDP and the baselines above (Figures 9.2 and 9.3), and find that

- Across all languages, SUBDP significantly outperforms DT with either XLM-R or CRISS word feature extractor. ST consistently improves over DT but is much less competitive than SUBDP, indicating that the gain of SUBDP over prior work is not simply from more powerful word features.
- While hard treebank projection using the method proposed by Lacroix et al. (2016) is quite competitive, SUBDP consistently produces competitive (Arabic, German, Spanish) or better (Hindi, Korean, Turkish, French, Italian) results.
- Comparing SUBDP to RandI, we find that initializing the target language parser with a trained source language (English in this work) parser helps improve performance across the board; therefore, source parser initialization should be considered as a general step in future work on zero-shot cross-lingual dependency parsing.

### 9.3.3 Analysis: Effect of Alignment Methods

Since most existing work has used only one-to-one alignment for annotation projection (Ma and Xia, 2014; Lacroix et al., 2016; Rasooli et al., 2021, *inter alia*), we would like to analyze the effect of introducing many-to-one alignment edges in SUBDP. We filter SimAlign BPE argmax to obtain a more conservative version, dropping all many-to-one edges (i.e., those that have a word linked to multiple edges),<sup>12</sup> and compare it to the BPE argmax algorithm (Table 9.2).

---

<sup>12</sup> This approach is different from Hard as it takes soft source trees as the input, yielding soft target trees as silver labels to train target language parsers.

Lang.	BPE argmax		1:1 only	
	LAS	UAS	LAS	UAS
ar	39.7	60.7	<b>40.2</b>	<b>61.1</b>
hi	<b>39.7</b>	<b>57.4</b>	38.7	56.5
ko	<b>31.1</b>	<b>51.3</b>	27.3	49.6
tr	<b>37.8</b>	<b>56.7</b>	33.3	55.8
avg. <i>distant</i>	<b>37.1</b>	<b>56.5</b>	34.8	55.8
de	71.7	81.6	<b>72.6</b>	<b>83.8</b>
es	67.3	79.7	<b>70.4</b>	<b>84.2</b>
fr	71.8	85.3	<b>72.6</b>	<b>87.7</b>
it	74.6	85.9	<b>76.0</b>	<b>88.8</b>
avg. <i>nearby</i>	71.4	83.1	<b>72.9</b>	<b>86.1</b>

Table 9.2: LAS and UAS on the Universal Dependencies v2.2 (Nivre et al., 2020) standard development set, averaged across five runs with different random seeds. 1:1 only denotes the filtered one-to-one alignments. The best LAS and UAS for each language are in boldface.

While the confident one-to-one alignment achieves further improvement on Arabic and all four nearby languages, we find that the many-to-one BPE argmax alignment is important to the superior transfer performance on Hindi, Korean, and Turkish. Given the fact that the scores are quite similar for Arabic, the results generally suggest using the many-to-one SimAlign BPE argmax alignments for transferring from English to distant languages while using the more confident one-to-one alignments for nearby languages.

### 9.3.4 Results: Multiple Source Languages

Following Schuster et al. (2019), we use Universal Dependencies v2.0 (McDonald et al., 2013) to evaluate zero-shot cross-lingual transfer from multiple source languages (Table 9.3).<sup>13</sup> For each language among German (de), Spanish (es), French (fr), Italian (it), Portuguese (pt), and Swedish (sv), annotated treebanks from all other languages and

<sup>13</sup>We do not report performance for Portuguese and Swedish as CRISSE does not cover them; however, the annotated treebanks in these languages are used as source treebanks when applicable.

Method	de	es	fr	it
Zhang and Barzilay (2015)	62.5	78.0	<b>78.9</b>	79.3
Guo et al. (2016)	65.0	79.0	77.7	78.5
Schuster et al. (2019) <sup>‡</sup>	61.7	76.6	76.3	77.1
DT (XLM-R) <sup>‡,*</sup>	73.1	82.2	75.5	79.5
SUBDP (XLM-R) <sup>‡,*</sup>	<b>78.5</b>	72.1	73.1	74.3
DT w/ SUBDP init. <sup>‡,*</sup>	76.1	<b>82.6</b>	77.7	<b>81.9</b>

Table 9.3: LAS on Universal Dependencies v2.0 (McDonald et al., 2013) standard test set. ‡: methods with minimal annotation. \*: results from our experiments; other results are taken from Schuster et al. (2019). The best number for each target language is in boldface.

English can be used for training and development purposes. For SUBDP, we generate bitext from all applicable source languages with CRISS.

SUBDP outperforms the previous state-of-the-art on German by 13.5 LAS, but underperforms the DT baseline on the other three languages. However, suppose we start with a trained SUBDP parser for a target language and use the standard training data (i.e., treebanks in other languages) to train further a bi-affine dependency parser (DT w/ SUBDP init.). In that case, we can achieve better results than DT across the board, obtaining competitive or even better LAS than methods that use extra annotations other than source treebanks (Zhang and Barzilay, 2015; Guo et al., 2016).

### 9.3.5 Results: Transfer with Supervised Bitext

We further evaluate SUBDP in another scenario where a few bitext pairs are available. We consider a larger set of eighteen target languages, including Arabic (ar), Czech (cs), German (de), Spanish (es), Finnish (fi), French (fr), Hindi (hi), Hungarian (hu), Italian (it), Japanese (ja), Korean (ko), Norwegian (no), Portuguese (pt), Russian (ru), Tamil (ta), Telugu (te), Vietnamese (vi), and Chinese (zh). We transfer from English to each target language with Wikimatrix bitext (Schwenk et al., 2021), where the examples are mined with an encoding similarity-based bitext miner trained with annotated bitext. We vary the number of Wikimatrix bitext pairs, selecting the number of pairs within the geometric sequence  $\{50 \times 2^k\}_{k=0}^9$ , leaving 10% of the examples for development.

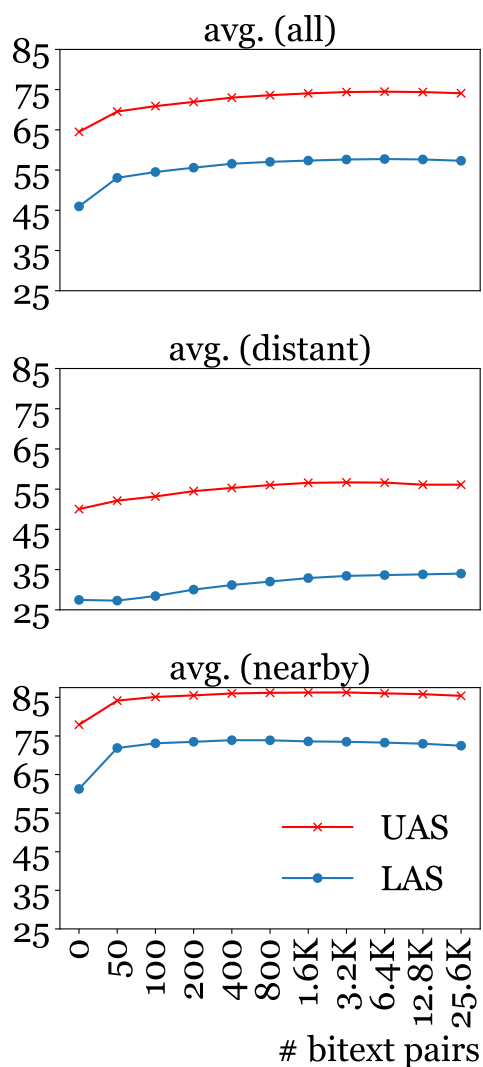


Figure 9.4: Averaged LAS and UAS on the Universal Dependencies v2.2 standard development set with respect to the number of bitext pairs. For each language, we run five times with different random seeds. The  $x$ -axis is on a log scale. Using zero bitext pairs corresponds to the direct transfer (DT; §9.3.2) baseline. All European languages are considered nearby, while the remaining are treated as distant languages.

On average and for nearby languages (Figure 9.4), we find that the performance of SUBDP with 50 pairs of bitext is quite close to that with 25K pairs of bitext. Although some distant languages generally require more bitext for further improvement, SUBDP outperforms the direct transfer baseline by a nontrivial margin with a small amount (e.g.,

800-1.6K pairs) of bitext.

## 9.4 Conclusion and Discussion

Our work is in line with recent work (Rasooli et al., 2021), which shows that cross-lingual transfer can be done effectively with weak supervision, such as Wikipedia links. Our results go further and study the setting of zero additional supervision beyond the source language treebank, demonstrating the potential of zero-shot cross-lingual dependency parsing with zero additional supervision, even between distant languages that do not share vocabulary or subwords. Our work suggests a new protocol for dependency annotation of low-resource languages: (1) train a pre-trained multilingual model following existing work such as XLM-R (Conneau et al., 2020) and CRISS (Tran et al., 2020), (2) annotate a small number of bitext pairs or generate bitext with trained unsupervised translation models, and (3) train a zero-shot cross-lingual dependency parser using SUBDP.

Our contribution to zero-shot cross-lingual dependency parsing is arguably orthogonal to contextualized representation alignment (Schuster et al., 2019; Wang et al., 2019), where pre-trained multilingual language models are finetuned for better transfer. In contrast, we use the frozen pre-trained models to extract features. In addition, projection quality controls by heuristics-based filtering (Rasooli and Collins, 2015) may also be combined with SUBDP to improve the performance.

Our results, on the other hand, demonstrate that multilingual pre-trained models may have more applications beyond representation-based direct transfer—information extracted from these models without further supervision (e.g., word alignment in this work) may further benefit downstream tasks (e.g., zero-shot cross-lingual dependency parsing in this work) with appropriate usage.

While this work depends on pre-trained multilingual models such as CRISS (Tran et al., 2020), which require extensive computational resources to train from scratch, SUBDP may be applied whenever bitext alignment and cross-lingual word embeddings are available. In addition, the required pre-trained cross-lingual models are useful for general purposes and can be applied to other downstream NLP tasks.

We suggest that SUBDP can be extended to other scenarios wherever relevant parallel signals are available, such as cross-lingual named entity recognition, cross-lingual constituency parsing, or zero-shot scene graph parsing for images using only the dependency

supervision in text. We leave the further exploration of SUBDP on other tasks and a more comprehensive cross-lingual parsing quality analysis for future work.



# Chapter 10

## Conclusion and Discussion

In this dissertation, we have explored the problem of learning language structures through grounding. Instead of following the supervision paradigm where the model is trained with explicit annotations of language structures, our key contribution is to propose a paradigm that learns these structures through arguably distant grounding signals. The grounding signals take various forms, including visual signals, acoustic signals, execution results of programs, and information from another language. These grounded settings offer advantages over pure text-based methods through two perspectives: (1) the cross-modal annotations are much easier to collect than explicit annotations required by supervised learning, as many of them exist naturally in the world, such as image captions, videos, and question-answer pairs, and (2) grounding signals naturally serve as bridges that connect language with the real world, offering the potential to learn more interpretable language structures.

The contents and findings presented in this dissertation are connected to multiple subareas in natural language processing, computational linguistics, and machine learning. We summarize the contributions of this dissertation in the following aspects:

- Chapters 3, 4 and 6 propose novel settings and models for grammar induction from visually grounded text and speech.
- Chapter 5 proposes an evaluation metric, *STRUCT-IOU*, for measuring the quality of induced speech constituency parse trees, which can also be applied to text constituency parsing evaluation.
- Chapter 6 propose a model that learns joint syntactic and semantic structures from

visual grounding signals and program execution results, enabling nearly perfect compositional generalization.

- Chapter 7 propose a decoding method that uses program execution results to guide the generation of code conditioned on natural language descriptions. For the first time, we show that few-shot natural language-to-code translation can achieve comparable performance to supervised methods, with awareness of program execution results.
- Chapters 8 and 9 propose to consider cross-lingual transfer within the paradigm of learning language structures through cross-lingual grounding, and introduce models and methods for cross-lingual word alignment and dependency parsing. Our systems achieve state-of-the-art performance on both tasks, respectively.

Most work in this dissertation is built based on a hypothesis that language structures are, to some extent, learnable through grounding. While the empirical results in this dissertation support this hypothesis, demonstrating that various forms of grounding signals improve performance over pure text-based methods on corresponding tasks, many open questions and challenges still need to be addressed in future work.

First, while there are shared features between text and grounding modalities, such as the shared semantics between image regions and words in image captioning, the discrepancy between these modalities is also significant—it is still arguable whether the grounding signals can provide sufficient information for learning language structures. For example, it has been clearly shown that visual grounding signals in VG-NSL are insufficient to retrieve all constituents, especially verb phrases, even in visually grounded settings (Table 3.1). In addition, the recent trend of large language models has shown that most of the grammatical rules of natural language can be learned implicitly from a large amount of text data. Related to this line of discussions, whether grounding signals can provide additional benefits over large-scale text data in learning language structures remains unclear. It would be interesting to design and implement methods that disentangle the contribution of each type of grounding signal, as well as the intrinsic information from text, and explore how to combine them effectively.

Second, in the cross-lingual grounding settings, due to the limitation of resources, we have not attributed the performance in a detailed way to the quality of the corpora, the quality of the cross-lingual alignment, or the difference between languages. Extending the experiment to a more diverse set of languages, especially the underrepresented and low-

resource ones, may reveal more insights into the effectiveness of cross-lingual grounding signals. This line also connects to historical language processing, especially those that lack a consensus on interpretations, where grounding in various forms may facilitate the understanding. It is also worth noting that different languages may carry cultural and historical information that is not directly translatable, and the cross-modal grounding signals may help discover these differences and similarities.

Third, many of the methods proposed in this dissertation are limited in terms of computational efficiency and scalability. For example, the time complexity for computing the STRUCT-IOU metric is bivariate quadratic, and G2L2 is not scalable to large-scale datasets due to the high computational cost of the program search while being polynomial. It would be interesting to explore more efficient methods to implement these algorithms through parallel computing, approximate search with conventional techniques or neural networks, or finding more efficient analytical solutions by exploiting the sparsity of the search space.

Finally, we have shown that grounded language learning can be meaningfully connected with syntactic and semantic structures; however, natural language is not limited to these two types of structures—this dissertation does not involve content related to discourse, pragmatics, and other types of linguistic structures. Additionally, although structure is everywhere with language, modeling linguistic phenomena does not necessarily imply being built based on structures—for example, it is unlikely that the grammatical genders in gendered languages or the classifiers in Mandarin Chinese have a direct correspondence with complex structures. We envision a future where grounding will benefit a more comprehensive set of linguistic tasks and facilitate the fundamental understanding of language.

# Bibliography

- [1] Sadaf Abdul-Rauf and Holger Schwenk. 2009. On the use of comparable corpora to improve SMT performance. In *EACL*. [126](#)
- [2] Omri Abend, Tom Kwiatkowski, Nathaniel J. Smith, Sharon Goldwater, and Mark Steedman. 2017. Bootstrapping language acquisition. *Cognition*, 164:116–143. [79](#)
- [3] Željko Agić, Anders Johannsen, Barbara Plank, Héctor Martínez Alonso, Natalie Schluter, and Anders Søgaard. 2016. Multilingual projection for parsing truly low-resource languages. *TACL*, 4:301–312. [135](#)
- [4] Wasi Ahmad, Zhisong Zhang, Xuezhe Ma, Eduard Hovy, Kai-Wei Chang, and Nanyun Peng. 2019. On difficulties of cross-lingual transfer with order differences: A case study on dependency parsing. In *NAACL*. [135](#)
- [5] Wasi Uddin Ahmad, Zhisong Zhang, Xuezhe Ma, Kai-Wei Chang, and Nanyun Peng. 2019. Cross-lingual dependency parsing with unlabeled auxiliary languages. In *CoNLL*. [135](#), [143](#)
- [6] Ekin Akyürek, Afra Feyza Akyürek, and Jacob Andreas. 2021. Learning to recombine and resample data for compositional generalization. In *ICLR*. [78](#), [100](#), [101](#)
- [7] Waleed Ammar, George Mulcaire, Miguel Ballesteros, Chris Dyer, and Noah A. Smith. 2016. Many languages, one parser. *TACL*, 4:431–444. [134](#)
- [8] Jacob Andreas. 2020. Good-enough compositional data augmentation. In *ACL*. [78](#)
- [9] Jacob Andreas and Dan Klein. 2016. Reasoning about pragmatics with neural listeners and speakers. In *EMNLP*. [39](#)

- [10] Jacob Andreas, Dan Klein, and Sergey Levine. 2017. Modular multitask reinforcement learning with policy sketches. In *ICML*. 79
- [11] Jacob Andreas, Marcus Rohrbach, Trevor Darrell, and Dan Klein. 2016. Learning to compose neural networks for question answering. In *NAACL-HLT*. 79
- [12] Jacob Andreas, Marcus Rohrbach, Trevor Darrell, and Dan Klein. 2016. Neural module networks. In *CVPR*. 94
- [13] Mikel Artetxe and Holger Schwenk. 2019. Margin-based parallel corpus mining with multilingual sentence embeddings. In *ACL*. 126, 127
- [14] Yoav Artzi and Luke Zettlemoyer. 2013. Weakly supervised learning of semantic parsers for mapping instructions to actions. *TACL*, 1:49–62. 78
- [15] Jacob Austin, Augustus Odena, Maxwell Nye, Maarten Bosma, Henryk Michalewski, David Dohan, Ellen Jiang, Carrie Cai, Michael Terry, Quoc Le, et al. 2021. Program synthesis with large language models. *arXiv preprint arXiv:2108.07732*. 104, 106, 110, 122
- [16] Mark C. Baker. 2001. *The Atoms of Language: The Mind’s Hidden Rules of Grammar*. Basic books. 28, 37, 50
- [17] Marco Baroni. 2020. Linguistic generalization and compositionality in modern artificial neural networks. *Philosophical Transactions of the Royal Society B.*, 375(1791):20190307. 78
- [18] Jon L. Bentley. 1977. Solutions to Klee’s rectangle problems. *Technical Report, Carnegie Mellon University*. 55, 58
- [19] Adam Berger, Peter F. Brown, Stephen A. Della Pietra, Vincent J. Della Pietra, John R. Gillett, John Lafferty, Robert L. Mercer, Harry Printz, and Lubos Ures. 1994. The candid system for machine translation. In *HLT*. 13
- [20] Saurabhchand Bhati, Jesús Villalba, Piotr Żelasko, Laureano Moro-Velazquez, and Najim Dehak. 2021. Segmental contrastive predictive coding for unsupervised word segmentation. *arXiv preprint arXiv:2106.02170*. 42

- [21] Peter J. Bickel and Kjell A. Doksum. 1977. *Mathematical statistics: basic ideas and selected topics, volumes I-II package*. HoldenDay Inc., Oakland, CA, USA. [106](#)
- [22] Philip Bille. 2005. A survey on tree edit distance and related problems. *Theoretical computer science*, 337(1-3):217–239. [74](#)
- [23] Yonatan Bisk, Ari Holtzman, Jesse Thomason, Jacob Andreas, Yoshua Bengio, Joyce Chai, Mirella Lapata, Angeliki Lazaridou, Jonathan May, Aleksandr Nisnevich, Nicolas Pinto, and Joseph Turian. 2020. Experience grounds language. In *EMNLP*. [16](#)
- [24] E. Black, S. Abney, D. Flickenger, C. Gdaniec, R. Grishman, P. Harrison, D. Hindle, R. Ingria, F. Jelinek, J. Klavans, M. Liberman, M. Marcus, S. Roukos, B. Santorini, and T. Strzalkowski. 1991. A procedure for quantitatively comparing the syntactic coverage of English grammars. In *Speech and Natural Language: Proceedings of a Workshop Held at Pacific Grove, California*. [4](#), [8](#), [29](#), [42](#), [47](#), [50](#), [57](#), [74](#)
- [25] Rens Bod. 2006. An all-subtrees approach to unsupervised parsing. In *ACL*. [22](#)
- [26] Stevo Bozinovski and Ante Fulgosi. 1976. The influence of pattern similarity and transfer learning upon training of a base perceptron B2. In *Proceedings of Symposium Informatica*, volume 3, pages 121–126. [18](#)
- [27] Joan Bresnan, Ash Asudeh, Ida Toivonen, and Stephen Wechsler. 2016. *Lexical-functional syntax*. John Wiley & Sons. [77](#)
- [28] Peter F. Brown, Stephen A. Della Pietra, Vincent J. Della Pietra, and Robert L. Mercer. 1993. The mathematics of statistical machine translation: Parameter estimation. *Comput. Linguist.*, 19(2):263–311. [126](#)
- [29] Roger W. Brown. 1957. Linguistic determinism and the part of speech. *The Journal of Abnormal and Social Psychology*, 55(1):1. [38](#)
- [30] Tom Brown, Benjamin Mann, Nick Ryder, Melanie Subbiah, Jared D. Kaplan, Prafulla Dhariwal, Arvind Neelakantan, Pranav Shyam, Girish Sastry, Amanda Askell, et al. 2020. Language models are few-shot learners. In *NeurIPS*. [106](#), [107](#)

- [31] Marc Brysbaert, Amy Beth Warriner, and Victor Kuperman. 2014. Concreteness ratings for 40 thousand generally known English word lemmas. *Behav. Res. Methods*, 46(3):904–911. [23](#), [31](#), [33](#), [35](#)
- [32] Razvan Bunescu and Marius Paşca. 2006. Using encyclopedic knowledge for named entity disambiguation. In *EACL*. [15](#)
- [33] Shu Cai and Kevin Knight. 2013. Smatch: an evaluation metric for semantic feature structures. In *ACL*. [57](#)
- [34] Sasha Calhoun, Jean Carletta, Jason M. Brenier, Neil Mayo, Dan Jurafsky, Mark Steedman, and David Beaver. 2010. The nxt-format switchboard corpus: a rich resource for investigating the syntax, semantics, pragmatics and prosody of dialogue. *Language resources and evaluation*, 44:387–419. [65](#)
- [35] Lluís Castrejon, Yusuf Aytar, Carl Vondrick, Hamed Pirsiavash, and Antonio Torralba. 2016. Learning aligned cross-modal representations from weakly aligned data. In *CVPR*. [39](#)
- [36] Joyce Y. Chai, Qiaozi Gao, Lanbo She, Shaohua Yang, Sari Saba-Sadiya, and Guangyue Xu. 2018. Language to action: Towards interactive task learning with physical agents. In *IJCAI*. [15](#), [16](#)
- [37] Khyathi Raghavi Chandu, Yonatan Bisk, and Alan W. Black. 2021. Grounding ‘grounding’ in nlp. In *Findings of ACL*. [16](#)
- [38] Eugene Charniak and Mark Johnson. 2001. Edit detection and parsing for transcribed speech. In *NAACL*. [55](#)
- [39] Eugene Charniak and Mark Johnson. 2005. Coarse-to-fine n-best parsing and MaxEnt discriminative reranking. In *ACL*. [8](#), [57](#)
- [40] Mark Chen, Jerry Tworek, Heewoo Jun, Qiming Yuan, Henrique Ponde de Oliveira Pinto, Jared Kaplan, Harri Edwards, Yuri Burda, Nicholas Joseph, Greg Brockman, et al. 2021. Evaluating large language models trained on code. *arXiv preprint arXiv:2107.03374*. [104](#), [105](#), [106](#), [107](#), [114](#)

- [41] Kyunghyun Cho, Bart van Merriënboer, Caglar Gulcehre, Dzmitry Bahdanau, Fethi Bougares, Holger Schwenk, and Yoshua Bengio. 2014. Learning phrase representations using RNN encoder–decoder for statistical machine translation. In *EMNLP*. 25
- [42] Do Kook Choe and Eugene Charniak. 2016. Parsing as language modeling. In *EMNLP*. 57
- [43] Jihun Choi, Kang Min Yoo, and Sang-goo Lee. 2018. Learning to compose task-specific tree structures. In *AAAI*. 22, 30, 33, 34
- [44] Noam Chomsky. 1957. *Syntactic Structures*. Mouton and Co. 1
- [45] Jan Chorowski, Grzegorz Ciesielski, Jarosław Dzikowski, Adrian Łańcucki, Ricard Marxer, Mateusz Opala, Piotr Pusz, Paweł Rychlikowski, and Michał Stypułkowski. 2021. Aligned contrastive predictive coding. In *Interspeech*. 42
- [46] Gordon Christie, Ankit Laddha, Aishwarya Agrawal, Stanislaw Antol, Yash Goyal, Kevin Kochersberger, and Dhruv Batra. 2016. Resolving language and vision ambiguities together: Joint segmentation & prepositional attachment resolution in captioned scenes. In *EMNLP*. 22, 39
- [47] Yoeng-Jin Chu and Tseng-hong Liu. 1965. On the shortest arborescence of a directed graph. *Scientia Sinica*, 14:1396–1400. 137
- [48] Herbert H. Clark and Susan E. Brennan. 1991. Grounding in communication. 16
- [49] John Cocke. 1969. *Programming languages and their compilers: Preliminary notes*. New York University. 83
- [50] Shay B. Cohen, Dipanjan Das, and Noah A. Smith. 2011. Unsupervised structure prediction with non-parallel multilingual guidance. In *EMNLP*. 134, 135
- [51] Michael Collins and Terry Koo. 2005. Discriminative reranking for natural language parsing. *Comput. Linguist.*, 31(1):25–70. 8, 57
- [52] Alexis Conneau, Kartikay Khandelwal, Naman Goyal, Vishrav Chaudhary, Guillaume Wenzek, Francisco Guzmán, Edouard Grave, Myle Ott, Luke Zettlemoyer,



- and Veselin Stoyanov. 2020. Unsupervised cross-lingual representation learning at scale. In *ACL*. [73](#), [126](#), [130](#), [136](#), [138](#), [144](#), [150](#)
- [53] James Cross and Liang Huang. 2016. Span-based constituency parsing with a structure-label system and provably optimal dynamic oracles. In *EMNLP*. [57](#)
- [54] Jacob Devlin, Ming-Wei Chang, Kenton Lee, and Kristina Toutanova. 2019. BERT: Pre-training of deep bidirectional transformers for language understanding. In *NAACL-HLT*. [126](#), [136](#), [138](#)
- [55] Li Dong and Mirella Lapata. 2018. Coarse-to-fine decoding for neural semantic parsing. In *ACL*. [106](#)
- [56] Timothy Dozat and Christopher D. Manning. 2017. Deep biaffine attention for neural dependency parsing. In *ICLR*. [137](#)
- [57] Andrew Drozdov, Pat Verga, Mohit Yadav, Mohit Iyyer, and Andrew McCallum. 2019. Unsupervised latent tree induction with deep inside-outside recursive autoencoders. In *NAACL-HLT*. [42](#), [78](#)
- [58] Ewan Dunbar, Nicolas Hamilakis, and Emmanuel Dupoux. 2022. Self-supervised language learning from raw audio: Lessons from the zero resource speech challenge. *IEEE Journal of Selected Topics in Signal Processing*, 16(6):1211–1226. [42](#)
- [59] Long Duong, Trevor Cohn, Steven Bird, and Paul Cook. 2015. Cross-lingual transfer for unsupervised dependency parsing without parallel data. In *CoNLL*. [134](#)
- [60] Greg Durrett and Dan Klein. 2015. Neural CRF parsing. In *ACL*. [57](#)
- [61] Greg Durrett, Adam Pauls, and Dan Klein. 2012. Syntactic transfer using a bilingual lexicon. In *EMNLP*. [134](#), [135](#)
- [62] Chris Dyer, Victor Chahuneau, and Noah A. Smith. 2013. A simple, fast, and effective reparameterization of IBM model 2. In *NAACL-HLT*. [126](#), [130](#), [138](#), [139](#)
- [63] Chris Dyer, Adhiguna Kuncoro, Miguel Ballesteros, and Noah A. Smith. 2016. Recurrent neural network grammars. In *NAACL-HLT*. [57](#)
- [64] Chris Dyer, Gábor Melis, and Phil Blunsom. 2019. A critical analysis of biased parsers in unsupervised parsing. *arXiv preprint arXiv:1909.09428*. [30](#)

- [65] Jack Edmonds. 1968. Optimum branchings. *Mathematics and the Decision Sciences, Part, 1*(335-345):25. [137](#)
- [66] Bryan Eikema and Wilker Aziz. 2020. Is MAP decoding all you need? the inadequacy of the mode in neural machine translation. In *Proc. of the 28th International Conference on Computational Linguistics*. [108](#)
- [67] Bryan Eikema and Wilker Aziz. 2022. Sampling-based approximations to minimum Bayes risk decoding for neural machine translation. In *EMNLP*. [108](#)
- [68] Desmond Elliott, Stella Frank, Loïc Barrault, Fethi Bougares, and Lucia Specia. 2017. Findings of the second shared task on multimodal machine translation and multilingual image description. In *WMT*. [21](#), [37](#)
- [69] Desmond Elliott, Stella Frank, Khalil Sima'an, and Lucia Specia. 2016. Multi30K: Multilingual English-German image descriptions. In *Proc. of the 5th Workshop on Vision and Language*. [21](#), [37](#), [46](#)
- [70] Kevin Ellis, Lionel Wong, Maxwell Nye, Mathias Sable-Meyer, Luc Cary, Lore Anaya Pozo, Luke Hewitt, Armando Solar-Lezama, and Joshua B. Tenenbaum. 2023. Dreamcoder: growing generalizable, interpretable knowledge with wake-sleep Bayesian program learning. *Philosophical Transactions of the Royal Society A*, 381(2251):20220050. [103](#)
- [71] Cristina Espana-Bonet, Adám Csaba Varga, Alberto Barrón-Cedeno, and Josef van Genabith. 2017. An empirical analysis of nmt-derived interlingual embeddings and their use in parallel sentence identification. *IEEE Journal of Selected Topics in Signal Processing*, 11(8):1340–1350. [126](#)
- [72] Fartash Faghri, David J. Fleet, Jamie Ryan Kiros, and Sanja Fidler. 2018. VSE++: Improving visual-semantic embeddings with hard negatives. In *BMVC*. [23](#)
- [73] Afsaneh Fazly, Afra Alishahi, and Suzanne Stevenson. 2010. A probabilistic computational model of cross-situational word learning. *Cognitive Science*, 34(6):1017–1063. [79](#)
- [74] Tommaso Fornaciari, Alexandra Uma, Silviu Paun, Barbara Plank, Dirk Hovy, and Massimo Poesio. 2021. Beyond black & white: Leveraging annotator disagreement via soft-label multi-task learning. In *NAACL*. [136](#)

- [75] Michael C. Frank and Noah D. Goodman. 2012. Predicting pragmatic reasoning in language games. *Science*, 336(6084):998–998. [103](#)
- [76] Zvi Galil. 1986. Efficient algorithms for finding maximum matching in graphs. *ACM Comput. Surv.*, 18(1):23–38. [46](#)
- [77] Tianyu Gao, Adam Fisch, and Danqi Chen. 2021. Making pre-trained language models better few-shot learners. In *ACL*. [106](#), [108](#)
- [78] Sarthak Garg, Stephan Peitz, Udhyakumar Nallasamy, and Matthias Paulik. 2019. Jointly learning to align and translate with transformer models. In *EMNLP*. [126](#), [129](#), [130](#)
- [79] Jon Gauthier, Roger Levy, and Joshua B. Tenenbaum. 2018. Word learning and the acquisition of syntactic–semantic overhypotheses. In *CogSci*. [38](#), [79](#), [103](#)
- [80] Vaibhava Goel and William J. Byrne. 2000. Minimum Bayes-risk automatic speech recognition. *Computer Speech & Language*, 14(2):115–135. [108](#)
- [81] Herbert P. Grice. 1975. Logic and conversation. In *Speech acts*, pages 41–58. Brill. [16](#)
- [82] Demi Guo, Yoon Kim, and Alexander Rush. 2020. Sequence-level mixed sample data augmentation. In *EMNLP*. [78](#), [100](#), [101](#)
- [83] Haohan Guo, Frank K. Soong, Lei He, and Lei Xie. 2019. Exploiting syntactic features in a parsed tree to improve end-to-end TTS. In *Interspeech*. [42](#)
- [84] Jiang Guo, Wanxiang Che, David Yarowsky, Haifeng Wang, and Ting Liu. 2015. Cross-lingual dependency parsing based on distributed representations. In *ACL*. [134](#), [135](#)
- [85] Jiang Guo, Wanxiang Che, David Yarowsky, Haifeng Wang, and Ting Liu. 2016. A representation learning framework for multi-source transfer parsing. In *AAAI*. [134](#), [135](#), [148](#)
- [86] Mandy Guo, Qinlan Shen, Yinfei Yang, Heming Ge, Daniel Cer, Gustavo Hernandez Abrego, Keith Stevens, Noah Constant, Yun-Hsuan Sung, Brian Strope, and Ray Kurzweil. 2018. Effective parallel corpus mining using bilingual sentence embeddings. In *WMT*. [126](#)

- [87] Wenjuan Han, Yong Jiang, and Kewei Tu. 2017. Dependency grammar induction with neural lexicalization and big training data. In *EMNLP*. [22](#)
- [88] Stevan Harnad. 1990. The symbol grounding problem. *Physica D: Nonlinear Phenomena*, 42(1-3):335–346. [6](#), [15](#), [16](#), [18](#)
- [89] David Harwath and James Glass. 2019. Towards visually grounded sub-word speech unit discovery. In *ICASSP*. [42](#)
- [90] David Harwath and James R. Glass. 2017. Learning word-like units from joint audio-visual analysis. In *ACL*. [42](#)
- [91] David Harwath, Adria Recasens, Dídac Surís, Galen Chuang, Antonio Torralba, and James Glass. 2018. Jointly discovering visual objects and spoken words from raw sensory input. In *ECCV*. [42](#)
- [92] David F. Harwath, Wei-Ning Hsu, and James R. Glass. 2020. Learning hierarchical discrete linguistic units from visually-grounded speech. In *ICLR*. [42](#)
- [93] Serhii Havrylov, Germán Kruszewski, and Armand Joulin. 2019. Cooperative learning of disjoint syntax and semantics. In *NAACL-HLT*. [2](#)
- [94] Junxian He, Zhisong Zhang, Taylor Berg-Kirkpatrick, and Graham Neubig. 2019. Cross-lingual syntactic transfer through unsupervised adaptation of invertible projections. In *ACL*. [135](#), [143](#)
- [95] Kaiming He, Georgia Gkioxari, Piotr Dollár, and Ross Girshick. 2017. Mask R-CNN. In *ICCV*. [90](#), [94](#)
- [96] Kaiming He, Xiangyu Zhang, Shaoqing Ren, and Jian Sun. 2016. Deep residual learning for image recognition. In *CVPR*. [31](#), [90](#)
- [97] Jack Hessel, David Mimno, and Lillian Lee. 2018. Quantifying the visual concreteness of words and topics in multimodal datasets. In *NAACL-HLT*. [23](#), [31](#), [32](#), [33](#), [35](#)
- [98] Felix Hill, Douwe Kiela, and Anna Korhonen. 2013. Concreteness and corpora: A theoretical and practical study. In *Proc. of CMCL*. [23](#)
- [99] Felix Hill and Anna Korhonen. 2014. Concreteness and subjectivity as dimensions of lexical meaning. In *ACL*. [23](#)

- [100] Felix Hill and Anna Korhonen. 2014. Learning abstract concept embeddings from multi-modal data: Since you probably can’t see what i mean. In *EMNLP*. 23
- [101] Felix Hill, Roi Reichart, and Anna Korhonen. 2014. Multi-modal models for concrete and abstract concept meaning. *TACL*, 2(1):285–296. 23
- [102] Geoffrey Hinton, Oriol Vinyals, and Jeffrey Dean. 2015. Distilling the knowledge in a neural network. In *NeurIPS Deep Learning and Representation Learning Workshop*. 136
- [103] Sepp Hochreiter and Jürgen Schmidhuber. 1997. Long short-term memory. *Neural Comput.*, 9(8):1735–1780. 30
- [104] Ari Holtzman, Peter West, Vered Shwartz, Yejin Choi, and Luke Zettlemoyer. 2021. Surface form competition: Why the highest probability answer isn’t always right. In *EMNLP*. 122
- [105] Yining Hong, Qing Li, Song-Chun Zhu, and Siyuan Huang. 2021. Vlgrammar: Grounded grammar induction of vision and language. In *ICCV*. 38
- [106] H. Hotelling. 1936. Relations between two sets of variates. *Biometrika*, 28(3-4):321–377. 18
- [107] Wei-Ning Hsu, Benjamin Bolte, Yao-Hung Hubert Tsai, Kushal Lakhota, Ruslan Salakhutdinov, and Abdelrahman Mohamed. 2021. HuBERT: Self-supervised speech representation learning by masked prediction of hidden units. *IEEE Trans. on Audio, Speech, and Language Processing*, 29:3451–3460. 47
- [108] Wei-Ning Hsu, David Harwath, Tyler Miller, Christopher Song, and James Glass. 2021. Text-free image-to-speech synthesis using learned segmental units. In *ACL*. 46
- [109] Phu Mon Htut, Kyunghyun Cho, and Samuel R. Bowman. 2018. Grammar induction with neural language models: An unusual replication. In *EMNLP*. 22, 30
- [110] Ronghang Hu, Jacob Andreas, Marcus Rohrbach, Trevor Darrell, and Kate Saenko. 2017. Learning to reason: End-to-end module networks for visual question answering. In *CVPR*. 79
- [111] Drew A. Hudson and Christopher D. Manning. 2018. Compositional attention networks for machine reasoning. In *ICLR*. 94

- [112] Rebecca Hwa, Philip Resnik, Amy Weinberg, Clara Cabezas, and Okan Kolak. 2005. Bootstrapping parsers via syntactic projection across parallel texts. *Natural language engineering*, 11(3):311–325. [135](#)
- [113] Masoud Jalili Sabet, Philipp Dufter, and Hinrich Schutze. 2020. SimAlign: High quality word alignments without parallel training data using static and contextualized embeddings. In *Findings of EMNLP*. [125](#), [126](#), [127](#), [129](#), [130](#), [132](#), [138](#), [139](#), [143](#)
- [114] Paria Jamshid Lou and Mark Johnson. 2020. Improving disfluency detection by self-training a self-attentive model. In *ACL*. [57](#), [65](#), [67](#)
- [115] Eric Jang, Shixiang Gu, and Ben Poole. 2017. Categorical reparameterization with Gumbel-softmax. In *ICLR*. [30](#)
- [116] Aren Jansen and Benjamin Van Durme. 2011. Efficient spoken term discovery using randomized algorithms. In *ASRU*. [42](#)
- [117] Zhengbao Jiang, Frank F. Xu, Jun Araki, and Graham Neubig. 2020. How can we know what language models know? *TACL*, 8:423–438. [106](#)
- [118] Lifeng Jin and William Schuler. 2020. Grounded PCFG induction with images. In *AAACL*. [78](#)
- [119] Justin Johnson, Bharath Hariharan, Laurens van der Maaten, Li Fei-Fei, C. Lawrence Zitnick, and Ross Girshick. 2017. CLEVR: A diagnostic dataset for compositional language and elementary visual reasoning. In *CVPR*. [80](#), [87](#), [88](#)
- [120] Aravind K. Joshi, Leon S. Levy, and Masako Takahashi. 1975. Tree adjunct grammars. *Journal of computer and system sciences*, 10(1):136–163. [1](#)
- [121] Armand Joulin, Edouard Grave, Piotr Bojanowski, Matthijs Douze, Herve Jégou, and Tomas Mikolov. 2016. FastText.zip: Compressing text classification models. *arXiv preprint arXiv:1612.03651*. [34](#)
- [122] Daniel Jurafsky and James H. Martin. 2000. *Speech and Language Processing*. Prentice Hall. [2](#), [6](#)
- [123] Jeremy G. Kahn, Matthew Lease, Eugene Charniak, Mark Johnson, and Mari Ostendorf. 2005. Effective use of prosody in parsing conversational speech. In *EMNLP*. [57](#)

- [124] Jeremy G. Kahn and Mari Ostendorf. 2012. Joint reranking of parsing and word recognition with automatic segmentation. *Computer Speech & Language*, 26(1):1–19. [55](#), [57](#)
- [125] Jeremy G. Kahn, Mari Ostendorf, and Ciprian Chelba. 2004. Parsing conversational speech using enhanced segmentation. In *NAACL*. [57](#)
- [126] Nobuyoshi Kaiki, Sakriani Sakti, and Satoshi Nakamura. 2021. Using local phrase dependency structure information in neural sequence-to-sequence speech synthesis. In *O-COCOSDA*. [42](#)
- [127] Herman Kamper. 2022. Word segmentation on discovered phone units with dynamic programming and self-supervised scoring. *IEEE Trans. on Audio, Speech, and Language Processing*, 31:684–694. [47](#), [48](#), [49](#), [53](#)
- [128] Herman Kamper, Aren Jansen, and Sharon Goldwater. 2017. A segmental framework for fully-unsupervised large-vocabulary speech recognition. *Computer Speech & Language*. [42](#)
- [129] Andrej Karpathy and Li Fei-Fei. 2015. Deep visual-semantic alignments for generating image descriptions. In *CVPR*. [23](#), [29](#)
- [130] Jungo Kasai, Keisuke Sakaguchi, Ronan Le Bras, Lavinia Dunagan, Jacob Morrison, Alexander Richard Fabbri, Yejin Choi, and Noah A. Smith. 2022. Bidimensional leaderboards: Generate and evaluate language hand in hand. In *NAACL-HLT*. [74](#)
- [131] Tadao Kasami. 1966. An efficient recognition and syntax-analysis algorithm for context-free languages. *Coordinated Science Laboratory Report no. R-257*. [83](#)
- [132] Charles K. Kemp, Amy Perfors, and Joshua B. Tenenbaum. 2006. Learning overhypotheses. In *CogSci*. [38](#)
- [133] Phillip Keung, Julian Salazar, Yichao Lu, and Noah A. Smith. 2020. Unsupervised bitext mining and translation via self-trained contextual embeddings. *TACL*, 8:828–841. [126](#)
- [134] Daniel Khashabi, Sewon Min, Tushar Khot, Ashish Sabharwal, Oyvind Tafjord, Peter Clark, and Hannaneh Hajishirzi. 2020. UNIFIEDQA: Crossing format boundaries with a single QA system. In *Findings of EMNLP*. [106](#)

- [135] Douwe Kiela, Felix Hill, Anna Korhonen, and Stephen Clark. 2014. Improving multi-modal representations using image dispersion: Why less is sometimes more. In *ACL*. [23](#)
- [136] Yoon Kim, Chris Dyer, and Alexander Rush. 2019. Compound probabilistic context-free grammars for grammar induction. In *ACL*. [47](#), [69](#), [78](#)
- [137] Diederik P. Kingma and Jimmy Ba. 2015. Adam: A method for stochastic optimization. In *ICLR*. [31](#), [142](#)
- [138] Ryan Kiros, Ruslan Salakhutdinov, and Richard S. Zemel. 2014. Unifying visual-semantic embeddings with multimodal neural language models. *arXiv preprint arXiv:1411.2539*. [23](#), [25](#), [27](#), [30](#), [36](#), [82](#)
- [139] Nikita Kitaev, Steven Cao, and Dan Klein. 2019. Multilingual constituency parsing with self-attention and pre-training. In *ACL*. [72](#)
- [140] Nikita Kitaev and Dan Klein. 2018. Constituency parsing with a self-attentive encoder. In *ACL*. [29](#), [42](#), [45](#), [46](#), [57](#), [70](#)
- [141] Dan Klein and Christopher D. Manning. 2002. A generative constituent-context model for improved grammar induction. In *ACL*. [8](#), [22](#)
- [142] Dan Klein and Christopher D. Manning. 2004. Corpus-based induction of syntactic structure: Models of dependency and constituency. In *ACL*. [22](#)
- [143] Dan Klein and Christopher D. Manning. 2005. Natural language grammar induction with a generative constituent-context model. *Pattern Recognition*, 38(9):1407–1419. [22](#)
- [144] Arne Köhn, Timo Baumann, and Oskar Dörfler. 2018. An empirical analysis of the correlation of syntax and prosody. In *Interspeech*. [42](#)
- [145] Satwik Kottur, José MF Moura, Devi Parikh, Dhruv Batra, and Marcus Rohrbach. 2018. Visual coreference resolution in visual dialog using neural module networks. In *ECCV*. [39](#)
- [146] Shankar Kumar and William Byrne. 2004. Minimum Bayes-risk decoding for statistical machine translation. In *NAACL-HLT*. [108](#)



- [147] Kemal Kurniawan, Lea Frermann, Philip Schulz, and Trevor Cohn. 2021. PPT: Parsimonious parser transfer for unsupervised cross-lingual adaptation. In *EACL*. [135](#), [143](#), [144](#)
- [148] Marie-Anne Lachaux, Baptiste Roziere, Marc Szafraniec, and Guillaume Lample. 2021. Dobf: A deobfuscation pre-training objective for programming languages. In *NeurIPS*. [106](#)
- [149] Ophélie Lacroix, Lauriane Aufrant, Guillaume Wisniewski, and François Yvon. 2016. Frustratingly easy cross-lingual transfer for transition-based dependency parsing. In *NAACL-HLT*. [xi](#), [132](#), [133](#), [134](#), [135](#), [145](#), [146](#)
- [150] Cheng-I Jeff Lai, Freda Shi, Puyuan Peng, Yoon Kim, Kevin Gimpel, Shiyu Chang, Yung-Sung Chuang, Saurabhchand Bhati, David Cox, David Harwath, Yang Zhang, Karen Livescu, and James Glass. 2023. Audio-visual neural syntax acquisition. In *ARSL*. [40](#), [55](#), [65](#), [74](#)
- [151] Brenden Lake and Marco Baroni. 2018. Generalization without systematicity: On the compositional skills of sequence-to-sequence recurrentlake networks. In *ICML*. [84](#), [87](#), [96](#), [100](#)
- [152] Matthew Lease and Mark Johnson. 2006. Early deletion of fillers in processing conversational speech. In *NAACL-HLT*. [57](#)
- [153] Yann LeCun, Léon Bottou, Yoshua Bengio, and Patrick Haffner. 1998. Gradient-based learning applied to document recognition. *Proceedings of the IEEE*, 86(11):2278–2324. [17](#)
- [154] Chia-ying Lee, Timothy J. O’donnell, and James Glass. 2015. Unsupervised lexicon discovery from acoustic input. *TACL*, 3:389–403. [42](#)
- [155] Brian Lester, Rami Al-Rfou, and Noah Constant. 2021. The power of scale for parameter-efficient prompt tuning. In *EMNLP*. [106](#)
- [156] Stephen C. Levinson. 1983. *Pragmatics*. Cambridge university press. [16](#)
- [157] Qing Li, Siyuan Huang, Yining Hong, and Song-Chun Zhu. 2020. A competence-aware curriculum for visual concepts learning via question answering. In *ECCV*. [93](#)

- [158] Xiang Lisa Li and Percy Liang. 2021. Prefix-tuning: Optimizing continuous prompts for generation. In *ACL*. [106](#)
- [159] Yujia Li, David Choi, Junyoung Chung, Nate Kushman, Julian Schrittwieser, Rémi Leblond, Tom Eccles, James Keeling, Felix Gimeno, Agustin Dal Lago, et al. 2022. Competition-level code generation with alphacode. *Science*, 378(6624):1092–1097. [104](#), [106](#)
- [160] Zhenghua Li, Min Zhang, and Wenliang Chen. 2014. Soft cross-lingual syntax projection for dependency parsing. In *COLING*. [135](#)
- [161] Percy Liang, Michael I. Jordan, and Dan Klein. 2013. Learning dependency-based compositional semantics. *Comput. Linguist.*, 39(2):389–446. [11](#)
- [162] Tsung-Yi Lin, Michael Maire, Serge Belongie, James Hays, Pietro Perona, Deva Ramanan, Piotr Dollár, and C. Lawrence Zitnick. 2014. Microsoft COCO: Common objects in context. In *ECCV*. [29](#), [46](#)
- [163] Xi Victoria Lin, Chenglong Wang, Luke Zettlemoyer, and Michael D. Ernst. 2018. Nl2bash: A corpus and semantic parser for natural language interface to the linux operating system. In *LREC*. [106](#), [110](#)
- [164] Wang Ling, Phil Blunsom, Edward Grefenstette, Karl Moritz Hermann, Tomáš Kočiský, Fumin Wang, and Andrew Senior. 2016. Latent predictor networks for code generation. In *ACL*. [106](#)
- [165] Pengfei Liu, Weizhe Yuan, Jinlan Fu, Zhengbao Jiang, Hiroaki Hayashi, and Graham Neubig. 2023. Pre-train, prompt, and predict: A systematic survey of prompting methods in natural language processing. *ACM Computing Surveys*, 55(9):1–35. [106](#)
- [166] Yinhan Liu, Sergey Edunov, Myle Ott, Naman Goyal, Jingfei Du, Dan Joshi, Dan Z. Chen, Omer Levy, Mike Lewis, Luke Zettlemoyer, et al. 2020. Multilingual denoising pre-training for neural machine translation. *arXiv preprint arXiv:2001.08210*. [137](#)
- [167] Yinhan Liu, Jiatao Gu, Naman Goyal, Xian Li, Sergey Edunov, Marjan Ghazvininejad, Mike Lewis, and Luke Zettlemoyer. 2020. Multilingual denoising pre-training for neural machine translation. *arXiv preprint arXiv:2001.08210*. [129](#), [130](#)

- [168] Paria Jamshid Lou, Yufei Wang, and Mark Johnson. 2019. Neural constituency parsing of speech transcripts. In *NAACL-HLT*. [42](#)
- [169] Cewu Lu, Ranjay Krishna, Michael Bernstein, and Li Fei-Fei. 2016. Visual relationship detection with language priors. In *ECCV*. [38](#)
- [170] Shuai Lu, Daya Guo, Shuo Ren, Junjie Huang, Alexey Svyatkovskiy, Ambrosio Blanco, Colin Clement, Dawn Drain, Daxin Jiang, Duyu Tang, Ge Li, Lidong Zhou, Linjun Shou, Long Zhou, Michele Tufano, MING GONG, Ming Zhou, Nan Duan, Neel Sundaresan, Shao Kun Deng, Shengyu Fu, and Shujie Liu. 2021. CodeXGLUE: A machine learning benchmark dataset for code understanding and generation. In *NeurIPS*. [106](#)
- [171] Lin Ma, Zhengdong Lu, Lifeng Shang, and Hang Li. 2015. Multimodal convolutional neural networks for matching image and sentence. In *CVPR*. [23](#)
- [172] Xuezhe Ma and Fei Xia. 2014. Unsupervised dependency parsing with transferring distribution via parallel guidance and entropy regularization. In *ACL*. [132](#), [133](#), [135](#), [136](#), [143](#), [146](#)
- [173] Jean Maillard and Stephen Clark. 2018. Latent tree learning with differentiable parsers: Shift-reduce parsing and chart parsing. In *Proc. of the Workshop on the Relevance of Linguistic Structure in Neural Architectures for NLP*. [22](#), [78](#)
- [174] Mateusz Malinowski, Marcus Rohrbach, and Mario Fritz. 2015. Ask your neurons: A neural-based approach to answering questions about images. In *ICCV*. [23](#)
- [175] Jiayuan Mao, Chuang Gan, Pushmeet Kohli, Joshua B. Tenenbaum, and Jiajun Wu. 2019. The Neuro-Symbolic Concept Learner: Interpreting Scenes, Words, and Sentences From Natural Supervision. In *ICLR*. [22](#), [79](#), [80](#), [83](#), [88](#), [90](#), [93](#), [94](#)
- [176] Jiayuan Mao, Freda Shi, Jiajun Wu, Roger P. Levy, and Joshua B. Tenenbaum. 2021. Grammar-based grounded lexicon learning. In *NeurIPS*. [2](#), [76](#)
- [177] Mitchell Marcus, Beatrice Santorini, and Mary Ann Marcinkiewicz. 1993. Building a large annotated corpus of English: The Penn treebank. *Comput. Linguist.*, 19(2). [8](#), [29](#), [70](#)

- [178] Alex Marin and Mari Ostendorf. 2014. Domain adaptation for parsing in automatic speech recognition. In *ICASSP*. [57](#)
- [179] David Mascharka, Philip Tran, Ryan Soklaski, and Arjun Majumdar. 2018. Transparency by design: Closing the gap between performance and interpretability in visual reasoning. In *CVPR*. [79](#), [94](#)
- [180] Michael McAuliffe, Michaela Socolof, Sarah Mihuc, Michael Wagner, and Morgan Sonderegger. 2017. Montreal forced aligner: Trainable text-speech alignment using Kaldi. In *Interspeech*. [46](#), [56](#)
- [181] David McClosky, Eugene Charniak, and Mark Johnson. 2006. Effective self-training for parsing. In *NAACL-HLT*. [8](#), [57](#)
- [182] Ryan McDonald. 2006. Discriminative training and spanning tree algorithms for dependency parsing. *University of Pennsylvania, PhD Thesis*. [10](#)
- [183] Ryan McDonald, Joakim Nivre, Yvonne Quirnbach-Brundage, Yoav Goldberg, Dipanjan Das, Kuzman Ganchev, Keith Hall, Slav Petrov, Hao Zhang, Oscar Täckström, Claudia Bedini, Núria Bertomeu Castelló, and Jungmee Lee. 2013. Universal dependency annotation for multilingual parsing. In *ACL*. [147](#), [148](#)
- [184] Ryan McDonald, Slav Petrov, and Keith Hall. 2011. Multi-source transfer of delexicalized dependency parsers. In *EMNLP*. [134](#)
- [185] Fergus McInnes and Sharon Goldwater. 2011. Unsupervised extraction of recurring words from infant-directed speech. In *CogSci*. [42](#)
- [186] Tao Meng, Nanyun Peng, and Kai-Wei Chang. 2019. Target language-aware constrained inference for cross-lingual dependency parsing. In *EMNLP*. [135](#), [143](#)
- [187] Antonio Valerio Miceli Barone and Rico Sennrich. 2017. A parallel corpus of python functions and documentation strings for automated code documentation and code generation. In *IJCNLP*. [106](#)
- [188] Sewon Min, Mike Lewis, Hannaneh Hajishirzi, and Luke Zettlemoyer. 2022. Noisy channel language model prompting for few-shot text classification. In *ACL*. [106](#)

- [189] Dimitri Coelho Mollo and Raphaël Millière. 2023. The vector grounding problem. *arXiv preprint arXiv:2304.01481*. [15](#)
- [190] Phoebe Mulcaire, Jungo Kasai, and Noah A. Smith. 2019. Polyglot contextual representations improve crosslingual transfer. In *NAACL*. [136](#)
- [191] Jiquan Ngiam, Aditya Khosla, Mingyu Kim, Juhan Nam, Honglak Lee, and Andrew Y. Ng. 2011. Multimodal deep learning. In *ICML*. [22](#)
- [192] Joakim Nivre. 2004. Incrementality in deterministic dependency parsing. In *Proceedings of the workshop on incremental parsing: Bringing engineering and cognition together*. [10](#)
- [193] Joakim Nivre. 2008. Algorithms for deterministic incremental dependency parsing. *Comput. Linguist.*, 34(4):513–553. [10](#)
- [194] Joakim Nivre, Marie-Catherine de Marneffe, Filip Ginter, Jan Hajič, Christopher D. Manning, Sampo Pyysalo, Sebastian Schuster, Francis Tyers, and Daniel Zeman. 2020. Universal Dependencies v2: An evergrowing multilingual treebank collection. In *LREC*. [x](#), [10](#), [134](#), [143](#), [147](#)
- [195] Franz Josef Och and Hermann Ney. 2003. A systematic comparison of various statistical alignment models. *Comput. Linguist.*, 29(1):19–51. [126](#), [130](#), [138](#)
- [196] Alex S. Park and James R. Glass. 2007. Unsupervised pattern discovery in speech. *IEEE Trans. on Audio, Speech, and Language Processing*, 16(1):186–197. [42](#)
- [197] Puyuan Peng and David Harwath. 2022. Word discovery in visually grounded, self-supervised speech models. In *Interspeech*. [40](#), [42](#), [44](#), [48](#), [49](#), [53](#)
- [198] Puyuan Peng, Shang-Wen Li, Okko Räsänen, Abdelrahman Mohamed, and David Harwath. 2023. Syllable segmentation and cross-lingual generalization in a visually grounded, self-supervised speech model. In *Interspeech*. [49](#)
- [199] Jan-Thorsten Peter, Arne Nix, and Hermann Ney. 2017. Generating alignments using target foresight in attention-based neural machine translation. *The Prague Bulletin of Mathematical Linguistics*, 108(1):27–36. [126](#)

- [200] Massimo Piattelli-Palmarini. 1980. *Language and learning: the debate between Jean Piaget and Noam Chomsky*. Harvard University Press. [2](#)
- [201] Steven Pinker. 1984. *Language Learnability and Language Development*. Cambridge University Press. [24](#), [38](#)
- [202] Telmo Pires, Eva Schlinger, and Dan Garrette. 2019. How multilingual is multilingual BERT? In *ACL*. [136](#)
- [203] Bryan A. Plummer, Liwei Wang, Chris M. Cervantes, Juan C. Caicedo, Julia Hockenmaier, and Svetlana Lazebnik. 2015. Flickr30k entities: Collecting region-to-phrase correspondences for richer image-to-sentence models. In *CVPR*. [15](#)
- [204] Carl Pollard and Ivan Sag. 1994. *Head-Driven Phrase Structure Grammar*. Chicago: University of Chicago Press and Stanford: CSLI Publications. [77](#)
- [205] Elias Ponvert, Jason Baldridge, and Katrin Erk. 2011. Simple unsupervised grammar induction from raw text with cascaded finite state models. In *ACL*. [22](#)
- [206] Adrien Pupier, Maximin Coavoux, Benjamin Lecouteux, and Jérôme Goulian. 2022. End-to-end dependency parsing of spoken french. In *Interspeech*. [42](#)
- [207] Maxim Rabinovich, Mitchell Stern, and Dan Klein. 2017. Abstract syntax networks for code generation and semantic parsing. In *ACL*. [106](#)
- [208] Alec Radford, Jeffrey Wu, Rewon Child, David Luan, Dario Amodei, Ilya Sutskever, et al. 2019. Language models are unsupervised multitask learners. *OpenAI blog*, 1(8):9. [106](#), [122](#)
- [209] Mohammad Sadegh Rasooli, Chris Callison-Burch, and Derry Tanti Wijaya. 2021. "wikily" neural machine translation tailored to cross-lingual tasks. *arXiv preprint arXiv:2104.08384*. [133](#), [135](#), [146](#), [150](#)
- [210] Mohammad Sadegh Rasooli and Michael Collins. 2015. Density-driven cross-lingual transfer of dependency parsers. In *EMNLP*. [135](#), [143](#), [150](#)
- [211] Mohammad Sadegh Rasooli and Michael Collins. 2017. Cross-lingual syntactic transfer with limited resources. *TACL*, 5:279–293. [135](#)

- [212] Mohammad Sadegh Rasooli and Michael Collins. 2019. Low-resource syntactic transfer with unsupervised source reordering. In *NAACL-HLT*. 135
- [213] Philip Resnik. 1999. Mining the web for bilingual text. In *ACL*. 126
- [214] Brian Roark, Mary P. Harper, Eugene Charniak, Bonnie J. Dorr, Mark Johnson, Jeremy G. Kahn, Yang Liu, Mari Ostendorf, John Hale, Anna Krasnyanskaya, et al. 2006. Sparseval: Evaluation metrics for parsing speech. In *LREC*. 42, 57, 74
- [215] Rudolf Rosa and Zdeněk Žabokrtský. 2015. KLcpos3 - a language similarity measure for delexicalized parser transfer. In *ACL*. 134
- [216] Olga Russakovsky, Jia Deng, Hao Su, Jonathan Krause, Sanjeev Satheesh, Sean Ma, Zhiheng Huang, Andrej Karpathy, Aditya Khosla, Michael Bernstein, Alexander C. Berg, and Li Fei-Fei. 2015. ImageNet large scale visual recognition challenge. *IJCV*, 115(3):211–252. 31
- [217] Victor Sanh, Lysandre Debut, Julien Chaumond, and Thomas Wolf. 2019. Distilbert, a distilled version of BERT: smaller, faster, cheaper and lighter. In *Proceedings of the 5th Workshop on Energy Efficient Machine Learning and Cognitive Computing*. 136
- [218] Raeid Saqur and Karthik Narasimhan. 2020. Multimodal graph networks for compositional generalization in visual question answering. In *NeurIPS*. 78
- [219] Torsten Scholak, Nathan Schucher, and Dzmitry Bahdanau. 2021. PICARD: Parsing incrementally for constrained auto-regressive decoding from language models. In *EMNLP*. 122
- [220] Philip Schulz, Wilker Aziz, and Khalil Sima'an. 2016. Word alignment without NULL words. In *ACL*. 139
- [221] Tal Schuster, Ori Ram, Regina Barzilay, and Amir Globerson. 2019. Cross-lingual alignment of contextual word embeddings, with applications to zero-shot dependency parsing. In *NAACL-HLT*. 134, 135, 136, 147, 148, 150
- [222] Holger Schwenk. 2018. Filtering and mining parallel data in a joint multilingual space. In *ACL*. 126

- [223] Holger Schwenk, Vishrav Chaudhary, Shuo Sun, Hongyu Gong, and Francisco Guzmán. 2021. WikiMatrix: Mining 135m parallel sentences in 1620 language pairs from wikipedia. In *EACL*. [148](#)
- [224] Djamé Seddah, Reut Tsarfaty, Sandra Kübler, Marie Candito, Jinho D. Choi, Richárd Farkas, Jennifer Foster, Iakes Goenaga, Koldo Gojenola Gallettebeitia, Yoav Goldberg, Spence Green, Nizar Habash, Marco Kuhlmann, Wolfgang Maier, Joakim Nivre, Adam Przepiórkowski, Ryan Roth, Wolfgang Seeker, Yannick Versley, Veronika Vincze, Marcin Woliński, Alina Wróblewska, and Eric Villemonte de la Clergerie. 2013. Overview of the SPMRL 2013 shared task: A cross-framework evaluation of parsing morphologically rich languages. In *Proceedings of the Fourth Workshop on Statistical Parsing of Morphologically-Rich Languages*. [72](#)
- [225] Satoshi Sekine and Michael Collins. 1997. Evalb bracket scoring program. [8](#), [29](#), [65](#)
- [226] Shane Settle, Kartik Audhkhasi, Karen Livescu, and Michael Picheny. 2019. Acoustically grounded word embeddings for improved acoustics-to-word speech recognition. In *ICASSP*. [15](#)
- [227] Yikang Shen, Zhouhan Lin, Chin-Wei Huang, and Aaron Courville. 2018. Neural language modeling by jointly learning syntax and lexicon. In *ICLR*. [22](#), [30](#), [32](#), [33](#), [34](#)
- [228] Yikang Shen, Zhouhan Lin, Athul Paul Jacob, Alessandro Sordoni, Aaron Courville, and Yoshua Bengio. 2018. Straight to the tree: Constituency parsing with neural syntactic distance. In *ACL*. [30](#)
- [229] Yikang Shen, Shawn Tan, Alessandro Sordoni, and Aaron Courville. 2019. Ordered neurons: Integrating tree structures into recurrent neural networks. In *ICLR*. [22](#), [30](#), [33](#), [34](#)
- [230] Freda Shi, Daniel Fried, Marjan Ghazvininejad, Luke Zettlemoyer, and Sida I. Wang. 2022. Natural language to code translation with execution. In *EMNLP*. [104](#)
- [231] Freda Shi, Kevin Gimpel, and Karen Livescu. 2022. Substructure distribution projection for zero-shot cross-lingual dependency parsing. In *ACL*. [132](#)
- [232] Haoyue Shi, Karen Livescu, and Kevin Gimpel. 2020. On the role of supervision in unsupervised constituency parsing. In *EMNLP*. [45](#), [74](#)



- [233] Haoyue Shi, Karen Livescu, and Kevin Gimpel. 2021. Substructure substitution: Structured data augmentation for nlp. In *Findings of ACL*. [136](#)
- [234] Haoyue Shi, Jiayuan Mao, Kevin Gimpel, and Karen Livescu. 2019. Visually grounded neural syntax acquisition. In *ACL*. [20](#), [41](#), [52](#), [78](#), [107](#)
- [235] Haoyue Shi, Jiayuan Mao, Tete Xiao, Yuning Jiang, and Jian Sun. 2018. Learning visually-grounded semantics from contrastive adversarial samples. In *COLING*. [23](#), [25](#)
- [236] Haoyue Shi, Luke Zettlemoyer, and Sida I. Wang. 2021. Bilingual lexicon induction via unsupervised bitext construction and word alignment. In *ACL*. [125](#), [130](#), [132](#), [136](#)
- [237] Haoyue Shi, Hao Zhou, Jiaze Chen, and Lei Li. 2018. On tree-based neural sentence modeling. In *EMNLP*. [30](#), [78](#)
- [238] Lei Shi, Cheng Niu, Ming Zhou, and Jianfeng Gao. 2006. A DOM tree alignment model for mining parallel data from the web. In *ACL*. [126](#)
- [239] Tianze Shi, Ozan Irsoy, Igor Malioutov, and Lillian Lee. 2021. Learning syntax from naturally-occurring bracketings. In *NAACL-HLT*. [78](#)
- [240] Taylor Shin, Yasaman Razeghi, Robert L. Logan IV, Eric Wallace, and Sameer Singh. 2020. AutoPrompt: Eliciting knowledge from language models with automatically generated prompts. In *EMNLP*. [106](#), [108](#)
- [241] N. Siddharth, Andrei Barbu, and Jeffrey Mark Siskind. 2014. Seeing what you’re told: Sentence-guided activity recognition in video. In *CVPR*. [22](#)
- [242] Carina Silberer, Vittorio Ferrari, and Mirella Lapata. 2017. Visually grounded meaning representations. *TPAMI*, 39(11):2284–2297. [23](#)
- [243] Carina Silberer and Mirella Lapata. 2012. Grounded models of semantic representation. In *EMNLP*. [23](#)
- [244] Noah A. Smith and Jason Eisner. 2006. Annealing structural bias in multilingual weighted grammar induction. In *ACL*. [22](#)

- [245] Richard Socher, Alex Perelygin, Jean Wu, Jason Chuang, Christopher D. Manning, Andrew Y. Ng, and Christopher Potts. 2013. Recursive deep models for semantic compositionality over a sentiment treebank. In *EMNLP*. 78
- [246] Valentin I. Spitzkovsky, Hiyani Alshawi, Angel X. Chang, and Daniel Jurafsky. 2011. Unsupervised dependency parsing without gold part-of-speech tags. In *EMNLP*. 22
- [247] Valentin I. Spitzkovsky, Hiyani Alshawi, and Daniel Jurafsky. 2010. From baby steps to leapfrog: How “less is more” in unsupervised dependency parsing. In *NAACL-HLT*. 22
- [248] Mark Steedman. 2000. *The Syntactic Process*. Cambridge, MA: MIT Press. 1, 12, 38, 77, 79, 80
- [249] Mitchell Stern, Jacob Andreas, and Dan Klein. 2017. A minimal span-based neural constituency parser. In *ACL*. 57
- [250] Ruisi Su, Shruti Rijhwani, Hao Zhu, Junxian He, Xinyu Wang, Yonatan Bisk, and Graham Neubig. 2021. Dependency induction through the lens of visual perception. In *CoNLL*. 39
- [251] Alane Suhr, Srinivasan Iyer, and Yoav Artzi. 2018. Learning to map context-dependent sentences to executable formal queries. In *NAACL-HLT*. 106
- [252] Ilya Sutskever, Oriol Vinyals, and Quoc V. Le. 2014. Sequence to sequence learning with neural networks. In *NeurIPS*. 100
- [253] Oscar Täckström, Ryan McDonald, and Joakim Nivre. 2013. Target language adaptation of discriminative transfer parsers. In *NAACL-HLT*. 135
- [254] Oscar Täckström, Ryan McDonald, and Jakob Uszkoreit. 2012. Cross-lingual word clusters for direct transfer of linguistic structure. In *NAACL-HLT*. 134
- [255] Kai Sheng Tai, Richard Socher, and Christopher D. Manning. 2015. Improved semantic representations from tree-structured long short-term memory networks. In *ACL*. 78
- [256] Zheng-Hua Tan, Najim Dehak, et al. 2020. rVAD: An unsupervised segment-based robust voice activity detection method. *Computer Speech & Language*. 44

- [257] Robert Endre Tarjan. 1977. Finding optimum branchings. *Networks*, 7(1):25–35. [137](#)
- [258] Marjorie Taylor and Susan A. Gelman. 1988. Adjectives and nouns: Children’s strategies for learning new words. *Child Development*, pages 411–419. [79](#)
- [259] Lucien Tesnière. 1959. *Éléments de Syntaxe Structurale*. Librairie C. Klincksieck, Paris. [1](#), [10](#)
- [260] Jörg Tiedemann. 2015. Improving the cross-lingual projection of syntactic dependencies. In *Proceedings of the 20th Nordic Conference of Computational Linguistics (NODALIDA)*. [135](#)
- [261] Jörg Tiedemann and Željko Agić. 2016. Synthetic treebanking for cross-lingual dependency parsing. *JAIR*, 55:209–248. [135](#)
- [262] Jörg Tiedemann, Željko Agić, and Joakim Nivre. 2014. Treebank translation for cross-lingual parser induction. In *CoNLL*. [135](#)
- [263] Ivan Titov and James Henderson. 2006. Bayes risk minimization in natural language parsing. *University of Geneva technical report*. [107](#)
- [264] Shubham Toshniwal, Haoyue Shi, Bowen Shi, Lingyu Gao, Karen Livescu, and Kevin Gimpel. 2020. A cross-task analysis of text span representations. In *Proceedings of the 5th Workshop on Representation Learning for NLP*. [142](#)
- [265] Chau Tran, Yuqing Tang, Xian Li, and Jiatao Gu. 2020. Cross-lingual retrieval for iterative self-supervised training. In *NeurIPS*. [126](#), [127](#), [129](#), [130](#), [136](#), [137](#), [144](#), [150](#)
- [266] Trang Tran and Mari Ostendorf. 2021. Assessing the use of prosody in constituency parsing of imperfect transcripts. In *Interspeech*. [42](#), [57](#)
- [267] Trang Tran, Shubham Toshniwal, Mohit Bansal, Kevin Gimpel, Karen Livescu, and Mari Ostendorf. 2018. Parsing speech: a neural approach to integrating lexical and acoustic-prosodic information. In *NAACL-HLT*. [42](#), [57](#)
- [268] Trang Tran, Jiahong Yuan, Yang Liu, and Mari Ostendorf. 2019. On the role of style in parsing speech with neural models. In *Interspeech*. [42](#)
- [269] Roy Tromble, Shankar Kumar, Franz Och, and Wolfgang Macherey. 2008. Lattice Minimum Bayes-Risk decoding for statistical machine translation. In *EMNLP*. [108](#)

- [270] Reut Tsarfaty, Joakim Nivre, and Evelina Andersson. 2012. Joint evaluation of morphological segmentation and syntactic parsing. In *ACL*. [57](#), [73](#), [74](#)
- [271] Yuan Tseng, Cheng-I Jeff Lai, and Hung-yi Lee. 2023. Cascading and direct approaches to unsupervised constituency parsing on spoken sentences. In *ICASSP*. [x](#), [42](#), [43](#), [54](#), [55](#), [65](#), [74](#)
- [272] Peter D. Turney, Yair Neuman, Dan Assaf, and Yohai Cohen. 2011. Literal and metaphorical sense identification through concrete and abstract context. In *EMNLP*. [23](#), [31](#), [33](#), [35](#)
- [273] Shubhi Tyagi, Marco Nicolis, Jonas Rohnke, Thomas Drugman, and Jaime Lorenzo-Trueba. 2020. Dynamic prosody generation for speech synthesis using linguistics-driven acoustic embedding selection. In *Interspeech*. [42](#)
- [274] Ashish Vaswani, Noam Shazeer, Niki Parmar, Jakob Uszkoreit, Llion Jones, Aidan N. Gomez, Lukasz Kaiser, and Illia Polosukhin. 2017. Attention is all you need. In *NeurIPS*. [100](#), [106](#)
- [275] Michael Wagner and Duane G. Watson. 2010. Experimental and theoretical advances in prosody: A review. *Language and cognitive processes*, 25(7-9):905–945. [42](#)
- [276] Bo Wan, Wenjuan Han, Zilong Zheng, and Tinne Tuytelaars. 2022. Unsupervised vision-language grammar induction with shared structure modeling. *ICLR*. [38](#), [41](#)
- [277] Xinyi Wang, Hieu Pham, Zihang Dai, and Graham Neubig. 2018. Switchout: an efficient data augmentation algorithm for neural machine translation. In *EMNLP*. [100](#)
- [278] Xuezhi Wang, Jason Wei, Dale Schuurmans, Quoc V. Le, Ed H. Chi, Sharan Narang, Aakanksha Chowdhery, and Denny Zhou. 2023. Self-consistency improves chain of thought reasoning in language models. In *ICLR*. [123](#)
- [279] Yuxuan Wang, Wanxiang Che, Jiang Guo, Yijia Liu, and Ting Liu. 2019. Cross-lingual BERT transformation for zero-shot dependency parsing. In *EMNLP*. [134](#), [135](#), [136](#), [150](#)
- [280] Sean Welleck, Ilia Kulikov, Stephen Roller, Emily Dinan, Kyunghyun Cho, and Jason Weston. 2020. Neural text generation with unlikelihood training. In *ICLR*. [116](#)

- [281] Michael Wick, Pallika Kanani, and Adam Pockock. 2016. Minimally-constrained multilingual embeddings via artificial code-switching. In *AAAI*. [134](#)
- [282] Adina Williams, Andrew Drozdov, and Samuel R. Bowman. 2018. Do latent tree learning models identify meaningful structure in sentences? *TACL*, 6:253–267. [22](#), [30](#), [32](#), [33](#)
- [283] Ronald J. Williams. 1992. Simple statistical gradient-following algorithms for connectionist reinforcement learning. *Mach. Learn.*, 8(3-4):229–256. [27](#)
- [284] Hao Wu, Jiayuan Mao, Yufeng Zhang, Weiwei Sun, Yuning Jiang, Lei Li, and Wei-Ying Ma. 2019. Unified visual-semantic embeddings: Bridging vision and language with structured meaning representations. In *CVPR*. [25](#), [38](#)
- [285] Qianhui Wu, Zijia Lin, Börje Karlsson, Jian-Guang Lou, and Biqing Huang. 2020. Single-/multi-source cross-lingual NER via teacher-student learning on unlabeled data in target language. In *ACL*. [136](#)
- [286] Chunyang Xiao, Marc Dymetman, and Claire Gardent. 2016. Sequence-based structured prediction for semantic parsing. In *ACL*. [106](#)
- [287] Tianbao Xie, Chen Henry Wu, Peng Shi, Ruiqi Zhong, Torsten Scholak, Michihiro Yasunaga, Chien-Sheng Wu, Ming Zhong, Pengcheng Yin, Sida I. Wang, et al. 2022. UnifiedSKG: Unifying and multi-tasking structured knowledge grounding with text-to-text language models. In *EMNLP*. [112](#)
- [288] Frank F. Xu, Zhengbao Jiang, Pengcheng Yin, Bogdan Vasilescu, and Graham Neubig. 2020. Incorporating external knowledge through pre-training for natural language to code generation. In *ACL*. [106](#)
- [289] Jiarui Xu, Shalini De Mello, Sifei Liu, Wonmin Byeon, Thomas Breuel, Jan Kautz, and Xiaolong Wang. 2022. GroupViT: Semantic segmentation emerges from text supervision. In *CVPR*. [17](#), [38](#)
- [290] Kexin Yi, Jiajun Wu, Chuang Gan, Antonio Torralba, Pushmeet Kohli, and Joshua B. Tenenbaum. 2018. Neural-Symbolic VQA: Disentangling Reasoning from Vision and Language Understanding. In *NeurIPS*. [94](#)

- [291] Pengcheng Yin, Bowen Deng, Edgar Chen, Bogdan Vasilescu, and Graham Neubig. 2018. Learning to mine aligned code and natural language pairs from stack overflow. In *2018 IEEE/ACM 15th international conference on mining software repositories (MSR)*. 106
- [292] Dani Yogatama, Phil Blunsom, Chris Dyer, Edward Grefenstette, and Wang Ling. 2017. Learning to compose words into sentences with reinforcement learning. In *ICLR*. 22
- [293] Shan You, Chang Xu, Chao Xu, and Dacheng Tao. 2017. Learning from multiple teacher networks. In *SIGKDD*. 136
- [294] Peter Young, Alice Lai, Micah Hodosh, and Julia Hockenmaier. 2014. From image descriptions to visual denotations: New similarity metrics for semantic inference over event descriptions. *TACL*, 2:67–78. 23, 37
- [295] Daniel H. Younger. 1967. Recognition and parsing of context-free languages in time  $n^3$ . *Information and control*, 10(2):189–208. 83
- [296] Haonan Yu, N. Siddharth, Andrei Barbu, and Jeffrey Mark Siskind. 2015. A compositional framework for grounding language inference, generation, and acquisition in video. *JAIR*, 52:601–713. 22
- [297] Tao Yu, Rui Zhang, Kai Yang, Michihiro Yasunaga, Dongxu Wang, Zifan Li, James Ma, Irene Li, Qingning Yao, Shanelle Roman, Zilin Zhang, and Dragomir Radev. 2018. Spider: A large-scale human-labeled dataset for complex and cross-domain semantic parsing and text-to-SQL task. In *EMNLP*. 106, 110
- [298] Weizhe Yuan, Graham Neubig, and Pengfei Liu. 2021. BARTScore: Evaluating generated text as text generation. In *Advances in Neural Information Processing Systems*. 106
- [299] John M. Zelle and Raymond J. Mooney. 1996. Learning to parse database queries using inductive logic programming. In *Proceedings of the national conference on artificial intelligence*. 11
- [300] Daniel Zeman and Philip Resnik. 2008. Cross-language parser adaptation between related languages. In *Proceedings of the IJCNLP-08 Workshop on NLP for Less Privileged Languages*. 134, 135

- [301] Thomas Zenkel, Joern Wuebker, and John DeNero. 2019. Adding interpretable attention to neural translation models improves word alignment. *arXiv preprint arXiv:1901.11359*. [126](#), [130](#)
- [302] Luke S. Zettlemoyer and Michael Collins. 2005. Learning to map sentences to logical form: Structured classification with probabilistic categorial grammars. In *UAI*. [11](#)
- [303] Hao Zhang and Daniel Gildea. 2008. Efficient multi-pass decoding for synchronous context free grammars. In *ACL*. [108](#)
- [304] Hongyi Zhang, Moustapha Cisse, Yann N. Dauphin, and David Lopez-Paz. 2017. mixup: Beyond empirical risk minimization. In *ICLR*. [100](#)
- [305] Meishan Zhang, Yue Zhang, and Guohong Fu. 2019. Cross-lingual dependency parsing using code-mixed treebank. In *EMNLP*. [135](#)
- [306] Songyang Zhang, Linfeng Song, Lifeng Jin, Kun Xu, Dong Yu, and Jiebo Luo. 2021. Video-aided unsupervised grammar induction. In *NAACL-HLT*. [41](#)
- [307] Yaodong Zhang. 2013. *Unsupervised speech processing with applications to query-by-example spoken term detection*. Ph.D. thesis, Massachusetts Institute of Technology. [42](#)
- [308] Yu Zhang, Zhenghua Li, and Min Zhang. 2020. Efficient second-order treeCRF for neural dependency parsing. In *ACL*. [107](#), [142](#)
- [309] Yuan Zhang and Regina Barzilay. 2015. Hierarchical low-rank tensors for multilingual transfer parsing. In *EMNLP*. [148](#)
- [310] Yanpeng Zhao and Ivan Titov. 2020. Visually grounded compound PCFGs. In *EMNLP*. [39](#), [41](#), [78](#)
- [311] Ruiqi Zhong, Tao Yu, and Dan Klein. 2020. Semantic evaluation for text-to-SQL with distilled test suites. In *EMNLP*. [120](#)
- [312] Zexuan Zhong, Dan Friedman, and Danqi Chen. 2021. Factual probing is [MASK]: Learning vs. learning to recall. In *NAACL*. [108](#)
- [313] Kangyan Zhou, Shrimai Prabhumoye, and Alan W. Black. 2018. A dataset for document grounded conversations. In *EMNLP*. [16](#)

- [314] Xiaodan Zhu, Parinaz Sobihani, and Hongyu Guo. 2015. Long short-term memory over recursive structures. In *ICML*. [78](#)